

# A STUDY ON POLLUTANT TRANSPORT IN A STREAM

## A THESIS

*Submitted in partial fulfilment of the  
requirements for the award of the degree*

*of*

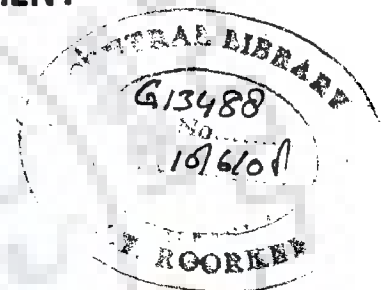
DOCTOR OF PHILOSOPHY

*in*

WATER RESOURCES DEVELOPMENT

*by*

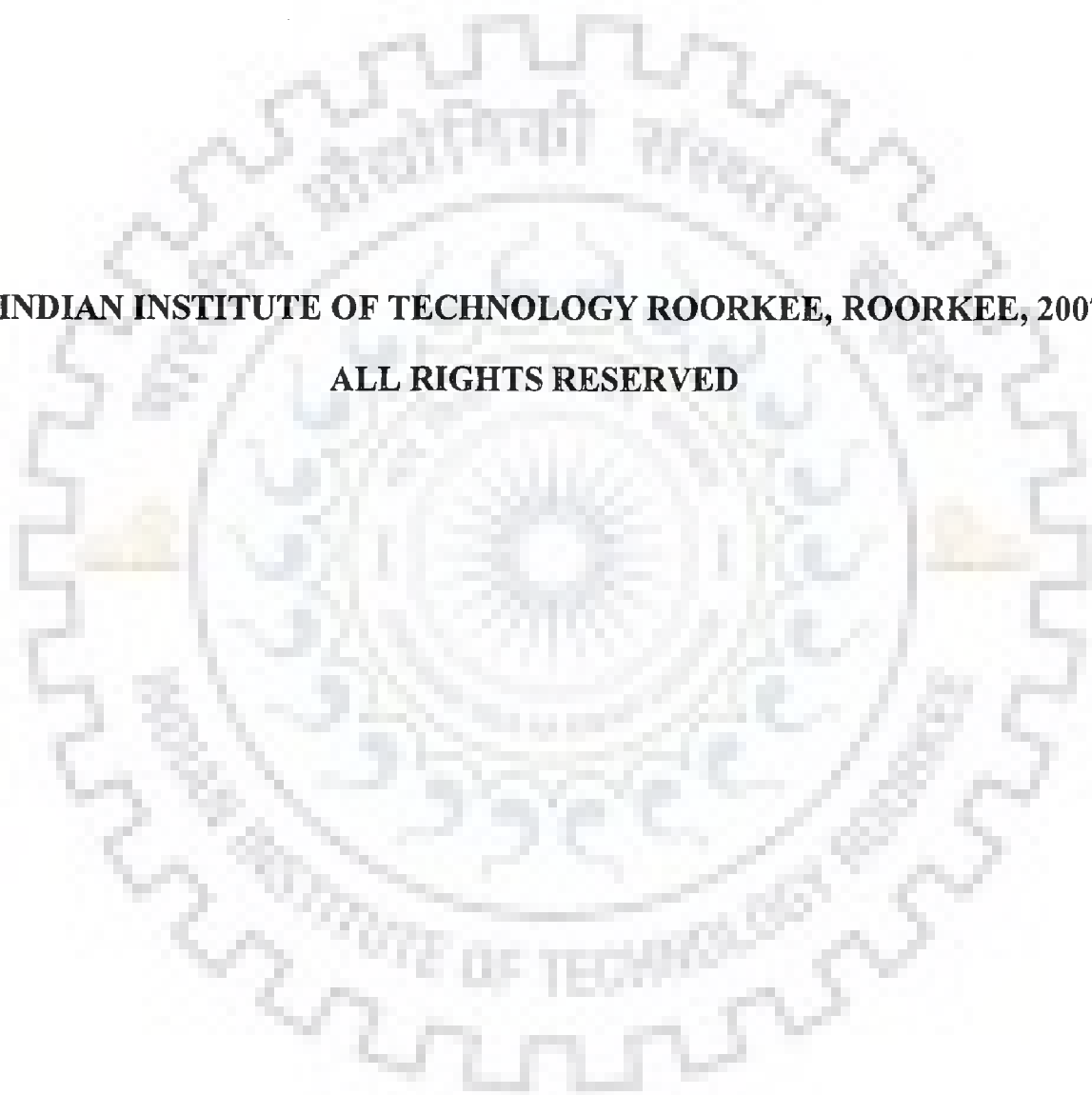
**MUTHUKRISHNAVELLAISAMY. K.**



DEPARTMENT OF WATER RESOURCES DEVELOPMENT & MANAGEMENT  
INDIAN INSTITUTE OF TECHNOLOGY ROORKEE  
ROORKEE-247 667 (INDIA)

JULY, 2007

**© INDIAN INSTITUTE OF TECHNOLOGY ROORKEE, ROORKEE, 2007**  
**ALL RIGHTS RESERVED**





# INDIAN INSTITUTE OF TECHNOLOGY ROORKEE ROORKEE

## CANDIDATE'S DECLARATION

I hereby certify that the work which is being presented in the thesis entitled **A STUDY ON POLLUTANT TRANSPORT IN A STREAM** in the partial fulfilment of the requirements for the award of the Degree of Doctor of Philosophy and submitted in the Department of Water Resources Development and Management of Indian Institute of Technology Roorkee, Roorkee is an authentic record of my own work carried out during a period of January 2003 to July 2007 under the supervision of Dr. G. C. Mishra, Emeritus Fellow, Dr. M. L. Kansal, Associate Professor, Water Resources Development and Management, Indian Institute of Technology Roorkee, Roorkee, and Dr. N C Ghosh, Scientist-F, National Institute of Hydrology, Roorkee.

The matter presented in this thesis has not been submitted by me for the award of any other degree of this or any other institute.

*Muthukrishnavellaisamy*  
(MUTHUKRISHNAVELLAISAMY. K.)

This is to certify that the above statement made by the candidate is correct to the best of our knowledge

Dr. N C Ghosh  
Scientist-F

Date: 9<sup>th</sup> July 2007

*Mansal*  
Dr. M. L. Kansal 9/7/07  
Associate Professor

*G. C. Mishra*  
Dr. G. C. Mishra  
Emeritus Fellow

The Ph.D Viva-Voce Examination of Mr. Muthukrishnavellaisamy. K., Research Scholar, has been held on .....

Signature of Supervisor(s)

Signature of External Examiner

equilibrium sorption of pollutant in each zone of the HCIS model, namely; plug flow and two thoroughly mixed zones of unequal residence time, a semi analytical solution for pollutant transport has been derived using Laplace transform technique. The hybrid cells in series model that incorporates adsorption (HCIS-A) is continuous in time and discrete in space. Response of the HCIS-A model closely matches with the finite difference solution of the differential equation governing advection dispersion and non-equilibrium adsorption.

Most of the pollutants entering to the river system are bio-degradable in nature. Due to this characteristic, the pollutants get decayed while being transported downstream. Considering first order decay at a specific rate, advection and dispersion, using HCIS model, the pollutant transport has been simulated. It is found that the concentration time profile derived from the hybrid cells in series model that incorporates decay (HCIS-D) matches with the analytical solution of advection dispersion decay equation model.

While a non-conservative pollutant enters a water course, depletion of dissolved oxygen (DO) takes place due to the consumption of oxygen by microbes to digest the bio-degradable pollutants. At the same time, depending on the deficit of DO, re-aeration process takes place in a specific rate. Considering, decay of pollutant, re-aeration of oxygen and advection dispersion transport in the HCIS model, an analytical solution has been derived for DO deficit. The response of the hybrid cells in series model that incorporate re-aeration (HCIS-R) closely matches with the numerical solution of Streeter-Phelps dispersion model. The Rinaldi (1979) approach very much over estimates the oxygen deficit.

Using least squares optimization method for a given sets of observed  $C-t$  profile, the pertinent model (HCIS or HCIS-A) can be identified and its parameters can be estimated to simulate the pollutant transport. That model, for which the tracer velocity matches with the mean flow velocity of the river, is the appropriate one.

To demonstrate the flexibility of the hybrid models to incorporate decay and adsorption processes,  $C-t$  profiles have been computed using the filed data of River Prahmani, in Orissa (India). For estimating the HCIS model parameters the longitudinal

dispersion co-efficient ( $D_L$ ) is required. In this study, by employing the regime channel concept to obtain channel geometry and flow characteristics and using Seo and Cheong's (1998) empirical formulae,  $D_L$  has been ascertained. The HCIS-D and HCIS-R models have been used to simulate the concentration of BOD and DO in the river stretch which is under grim of pollutant threat. The maximum concentration at Talcher is about 22.5 mg / L due to continuous discharge of waste at Tikira. It is observed, the BOD concentration in river Brahmani down stream of Rengali dam and prior to the waste disposal site at Tikira is already 12.6 mg / L. Thus, to satisfy the water quality requirement of 3 mg / L as BOD at Talcher, the effluents dumped to river Brahmani between Rengali and Talcher including that at Tikira confluence require prior treatment. The study could be further extended for pollutant-stream-aquifer interaction. Pollutant transport governed by non-linear non-equilibrium adsorption isotherm of pollutant, effect of sediment transport on pollutant transport need to be investigated.



## ACKNOWLEDGEMENT

---

I am immensely grateful to my supervisors Prof. G. C. Mishra, Emeritus Fellow, Dr. M. L. Kansal, Associate Professor, Dept. of WRD & M, IIT Roorkee and Dr. N. C. Ghosh, Scientist-F, National Institute of Hydrology Roorkee for their stipulated guidance, unwavering support and encouragement. This thesis could not have attained its present form, both in content and presentation, without their active interest, direction and guidance. I wish to take a chance to express my wholehearted thanks to Dr. N. C. Ghosh, who has devoted his invaluable time and took personal care in motivating me whenever I was disheartened due to tough in the research.

I wish to thank Prof. S. K. Tripathi, Professor and Head, Department of WRD & M, IIT Roorkee for his help and support throughout the course of my research work. I am thankful to Prof. Nayan Sharma, Professor and Chairman, Departmental Research Committee, for his help and support throughout the course of my PhD work. I also express my sincere thanks to Prof. C. S. P. Ohja, Professor, Department of Civil Engineering, and Dr. D. K. Srivastava, Professor, Department of Hydrology, members, Student Research Committee, for giving their valuable suggestions and words of encouragement.

I express my thanks to Dr. M. Perumal, Associate Professor, Department of Hydrology, members, Student Research Committee, for giving their valuable suggestions and words of encouragement. I also express my sincere thanks to all distinguished faculty and staff members of Department of WRD & M, IIT Roorkee for their suggestions and timely help.

I would like to thank to Er. K. C. Palo, Department of Water Resources, Orissa and Dr. Aman Sharma, WAPCOS, Gurgaon for providing necessary data for this study.

I express my sincere thanks to Prof. Y. B. G. Varma, Retd. Professor, IIT Madras, Chennai, for his encouragement and motivation to carryout the research. I must express my sincere thanks to Mr.Srinivasan, Scientist-C, CBRI, Roorkee, for his support.

I wish to express my thanks to my fellow scholar Mr.K.Saravanan for giving tips to debug the computer programmes. The helps by Mr.P. Purushothaman, Mr. S. Saravanan

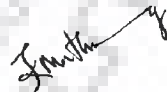
and Mrs. K. Prava Samal require a special mention. I also express my thanks to fellow scholars Mr.Dilip. K. Barrik, Mr. R. Rajinikanth, Mr.Arivazhagan, N, Mr.Felix Regin, A, Mr.Prabakaran.S, Mr.R. Ramsankar, Mr. Srinivasan, Dr. N. Saravanan and all other colleagues for their help and motivation.

Thanks are also due to Mrs. Ruchira Ghosh and Mrs. Goldy Kansal for their support and encouragement during the period of study.

Words can't express my heartfelt thanks to Dr. G. C. Mishra for his consistent support and understanding, special thanks are due to Mrs. Geetanjali Mishra for always encouraging and caring for me. I express my special thanks to them from son hood.

I express my deep gratitude to my Father, Mr. K. Kumarasamy, and Mother, Mrs. K. Dhanalaksmi, for their wholehearted support and sacrifice during the course of this research. I am also thankful to my sisters, Mrs. Vijaya Velumani and Mrs. Rathina, brother in-laws for their direct and indirect support in accomplishing this task with special mention of my sororal nephews, Master. Monish and Master Vedhanth for their encouraging smile and cheerful looks. Thanks are due to my aunty, Mrs. K. Parameswari and uncle, Mr. P. Palanisamy for their words of encouragement.

Above all I express my gratitude from the core of my heart to my family deity for giving courage, strength and patience to carry out my Research work. This thesis could not be successful without Lord's support and direction.

  
(Muthukrishnavellaisamy. K.)



# CONTENTS

	<b>Page No.</b>
<b>CANDIDATE'S DECLARATION</b>	
<b>ABSTRACT</b>	i
<b>ACKNOWLEDGEMENTS</b>	v
<b>CONTENTS</b>	vii
<b>LIST OF TABLES</b>	xiii
<b>LIST OF FIGURES</b>	xv
<b>NOMENCLATURE</b>	xxi
<b>CHAPTER 1 INTRODUCTION</b>	
1.1 INTRODUCTION	1
1.2 OBJECTIVES OF THE STUDY	4
1.3 ORGANIZATION OF THE THESIS	4
<b>CHAPTER 2 REVIEW OF LITERATURE</b>	
2.1 INTRODUCTION	7
2.2 STUDIES BASED ON THE ADE MODEL	10
2.3 MIXING CELLS MODELS	15
2.4 COMPARISON OF THE HCIS MODEL WITH THE CIS, ADZ AND ADE MODELS	18
2.5 ADSORPTION/DESORPTION PROCESSES	20
2.6 REACTIVE POLLUTANTS TRANSPORT	24
2.7 CONCLUSIONS	26
<b>CHAPTER 3 TRANSPORT OF CONSERVATIVE POLLUTANTS CONSIDERING NON- EQUILIBRIUM SORPTION</b>	
3.1 INTRODUCTION	29
3.2 STATEMENT OF THE PROBLEM	30

3.3	FORMULATION OF MODEL	31
3.3.1	Derivation of Concentration of Pollutant in the Plug Flow Zone	31
3.3.2	Unit Step Response Function for the First Thoroughly Mixing Zone	39
3.3.3	Unit Step Response Function for the Second Thoroughly Mixing Zone	44
3.3.4	Derivation of Concentration of Pollutant by Discrete Kernel Approach	45
3.4	COMPARISON OF HCIS-A MODEL WITH THE ADE MODEL CONSIDERING NON- EQUILIBRIUM FREUNDLICH ADSORPTION ISOTHERM	47
3.5	RESULTS AND DISCUSSION	51
3.5	CONCLUSIONS	61
<b>CHAPTER 4</b>	<b>POLLUTANTS TRANSPORT WITH FIRST ORDER REACTION KINETICS</b>	
4.1	INTRODUCTION	63
4.2	STATEMENT OF THE PROBLEM	63
4.3	FORMULATION OF MODEL	64
4.3.1	Derivation of Concentration of Pollutant in the Plug Flow Zone	64
4.3.2	Derivation of Concentration of Pollutant in the First Thoroughly Mixing Zone	65
4.3.3	Derivation of Concentration of Pollutant in the Second Thoroughly Mixed Zone	68
4.4	ESTIMATION OF CONCENTRATION OF POLLUTANT USING CONVOLUTION	70

	TECHNIQUE	
4.5	RESULTS AND DISCUSSION	71
4.6	CONCLUSIONS	75
<b>CHAPTER 5</b>	<b>POLLUTANT TRANSPORT WITH</b>	
	<b>DE-OXYGENATION AND RE-AERATION</b>	
5.1	INTRODUCTION	77
5.2	STATEMENT OF THE PROBLEM	78
5.3	FORMULATION OF MODEL	79
5.3.1	Derivation of DO Concentration in the Plug Flow Zone	79
5.3.2	Derivation of DO Concentration in the First Thoroughly Mixed Zone	82
5.3.3	Derivation of DO Concentration in the Second Thoroughly Mixed Zone	85
5.4	DERIVATION OF DO DEFICIT AT SECOND AND SUBSEQUENT HYBRID UNITS	93
5.5	COMPARISON OF HCIS-R MODEL WITH STREETER-PHELPS DISPERSION MODEL	95
5.6	RESULTS AND DISCUSSION	99
5.7	CONCLUSIONS	105
<b>CHAPTER 6</b>	<b>PARAMETER ESTIMATION OF HYBRID</b>	
	<b>MODELS</b>	
6.1	INTRODUCTION	107
6.2	LEAST SQUARES OPTIMIZATION	108
6.2.1	The HCIS Model	109
6.2.2	The HCIS Model with Adsorption (HCIS-A)	110
6.3	OBSERVED DATA	112
6.4	SELECTION OF APPROPRIATE MODEL	114

6.5	RESULTS AND DISCUSSION	117
6.6	CONCLUSIONS	120
<b>CHAPTER 7</b>	<b>PERFORMANCE EVALUATION OF HYBRID MODELS USING FIELD DATA</b>	
7.1	INTRODUCTION AND STUDY AREA DESCRIPTION	121
7.2	DATA REQUIREMENT	122
7.3	FLOW DATA AND ROUTING	122
7.4	PARTICLE SIZE ANALYSIS FOR THE BED MATERIALS OF RIVER BRAHMANI AND SILT FACTOR	127
7.5	REGIME CHANNEL CONCEPT	128
7.6	DETERMINATION OF LONGITUDINAL DISPERSION CO-EFFICIENT	129
7.7	RIVER REACH DISCRETIZATION AND PARAMETER ESTIMATION	130
7.8	POLLUTION DATA	130
7.9	SIMULATION OF BOD	131
7.10	SIMULATION OF DO	139
7.11	CONCLUSIONS	144
<b>CHAPTER 8</b>	<b>CONCLUSIONS</b>	
8.1	GENERAL	147
8.2	CONCLUSIONS FROM PRESENT STUDY	147
8.3	SCOPE OF FUTURE STUDY	150
<b>REFERENCES</b>		151

<b>APPENDICES:</b>	<b>APPENDIX A (Ref. Chapter 2)</b>	
A1.	The HCIS Model	167
	<b>APPENDIX B (Ref. Chapter 3)</b>	
B1.	Formulation of Equation for Pollutant Transport in Plug Flow Zone	171
	<b>APPENDIX C (Ref. Chapter 6)</b>	
C1.	The HCIS Model	173
C2.	The HCIS Model with Adsorption	174
	<b>APPENDIX D (Ref. Chapter 6)</b>	
	<b>ESTIMATION OF STREAM WATER QUALITY PARAMETER USING REGIME CHANNEL THEORY</b>	
D1.	GENERAL	177
D2.	EMPIRICAL METHODS	177
D3.	REGIME CHANNEL CONCEPT	178
	<b>APPENDIX E (Ref. Chapter 7)</b>	
E1.	MUSKINGUM-CUNGE METHOD	181



## LIST OF TABLES

Table No	Title	Page No
2.1	Methods suggested by investigators for estimation of $D_L$	13
6.1	Comparison of the estimated parameters with the true parameters ( $\alpha = 1.7m$ in, $T_1 = 2.3$ min, $T_2 = 6.0$ min) for different % of $S_d$ for HCIS model	113
6.2	Comparison of the estimated parameters with the true parameters ( $\alpha = 1.7m$ in, $T_1 = 2.3$ min, $T_2 = 6.0$ min, $R_D = 0.1$ per min) for different % of $S_d$ for HCIS-A model	113
7.1	Average flow rates at various sections of River Brahmani	127
7.2	Channel geometry estimation corresponding to average flow rate (Non-monsoon) and silt factor	128
7.3	Channel geometry estimation corresponding to average flow rate (Monsoon) and silt factor	128
7.4	Estimated longitudinal dispersion co-efficient during non-monsoon period	129
7.5	Estimated longitudinal dispersion co-efficient during monsoon period	129
7.6	Water quality data in river Brahmani	130
7.7	Water quality data in river Tikira	131
7.8	Parameters estimated corresponding to the low and high flow rates of river Brahmani	141





## LIST OF FIGURES

Figure No	Title	Page No
2.1	The first process unit of the HCIS model	17
2.2	Comparison of concentration-time distribution profiles generated by different models for a unit impulse input; each distribution represents same residence time = 10 min.	19
2.3	Comparison of concentration-time distribution profiles generated by different models for a unit impulse input; each distribution represents same residence time = 10 min.	20
3.1	Conceptualized unit of Hybrid Cells in Series Model incorporating adsorption	31
3.2	Pollutant transport through plug flow zone for a unit step input.	31
3.3	Exclusive pollutant transport through 1 <sup>st</sup> thoroughly mixed zone for a unit step input.	40
3.4	Exclusive pollutant transport through 2 <sup>nd</sup> thoroughly mixed zone for a unit step input.	45
3.5	Composed series of hybrid units representing a stream reach of $n \Delta x$ length.	47
3.6	Impulse response functions of HCIS-A model and numerical solution of Eq. (3.67) at $x = 200$ m	50
3.7	Concentration – time profile at the end of the plug flow zone (34 m) for different values of $R_D$ and $\alpha = 1.7$ min; $u = 20$ m / min; $\frac{\phi W_p D_B}{A} = 0.1$	54
3.8	Concentration – time distribution in water and soil column at the end of the plug flow zone (34 m) for $R_D = 0.25$ per min and $\alpha = 1.7$ min; $u = 20$ m / min; $\frac{\phi W_p D_B}{A} = 0.1$	54
3.9	Spatial distribution of effluent concentration in the plug flow zone for different values of $R_D$ (=0.0, 0.1 and 0.25 per min) and $\alpha = 1.7$ min; $u = 20$ m / min; $\frac{\phi W_p D_B}{A} = 0.1$	55

3.10	Unit step response function of a thoroughly mixed zone for different values of $R_D$ and residence time is 2.3 min; $u = 20$ m / min; $\frac{\phi W_P D_B}{A} = 0.5$	55
3.11	Unit step response function of a thoroughly mixed zone for different values of residence time ( $T$ ), for $R_D = 0.1$ per min; $u = 20$ m / min; $\frac{\phi W_P D_B}{A} = 0.5$	56
3.12	Unit step responses of HCIS-A model for Adsorption rate $R_D = 0, 0.1$ and $1.0$ per min; $\alpha = 1.7$ min, $T_1 = 2.3$ min, $T_2 = 6.0$ min and Porosity $\phi = 0.2$	57
3.13	Unit pulse responses of HCIS-A model for Adsorption rate $R_D = 0, 0.1$ and $1.0$ per min; $\alpha = 1.7$ min, $T_1 = 2.3$ min, $T_2 = 6.0$ min and Porosity $\phi = 0.2$	57
3.14	Step responses of the ADE model ( $u = 20$ m/ min; $D_L = 1000$ m <sup>2</sup> /min) and the HCIS model in absence of adsorption for $\alpha = 1.7$ min, $T_1 = 2.3$ min, $T_2 = 6.0$ min.	58
3.15	Unit pulse responses of the ADE model ( $u = 20$ m/ min; $D_L = 1000$ m <sup>2</sup> /min) and the HCIS model in absence of adsorption for $\alpha = 1.7$ min, $T_1 = 2.3$ min, $T_2 = 6.0$ min	58
3.16	Unit pulse responses of the HCIS-A model, with adsorption rate co-efficient, $R_D = 0.0$ and $0.1$ per min, at the end of first ( $n = 1$ ), second ( $n = 2$ ), fifth ( $n = 5$ ) and tenth ( $n = 10$ ) hybrid units for $\alpha = 1.7$ min, $T_1 = 2.3$ min, $T_2 = 6.0$ min, $u = 20$ m/min and $\Delta x = 200$ m.	59
3.17	Unit pulse responses of the HCIS-A model for different values of porosity	60
3.18	Variation of Peak concentration with porosity at the end of 1 <sup>st</sup> and 5 <sup>th</sup> hybrid units for $\alpha = 1.7$ min, $T_1 = 2.3$ min, $T_2 = 6.0$ min, $W_P = 10$ m, $D_B = 1$ m, $A = 20$ m <sup>2</sup> and size of one hybrid unit, $\Delta x = 200$ m corresponding to $P_e = 4$ , $u = 20$ m/min, $D_L = 1000$ m <sup>2</sup> /min	60
4.1	Conceptualized unit of Hybrid Cells in Series Model	64
4.2	Pollutant transport through plug flow zone for a unit step input	64
4.3	Pollutant transport through 1 <sup>st</sup> thoroughly mixed zone	66
4.4	Pollutant transport through 2 <sup>nd</sup> thoroughly mixed zone	68
4.5	Composed series of hybrid units representing a stream reach of $n\Delta x$ length	70
4.6	Unit pulse responses of ADDE model ( $u = 20$ m/ min; $D_L = 1000$ m <sup>2</sup> / min and at 200 m) and HCIS-D model ( $\alpha = 1.7$ min; $T_1 = 2.3$ min; $T_2 = 6.0$ min; $\Delta x = 200$ m) for decay rate co-efficient, $k_1 = 0.0$ and $0.1$ per min.	72

4.7	Unit step responses of the HCIS-D model, with decay rate coefficient, $k_f = 0.0$ and $0.1$ per min, at the end of first ( $n = 1$ ), second ( $n = 2$ ), fourth ( $n = 4$ ) and fifth ( $n = 5$ ) hybrid units for $\alpha = 1.7$ min, $T_1 = 2.3$ min, $T_2 = 6.0$ min, $u = 20$ m / min and $\Delta x = 200$ m	73
4.8	Unit pulse responses of the HCIS-D model, with decay rate coefficient, $k_f = 0.0$ and $0.1$ per min, at the end of first ( $n = 1$ ), second ( $n = 2$ ), fourth ( $n = 4$ ) and fifth ( $n = 5$ ) hybrid units for $\alpha = 1.7$ min, $T_1 = 2.3$ min, $T_2 = 6.0$ min, $u = 20$ m / min and $\Delta x = 200$ m	74
4.9	Variation of Peak concentration with number of hybrid units, $n$ for different values of decay rate co-efficient, $k_f$ ( $0.0, 0.05, 0.1$ and $0.25$ per min) for $\alpha = 1.7$ min, $T_1 = 2.3$ min, $T_2 = 6.0$ min, $W_p = 10$ m, $D_B = 1$ m, $A = 20$ m <sup>2</sup> and $\Delta x = 200$ m corresponding to $P_e = 4$ , $u = 20$ m/min, $D_L = 000$ m <sup>2</sup> /min	75
5.1	Conceptual hybrid unit to represent the transport, decay and re-aeration processes.	78
5.2	Impulse responses of HCIS-R model, Numerical solution of BOD-DO Equation with dispersion (Eq. 2.19), approximate Streeter-Phelps model with dispersion (approximated from Eq. 2.19)	98
6.1	Flow chart showing the procedure to select an appropriate model and estimation of its parameters to simulate given observed data (C-t profile)	116
6.2	Observed and Computed C-t profiles by HCIS ( $\alpha = 1.704$ min, $T_1 = 2.272$ min, $T_2 = 6.03$ min) and HCIS-A ( $\alpha = 1.671$ min, $T_1 = 2.918$ min, $T_2 = 4.428$ min, $R_D = 0.266$ per min) models with estimated parameters at $x = 1000$ m and $2000$ m down stream.	119
6.3	Observed and Computed C-t profiles by HCIS ( $\alpha = 1.724$ min, $T_1 = 1.882$ min, $T_2 = 7.012$ min) and HCIS-A ( $\alpha = 1.704$ min, $T_1 = 2.27$ min, $T_2 = 6.01$ min, $R_D = 0.103$ per min) models with estimated parameters at $x = 1000$ m and $2000$ m down stream.	119
7.1	Location map showing River Brahmani and its tributary Tikira (Digitized from Google Earth)	123
7.2	Computed Flow Rate of River Brahmani and Tikira at specific locations	124
7.3	Flow hydrograph with out and with correction at a location after Tikira	125
7.4	Observed and computed flow rates before correction at Talcher	125
7.5	Observed and computed flow rates after correction at Talcher	126
7.6	Seasonal average computed flow rate at Talcher	126
7.7	Grain size distribution curve of bed sediment samples collected from Brahmani	127

7.8	Impulse response functions of HCIS-D and ADDE models at 3.857 km from Tikira confluence for $Q = 239.17 \text{ m}^3 / \text{s}$ , $C_R = 24.03 \text{ mg} / \text{L}$ ; $u = 55.65 \text{ m} / \text{min}$ $D_L = 29359.92 \text{ m}^2 / \text{min}$ , $\Delta x = 3857 \text{ m}$ , $\alpha = 20.267 \text{ min}$ ; $T_1 = 25.335 \text{ min}$ ; $T_2 = 23.706 \text{ min}$ and $k_1 = 0.23 \text{ per day}$	132
7.9	Impulse response functions of HCIS-D model at different locations from Tikira confluence for $C_R = 24.03 \text{ mg} / \text{L}$ , $k_1 = 0.23 \text{ per day}$ , $Q = 239.17 \text{ m}^3 / \text{s}$ , $\alpha = 20.267 \text{ min}$ ; $T_1 = 25.335 \text{ min}$ and $T_2 = 23.706 \text{ min}$ , $u = 55.65 \text{ m} / \text{min}$ and $\Delta x = 3857 \text{ m}$ .	133
7.10	Step response functions of HCIS-D model at different locations for $C_R = 24.03 \text{ mg} / \text{L}$ , $k_1 = 0.23 \text{ per day}$ , $Q = 239.17 \text{ m}^3 / \text{s}$ , $\alpha = 20.267 \text{ min}$ ; $T_1 = 25.335 \text{ min}$ and $T_2 = 23.706 \text{ min}$ .	134
7.11	Impulse response functions of HCIS-D model at different locations from Tikira confluence for $C_R = 43.61 \text{ mg} / \text{L}$ , $k_1 = 0.23 \text{ per day}$ for flow rate, $Q = 79.72 \text{ m}^3 / \text{s}$ and corresponding parameters: $\alpha = 16.53 \text{ min}$ ; $T_1 = 20.657 \text{ min}$ , $T_2 = 15.687 \text{ min}$ , $u = 46.34 \text{ m} / \text{min}$ and $\Delta x = 2450 \text{ m}$	135
7.12	Step response functions of HCIS-D model at different locations from Tikira confluence for $C_R = 43.61 \text{ mg} / \text{L}$ , $k_1 = 0.23 \text{ per day}$ for flow rate, $Q = 79.72 \text{ m}^3 / \text{s}$ and corresponding parameters: $\alpha = 16.53 \text{ min}$ ; $T_1 = 20.657 \text{ min}$ , $T_2 = 15.687 \text{ min}$ $u = 46.34 \text{ m} / \text{min}$ and $\Delta x = 2450 \text{ m}$	136
7.13	Impulse response functions of HCIS-D model at different locations from Tikira confluence for $C_R = 15.13 \text{ mg} / \text{L}$ , $k_1 = 0.23 \text{ per day}$ for flow rate, $Q = 1127.84 \text{ m}^3 / \text{s}$ and corresponding parameters: $\alpha = 22.99 \text{ min}$ ; $T_1 = 28.74 \text{ min}$ , $T_2 = 41.92 \text{ min}$ , $u = 72.07 \text{ m} / \text{min}$ and $\Delta x = 6750 \text{ m}$ .	137
7.14	Step response functions of HCIS-D model at different locations from Tikira confluence for $C_R = 15.13 \text{ mg} / \text{L}$ , $k_1 = 0.23 \text{ per day}$ for flow rate, $Q = 1127.84 \text{ m}^3 / \text{s}$ and corresponding parameters: $\alpha = 22.99 \text{ min}$ ; $T_1 = 28.74 \text{ min}$ , $T_2 = 41.92 \text{ min}$ , $u = 72.07 \text{ m} / \text{min}$ and $\Delta x = 6750 \text{ m}$	138
7.15	Unit step response functions for different values of $k_1$ during lean flow ( $Q = 239.17 \text{ m}^3 / \text{s}$ )	139
7.16	Impulse response functions of HCIS-R model at different locations from Tikira confluence for $C_R = 24.03 \text{ mg} / \text{L}$ , boundary deficit, $D_0 = 1.76 \text{ mg} / \text{L}$ , $k_1 = 0.23 \text{ per day}$ , $k_2 = 4 \text{ per day}$ , $Q = 239.17 \text{ m}^3 / \text{s}$ , $\alpha = 20.267 \text{ min}$ ; $T_1 = 25.335 \text{ min}$ , $T_2 = 23.706 \text{ min}$ , $u = 55.65 \text{ m} / \text{min}$ and $\Delta x = 3857 \text{ m}$	140
7.17	Step response function of HCIS-R model at Talcher for $C_R = 24.03 \text{ mg} / \text{L}$ , boundary deficit, $D_0 = 1.76 \text{ mg} / \text{L}$ , $k_1 = 0.23 \text{ per day}$ , $k_2 = 4 \text{ per day}$ , $Q = 239.17 \text{ m}^3 / \text{s}$ , $\alpha = 20.267 \text{ min}$ ; $T_1 = 25.335 \text{ min}$ , $T_2 = 23.706 \text{ min}$ , $u = 55.65 \text{ m} / \text{min}$ and $\Delta x = 3857 \text{ m}$ .	141

7.18	Impulse response functions of HCIS-R model at different locations from Tikira confluence for $C_R = 43.61$ mg / L, boundary deficit, $D_0 = 2.4$ mg / L, $k_1 = 0.23$ per day, $k_2 = 4$ per day, $Q = 79.72$ m <sup>3</sup> / s, $\alpha = 16.53$ min; $T_1 = 20.657$ min, $T_2 = 15.687$ min, $u = 46.34$ m / min and $\Delta x = 2450$ m	142
7.19	Step response function of HCIS-R model at Talcher for $C_R = 43.61$ mg / L, boundary deficit, $D_0 = 2.4$ mg / L, $k_1 = 0.23$ per day, $k_2 = 4$ per day, $Q = 79.72$ m <sup>3</sup> / s, $\alpha = 16.53$ min; $T_1 = 20.657$ min, $T_2 = 15.687$ min, $u = 46.34$ m / min and $\Delta x = 2450$ m	143
7.20	Impulse response functions of HCIS-R model at different locations from Tikira confluence for $C_R = 15.13$ mg / L, boundary deficit, $D_0 = 1.48$ mg / L, $k_1 = 0.23$ per day, $k_2 = 4$ per day, $Q = 1127.84$ m <sup>3</sup> / s, $\alpha = 22.99$ min; $T_1 = 28.74$ min, $T_2 = 41.92$ min, $u = 72.07$ m / min and $\Delta x = 6750$ m	143
7.21	Step response function of HCIS-R model at Talcher for $C_R = 15.13$ mg / L, boundary deficit, $D_0 = 1.48$ mg / L, $k_1 = 0.23$ per day, $k_2 = 4$ per day, $Q = 1127.84$ m <sup>3</sup> / s, $\alpha = 22.99$ min; $T_1 = 28.74$ min, $T_2 = 41.92$ min, $u = 72.07$ m / min and $\Delta x = 6750$ m.	144
A1	The first process unit of the HCIS model	167
A2	A Hybrid-cells-in-series Model ( $\alpha$ = time to replace fluid in the plug flow zone, $T_1$ and $T_2$ = residence times of solute in the 1 <sup>st</sup> and 2 <sup>nd</sup> thoroughly mixed reservoirs respectively, $\Delta x$ = size of one unit of the hybrid model)	169
B1	A control volume within the plug flow zone, considered for mass balance	171
D1	Variation of $D_L/H U_*$ versus $W/H$ ; Using empirical formulae suggested by various investigators for estimation of $D_L$ in natural streams	180
E1	Space-Time discretization of kinematic wave equation paralleling Muskingum method	181





## NOMENCLATURE

$\alpha$	Residence time of plug flow zone
$\delta (.)$	Dirac delta function
$\varepsilon$	Least square error
$\phi$	porosity
$\Delta x$	Space step
$\Delta R_D$	Increment of $R_D$
$\Delta t$	Time step
$\Delta T_1$	Increment of $T_1$
$\Delta T_2$	Increment of $T_2$
$\Delta \alpha$	Increment of $\alpha$
$A$	cross-sectional area of flow
$a (l, t)$	Auxiliary variable
$A_s$	Storage zone area
$C$	solute concentration
$C(x, t)$	solute concentration in $x$ and $t$
$C^*$	Laplace transform of $C$
$C_{DO}$	Dissolved oxygen concentration
$C_i$	Initial concentration
$C_L$	Lateral concentration input
$C_P(\alpha u, t)$	Concentration of pollutant at the end of plug flow zone
$C_R$	Boundary concentration
$C_s(x, t)$	Adsorbed concentration in $x$ and $t$
$C_s^*$	Laplace transform of $C_s$
$C-t$	Concentration - time
$D^*$	Laplace transform deficit, $D$
$D_0$	Boundary deficit
$D_L$	longitudinal dispersion co-efficient
DO	Dissolved Oxygen
$erf (.)$	error function
$erfc (.)$	complimentary error function
$f_L$	silt factor

$H$	Depth of flow
$I_1$	Modified Bessel function of first kind
$J(*, *)$	J - function
$k_1$	Decay rate co-efficient
$k_2$	Re-aeration rate co-efficient
$k_C$	Computed concentration
$K_{D-CR U}(t)$	unit step response function of deficit with respect to $C_R$
$k_{D-CR U}(t)$	unit impulse response function of deficit with respect to $C_R$
$K_{D-D_0}(t)$	unit step response function of deficit with respect to $D_0$
$k_{D-D_0 U}(t)$	unit impulse response function of deficit with respect to $D_0$
$K_{HCIS-A}$	unit step response function of hybrid model with adsorption
$k_{HCIS-A}$	unit impulse response function of hybrid model with adsorption
$K_{HCIS-D}$	unit step response function of hybrid model with decay
$k_{HCIS-D}$	unit impulse response function of hybrid model with decay
$K_{HCIS-R}$	unit step response function of hybrid model with re-aeration
$k_{HCIS-R}$	unit impulse response function of hybrid model with re-aeration
$M$	mass injected
$M_1$	First moment
$M_2$	Second moment
$M_r$	$r^{\text{th}}$ moment
$M_s$	Mass adsorbed
$n$	Number (cell number)
$P_e$	Peclet number
$Q$	flow rate
$q_0$	Reference discharge per unit width of the flow
$R$ or $R_h$	Hydraulic radius
$R_D$	Adsorption rate co-efficient
$S$	Slope
$s$	Laplace domain variable
$S_d$	Standard deviation
$S_{DO}$	Saturated DO
$t$	time
$T_1$	Residence time of 1 <sup>st</sup> mixed zone



$T_2$	Residence time of 1 <sup>st</sup> mixed zone
$t_P$	Time to peak
$u$ or $\bar{u}$	mean flow velocity
$\hat{u}$	Tracer velocity
$U(.)$	Step function
$U_*$	Shear flow velocity
$W$	Width of the channel
$W_P$	Wetted perimeter of the channel
$x$	distance
$X$	Weighting factor of muskingum-cunge method



# CHAPTER 1

## INTRODUCTION

---

### 1.1 INTRODUCTION

Streams are the major source to meet the domestic, industrial and agricultural water needs. Due to urbanization and industrialization, the quantum of pollutants load to the streams has increased many folds. This has resulted in the worsening of stream water quality, as the assimilation capacity of the streams is inadequate. Consequently, it endangers the associated ecosystem of the streams. In order to control the stream water pollution, it is essential to know the rate at which the streams are capable to disperse the pollutants it receives. Also, it is imperative to be acquainted with the knowledge of pollutants transport for the determination of its concentration along the stream courses and for regulating the pollutants disposal to the streams.

Pollutants originating from domestic, industrial and agricultural sectors can be grouped into two categories, such as; conservative and non-conservative. Conservative pollutants are those which do not degrade in the receiving water; however, they may change form or their media association. Non-conservative pollutants are those which degrade in the receiving water. Some of the important water quality constituents and indices of pollution are: Temperature, Biochemical Oxygen Demand (BOD), Dissolved Oxygen (DO), Total Dissolved Solids (TDS) and Chlorides. Out of these, Temperature, TDS and Chloride are conservative in nature and temperature is a catalyst of kinetics of non-conservative pollutants like BOD and DO. Pollution problem in streams could be due to the transport of both conservative and non-conservative pollutants. When a pollutant mass is injected into a stream, the concentrated pollutant mass is advected by the flowing water and at the same time the pollutants domain spreads in all directions under the action of turbulent diffusion leading to an almost uniform concentration over the whole cross section of the stream. During the pollutant's transport, some fractions of the pollutant are

sorbed from the stream water by the stream bed soils and sediments. The reverse process takes place while the concentration of pollutant in stream water is less than that in bed sediments. These processes are known as adsorption and desorption respectively. Sorptive exchange of the pollutants is non-equilibrium in nature because of the complication of these sorption processes and it assumes that the equilibrium is not reached instantaneously. If the injected pollutant is of non-conservative type, degradation of pollutants takes place along with these processes.

Waste water treatment and disposal for controlling the environmental pollution requires accurate prediction of pollutant transport. Pollutant transport processes are basically three-dimensional: However, it has been described by many researchers (Fischer, 1967, 1968; Sayre, 1968; Chatwin, 1970, 1971; Holley and Tasi, 1977) that in a stream away from the source, pollutants' transport can adequately be described by a one-dimensional process along the longitudinal direction.

There are several methods of solving pollutant transport models, e.g. finite difference, analytical and hybrid methods. The finite difference methods give second order accurate results. The advection dispersion equation (ADE) model is a well known model for solving solute transport problems. But ADE model has limitations in practical applications (Young & Wallis, 1993; Fischer, 1967; 1968; Thackston & Krenkel, 1967; Sooky, 1969; Day & Wood, 1969; Fischer et al., 1979; Chatwin, 1980; Chatwin & Allen, 1985; Van Genuchten & Jury, 1987). Cells-in-Series (CIS) model (Bear, 1972; Banks, 1974; Vander Molen, 1979; Beltaos, 1980; Van Ommen, 1985; Stefan & Demetropoulos, 1981; Yurtsever, 1983; Beven & Young, 1988; Young & Wallis, 1993; Wang & Chen, 1996) could be an alternative method to the ADE model to simulate the solute transport. However, due to the limitations, CIS model restricts its usefulness to the solute transport in rivers to simulate the longitudinal dispersion (Stefan & Demetropoulos, 1981; Rutherford, 1994; Ghosh, 2001; Ghosh et al., 2004). Aggregated Dead Zone (ADZ) model (Beer & Young, 1983) incorporates advective time delay to the dead zone approach and brought improvement in the simulation of solute transport.

However, there exist a practical difficulty in identifying and estimating the model coefficients (Rutherford, 1994)

The limitations of CIS and ADZ models have been tackled by using conceptualized hybrid cells in series (HCIS) model (Ghosh, 2001; Ghosh, et al., 2004). One hybrid unit of this HCIS model consists of a plug flow zone of residence time  $\alpha$  and two thoroughly mixed zones of unequal residence times  $T_1$  and  $T_2$  and all these zones are connected in series. This HCIS model has been conceptualized to simulate the advection and dispersion of the solute. As HCIS model has been shown most promising to simulate solute transport in streams, it has been considered as a base of the present study. Simulating non-equilibrium sorption isotherm processes along with advection and dispersion is a difficult task due to the complexity of the adsorption and desorption processes (Cameron and Klute, 1977). Assuming simplified non-equilibrium adsorption isotherm in HCIS model, Ghosh (2001) numerically estimated the solute concentration in a river. In the present study, the simplified non-equilibrium Freundlich adsorption isotherm has been considered to estimate the pollutants concentration in all zones of the HCIS model. Using Laplace transform technique, an attempt has been made to find an analytical solution of non-equilibrium sorption for A-D pollutants transport in a stream.

In order to estimate the model parameters, it is required to know the values of flow velocity ( $u$ ) and dispersion coefficient ( $D_L$ ). Flow velocity ( $u$ ) can be estimated by using a straightforward approach; however, a unique method for estimation of dispersion coefficient ( $D_L$ ) is yet to be derived. There are number of theoretical, experimental and empirical formulae available for estimation of  $D_L$ . Most of the empirical formulae depict that  $D_L$  is a function of stream's geometry and flow characteristics, which eventually inform that if hydraulic geometry of a stream downstream of pollution source for a given flow condition is known *a priori*, one can reasonably estimate the value of  $D_L$  using a suitable empirical formula. If only flow rate ( $Q$ ) is known, using regime channel concepts, the hydraulic geometry of a stream can be determined. The regime channel concept dictates that the stream geometry is the function of silt factor ( $f_L$ ) and the flow rate ( $Q$ ). The silt factor and flow rate vary in space and time and to change the stream geometry accordingly.

Having estimated velocity, and  $D_L$ , using convolution technique or numerical methods, one can predict/forecast the possible threat expected to the downstream. For changing velocity, which is normally caused due to non-uniform flow,  $D_L$  will also change. The transport of pollutant in a non-uniform flow condition is also an important aspect of pollutant transport.

The present study also deals with pollutants of non-conservative type. The organic substances of non-conservative type usually cause serious damage to the aquatic life supported by a stream by increasing BOD load and decreasing the DO concentration. A stream has a limiting self-cleansing capacity of organic substances; which depends upon flow rate and the stream's geometry besides the constituent kinetic and some meteorological variables. For a given load of organic substances in a stream, the first order reaction kinetic has been coupled with advection and dispersion in HCIS model to predict the pollutant transport. In order to explain the proposed philosophy, a case study of Brahmani River in India has been considered. The methodology has been applied and philosophy has been validated by verifying the results in a particular reach of this river.

## **1.2 OBJECTIVES OF THE STUDY**

The research work envisaged in the present dissertation, is:

1. Investigation of adsorption of the pollutants by the streambed material for conservative pollutants.
2. Investigation of decay of pollutants for non-conservative pollutants.
3. Investigation of a method to estimate  $D_L$ , knowing stream flow only using the concept of regime channel, and to estimate  $D_L$  for non-uniform flow conditions.

## **1.3 ORGANIZATION OF THE THESIS**

The thesis has been organized into the following chapters:

### *Chapter 1: Introduction*

This chapter covers the general introduction and the importance of pollutant transport in streams.

## *Chapter 2: Literature Review*

This chapter covers the critical review of the previous investigations on transport of conservative and non-conservative solutes. The review is focused on advection dispersion equation (ADE) model, cells-in-series (CIS) model, aggregated dead zone (ADZ) model, transient storage (TS) model and hybrid cells in series (HCIS) model and longitudinal dispersion co-efficient ( $D_L$ ).

## *Chapter 3: Transport of conservative pollutants considering non-equilibrium sorption*

This chapter elucidates the model formulation for the problem of conservative pollutants, which undergo sorption. HCIS-A model has been conceptualized to simulate advection, dispersion and adsorption of pollutants in all the zones (Plug flow zone and two thoroughly mixed zones of unequal residence time) and represented in terms of differential equations. Laplace transform technique has been used to solve the differential equations. Also, characteristics of the  $C-t$  profiles for a conservative pollutant in a stream with adsorbing stream bed and soil sediments are demonstrated.

## *Chapter 4: Pollutants transport with first order reaction kinetics*

This chapter explains the formulation of the model and mathematical solution for the Non-conservative pollutants, which undergo decay. HCIS-D model has been conceptualized to simulate advection, dispersion and first order decay of pollutants in all the zones. The governing differential equations have been solved by using Laplace transform technique.

## *Chapter 5: Pollutant transport with de-oxygenation and re-aeration*

This chapter discusses the problem of non-conservative pollutants transport in a stream for deoxygenation – reaeration. HCIS-R model has been conceptualized to simulate advection, dispersion, deoxygenation and reaeration. Adopting concept of DO deficit, the problem has been solved by using Laplace transform technique.

### *Chapter 6: Parameter estimation of hybrid models*

This chapter deals with the estimation of parameters of HCIS model. The three model parameters ( $\alpha$ ,  $T_1$  and  $T_2$ ) and adsorption rate constant ( $R_D$ ) have been estimated by Least Squares Optimization method using synthetic observed data with 0%, 5%, 10% and 20% random errors.

This Chapter also discusses the usage of regime channel concept to estimate the channel geometry and flow characteristics from flow rate and silt factor only. The estimated channel geometry and flow characteristics are further used to estimate the longitudinal dispersion Co-efficient.

### *Chapter 7: Performance evaluation of hybrid models using field data*

This chapter examines the performance of the HCIS model by comparing the results with observed values in the field. The flexibility and advantage of HCIS model to simulate the pollutants transport has been demonstrated with the field data as a case study for Brahmani River, in Orissa, India.

### *Chapter 8: Conclusions.*

This chapter highlights the key findings of the investigation and the conclusions. Also, it briefs the specific contributions of the present study and the scope of future work.



## CHAPTER 2

### LITERATURE REVIEW

---

#### 2.1 INTRODUCTION

The solute transport process in a stream or river depends upon the mixing mechanisms as well as physical, chemical and biological properties of the contaminant. But this process is caused primarily by the interaction of two basic phenomena – differential advection and cross-sectional diffusion. Adolph Fick in 1855 developed the analogy between the molecular diffusion and the heat transfer by conduction using the Fourier's law of heat flow. Based on the diffusion laws given by Fick, Sir G. I. Taylor in 1921 first studied the theory of diffusion for fluid with uniform velocity and established the concept of diffusion by continuous movements. Later on, Taylor (1953, 1954) described the mechanism of dispersion both for laminar and turbulent flow conditions.

The mixing process in moving fluid is described by two basic phenomena; advection and diffusion. Advection is the bodily movement of fluid particles resulting from an imposed current. The scattering of the fluid particles by turbulent motion on a microscopic scale due to *Brownian motion* is termed as molecular diffusion. Scattering of particles by the interaction of differential advection and cross sectional diffusion on macroscopic scale is known as dispersion. In open channel flows, dispersion is attributed to both molecular diffusion and velocity variations caused by shear stress. Shear flow support lateral and vertical gradients of longitudinal velocity. Due to non-uniformity in the velocity gradient along longitudinal direction, some solute particles travel faster and some slower than the mean flow velocity. This results in continuous scattering of solute particles within the channel cross-section via transverse and vertical processes. Further it is important to know the rate at which the solute cloud spreads out, attenuation of peak concentration, and the concentration distribution along the flow direction.

In a river, near to the source normally mixing and transport of solute particles take place in all three directions, viz. vertical, transverse and longitudinal direction. However,



away from the source, transport of solute particles eventually becomes one-dimensional process (Fischer, 1967, 1968; Chatwin, 1970, 1971; Holley and Tasi, 1977). The equation describing the spatial and temporal effects of advection and dispersion on solute concentration along longitudinal direction was derived from the principle of conservation of mass together with the Fick's Law of diffusion. The differential equation of solute transport, resulting from the conservation of mass together with the Fick's Law of diffusion in a controlled volume, is given by:

$$\frac{\partial(AC)}{\partial t} = -\frac{\partial(Au C)}{\partial x} + \frac{\partial}{\partial x}\left(AD_L \frac{\partial C}{\partial x}\right) \quad (2.1)$$

where,  $C$  is the solute concentration ( $ML^{-3}$ ),  $u$  is the mean flow velocity ( $LT^{-1}$ ),  $D_L$  is longitudinal dispersion co-efficient ( $L^2T^{-1}$ ),  $A$  is the cross-sectional area of flow ( $L^2$ ),  $x$  is distance ( $L$ ) and  $t$  is the time ( $T$ ).

For a constant  $A$  and  $u$  i.e., for uniform flow velocity in a regular channel, Eq. (2.1) simplifies to the well-known Advection dispersion equation (ADE) (Fischer, 1967 and Fischer et al. 1979):

$$\frac{\partial C}{\partial t} = -u \frac{\partial C}{\partial x} + D_L \frac{\partial^2 C}{\partial x^2} \quad (2.2)$$

Eq. (2.2) is also known as Fickian dispersion model.

Following assumptions are implied in the derivation of Eq. (2.2):

1. the fluid is incompressible, and the tracer is neutrally buoyant, i.e., hydrodynamically indistinguishable from the surrounding fluid;
2. velocity varies along vertical direction;
3. the tracer concentration varies along the longitudinal direction,  $x$ , with the flow, and time, and the flow cross-section is independent of longitudinal distance and time; and
4.  $D_L$  is constant for a given flow system.

Since the development of the ADE model, it has been widely accepted and extensively used (Fischer, 1967, 68; Sooky 1969; Chatwin 1970; 1971; Bear, 1972; Banks, 1974; Cameron and Klute, 1977; Holley & Tsai 1977; Fischer et al. 1979; Bencala and

Walters, 1983; Runkel and Broshears, 1991; Runkel and Chapra, 1993; Hart, 1995; Runkel, 1998; Lees et al., 2000) as a standard model for study of solute transport and longitudinal dispersion in streams and other areas.

Numerous factors influence mixing and transport of solute in natural streams. These are: i) channel side and bed irregularities, ii) channel curvature, iii) presence of dead zones and hyporheic zones, iv) Geo-morphology of the streambed, etc. Additionally, a number of processes, in addition to the advection and dispersion, affect the transport of solute. These are: i) retardation, ii) sorption iii) decay or growth of the constituents. By employing particular processes and factors as applicable to a stream with the two primary mechanisms – advection and dispersion, the ADE model had been extended widely to simulate complex processes of solute transport in streams and rivers (Bencala and Walters, 1983; Runkel and Broshears, 1991; Runkel and Chapra, 1993; Hart, 1995; Runkel, 1998; Lees et al., 2000). Inaccurate simulation of  $C-t$  profiles and estimation difficulties of  $D_L$  in many natural streams created doubt to many investigators (Day, 1975; Chatwin, 1980; Chatwin and Allen, 1985) about the validity of the ADE model to natural streams, particularly in rivers where non-homogeneous turbulent mixing prevails. The argument owed was to the limiting assumptions of the ADE model (Young and Wallis, 1993). As there were no widely accepted alternate models, the ADE model continued to application as standard model for dispersion studies in streams or rivers, even in complex cases despite recognizing its limitations. Over last three decades, as alternate to the ADE model, a number of conceptual models have been developed and applied successfully for simulating solute transport in streams.

The following sections present and critically review the usage and performance of various solute transport models, which mainly focus on:

1. Advection-Dispersion Equation Model
2. Conceptual Mixing Cells Models

Thereafter, the application of the above models for simulation of various processes like Adsorption / Desorption, process due to hyporheic zone and decay have been discussed:

## 2.2 STUDIES BASED ON THE ADE MODEL

Eq. (2.2) represents a partial differential equation (PDE) of dependant variable  $C$  as function of  $x$  and  $t$ . Ogata and Banks (1961) gave the analytical solution of the Eq (2.2) for a steady and uniform flow using the initial condition  $C(x, 0) = 0$  with a step input  $C(0, t) = C_R$  applied at the boundary. The solution given by Ogata and Banks (1961) is:

$$C(x, t) = \frac{C_R}{2} \left\{ \operatorname{erfc} \left[ \frac{x - ut}{2\sqrt{D_L t}} \right] + \exp \left( \frac{xu}{D_L} \right) \operatorname{erfc} \left[ \frac{x + ut}{2\sqrt{D_L t}} \right] \right\} \quad (2.3)$$

where,  $\operatorname{erfc}(\cdot)$  is a complimentary error function  $= 1 - \operatorname{erf}(\cdot)$ ,  $\operatorname{erf}(z)$  is the error function of  $z$ , which is expressed as  $\operatorname{erf}(z) = \frac{2}{\sqrt{\pi}} \int_0^z e^{-\xi^2} d\xi$ ,  $x$  is distance,  $t$  is the time after input and

$C(x, t)$  is concentration of solute at a distance  $x$  and time  $t$  from the input.

The response function of Eq. (2.2) due to an impulse input of magnitude  $C_R$  applied at the boundary, which is the derivative of Eq. (2.3) with respect to time, is given by:

$$c(x, t) = \frac{C_R x}{2t \sqrt{\pi D_L t}} \exp \left\{ - \left[ \frac{(x - ut)^2}{4 D_L t} \right] \right\} \quad (2.4)$$

where,  $c(x, t)$  is the response of impulse input at a distance,  $x$  and time  $t$  since injection of solute. Eqs. (2.3) and (2.4) clearly indicate that for computation of concentration of solute at any distance,  $x$  and time  $t$ , one requires prior estimation of two basic parameters,  $u$  and  $D_L$ .

The analytical solution (Eq. 2.3) to Eq. (2.2) given by Ogata and Banks (1961) is considered to be the exact solution for idealized condition. After Ogata and Banks (1961), many other investigators (Sooky 1969; Chatwin 1970; 1971; Holley & Tsai 1977) derived solutions to Eq. (2.2) in different ways, which are similar to Eq (2.4). Sayre (1968) considered the cross sectional mass of instantaneous input in the impulse response function of the following form; and satisfying the under mentioned boundary conditions had studied the solute transport in a stream.

$$C(x, t) = \frac{M}{2A \sqrt{\pi D_L t}} \exp \left\{ - \left[ \frac{(x - \bar{u}t)^2}{4 D_L t} \right] \right\} \quad (2.5)$$

The boundary conditions used for studying the solute transport in stream using Eq. (2.5)

were:

$$\int_0^{\infty} A(x) C(x,t) dx = M \quad \text{for all } t$$

$$C(\infty, t) = 0 \quad \text{for } t \geq 0$$

$$\frac{\partial C}{\partial x} \Rightarrow 0 \quad \text{as } t \Rightarrow \infty$$

where,  $M$  = mass injected (M), and  $A$  = cross sectional area ( $L^2$ ). Eq. (2.5) is also known as Taylor solution.

Fischer (1967; 1968) studied the dispersion in open channels extensively and suggested a convolution integral (routing method) using Taylor solution for computing the downstream tracer distribution corresponding to an observed upstream concentration-time ( $C$ - $t$ ) profile:

$$C(x_2, t) = \int_{-\infty}^{+\infty} \left\{ C(x_1, \tau) \left[ \frac{u}{\sqrt{4\pi D_L (t_2 - t_1)}} \exp\left(-\frac{u^2 (t_2 - t_1 - t + \tau)^2}{4D_L (t_2 - t_1)}\right) \right] \right\} d\tau. \quad (2.6)$$

where,  $C(x_2, t)$  = predicted value of concentration at station  $x_2$  at time  $t$ ;  $C(x_1, t)$  = value of concentration at station  $x_1$  at time  $t$ ; and  $t_1, t_2$  = respective times of passage of the tracer cloud through two stations and have been calculated assuming that the cross sectional mean velocity  $u$  is equal to the velocity of tracer cloud.

Barnett (1983) suggested an alternative method for routing a  $C$ - $t$  profile. He considered a different form of solution to Eq. (2.2), which is also called as Hayami solution.

$$C(x,t) = \frac{M x}{A u t \sqrt{4 \pi D_L t}} \exp\left[-\frac{(x - u t)^2}{4D_L t}\right] \quad (2.7)$$

Eq. (2.7) is Eq. (2.5) multiplied by  $\left(\frac{x}{u t}\right)$ . It satisfies the boundary condition  $C(0, t) = 0$  when a tracer slug of mass  $M$  is introduced over an infinitesimally small time interval. Barnett suggested that the advantage of using Eq. (2.7) is that it could route an observed  $C$ - $t$  profile without requiring the frozen cloud approximation. Both Taylor (Eq. 2.5) and

Hayami (Eq. 2.7) solutions give similar results at moderately large  $x$  and  $t$  but they differ significantly in their behavior at a very small value of  $t$ .

During period from 1960 to 1985, many other investigators (Fischer 1967; Thackston and Krenkel 1967; Sooky 1969; Day and Wood 1976; Fischer et al. 1979; Chatwin 1980; Chatwin and Allen 1985) have also used the Fickian dispersion model to study solute transport in rivers for various complexities, and reported the practical difficulties in application of Fickian dispersion model to field conditions owing to difficulties in establishing a logical method to estimate  $D_L$ .

In order to account for variability of field conditions, where analytical solutions fall short to satisfactorily field representation, many investigators used numerical methods to the advection dispersion equation of one, two and three-dimensional cases in open channels. Yotsukura and Fiering (1964) studied transport of solute in open channel by deriving numerical solutions for two-dimensional turbulent flows considering logarithmic velocity distribution. Fischer (1966) proposed a numerical simulation to two-dimensional diffusion equation for predicting the concentration distribution at the convective period performing step-by-step simulation of diffusion process. In addition to the investigations mentioned above, many other researchers (Holley, 1977; Keefer and Jobson, 1978; Fischer et al., 1979; Holley, 1983; Koussis, 1983) suggested various mathematical and numerical schemes for solving the convective diffusion equation, which were either mathematically very complex or had shown problem of overshoot and undershoot due to the numerical dispersion.

It is clearly evident that the use of the ADE, whether in its analytical form or numerical scheme, one requires estimation of  $u$  and  $D_L$  *a priori*. In most cases,  $u$  can be measured or estimated relatively easily and quite accurately from the knowledge of gauged flows or by application of flow resistance equation. The situation is, however, not straightforward with regard to  $D_L$ . Thus, the accuracy in simulation of tracer cloud transport depends on the value of  $D_L$  (Holley and Tsai, 1977). The compilation work of many investigators (Bansal, 1971; Elhadi and Davar, 1976; and Elhadi *et al.*, 1984; ERL, 1985) reported a wide range of  $D_L$  values which have been estimated either by theoretical

or by experimental bases or by empirical formulae. Table 2.1 presents a compilation of methods suggested by various investigators for estimation of  $D_L$  in a stream.

**Table 2.1: Methods suggested by investigators for estimation of  $D_L$**

S. No	Investigators	Equation	Method
1.	Taylor, 1921	$\frac{d\sigma^2}{dt} = 2D$ ; where, $\sigma^2$ is the variance of solute distribution and $D$ is the diffusion co-efficient.	Experimental
2.	Chatwin, 1971; Valentine and Wood, 1979	$D_L = \frac{\bar{u}^3}{2} \frac{d\sigma_x^2}{dx}$ ; where, $\bar{u}$ is the average flow velocity, $\sigma_x$ is the spatial variances of concentration distribution.	Experimental
3.	Elder, 1959	$D_L = \left[ \frac{0.404}{\kappa^3} + \frac{\kappa}{6} \right] y U_*$ ; where $\kappa$ is the Von Karman's coefficient, and $U_*$ is the shear velocity, and $y$ is the vertical distance.	Theoretical
4.	Fischer et al., 1979	$D_L = -\frac{1}{A} \int_0^B \bar{u} y \int_0^y \frac{1}{\varepsilon_t} \int_0^B \bar{u}' y dy dy dy$ where $\bar{u}'$ is the deviation of velocity from the cross sectional mean velocity, $y$ is the depth of flow, and $\varepsilon_t$ is the transverse mixing coefficient.	Theoretical
5.	Taylor, 1954	$D_L = 10.1 U_* r$ ; where $U_*$ is the shear flow velocity, and $r$ is the radius of the pipe.	Empirical
6.	Elder, 1959	$D_L = 6.3 U_* H$ ; where $H$ is the flow depth	Empirical

7.	Yotsukura and Fiering, 1964	$D_L = 9.0 \text{ to } 13.0 U_* H;$	Empirical
8.	Fischer, 1966	$D_L = 0.011 u^2 W^2 / U_* H$ where $W$ is the width of the stream, and $u$ is the mean flow velocity.	Empirical
9.	Thackston and Krenkal, 1967	$D_L = 7.25 U_* H \{u / U_*\}^{1/4}$	Empirical
10.	Sumer, 1969	$D_L = 6.23 U_* H$	Empirical
11	Fukuoka and Sayre, 1973	$D_L / R U_* = 0.8 \{r_c^2 / L_B H\}^{1.4}$ where $R$ is the hydraulic depth, $r_c$ is the radius of curvature	Empirical
12.	McQuivey and Keefer, 1974	$D_L = 0.058 Q / SW$	Empirical
11.	Jain, 1976	$D_L = u^2 W^2 / k A U_*$	Empirical
12.	Beltaos, 1978	$D_L / R U_* = \alpha \{W / R\}^2$	Empirical
13.	Liu, 1978	$D_L = Q^2 / 2 U_* R^3 \{U_* / u\}^2$	Empirical
14.	Magazine, 1983	$D_L / R_b U_* = D_L / R_w U_* = 75.86 Pr^{1.632}$ $Pr = C_w \sqrt{g} \{x/h\}^{0.3} \{x_1/b\}^{0.3} \{1.5 + e/h\}$	Empirical
15.	Marivoet and Craenenbroec, 1986	$D_L = 0.0021 u^2 W^2 / U_* H$	Empirical
16.	Asai et al., 1991	$D_L / U_* H = 2.0 \{W / R\}^{1.5}$	Empirical
17.	Ranga Raju et al., 1997	$D_L / q S = 0.4 P_f$ where $P_f = \{W / R\}^{2.16} \{u / U_*\}^{-0.82} \{S\}^{-0.2}$	Empirical
18.	Koussis and Mirasol, 1998	$D_L = \Phi \sqrt{(gRS) / H} \{W\}^2$	Empirical
19.	Seo & Cheong, 1998	$D_L / U_* H = 5.915 \{W / H\}^{0.628} \{u / U_*\}^{1.428}$	Empirical
20.	Kezhong and Yu, 2000	$D_L / U_* H = 3.5 \{W / H\}^{1.125} \{u / U_*\}^{0.25}$	Empirical



Empirical formulae indicate that  $D_L$  is a function of stream flow characteristic and stream geometry. By analyzing empirical formulae, Seo and Cheong (1998) suggested a generalized functional relationship of  $D_L$  with flow characteristic and geometry of a stream of the following form:

$$\frac{D_L}{U_* H} = a \left( \frac{W}{H} \right)^b \left( \frac{u}{U_*} \right)^c \quad (2.8)$$

where,  $W$  is the channel width (L),  $H$  is the depth of the flow (L),  $U$  is the average velocity ( $LT^{-1}$ ),  $U_*$  is the shear velocity ( $LT^{-1}$ ), and  $a$ ,  $b$ ,  $c$  are constants.

Table 2.1 also reveals that estimation of  $D_L$  is neither a simple nor a straightforward approach, as the values of  $D_L$  computed by any two methods differ significantly. The theoretical methods are data expensive viz., require measurements of point velocities along vertical and transverse direction; experimental bases require observations of  $C-t$  profiles at two downstream sites. Nevertheless, how  $D_L$  changes with the change in flow velocity at other downstream locations in a stream can't be known when  $D_L$  is estimated using experimental methods. On the other hand, the empirical formulae show a wide range of variability in  $D_L$  when compared with each other.

### 2.3 MIXING CELLS MODELS

As alternate to the ADE model, the Cells-In-Series (CIS) approach has been extensively used by many investigators (Bear 1972; Banks 1974; Van der Molen 1979; Beltaos 1980; Stefan and Demetracopoulos 1981; Yurtsever 1983; Beven and Young 1988; Young and Wallis 1993; Wang and Chen 1996) for study of solute transport in flowing medium. In the CIS model, a reach length of a river is assumed to be comprised of a number of thoroughly mixed cells of equal residence time; the concentration of the effluent from a particular cell is equal to the concentration within the cell; output from a preceding cell forms input to the succeeding cell, and time is reckoned since injection of solute into the first cell. Comparing the CIS model with Ogata and Banks solution to the ADE model, Banks (1974) had shown that the CIS model does not adequately simulate the advection



component. Stefan and Demetracopoulos (1981) have also reported the limitations of the CIS model. These limitations are:(i) the CIS model does not reproduce persistence skewness in concentration-time profiles usually observed in tracer data from rivers, (ii) the travel time, rate of dispersion and the skewness are function of the number of cells and these parameters can't be varied independently, which restricts the usefulness of the model. However, the advantage in formulation of the CIS model is that the governing second order partial differential equation is reduced to a first order ordinary differential equation.

To remove the discrepancy in simulating advection component, Beer and Young (1983) introduced a variant on the CIS model, which is designated as the Aggregated Dead Zone (ADZ) model. In the ADZ model, dead-zone processes were considered as the major physical cause of dispersion in natural streams. The main difference in the ADZ model from the CIS model is that, in the ADZ model, a pure time delay was introduced into the input concentration, which allowed advection and dispersion to be de-coupled (Rutherford 1994). If the time delay component is zero, the ADZ model breakdowns to the CIS model. Beer and Young (1983) have postulated that a correct order of the ADZ model describes the observed  $C-t$  profiles closely. However, the difficulties with the ADZ model are determination of model orders and estimation of the model parameters (Lees et al., 2000). Beer and Young (1984) have chosen the time series method (Young 1984) for estimation of model parameters.

Considering the performance of the mixing cell concept for its characteristics to describe the dispersion, and the time delay component for its uniqueness to depict the pure advection, Ghosh (2001) and Ghosh et al., (2004) developed a conceptualized Hybrid-Cells-In-Series (HCIS) model to simulate advection-dispersion governed solute transport for a conservative solute transport in a river. The HCIS model seems to overcome the limitations of the ADE, the CIS and the ADZ models. The conceptualized HCIS model is comprised of a plug flow zone of residence time,  $\alpha$  and two thoroughly mixed zones of unequal residence times,  $T_1$  and  $T_2$ ; all connected in series, as shown in Fig. 2.1.

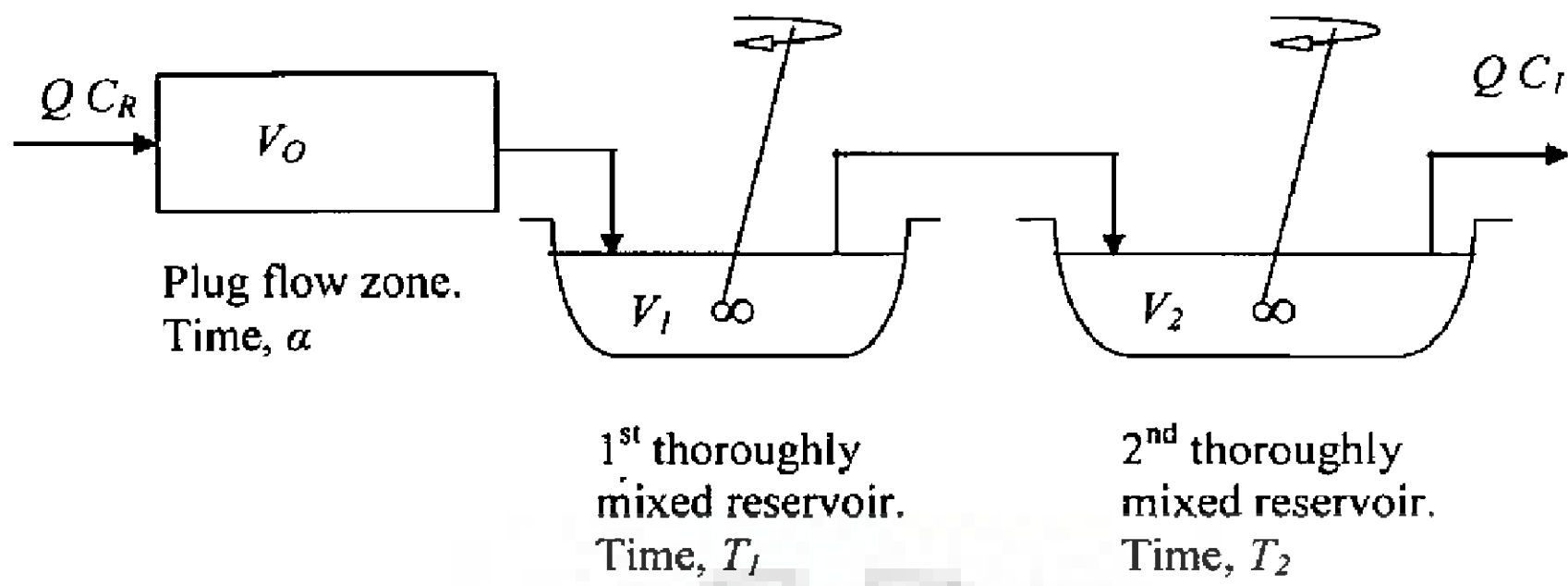


**Fig. 2.1: The first process unit of the HCIS model**

The movement of solute in the plug flow zone represents the pure advection, and transport through the mixing reservoirs represents both advection and dispersion. Under steady and uniform flow conditions, the  $C-t$  graphs at  $n \Delta x$ ,  $n = 1, 2, 3, \dots$  ( $\Delta x =$  basic process unit size) generated by the HCIS model have been found identical to that as predicted by the analytical solution of the ADE (Ogata and Banks, 1961) when the size of the basic process unit,  $\Delta x$ , is equal to or more than  $4D_L/u$  (Ghosh *et al.*, 2004), where  $u =$  mean flow velocity ( $LT^{-1}$ ), and  $D_L =$  longitudinal dispersion coefficient ( $L^2T^{-1}$ ), or chosen satisfying the condition of Peclet number,  $P_e = (\Delta x u)/D_L \geq 4$ . The linear dimension of the HCIS model, i.e., size of each process unit,  $\Delta x = (\alpha + T_1 + T_2) u$ , outlines the dispersion of solute cloud along the longitudinal flow direction. The mathematical structure and its characteristics equations of the HCIS model have been given in the Appendix A.

By assuming that, (i) the reach length downstream from a point source of pollution in a stream is comprised of a series of equal size hybrid process units, and (ii) the output from the preceding process unit is the input to the succeeding process unit, the response of the  $n^{\text{th}}$  hybrid process unit,  $n \geq 2$ , consequent to any perturbation at the inlet boundary of the first hybrid unit can be obtained by applying simple convolution technique as:

$$C(n\Delta x, t) = \int_0^t C\{(n-1)\Delta x, \tau\} k_h(\alpha, T_1, T_2, t-\tau) d\tau \quad (2.9)$$

where  $C((n-1)\Delta x, \tau)$  = output from  $(n-1)^{\text{th}}$  unit. In particular, for  $n=1$ , consequent to a unit impulse perturbation, output of the 1<sup>st</sup> hybrid unit  $C(\Delta x, t) = k_h(\alpha, T_1, T_2, t)$ .

The advantages of the HCIS model as reported by Ghosh et al., (2004) are:

1. the mathematical derivation of the HCIS model follows an ordinary differential equation.
2. the HCIS model simulates closely the advection-dispersion governed solute transport.
3. the parameters of the model can also be determined from the measurement of single  $C-t$  profile.
4. the HCIS model overcomes weaknesses of the CIS and the ADZ model.
5. In the HCIS model, pure advection is represented by an explicitly derived time parameter besides representation of advection and dispersion components implicitly by two time parameters.
6. Alike the ADE model, natural adsorption and desorption, transient storage, growth and decay components can be incorporated into the HCIS model comparatively more easily.

#### **2.4 COMPARISON OF THE HCIS MODEL WITH THE CIS, ADZ AND ADE MODELS**

The CIS, ADZ, and the HCIS are conceptual models in which dispersion is induced by assuming the cells to be thoroughly mixed reservoirs. The ADZ and the HCIS models contain a plug flow component, whereas, the CIS model does not have it, implying that a pure advection component of solute transport is represented exclusively by the ADZ and the HCIS model. An advection component is otherwise implicitly present in all the models as the flow velocity governs the residence time in a cell. These models are discrete in space domain and continuous in time domain. The CIS has one time constant, the ADZ has two, and the HCIS has three time constants.

Assuming the time lag in the ADZ model to be equal to the residence time in the plug flow zone of the HCIS model, and considering that all the models have equal total

residence time, the  $C-t$  profile generated by each model will be as shown in Fig. 2.2. A single unit of the CIS or the ADZ model does not show a rising limb. Therefore, a minimum of two units is needed in the ADZ and in the CIS model to simulate a skewed  $C-t$  profile. While a single hybrid unit of the HCIS model simulates a skewed  $C-t$  profile since two cells are embedded together. Further, sub-dividing the lag time and the residence time of the ADZ model, and the total residence time in the CIS model equally in two parts, the  $C-t$  distributions simulated by the ADZ and the CIS model will be as shown in Fig. 2.3. One can observe from Fig. 2.3 that the second unit of the ADZ and the CIS model generate skewed  $C-t$  profile like that of the ADE and the HCIS models. Neither of the  $C-t$  distribution including that of the ADE model is Gaussian. However, the concentration-space distributions simulated by all the models are Gaussian.

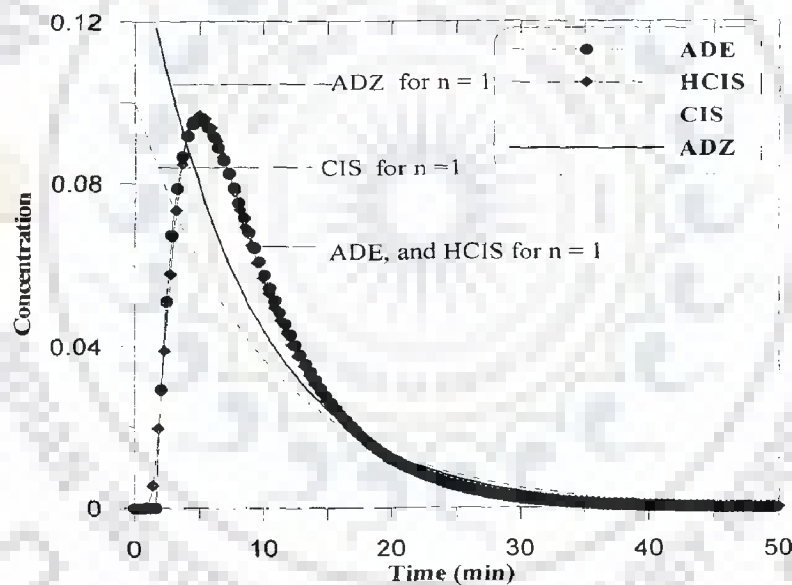


**Fig. 2.2:** Comparison of concentration-time distribution profiles generated by different models for a unit impulse input; each distribution represents same residence time = 10 min.

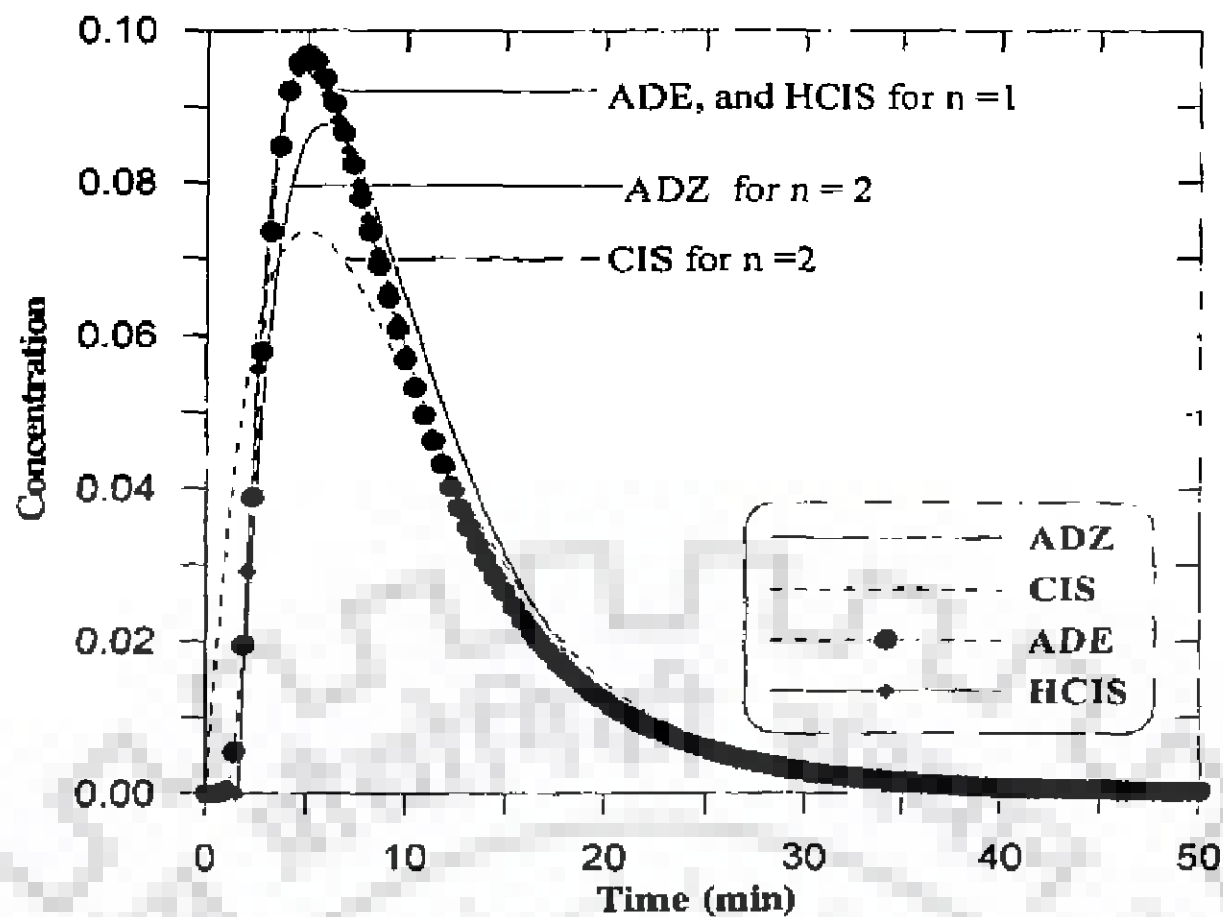


**Fig. 2.3: Comparison of concentration-time distribution profiles generated by different models for a unit impulse input; each distribution represents same residence time = 10 min.**

## **2.5 ADSORPTION/DESORPTION PROCESSES**

Various processes in addition to primary mechanisms of advection-dispersion determine the fate and transport of solutes in streams. One such important process controlling the solute concentration in streams is adsorption and desorption to and from bed sediments below the water column. Many investigators (Deacon and Driver, 1999; Jain and Sharma, 2002; Perk *et al.*, 2006) have reported strong association of numerous toxic chemicals both organic and inorganic with sediments below water column in streams. Adsorption and desorption take place under non-equilibrium conditions. Investigations coupling adsorption and desorption isotherm with the advection-dispersion processes in a stream are rarely available in literature. However, adsorption isotherms studies are found more referred in soil-water and groundwater contamination problems. From soil-water column and groundwater studies, many investigators (Cameron and Klute, 1977; Bear and

Bachmat, 1990; Bajracharya and Barry, 1992) demonstrated that the adsorption process attenuates concentration of pollutants.

Numerous investigators (Hays et al., 1966; Nordin and Troutman, 1980; Bencala and Walters, 1983; Bencala et al., 1990; Runkel and Broshears, 1991; Runkel and Chapra, 1993; Czernuszenko and Rowinski, 1997; Runkel, 1998; Worman, 1998; Worman et al., 2002) reported that solute transport in stream is influenced by the presence of dead zones or stagnation zones along the streambeds and sides. The physical process representing the effects of these zones has been termed as transient storage (Bencala and Walters, 1983). Transient storage has been noted in many small streams, where solutes are temporarily detained in small eddies and stagnant zones of water that are stationary relative to the faster moving waters near the centre of the channel. In addition, significant portions of the flow move through the coarse gravel of the streambed and the porous areas within the stream bank. The travel time for solutes carried through these porous areas is significantly longer than that for solutes travelling within the water column.

Bencala and Walters (1983) studied the effect of dead zone by coupling a non-linear sorption type isotherm with the classical ADE model. The coupled process has been named as the Transient Storage (TS) model. The TS model has been expressed by the following governing partial differential equations:

$$\frac{\partial C}{\partial t} + u \frac{\partial C}{\partial x} = D_L \frac{\partial^2 C}{\partial x^2} + \alpha (C_s - C) \quad (2.10)$$

$$\frac{\partial C_s}{\partial t} = \alpha \frac{A}{A_s} (C - C_s) \quad (2.11)$$

where  $C_s$  is the concentration in the storage zone ( $ML^{-3}$ ),  $C$  is the concentration in the main stream ( $ML^{-3}$ ),  $A_s$  is the area of the storage zone ( $L^2$ ),  $A$  is the area of the main stream ( $L^2$ ),  $\alpha$  is the mass exchange rate constant ( $T^{-1}$ ).

The assumptions underlined in their study were:

1. There exist storage zones and these are assumed to be stagnant relative to the longitudinal flow of the stream.
2. Within the storage zone, solute is uniformly distributed.



3. First order kinetic has been assumed to the exchange of mass between the mainstream and storage zone

Several other transient storage models were found in literature, which have been developed considering either main channel flow in conjunction with mass exchange in stagnant water zones or first-order mass exchange between the main channel and a storage zone (Hays et al., 1966; Nordin and Troutman, 1980; Bencala and Walters, 1983; Bencala et al., 1990; Czernuszenko and Rowinski, 1997). Worman (1998) considered the exchange of solute from the main channel to a storage zone to be governed by a diffusion equation and presented an analytical solution neglecting dispersion in the main channel. Worman et al. (2002) described a model that couples longitudinal solute transport in streams with solute advection along a continuous distribution of hyporheic flow paths. Runkel and Chapra (1993) developed a one-dimensional Transport with Inflow and Storage (OTIS) model and presented analysis of an implicit finite difference approximation by considering first-order mass exchange between the main channel and a storage zone (Runkel and Broshears, 1991; Runkel and Chapra, 1993). The model was later extended as OTIS-P (Runkel, 1998), and has been used extensively.

Hart (1995) presented an alternative formulation of the storage model by considering stochastic process and derived an analytical expression for the density function of a conservative solute. The governing equation considered for the model was,

$$\frac{Q}{A} \frac{\partial C}{\partial x} = \frac{1}{A} \frac{\partial}{\partial x} \left( AD \frac{\partial C}{\partial x} \right) + k_1 (B - C) + k_L (C_L - C) \quad (2.12)$$

and

$$\frac{\partial B}{\partial t} = k_2 (C - B) \quad (2.13)$$

where  $k_1$  is the exchange co-efficient from free flowing water to the storage zone ( $T^{-1}$ ),  $k_2$  is the exchange co-efficient from the storage zone to the free flowing water ( $T^{-1}$ ),  $k_L$  is the exchange co-efficient for lateral inflow ( $T^{-1}$ ),  $C_L$  is the concentration of the solute in the lateral inflow ( $ML^{-3}$ ),  $B$  is the concentration of solute trapped in the transient storage zone ( $ML^{-3}$ ) and  $C$  is the concentration of solute in the stream ( $ML^{-3}$ ).

De Smedt F et al. (2005) gave an analytical solution for solute transport in rivers including the effects of transient storage in which the traditional advection–dispersion equation for transport in the main channel was linked to a first order mass exchange term between the main channel and the transient storage zone. The governing equation considered for the model was,

$$\frac{\partial C}{\partial t} = D \frac{\partial^2 C}{\partial x^2} - v \frac{\partial C}{\partial x} - \alpha (C - C_s) \quad (2.14)$$

$$\beta \frac{\partial C_s}{\partial t} = \alpha (C - C_s) \quad (2.15)$$

where  $C$  and  $C_s$  are the cross sectional averaged solute concentrations respectively in the main channel and the storage zone ( $ML^{-3}$ ).  $D_L$  is the cross sectional averaged longitudinal dispersion co-efficient in the main channel ( $L^2T^{-1}$ ).  $\alpha$  is the mass exchange co-efficient between main channel and storage zone ( $T^{-1}$ ),  $\beta$  is the ratio between the storage zone and main channel cross sectional area. They used convolution theorem of the Laplace transform to solve Eq. (2.14) and (2.15) and a close form analytical solution was given by

$$C(x, t) = \int_0^t \left[ \alpha + \left( \frac{x^2 - v^2 \tau^2}{4D\tau^2} - \frac{1}{2\tau} - \alpha \right) J \left( \alpha \tau, \frac{\alpha(t-\tau)}{\beta} \right) - \alpha J \left( \frac{\alpha(t-\tau)}{\beta}, \alpha \tau \right) \right] C_0(x, \tau) d\tau \quad (2.16)$$

where,  $C_0$  is the solution of the classical advection dispersion equation,  $J(*, *)$  is the  $J$  – function.

The integral appearing in Eq. (2.16) is an improper integral as the integrand becomes infinite at  $\tau=0$ . By making a substitution  $\tau = 1/\mu$ ,  $d\tau = -(1/\mu^2) d\mu$ , Eq. (2.16) is reduced to

$$\int_{1/t}^{\infty} \left[ \alpha + \left( \frac{x^2 - v^2/\mu^2}{4D/\mu^2} - \frac{\mu}{2} - \alpha \right) J \left( \alpha/\mu, \frac{\alpha(t-1/\mu)}{\beta} \right) - \alpha J \left( \frac{\alpha(t-1/\mu)}{\beta}, \alpha/\mu \right) \right] C_0(x, 1/\mu) (1/\mu^2) d\mu$$

This integral is also improper, as the limit has gone to infinite. However the value of the integrand is 0 at the upper limit.

The processes of solute transport as considered in the transient storage model are nearly similar as that of the adsorption/desorption processes, except the differences of transport media, and their extent. In case of transient storage model, the exchange of solute is between the main channel flow and the stagnation or dead zone, and vice-versa, while



for adsorption /desorption, the exchange of solute takes place between the water column and the sediment bed, and vice-versa.

## 2.6 REACTIVE POLLUTANTS TRANSPORT

Stream water quality modeling has a long history since development of Streeter and Phelps equation in year 1925 for DO-BOD modeling. After Streeter and Phelps, several concepts were introduced (Bhargava, 1983; Bobba et al., 1983; Barnwell, 1985; Thomman and Muller, 1987; Choudhary et al., 1990; Jolanki, 1997; Guymer, 1998; Sharma et al., 2000). All these approaches assumed that the substances present in the water decay according to a first order reaction, i.e., the rate of loss of the substance is proportional to its concentration at any time. However, the one-dimensional equation describing the advection-dispersion-decay of pollutants for time varying concentration of reactive pollutants in a stream due to steady and uniform flow conditions is given by:

$$\frac{\partial C}{\partial t} = -u \frac{\partial C}{\partial x} + D_L \frac{\partial^2 C}{\partial x^2} - \lambda C \quad (2.16)$$

where  $C$  is the concentration of reactive pollutants ( $ML^{-3}$ ),  $x$  is distance (L),  $t$  is time (T),  $u$  is the mean flow velocity ( $LT^{-1}$ ),  $D_L$  is the longitudinal dispersion coefficient ( $L^2T^{-1}$ ), and  $\lambda$  is the decay rate coefficient ( $T^{-1}$ ).

Later on, the approximate dispersion model for BOD-DO has been derived by extending the Streeter-Phelps model in the form (Source: Rinaldi et al., 1979)

$$\frac{\partial b}{\partial t} + v \frac{\partial b}{\partial l} - D \frac{\partial^2 b}{\partial l^2} = -k_1 b \quad (2.17)$$

$$\frac{\partial d}{\partial t} + v \frac{\partial d}{\partial l} - D \frac{\partial^2 d}{\partial l^2} = k_1 b - k_2 d \quad (2.18)$$

where  $b$  is the BOD concentration ( $ML^{-3}$ ),  $d$  is the DO deficit ( $ML^{-3}$ ),  $v$  is the flow velocity ( $LT^{-1}$ ),  $D$  is the longitudinal dispersion co-efficient ( $L^2T^{-1}$ ),  $k_1$  is the decay rate co-efficient ( $T^{-1}$ ) and  $k_2$  is the re-aeration rate constant ( $T^{-1}$ ).

By defining the auxiliary variable,  $a$

$$a = d + \frac{k_1}{k_1 - k_2} b \quad (2.19)$$

Eq. (2.18) was simplified and analytical solution,  $a(l, t)$  was obtained. From Eq. (2.19), the solution for DO deficit has been deduced. Dobbins' criterion (Dobbins, 1964) says that the effect of dispersion is negligible as far as steady state conditions are concerned.

Young and Beck (1974) joined together two of the most well known simplifying assumptions: i) the river to be constituted by a sequence of reaches ii) each reach is a perfectly mixed reactor. The approximate dispersion model for BOD-DO has the same structure as the so-called continuously stirred tank reactor (CSTR) model heuristically proposed by them.

De Smedt F (2006) gave analytical solutions for solute transport in rivers including the effects of transient storage and first order decay. The solute transport model considers an advection–dispersion equation for transport in the main channel linked to a first order decay and to a first order mass exchange between the main channel and the transient storage zones. This new analytical solutions are suitable for both conservative and non-conservative solute. However, like Eq. (2.16), it has the similar problem of singularity in  $\left( \frac{x^2 - v^2 \tau^2}{4D\tau^2} - \frac{1}{2\tau} - \alpha - \lambda + \lambda_s \right)$  term, in which  $\lambda$  is first order decay coefficient in the main stream;  $\lambda_s$  is first order decay coefficient in the dead zone.

- Incorporating kinetics of reactive components with the ADE model, transport of non-conservative pollutants in streams are normally studied as a standard practice. The question that remains valid, even for transport of reactive pollutants is estimation of logical value of  $D_L$  for natural streams.

Re-aeration rate constant,  $k_2$  is one of the important parameters for stream water quality modeling. It is the rate at which oxygen in dissolved form is introduced in the water column. Many researchers (O'Connor and Dobbins, 1958; Owens et al., 1964; Langbein and Durum, 1967; Thackston and Krenkel, 1969; and Moog and Jirka, 1998) have derived different empirical formulae to estimate  $k_2$ .

## 2.7 CONCLUSIONS

From the literature review, following conclusions are drawn.

1. The ADE model has been used as a classical approach based on the physical theory for solute transport in the streams. However, difficulty in estimation of  $D_L$  poses the major hurdle in its straightforward application.
2. The applications of conceptual potential alternatives to the ADE model, namely the CIS and the ADZ models have their own limitations. The CIS model has limitation toward simulating advection component, while the ADZ model faces complexity in selecting the model order.
3. The HCIS model simulates advection-dispersion governed solute transport as depicted by the ADE model under steady and uniform flow conditions closely when size of the basic process unit of the HCIS model is equal to or greater than  $4D_L/u$  or is chosen satisfying the condition of Peclet number,  $P_e = (\Delta x u)/D_L \geq 4$ .
4. The HCIS model is a three-parameter model discrete in space and continuous in time domain. Alike the ADE, the HCIS model also represents Gaussian distribution of the concentration-space and asymmetric of the concentration-time variation.
5. The parameters of the HCIS model can be determined from the measurement of single  $C-t$  profile without invoking measurements of  $u$  and  $D_L$ .
6. In the HCIS model, pure advection is represented by an explicitly derived time parameter, and it also represents the advection and dispersion components implicitly by two time parameters. Whereas, in the ADE model, both advection and dispersion are represented implicitly by  $u$  and  $D_L$ . The HCIS is a simple semi-analytical model and can accommodate non-homogeneity character of the system.
7. Alike in the ADE model, natural adsorption and desorption, transient storage, growth and decay components can be incorporated into the HCIS model.
8. Thus, the HCIS model seems to have overcome the weaknesses of the ADE, the CIS, and the ADZ model. Considering the strength and the flexibility of the HCIS model, it can be extended to the study of solute transport in streams for resolving the model complexities of various processes like adsorption/desorption,

stagnation and hyporheic zones, and non-conservative nature of the pollutants. The present study aims at extending the HCIS model for analyzing the adsorption/desorption mechanism for a conservative as well as non-conservative substance.



## CHAPTER 3

# TRANSPORT OF CONSERVATIVE POLLUTANTS CONSIDERING NON-EQUILIBRIUM SORPTION

---

### 3.1 INTRODUCTION

In developing countries, streams and rivers are being exploited unwisely as means for waste disposal from domestic, industrial and agricultural sectors beyond their assimilating power of the streams. When the pollutants are disposed into water bodies, some basic processes like advection, diffusion, dispersion and decay take place. During transport of the solute, the bed soils and sediments adsorb some portion of the pollutants. The reverse process takes place when the concentration of pollutant is reduced in the moving water. The exchange of the pollutants between the solid and liquid phases is non-equilibrium in nature. Simulating non-equilibrium sorption processes along with advection and dispersion, which govern the transport of the pollutants, is a difficult task due the complexity of the adsorption and desorption processes (Cameron and Klute, 1977). Ghosh (2001) conceptualized a Hybrid Cells-in-Series (HCIS) model to simulate the transport of conservative solute in river. By discretising the time domain, and adopting Freundlich non-equilibrium adsorption isotherm in HCIS model, Ghosh (2001) estimated the concentration of conservative solute in a river. Scientific studies (Cameron and Klute, 1977; Bear and Bachmat, 1990; Bajracharya and Barry, 1992) illustrate that the adsorption processes more attenuate the concentration of the pollutants. So an exact simulation of the pollutants' transport is essential to ascertain the assimilation capacity of rivers. In this study, it has been assumed that the non-equilibrium Freundlich adsorption isotherm governs adsorption-desorption process. A semi analytical solution for pollutant transport in a stream consequence to advection, dispersion and adsorption has been derived using the Laplace transform technique and HCIS model.

### 3.2 STATEMENT OF THE PROBLEM

Consider a conceptualized hybrid cells in series model as shown in Fig. 3.1 with adsorption (HCIS-A) consisting of a plug flow zone and two thoroughly mixed zones of different residence time all connected in series. Let the initial concentration of pollutant in each zone be  $C_i$ . The boundary concentration changes from  $C_i$  to  $C_R$  at  $t = 0$ . In the plug flow zone, the fluid gets replaced in a time  $\alpha$ , which is equal to the ratio of the volume of plug flow zone to the volumetric throughput or stream flow rate. In the first thoroughly mixed zone, the residence time of fluid is  $T_1$ . In the second thoroughly mixed zone, the residence time is  $T_2$ . Let the flow rate be  $Q \text{ m}^3 / \text{unit time}$  and flow be under steady state condition. Let the exclusively plug flow zone is as shown in Fig. 3.2. The plug flow zone is conceptualized as a series of compartments. The length of each compartment is  $\Delta x_p$  and velocity of water is  $u$ . A plume of water in each compartment stays for a time interval  $\Delta x_p / u$  and then replaced by an incoming plume. Such replacements take place in all compartments in the plug flow zone simultaneously. This means, in any compartment there is no intermixing of the pollutant with the pollutants in either the leading or the following compartments. While moving to downstream, the pollutant loses some fraction of its concentration due to adsorption activity by the riverbed materials. Adsorption of pollutant is assumed to follow the simplified Freundlich adsorption isotherm of non-equilibrium type. Within the advanced moving front in the plug flow zone in a particular compartment at  $x_0$ , the rate of adsorption is given by:

$$\frac{dC_s(x_0, t)}{dt} = R_D [C(x_0, t) - C_s(x_0, t)] \quad (3.1)$$

where,  $R_D$  is proportionality constant ( $T^{-1}$ ),  $C_s(x_0, t)$  is the concentration of pollutant adsorbed ( $ML^{-3}$ ),  $C(x_0, t)$  is the concentration of pollutant in the water column ( $ML^{-3}$ ),  $t$  is the time (T). It is aimed to predict the temporal and spatial distribution of solute concentration in a stream that is conceptualized as a series of hybrid cells.

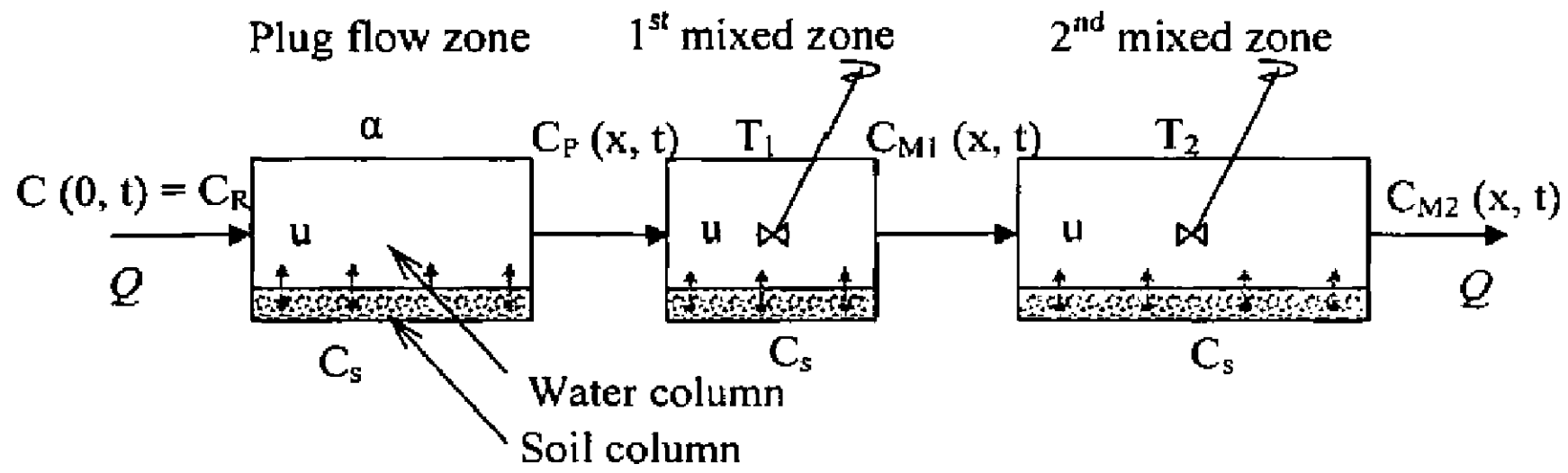


**Fig. 3.1: Conceptualized unit of Hybrid Cells in Series Model incorporating adsorption**

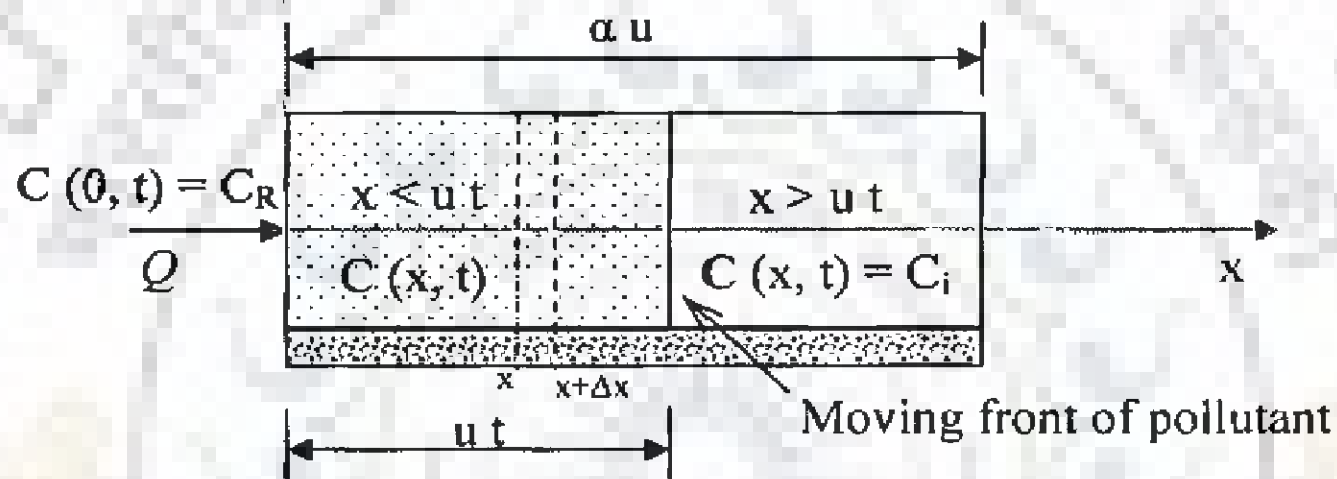


**Fig. 3.2: Pollutant transport through plug flow zone for a unit step input.**

### 3.3 FORMULATION OF MODEL

#### 3.3.1 Derivation of Concentration of Pollutant in the Plug Flow Zone

Consider a control volume which consists of water column and soil column within the plug flow zone. The pollutant transported thorough water column gets adsorbed by the materials of soil column or exchanged with adjacent pore water. Let the concentration of the pollutant in the water column be  $C(x, t)$ . In a small time interval  $\Delta t$ , some fraction of the pollutant is adsorbed, and then the remaining pollutant in the water column is moved forward to the next control volume in which concentration is  $C(x+\Delta x_p, t+\Delta t)$ . Within each control volume in the water column the pollutant is uniformly distributed. For a steady state flow condition, the mass balance equation is



$$\begin{aligned}
& Q \Delta t C(x, t) - W_p D_B \Delta x_p \phi \left\{ \left[ \frac{C_s(x, t + \Delta t) + C_s(x + \Delta x_p, t + \Delta t)}{2} \right] - \left[ \frac{C_s(x, t) + C_s(x + \Delta x_p, t)}{2} \right] \right\} \\
& = Q \Delta t C(x + \Delta x_p, t + \Delta t) \tag{3.2}
\end{aligned}$$

Using Taylor series of expansion,

$$C_s(x, t + \Delta t) = C_s(x, t) + \frac{\partial C_s(x, t)}{\partial t} \Delta t + \dots$$

$$C_s(x + \Delta x_p, t) = C_s(x, t) + \frac{\partial C_s(x, t)}{\partial x} \Delta x_p + \dots$$

$$C_s(x + \Delta x_p, t + \Delta t) = C_s(x, t) + \frac{\partial C_s(x, t)}{\partial t} \Delta t + \frac{\partial C_s(x, t)}{\partial x} \Delta x_p + \frac{\partial}{\partial x} \left( \frac{\partial C_s(x, t)}{\partial t} \Delta t \right) \Delta x_p + \dots$$

$$C(x + \Delta x_p, t + \Delta t) = C(x, t) + \frac{\partial C(x, t)}{\partial t} \Delta t + \frac{\partial C(x, t)}{\partial x} \Delta x_p + \frac{\partial}{\partial x} \left( \frac{\partial C(x, t)}{\partial t} \Delta t \right) \Delta x_p + \dots$$

Incorporating these in Eq. (3.2)

$$\begin{aligned}
& Q \Delta t \left[ C(x, t) + \frac{\partial C(x, t)}{\partial t} \Delta t + \frac{\partial C(x, t)}{\partial x} \Delta x_p + \frac{\partial}{\partial x} \left( \frac{\partial C(x, t)}{\partial t} \Delta t \right) \Delta x_p \right] - Q \Delta t C(x, t) \\
& = - \frac{\phi W_p D_B \Delta x_p}{2} \left\{ \left[ \left( C_s(x, t) + \frac{\partial C_s(x, t)}{\partial t} \Delta t \right) + \left( C_s(x, t) + \frac{\partial C_s(x, t)}{\partial t} \Delta t + \frac{\partial C_s(x, t)}{\partial x} \Delta x_p \right) \right. \right. \\
& \quad \left. \left. + \frac{\partial}{\partial x} \left( \frac{\partial C_s(x, t)}{\partial t} \Delta t \right) \Delta x_p \right] - \left[ C_s(x, t) + \left( C_s(x, t) + \frac{\partial C_s(x, t)}{\partial x} \Delta x_p \right) \right] \right\}
\end{aligned}$$

Neglecting higher order terms in Taylor series of expansion and simplifying by equating  $Q = u A$  and  $u = \Delta x_p / \Delta t$ ,

$$\frac{\partial C(x, t)}{\partial t} = - u \frac{\partial C(x, t)}{\partial x} - \frac{\phi W_p D_B}{A} \frac{\partial C_s(x, t)}{\partial t} \tag{3.3}$$

where,  $C(x, t)$  is concentration of pollutant in the water column ( $ML^{-3}$ ),  $C_s(x, t)$  is concentration of pollutant in the soil column ( $ML^{-3}$ ),  $W_p$  is the wetted surface area per unit length of the stream (L),  $D_B$  is the average thickness of the adsorbing layer surrounding the wetted perimeter of the stream (L),  $u$  is the flow velocity ( $LT^{-1}$ ),  $\phi$  is the porosity,  $A$  is the cross sectional area of flow ( $L^2$ ),  $x$  is the distance from the point of injection (L), and  $t$  is



the time (T). Alternatively, the formulation of Eq. (3.3) has been done using Chain rule or Euler's principle as given in Appendix B.

The initial and boundary conditions to be satisfied for Eq. (3.3) are:

$$C(x, 0) = 0, \quad x > 0; \quad (3.4 \text{ a})$$

$$C_s(x, 0) = 0, \quad x > 0; \quad (3.4 \text{ b})$$

$$C(0, t) = C_R, \quad t \geq 0; \quad (3.4 \text{ c})$$

$$C_s(x, \infty) = C_R, \quad x > 0. \quad (3.4 \text{ d})$$

Taking Laplace transform for the Eq. (3.3)

$$\mathcal{L}\left(\frac{\partial C}{\partial t}\right) = s C^* - C e^{-st} \Big|_{t=0} = s C^* \quad (3.5)$$

$$\mathcal{L}\left(\frac{\partial C}{\partial x}\right) = \frac{dC^*}{dx} \quad (3.6)$$

$$\mathcal{L}\left(\frac{\partial C_s}{\partial t}\right) = s C_s^* - C_s e^{-st} \Big|_{t=0} = s C_s^* \quad (3.7)$$

where,  $C^*$ ,  $C_s^*$  are the Laplace Transforms of  $C$  and  $C_s$ , and  $s$  is the Laplace domain variable for time.

From Eq. (3.1), for constant input 'C',  $C_s(t)$  is given by

$$C_s(t) = C \left[ 1 - e^{-R_D t} \right] \quad (3.8)$$

In the plug flow zone, the input to any particular control volume will not be constant over different time while adsorption of pollutant takes place by stream bed materials. Consider the variable input  $C(\tau)$ , in that case  $C_s$  can be expressed as:

$$C_s(t) = \int_0^t C(\tau) k_s(t-\tau) d\tau \quad (3.9)$$

where,  $k_s$  is unit impulse response in respect of  $C_s$ . From Eq. (3.8)  $k_s(t) = R_D e^{-R_D t}$

Eq. (3.9) can be written as:

$$C_s(x, t) = \int_0^t C(x, \tau) k_s(x, t-\tau) d\tau \quad (3.10)$$

Now taking Laplace Transform for Eq. (3.10) by using Faultang theorem (Abramowitz and Stegun, 1970):

$$\mathcal{L}(C_s(x,t)) = \mathcal{L}\left(\int_0^t C(x,\tau) k_s(x,t-\tau) d\tau\right) = C^* k_s^* \quad (3.11 a)$$

Eq. (3.11 a) can be rewritten as follows:

$$\mathcal{L}(C_s(x,t)) = \mathcal{L}\left(\int_0^{x/u} C(x,\tau) k_s(x,t-\tau) d\tau + \int_{x/u}^t C(x,\tau) k_s(x,t-\tau) d\tau\right) = C^* k_s^* \quad (3.11 b)$$

At any  $x$ ,  $C(x, t) = 0$  for  $0 \leq t < x/u$ . Until the time  $t < x/u$ , the pollutant front does not travel the distance  $x$ . So at any distance  $x$  within the plug flow zone, the concentration of pollutant will be zero up to the time  $x/u$ .

Hence, Eq. (3.11 b) becomes

$$\mathcal{L}(C_s(x,t)) = \mathcal{L}\left(\int_{x/u}^t C(x,\tau) k_s(x,t-\tau) d\tau\right) = C^* k_s^* \quad (3.12)$$

where,  $C^*$  and  $k_s^*$  are the Laplace transforms of  $C$  and  $k_s$  respectively.

Eq. (3.8) can be modified to express  $C_s(x, t)$  for the constant input 'C' injected at a distance of  $x$  to a particular control volume as follows

$$C_s(x,t) = C \left(1 - e^{-R_D(t-x/u)}\right) \quad (3.13)$$

Eq. (3.13) is valid for  $t \geq x/u$

Differentiating Eq. (3.13) with respect to  $t$

$$k_s(x,t) = \frac{d}{dt} \left(\frac{C_s(x,t)}{C}\right) = R_D e^{-R_D(t-x/u)} \quad (3.14)$$

Taking Laplace Transform for Eq. (3.14)

$$\mathcal{L}(k_s(x,t)) = R_D \int_0^{\infty} e^{-R_D(t-x/u)} e^{-st} dt = R_D e^{R_D x/u} \left(\frac{1}{s + R_D}\right) \quad (3.15)$$

Substituting Eq. (3.15) in Eq. (3.12)

$$C_s^* = C^* R_D e^{R_D x/u} \left(\frac{1}{s + R_D}\right) \quad (3.16)$$

Substituting Eq. (3.16) in Eq. (3.7)

$$\mathcal{L}\left(\frac{\partial C_s}{\partial t}\right) = sC^* R_D e^{R_D x/u} \left(\frac{1}{s+R_D}\right) \quad (3.17)$$

Now Laplace Transform of Eq. (3.3) can be written incorporating Eqs. (3.5), (3.6) and (3.17) as

$$sC^* = -u \frac{dC^*}{dx} - \frac{\phi W_P D_B}{A} sC^* R_D e^{R_D x/u} \left(\frac{1}{s+R_D}\right) \quad (3.18)$$

Rearranging Eq. (3.18)

$$\frac{dC^*}{C^*} = - \left[ \frac{\phi W_P D_B R_D}{uA} e^{R_D x/u} \left(\frac{s}{s+R_D}\right) + \frac{s}{u} \right] dx \quad (3.19)$$

Integrating Eq. (3.19),

$$\ln C^* = - \frac{\phi W_P D_B}{A} \left(\frac{s}{s+R_D}\right) e^{R_D x/u} - s \frac{x}{u} + E \quad (3.20)$$

where,  $E$  is a constant of integration.

For  $x = 0$ ;  $C = C_R$  from condition given in Eq. (3.4 c).

$$C^*(0, s) = C_R \int_0^{\infty} e^{-st} dt = \frac{C_R}{s}$$

Hence,

$$E = \ln\left(\frac{C_R}{s}\right) + \frac{\phi W_P D_B}{A} \left(\frac{s}{s+R_D}\right) \quad (3.21)$$

Substituting Eq. (3.21) in Eq. (3.20),

$$\ln\left(\frac{C^*}{C_R/s}\right) = - \frac{\phi W_P D_B}{A} \left(e^{R_D x/u} - 1\right) \left(\frac{s}{s+R_D}\right) - s \frac{x}{u} \quad (3.22)$$

Hence,

$$\begin{aligned} C^* &= \frac{C_R}{s} \exp \left\{ - \frac{\phi W_P D_B}{A} \left(e^{R_D x/u} - 1\right) \left(\frac{s}{s+R_D}\right) - s \frac{x}{u} \right\} \\ &= \frac{C_R}{s} \exp \left\{ - \frac{\phi W_P D_B}{A} \left(e^{R_D x/u} - 1\right) \left(1 - \frac{R_D}{s+R_D}\right) - s \frac{x}{u} \right\} \end{aligned} \quad (3.23)$$

$$\begin{aligned}
&= \frac{C_R}{s} \exp \left\{ - \left[ \frac{\phi W_P D_B}{A} \left( e^{R_D x/u} - 1 \right) \right] + \left[ \frac{\phi W_P D_{B'}}{A} \left( e^{R_D x/u} - 1 \right) \left( \frac{R_D}{s + R_D} \right) \right] - s \frac{x}{u} \right\} \\
&= \frac{C_R}{s} \exp \left\{ - \frac{\phi W_P D_B}{A} \left( e^{R_D x/u} - 1 \right) \right\} \exp \left\{ \frac{\phi W_P D_{B'}}{A} \left( e^{R_D x/u} - 1 \right) \left( \frac{R_D}{s + R_D} \right) \right\} \exp \left[ -s \frac{x}{u} \right]
\end{aligned}$$

$$C^* = \frac{C_R}{s} \exp\{\beta\} \exp\left(\frac{\eta}{s + R_D}\right) \exp\left(-s \frac{x}{u}\right) \quad (3.24)$$

$$\text{where, } \beta = -\frac{\phi W_P D_B}{A} \left( e^{R_D x/u} - 1 \right); \quad \eta = \frac{\phi W_P D_{B'} R_D}{A} \left( e^{R_D x/u} - 1 \right)$$

After  $C^*$  is obtained, the original solution  $C$  is obtained by finding the inverse Laplace Transform for Eq. (3.24).

$$C = \mathcal{L}^{-1}\{C^*\} = C_R \exp\{\beta\} \mathcal{L}^{-1}\left\{\frac{1}{s} \exp\left(-s \frac{x}{u}\right) \exp\left[\frac{\eta}{s + R_D}\right]\right\} \quad (3.25)$$

From the table of Laplace transform,  $\mathcal{L}^{-1}\left\{\frac{1}{s} f(s)\right\} = \int_0^t F(\tau) d\tau$ , where,  $F = \mathcal{L}^{-1}(f)$

$$\mathcal{L}^{-1}\left\{\frac{1}{s} e^{-s \frac{x}{u}} e^{\left[\frac{\eta}{s + R_D}\right]}\right\} = \int_0^t \left[ \mathcal{L}^{-1}\left\{e^{-s \frac{x}{u}} e^{\left[\frac{\eta}{s + R_D}\right]}\right\} \right] d\tau \quad (3.26)$$

Expanding the exponential term  $e^{\frac{\eta}{s + R_D}}$

$$\mathcal{L}^{-1}\left\{e^{-s \frac{x}{u}} e^{\left[\frac{\eta}{s + R_D}\right]}\right\} = \mathcal{L}^{-1}\left\{e^{-s \frac{x}{u}} \left[1 + \frac{\eta}{s + R_D} + \frac{\eta^2}{2! (s + R_D)^2} + \frac{\eta^3}{3! (s + R_D)^3} + \dots\right]\right\}$$

From the table of Laplace transform,  $\mathcal{L}^{-1}\{e^{-as}\} = \delta(t - a)$

$$\mathcal{L}^{-1}\{e^{-as} f(s)\} = \begin{cases} F(t - a)U(t - a) & t \geq a \\ 0 & t < a \end{cases}$$

where,  $F = \mathcal{L}^{-1}(f)$  and  $U(t - a)$  is step function and  $\delta(t - a)$  is Dirac delta function.

$$\begin{aligned}
\mathcal{L}^{-1}\left\{e^{-s \frac{x}{u}} e^{\left[\frac{\eta}{s + R_D}\right]}\right\} &= \delta\left(t - \frac{x}{u}\right) + U\left(t - \frac{x}{u}\right) \left[ \frac{\eta}{1!} e^{-R_D \left(t - \frac{x}{u}\right)} \right. \\
&\quad \left. + \frac{\eta^2}{2!} \frac{\left(t - \frac{x}{u}\right)}{1!} e^{-R_D \left(t - \frac{x}{u}\right)} + \frac{\eta^3}{3!} \frac{\left(t - \frac{x}{u}\right)^2}{2!} e^{-R_D \left(t - \frac{x}{u}\right)} + \dots \right]
\end{aligned}$$

$$\begin{aligned}
&= \delta\left(t - \frac{x}{u}\right) + U\left(t - \frac{x}{u}\right) \eta e^{-R_D\left(t - \frac{x}{u}\right)} \left\{ 1 + \frac{\eta}{2!} \frac{\left(t - \frac{x}{u}\right)}{1!} + \frac{\eta^2}{3!} \frac{\left(t - \frac{x}{u}\right)^2}{2!} + \dots \right\} \\
&= \delta\left(t - \frac{x}{u}\right) + U\left(t - \frac{x}{u}\right) \eta e^{-R_D\left(t - \frac{x}{u}\right)} \left\{ \sum_{j=0}^{\infty} \frac{\left[\eta\left(t - \frac{x}{u}\right)\right]^j}{(j+1)! j!} \right\} \quad (3.27 \text{ a})
\end{aligned}$$

where,  $\delta(t-x/u)$  is the Dirac delta function.

Rewriting Eq. (3.27 a),

$$\mathcal{L}^{-1} \left\{ e^{-s\frac{x}{u}} e^{\frac{\eta}{s+R_D}} \right\} = \delta\left(t - \frac{x}{u}\right) + U\left(t - \frac{x}{u}\right) \eta e^{-R_D\left(t - \frac{x}{u}\right)} \left\{ \sum_{j=0}^{\infty} \frac{\left[ \frac{1}{4} \left( 2 \sqrt{\eta\left(t - \frac{x}{u}\right)} \right)^2 \right]^j}{\Gamma(j+2) j!} \right\} \quad (3.27 \text{ b})$$

Eq. (3.27 b) can be expressed alternatively as follows (Abramowitz and Stegun, 1970):

$$\mathcal{L}^{-1} \left\{ e^{-s\frac{x}{u}} e^{\frac{\eta}{s+R_D}} \right\} = \delta\left(t - \frac{x}{u}\right) + U\left(t - \frac{x}{u}\right) \eta e^{-R_D\left(t - \frac{x}{u}\right)} \left\{ \frac{1}{\sqrt{\eta\left(t - \frac{x}{u}\right)}} I_1\left(2 \sqrt{\eta\left(t - \frac{x}{u}\right)}\right) \right\} \quad (3.27 \text{ c})$$

where,  $I_1$  is the Modified Bessel function of first kind and first order.

Incorporating Eq. (3.27 c) in Eq. (3.26),

$$\begin{aligned}
\mathcal{L}^{-1} \left( \frac{1}{s} e^{-s\frac{x}{u}} e^{\frac{\eta}{s+R_D}} \right) &= \int_0^t \delta\left(\tau - \frac{x}{u}\right) d\tau \\
&+ \int_0^t U\left(\tau - \frac{x}{u}\right) \eta e^{-R_D\left(\tau - \frac{x}{u}\right)} \left\{ \frac{1}{\sqrt{\eta\left(\tau - \frac{x}{u}\right)}} I_1\left(2 \sqrt{\eta\left(\tau - \frac{x}{u}\right)}\right) \right\} d\tau \quad (3.28) \\
&= I_{n1} + I_{n2}
\end{aligned}$$

where,  $I_{n1}$  and  $I_{n2}$  are the first and the second integral in Eq. (3.28).

$$I_{n1} = \int_0^t \delta\left(\tau - \frac{x}{u}\right) d\tau = U\left(t - \frac{x}{u}\right) \quad (3.29)$$

$$I_{n2} = \sqrt{\eta} \int_0^t U\left(\tau - \frac{x}{u}\right) e^{-R_D\left(\tau - \frac{x}{u}\right)} \frac{1}{\sqrt{\tau - \frac{x}{u}}} I_1\left(2\sqrt{\eta\left(\tau - \frac{x}{u}\right)}\right) d\tau$$

$U(\tau - x/u) = 0$  for  $\tau < x/u$  and  $U(\tau - x/u) = 1$  for  $\tau \geq x/u$

Hence,

$$I_{n2} = \sqrt{\eta} \int_{x/u}^t U\left(\tau - \frac{x}{u}\right) e^{-R_D\left(\tau - \frac{x}{u}\right)} \frac{1}{\sqrt{\tau - \frac{x}{u}}} I_1\left(2\sqrt{\eta\left(\tau - \frac{x}{u}\right)}\right) d\tau$$

To remove the singularity at  $\tau = \frac{x}{u}$ , let us substitute,  $\tau - \frac{x}{u} = \mu^2$ ;  $d\tau = 2\mu d\mu$ .

$$\begin{aligned} I_{n2} &= \sqrt{\eta} \int_0^{\sqrt{t - \frac{x}{u}}} e^{-R_D \mu^2} \frac{1}{\mu} I_1(2\sqrt{\eta} \mu) 2\mu d\mu \\ &= 2\sqrt{\eta} \int_0^{\sqrt{t - \frac{x}{u}}} e^{-R_D \mu^2} I_1(2\sqrt{\eta} \mu) d\mu \end{aligned} \quad (3.30)$$

The limits of integration are changed for performing numerical integration for Eq. (3.30), by Gauss quadrature formula.

Let,  $\mu = a + b\nu$

where, a and b are unknown constants,  $\nu$  is another dummy variable.

At the lower limit  $\mu = 0$ ,  $\nu = -1$ ; hence,  $a - b = 0$ .

At the upper limit  $\mu = \sqrt{t - \frac{x}{u}}$ ,  $\nu = +1$ ; hence,  $a + b = \sqrt{t - \frac{x}{u}}$

Solving,  $a = b = \frac{\sqrt{t - \frac{x}{u}}}{2}$

Substituting  $\mu = \frac{\sqrt{t - \frac{x}{u}}}{2}(1 + \nu)$  and  $d\mu = \frac{\sqrt{t - \frac{x}{u}}}{2} d\nu$  in Eq. (3.30)

$$I_{n2} = \sqrt{\eta \left( t - \frac{x}{u} \right)} \int_{-1}^{+1} e^{-R_D \left[ \frac{\sqrt{t - \frac{x}{u}}}{2} (1+\nu) \right]^2} I_1 \left[ \sqrt{\eta \left( t - \frac{x}{u} \right)} (1+\nu) \right] d\nu \quad (3.31)$$

Incorporating Eq. (3.29) and Eq. (3.31) in Eq. (3.28)

$$\mathcal{L}^{-1} \left\{ \frac{1}{s} e^{-s \frac{x}{u}} e^{\left[ \frac{\eta}{s+R_D} \right]} \right\} = \left\{ U \left( t - \frac{x}{u} \right) + \sqrt{\eta \left( t - \frac{x}{u} \right)} \int_{-1}^{+1} e^{-R_D \left[ \frac{\sqrt{t - \frac{x}{u}}}{2} (1+\nu) \right]^2} I_1 \left[ \sqrt{\eta \left( t - \frac{x}{u} \right)} (1+\nu) \right] d\nu \right\}$$

Finally the solution  $C(x, t)$  is obtained by substituting  $\omega$ ,  $\eta$  &  $\mathcal{L}^{-1} \left\{ \frac{1}{s} e^{-s \frac{x}{u}} e^{\left[ \frac{\eta}{s+R_D} \right]} \right\}$  in Eq.

(3.25) as:

$$C(x, t) = C_R \exp \left[ - \frac{\phi W_p D_B \left( e^{R_D \frac{x}{u}} - 1 \right)}{A} \right] \left\{ 1 + \sqrt{\frac{\phi W_p D_B R_D \left( e^{R_D \frac{x}{u}} - 1 \right) \left[ t - \frac{x}{u} \right]}{A}} \int_{-1}^{+1} \exp \left[ -R_D \left( \frac{\sqrt{t - \frac{x}{u}}}{2} (1+\nu) \right)^2 \right] I_1 \left[ \frac{\phi W_p D_B R_D \left( e^{R_D \frac{x}{u}} - 1 \right) \left[ t - \frac{x}{u} \right]}{A} (1+\nu) \right] d\nu \right\} \quad (3.32)$$

which is valid for  $t \geq x/u$ . The response at the end of plug flow zone is  $C_P(a u, t)$  then described by Eq. (3.32).

### 3.3.2 Unit Step Response Function for the First Thoroughly Mixed Zone

Consider the first thoroughly mixed zone as shown in Fig. 3.3. The output of the plug flow zone enters the first thoroughly mixed zone after traveling a distance  $au$ . In order to find the solute concentration in the first thoroughly mixed zone, we first derive exclusively the unit step response function for the first thoroughly mixed zone. Consider a unit step input  $C_R$ , and perform the mass balance in the first thoroughly mixed zone over a time interval  $t$  to  $t + \Delta t$ .

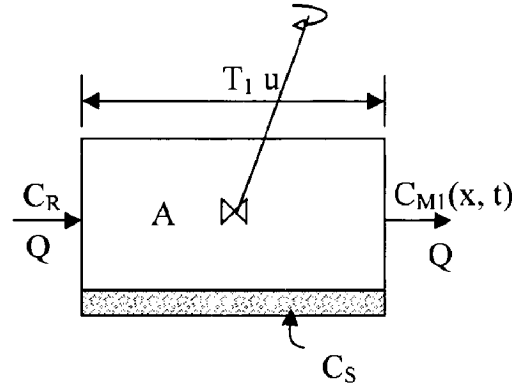


**Fig. 3.3: Exclusive pollutant transport through 1<sup>st</sup> thoroughly mixed zone for a unit step input.**

Expressing the mass balance equation in discrete form,

$$C_R u A \Delta t = C_{M1} u A \Delta t + V_1 \Delta C_{M1} + \Delta M_s \quad (3.33)$$

In which, the term in left side is the mass entering, the first term in right side is the mass leaving, the second term is change of mass within the zone and the third term is the mass adsorbed.

Rearranging the above,

$$C_R = C_{M1} + \frac{V_1}{u A} \frac{\Delta C_{M1}}{\Delta t} + \frac{1}{u A} \frac{\Delta M_s}{\Delta t}$$

$$C_R = C_{M1} + T_1 \frac{\Delta C_{M1}}{\Delta t} + \frac{T_1}{V_1} \frac{\Delta M_s}{\Delta t} \quad (3.34)$$

where,  $C_R$  is influent concentration ( $ML^{-3}$ ),  $C_{M1}$  is the pollutant concentration of the effluent of the first thoroughly mixed zone ( $ML^{-3}$ ),  $M_s$  is the mass of the pollutant adsorbed by the stream bed materials (M),  $V_1$  is the volume of the first thoroughly mixed zone ( $L^3$ ),  $T_1$  is the residence time of the first thoroughly mixed zone (T).

Eq. (3.34) is reduced to differential form as follows:

$$C_R = C_{M1} + T_1 \frac{dC_{M1}}{dt} + \frac{T_1}{V_1} \frac{dM_s}{dt} \quad (3.35)$$

where,  $M_s = \phi W_p D_B \Delta x_l C_s$  and  $V_1 = A \Delta x_l$

Substituting these and rearranging the Eq. (3.35),



$$\frac{dC_{M1}}{dt} = \frac{C_R}{T_1} - \frac{C_{M1}}{T_1} - \frac{\phi W_p D_B}{A} \frac{dC_s}{dt} \quad (3.36)$$

In the 1<sup>st</sup> thoroughly mixed zone, adsorption of pollutant by bed materials follows the Freundlich non-equilibrium adsorption isotherm, which is expressed as:

$$\frac{dC_s}{dt} = R_D(C_{M1} - C_s) \quad (3.37)$$

Eq. (3.36) and (3.37) are first order differential equations, containing two dependant variables ( $C_{M1}$  and  $C_s$ ). These are segregated into two different second order differential equations as follows:

Substituting Eq. (3.37) in Eq. (3.36),

$$\frac{dC_{M1}}{dt} = \frac{C_R}{T_1} - \frac{C_{M1}}{T_1} - \frac{\phi W_p D_B R_D C_{M1}}{A} + \frac{\phi W_p D_B R_D C_s}{A} \quad (3.38)$$

Expressing Eq. (3.38) as,

$$\frac{dC_{M1}}{dt} = a_1 C_{M1} + a_2 C_s + a_3 \quad (3.39)$$

$$\text{where, } a_1 = -\frac{1}{T_1} - \frac{\phi W_p D_B R_D}{A}; \quad a_2 = \frac{\phi W_p D_B R_D}{A}; \quad \text{and } a_3 = \frac{C_R}{T_1}$$

Let us express Eq. (3.37) as,

$$\frac{dC_s}{dt} = a_4 C_{M1} + a_5 C_s \quad (3.40)$$

where,  $a_4 = R_D$  &  $a_5 = -R_D$

Differentiating Eq. (3.39) with respect to  $t$

$$\frac{d^2 C_{M1}}{dt^2} = a_1 \frac{dC_{M1}}{dt} + a_2 \frac{dC_s}{dt} \quad (3.41)$$

Substituting Eq. (3.40) in Eq. (3.41)

$$\frac{d^2 C_{M1}}{dt^2} = a_1 \frac{dC_{M1}}{dt} + a_2 (a_4 C_{M1} + a_5 C_s) \quad (3.42)$$

From Eq. (3.39),

$$C_s = \frac{1}{a_2} \left( \frac{dC_{M1}}{dt} - a_1 C_{M1} - a_3 \right) \quad (3.43)$$

Substituting Eq. (3.43) in Eq. (3.42),

$$\frac{d^2 C_{M1}}{dt^2} = a_1 \frac{dC_{M1}}{dt} + a_2 \left\{ a_4 C_{M1} + a_5 \frac{1}{a_2} \left( \frac{dC_{M1}}{dt} - a_1 C_{M1} - a_3 \right) \right\} \quad (3.44)$$

Rearranging, Eq. (3.44) reduces to

$$\frac{d^2 C_{M1}}{dt^2} - (a_1 + a_5) \frac{dC_{M1}}{dt} + (a_1 a_5 - a_2 a_4) C_{M1} + a_3 a_5 = 0 \quad (3.45)$$

For solving Eq. (3.45), the Complementary Function and Particular Integral are found as follows:

The Complementary Function is

$$CF = A_1 e^{\lambda_1 t} + B_1 e^{\lambda_2 t}$$

The Particular Integral is:

$$PI = \frac{1}{\{D^2 - (a_1 + a_5)D + (a_1 a_5 - a_2 a_4)\}} (-a_3 a_5)$$

where,  $D$  is the differential operator.

Since  $(-a_3 a_5)$  is constant, the particular integral is:

$$PI = \frac{-a_3 a_5}{(a_1 a_5 - a_2 a_4)} = C_R$$

Complete Solution is

$$C_{M1} = A_1 e^{\lambda_1 t} + B_1 e^{\lambda_2 t} + C_R \quad (3.46)$$

$$\text{where, } \lambda_1 = \frac{(a_1 + a_5) + \sqrt{(a_1 - a_5)^2 + 4a_2 a_4}}{2}; \lambda_2 = \frac{(a_1 + a_5) - \sqrt{(a_1 - a_5)^2 + 4a_2 a_4}}{2}$$

Similarly differentiating Eq. (3.40) with respect to  $t$

$$\frac{d^2 C_s}{dt^2} = a_4 \frac{dC_{M1}}{dt} + a_5 \frac{dC_s}{dt} \quad (3.47)$$

Substituting Eq. (3.39) in Eq. (3.47),

$$\frac{d^2 C_s}{dt^2} = a_4 (a_1 C_{M1} + a_2 C_s + a_3) + a_5 \frac{dC_s}{dt} \quad (3.48)$$

From Eq. (3.40),

$$C_{M1} = \frac{1}{a_4} \left( \frac{dC_s}{dt} - a_5 C_s \right) \quad (3.49)$$

Substituting Eq. (3.49) in Eq. (3.48),

$$\frac{d^2C_s}{dt^2} = a_4 \left\{ a_1 \frac{1}{a_4} \left( \frac{dC_s}{dt} - a_5 C_s \right) + a_2 C_s + a_3 \right\} + a_5 \frac{dC_s}{dt} \quad (3.50)$$

Rearranging and incorporating  $a_3 a_4 = -a_3 a_5$ , Eq. (3.50) reduces to

$$\frac{d^2C_s}{dt^2} - (a_1 + a_5) \frac{dC_s}{dt} + (a_1 a_5 - a_2 a_4) C_s + a_3 a_5 = 0 \quad (3.51)$$

Solving Eq. (3.51) by finding Complementary Function and Particular Integral,

$$C_s = A_2 e^{\lambda_1 t} + B_2 e^{\lambda_2 t} + C_R \quad (3.52)$$

$$\text{where, } \lambda_1 = \frac{(a_1 + a_5) + \sqrt{(a_1 - a_5)^2 + 4a_2 a_4}}{2}; \lambda_2 = \frac{(a_1 + a_5) - \sqrt{(a_1 - a_5)^2 + 4a_2 a_4}}{2}$$

Differentiating Eq. (3.46) and Eq. (3.52) with respect to  $t$ ,

$$\frac{dC_{M1}}{dt} = A_1 \lambda_1 e^{\lambda_1 t} + B_1 \lambda_2 e^{\lambda_2 t} \quad (3.53)$$

$$\frac{dC_s}{dt} = A_2 \lambda_1 e^{\lambda_1 t} + B_2 \lambda_2 e^{\lambda_2 t} \quad (3.54)$$

Applying initial and boundary conditions in Eq. (3.46), Eq. (3.52), Eq. (3.53) and Eq. (3.54), i.e

at  $t = 0$ ;  $C_{M1} = 0$ ;  $\frac{dC_{M1}}{dt} = \frac{C_R}{T_1}$ ; &  $C_s = 0$ , the following relations are obtained:

$$A_1 + B_1 + C_R = 0$$

$$A_2 + B_2 + C_R = 0$$

$$A_1 \lambda_1 + B_1 \lambda_2 = \frac{C_R}{T_1}$$

$$A_2 \lambda_1 + B_2 \lambda_2 = 0$$

Solving the above,

$$A_1 = \frac{C_R \left( \lambda_2 + \frac{1}{T_1} \right)}{\lambda_1 - \lambda_2}; \quad B_1 = \frac{-C_R \left( \lambda_1 + \frac{1}{T_1} \right)}{\lambda_1 - \lambda_2}$$

$$A_2 = \frac{C_R \lambda_2}{\lambda_1 - \lambda_2}; \quad B_2 = \frac{-C_R \lambda_1}{\lambda_1 - \lambda_2}$$

Substituting these in Eq. (3.46) and Eq. (3.52) the concentration of the pollutant at the outlet of the first thoroughly mixed zone and the concentration of the pollutant adsorbed by the stream bed materials are found as:

$$C_{M1} = C_R \left\{ 1 + \left( \frac{\lambda_2 + \frac{1}{T_1}}{\lambda_1 - \lambda_2} \right) e^{\lambda_1 t} - \left( \frac{\lambda_1 + \frac{1}{T_1}}{\lambda_1 - \lambda_2} \right) e^{\lambda_2 t} \right\} \quad (3.55)$$

$$C_s = C_R \left\{ 1 + \left( \frac{\lambda_2}{\lambda_1 - \lambda_2} \right) e^{\lambda_1 t} - \left( \frac{\lambda_1}{\lambda_1 - \lambda_2} \right) e^{\lambda_2 t} \right\} \quad (3.56)$$

$$\text{where, } \lambda_1 = \frac{(a_1 + a_5) + \sqrt{(a_1 - a_5)^2 + 4a_2 a_4}}{2}; \quad \lambda_2 = \frac{(a_1 + a_5) - \sqrt{(a_1 - a_5)^2 + 4a_2 a_4}}{2}$$

$$a_1 = -\frac{1}{T_1} - \frac{\phi W_P D_B R_D}{A}; \quad a_2 = \frac{\phi W_P D_B R_D}{A}; \quad a_4 = R_D \quad \& \quad a_5 = -R_D$$

For any value of  $\phi$ ,  $W_P$ ,  $D_B$ ,  $R_D$ ,  $T_1$ ,  $A$ ,  $C_R$ , the root of Eq. (3.51),  $\lambda_2$  will be negative as  $a_1$  and  $a_5$  having negative value. Substituting  $a_1$ ,  $a_2$ ,  $a_4$ , and  $a_5$  in expression of  $\lambda_1$  and canceling out the common terms, it can be noted that  $|(a_1 + a_5)| > \left| \sqrt{(a_1 - a_5)^2 + 4a_2 a_4} \right|$ . So the other root of Eq. (3.51),  $\lambda_1$  is always negative.

### 3.3.3 Unit Step Response Function for the Second Thoroughly Mixed Zone

The second thoroughly mixed zone, shown in Fig. 3.4, differs from the first only in the residence time ( $T_2$ ). Performing mass balance in the second mixed zone over a time interval  $t$  to  $t + \Delta t$  for a unit step input of  $C_R$ , the concentration of pollutant in the second mixed zone can be derived in the similar manner as carried out for the first thoroughly mixed zone.

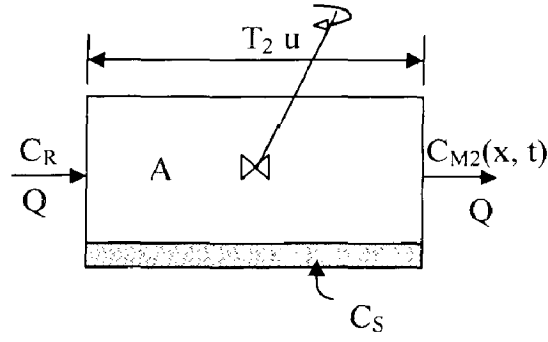


**Fig. 3.4: Exclusive pollutant transport through 2<sup>nd</sup> thoroughly mixed zone for a unit step input.**

The step response function of the second thoroughly mixed zone and the concentration of the pollutant adsorbed by the stream bed materials for a step input can be written as:

$$C_{M2} = C_R \left\{ 1 + \left( \frac{\hat{\lambda}_2 + \frac{1}{T_2}}{\hat{\lambda}_1 - \hat{\lambda}_2} \right) e^{\hat{\lambda}_1 t} - \left( \frac{\hat{\lambda}_1 + \frac{1}{T_2}}{\hat{\lambda}_1 - \hat{\lambda}_2} \right) e^{\hat{\lambda}_2 t} \right\} \quad (3.57)$$

$$C_s = C_R \left\{ 1 + \left( \frac{\hat{\lambda}_2}{\hat{\lambda}_1 - \hat{\lambda}_2} \right) e^{\hat{\lambda}_1 t} - \left( \frac{\hat{\lambda}_1}{\hat{\lambda}_1 - \hat{\lambda}_2} \right) e^{\hat{\lambda}_2 t} \right\} \quad (3.58)$$

$$\text{where, } \hat{\lambda}_1 = \frac{(\hat{a}_1 + \hat{a}_5) + \sqrt{(\hat{a}_1 - \hat{a}_5)^2 + 4\hat{a}_2\hat{a}_4}}{2}; \quad \hat{\lambda}_2 = \frac{(\hat{a}_1 + \hat{a}_5) - \sqrt{(\hat{a}_1 - \hat{a}_5)^2 + 4\hat{a}_2\hat{a}_4}}{2}$$

$$\hat{a}_1 = -\frac{1}{T_2} - \frac{\phi W_p D_B R_D}{A}; \quad \hat{a}_2 = \frac{\phi W_p D_B R_D}{A}; \quad \hat{a}_4 = R_D \quad \& \quad \hat{a}_5 = -R_D$$

### 3.3.4 Derivation of Concentration of Pollutant by Discrete Kernel Approach

The Eq. (3.32), Eq. (3.55) and Eq. (3.57) give the individual step response function of plug flow zone and the two thoroughly mixed zones where in adsorption is taking place. Using these basic solutions, the unit step response function of a hybrid unit is derived using convolution technique. Consider a unit step input injected at the entrance of the plug flow zone. The output from plug flow zone is the input to the 1<sup>st</sup> mixed zone and consecutively

to the 2<sup>nd</sup> mixed zone. For the unit step input at the inlet of plug flow zone, the response at the end of 1<sup>st</sup> thoroughly mixed zone can be derived as follows

$$\begin{aligned}
 C_1(t) &= \int_0^t \frac{dC_p(\tau)}{d\tau} K_{M1}(t-\tau) d\tau \\
 &= \int_0^{\Delta t} \frac{dC_p(\tau)}{d\tau} K_{M1}(t-\tau) d\tau + \int_{\Delta t}^{2\Delta t} \frac{dC_p(\tau)}{d\tau} K_{M1}(t-\tau) d\tau + \\
 &\quad \dots + \int_{(n-1)\Delta t}^{n\Delta t} \frac{dC_p(\tau)}{d\tau} K_{M1}(t-\tau) d\tau
 \end{aligned} \tag{3.59}$$

where,  $K_{M1}$  is the unit step response function of the 1<sup>st</sup> thoroughly mixed zone;  $C_p(t)$  is the response of the plug flow zone to a step input.

Let a ramp kernel co-efficient  $\delta_{M1}(m, \Delta t)$  be defined as:

$$\delta_{M1}(m, \Delta t) = \frac{1}{\Delta t} \int_0^{\Delta t} K_{M1}(m\Delta t - \tau) d\tau \tag{3.60}$$

where,  $m$  is an integer.

Incorporating  $K_{M1}(m\Delta t - \tau)$  in Eq. (3.60)

$$\delta_{M1}(m, \Delta t) = \frac{1}{\Delta t} \int_0^{\Delta t} \left\{ 1 + \frac{\lambda_2 + \frac{1}{T_1}}{\lambda_1 - \lambda_2} e^{\lambda_1(m\Delta t - \tau)} - \frac{\lambda_1 + \frac{1}{T_1}}{\lambda_1 - \lambda_2} e^{\lambda_2(m\Delta t - \tau)} \right\} d\tau \tag{3.61}$$

Performing the integration

$$\delta_{M1}(m, \Delta t) = \frac{1}{\Delta t} \left\{ \Delta t + \frac{1}{\lambda_1} \left( \frac{\lambda_2 + \frac{1}{T_1}}{\lambda_1 - \lambda_2} \right) e^{\lambda_1 m \Delta t} (1 - e^{-\lambda_1 \Delta t}) - \frac{1}{\lambda_2} \left( \frac{\lambda_1 + \frac{1}{T_1}}{\lambda_1 - \lambda_2} \right) e^{\lambda_2 m \Delta t} (1 - e^{-\lambda_2 \Delta t}) \right\} \tag{3.62}$$

The concentration  $C_1(n\Delta t)$  of the first thoroughly mixed zone is

$$C_1(n\Delta t) = \sum_{\gamma=1}^n \{ C_p(\gamma\Delta t) - C_p((\gamma-1)\Delta t) \} \delta_{M1}[(n-\gamma+1), \Delta t] \tag{3.63}$$

$C_1(n\Delta t)$  is the input to the 2<sup>nd</sup> thoroughly mixed zone. Using the ramp kernel of the second thoroughly mixed zone, the concentration of the solute in the second mixed zone is

$$K_{HCIS-A}(n\Delta t) = C_2(n\Delta t) = \sum_{\gamma=1}^n \{ C_1(\gamma\Delta t) - C_1((\gamma-1)\Delta t) \} \delta_{M2}[(n-\gamma+1), \Delta t] \tag{3.64}$$

The kernel co-efficient  $\delta_{M1} (m \Delta t)$  and  $\delta_{M2} (m \Delta t)$  are similar except in the residence time (i.e.  $T_1$  and  $T_2$ ). The Eq. (3.64) predicts the concentration of pollutant at the end of one hybrid unit for a unit step input injected at the entrance of the plug flow zone. For a unit pulse input, the unit pulse response function  $\delta_{HCIS-A} (n, \Delta t)$  is

$$k_{HCIS-A} (n, \Delta t) = \delta_{HCIS-A} (n, \Delta t) = \frac{K_{HCIS-A} (n\Delta t) - K_{HCIS-A} ((n-1)\Delta t)}{\Delta t} \quad (3.65)$$

Let the stream reach downstream of a point source of pollution be composed of a series of equal size hybrid units each having linear dimension  $\Delta x$  and consisting of a plug flow zone, and two unequal thoroughly mixed reservoirs, as shown in Fig. 3.5.

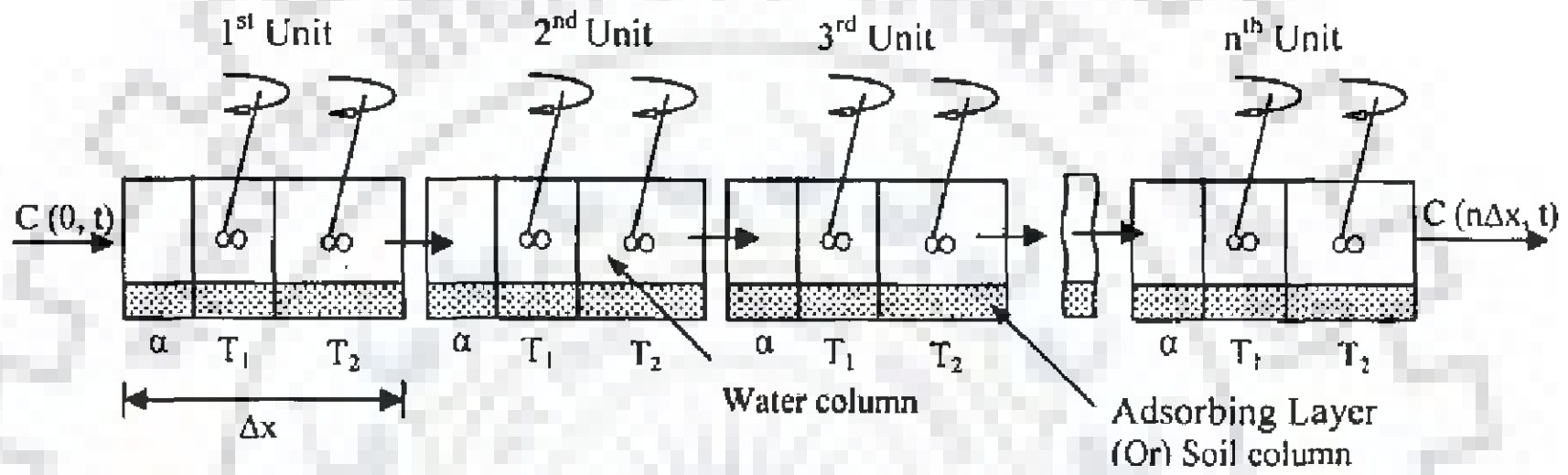


**Fig. 3.5: Composed series of hybrid units representing a stream reach of  $n \Delta x$  length.**

Using the convolution technique, the response of the  $i$ th hybrid unit,  $i \geq 2$ , is expressed as

$$C(i \Delta x, n \Delta t) = \sum_{\gamma=1}^n C((i-1) \Delta x, \gamma) \delta_{HCIS-A} (n-\gamma+1, \Delta t) \quad (3.66)$$

### 3.4 COMPARISON OF HCIS-A MODEL WITH THE ADE MODEL CONSIDERING NON-EQUILIBRIUM FREUNDLICH ADSORPTION ISOTHERM

One can formulate the Fickian based advection dispersion adsorption equation model as:

$$\frac{\partial C}{\partial t} = -u \frac{\partial C}{\partial x} + D_L \frac{\partial^2 C}{\partial x^2} - \frac{\phi W_P D_B}{A} \frac{\partial C_S}{\partial t} \quad (3.67)$$

where,  $C$  is the concentration of pollutant in the water column ( $ML^{-3}$ ),  $C_s$  is the concentration of pollutant in the soil column ( $ML^{-3}$ ),  $W_P$  is the wetted surface area per unit

length of the stream ( $L$ ),  $D_B$  is the average thickness of the adsorbing layer surrounding the wetted perimeter of the stream ( $L$ ),  $u$  is the flow velocity ( $LT^{-1}$ ),  $D_L$  is the longitudinal dispersion co-efficient ( $L^2T^{-1}$ ),  $\phi$  is the porosity,  $A$  is the cross sectional area of flow ( $L^2$ ),  $x$  is the distance from the point of injection ( $L$ ), and  $t$  is the time ( $T$ ).

The initial and boundary conditions to be satisfied for Eq. (3.67) are:

$$C(x, 0) = 0, \quad x > 0;$$

$$C_s(x, 0) = 0, \quad x > 0;$$

$$C(0, t) = C_R, \quad t \geq 0;$$

$$C_s(x, \infty) = C_R, \quad x > 0.$$

Adsorption of pollutant can be assumed to follow the simplified Freundlich adsorption isotherm of non-equilibrium equation

$$\frac{dC_s}{dt} = R_D [C - C_s] \quad (3.68)$$

where,  $R_D$  is proportionality constant ( $T^{-1}$ ),  $C$  is the concentration of pollutant in the water column ( $ML^{-3}$ ),  $C_s$  is the concentration of pollutant in the soil column ( $ML^{-3}$ ).

Many investigators (Hays et al., 1966; Nordin and Troutman, 1980; Bencala and Walters, 1983; Bencala et al., 1990; Runkel and Broshears, 1991; Runkel and Chapra, 1993; Czernuszenko and Rowinski, 1997; Runkel, 1998; Worman, 1998; Worman et al., 2002) have solved equations similar to Eq. (3.67) and (3.68) by numerical and semi-analytical methods. For demonstration, Eq. (3.67) and (3.68) are solved numerically by explicit scheme considering forward and central differences in time and space respectively.

The finite difference form of Eq. (3.67) is

$$\frac{C(x, t + \Delta t) - C(x, t)}{\Delta t} = -u \frac{C(x + \Delta x, t) - C(x - \Delta x, t)}{2\Delta x} + D_L \frac{C(x + \Delta x, t) - 2C(x, t) + C(x - \Delta x, t)}{(\Delta x)^2} - \frac{\phi W_p D_B}{A} \frac{C_s(x, t + \Delta t) - C_s(x, t)}{\Delta t} \quad (3.69)$$

The finite difference form of Eq. (3.68) is



$$\frac{C_s(x, t + \Delta t) - C_s(x, t)}{\Delta t} = R_D [C(x, t) - C_s(x, t)] \quad (3.70)$$

Combining Eq. (3.69) and (3.70) we obtain

$$\begin{aligned} C(x, t + \Delta t) = & C(x, t) \left[ 1 - \frac{2D_L \Delta t}{(\Delta x)^2} - \frac{\phi W_p D_B}{A} R_D \Delta t \right] + C(x + \Delta x, t) \left[ -\frac{u \Delta t}{2\Delta x} + \frac{D_L \Delta t}{(\Delta x)^2} \right] \\ & + C(x - \Delta x, t) \left[ \frac{u \Delta t}{2\Delta x} + \frac{D_L \Delta t}{(\Delta x)^2} \right] + C_s(x, t) \left[ \frac{\phi W_p D_B}{A} R_D \Delta t \right] \end{aligned} \quad (3.71)$$

Letting  $x = i \Delta x$ ,  $t = j \Delta t$

$$\begin{aligned} C(i, j + 1) = & C(i, j) \left[ 1 - \frac{2D_L \Delta t}{(\Delta x)^2} - \frac{\phi W_p D_B}{A} R_D \Delta t \right] + C(i + 1, j) \left[ -\frac{u \Delta t}{2\Delta x} + \frac{D_L \Delta t}{(\Delta x)^2} \right] \\ & + C(i - 1, j) \left[ \frac{u \Delta t}{2\Delta x} + \frac{D_L \Delta t}{(\Delta x)^2} \right] + C_s(i, j) \left[ \frac{\phi W_p D_B}{A} R_D \Delta t \right] \end{aligned} \quad (3.72)$$

where  $i = 1, 2, \dots, Imax$  and  $j = 0, 1, \dots, Jmax$ ;  $C(0, j) = C_R$  and  $C_s(i, 0) = 0$ .

$\Delta x Imax$  is the distance of interest from point of injection and  $\Delta t Jmax$  is the observation time of interest from time of injection.

Unit impulse response function is given by

$$k(i, j) = \frac{C(i, j + 1) - C(i, j)}{\Delta t} \quad (3.73)$$

The unit impulse response of Eq. (3.67) is computed from Eq. (3.73) and compared with that of HCIS-A model given by Eq. (3.65) for the following set of data:  $\alpha = 1.70 \text{ min}$ ;

$T_1 = 2.3 \text{ min}$ ;  $T_2 = 6.0 \text{ min}$ ;  $\Delta x = 200 \text{ m}$ ;  $\frac{\phi W_p D_B}{A} = 0.2$ ;  $u = 20 \text{ m/min}$ ;  $D_L = 1000 \text{ m}^2/\text{min}$

and  $R_D = 0.1 \text{ per min}$ . In order to avoid oscillations in the explicit scheme, the space and time grid size have been chosen as 20 m and 0.05 min respectively in such a way that  $u \Delta t > \Delta x / 10$ . The responses at 200 m from the point of injection have been presented in Fig.

3.6. From Fig. 3.6, it can be noted that the response of HCIS-A model closely matches with the numerical solution of Eq. (3.67).

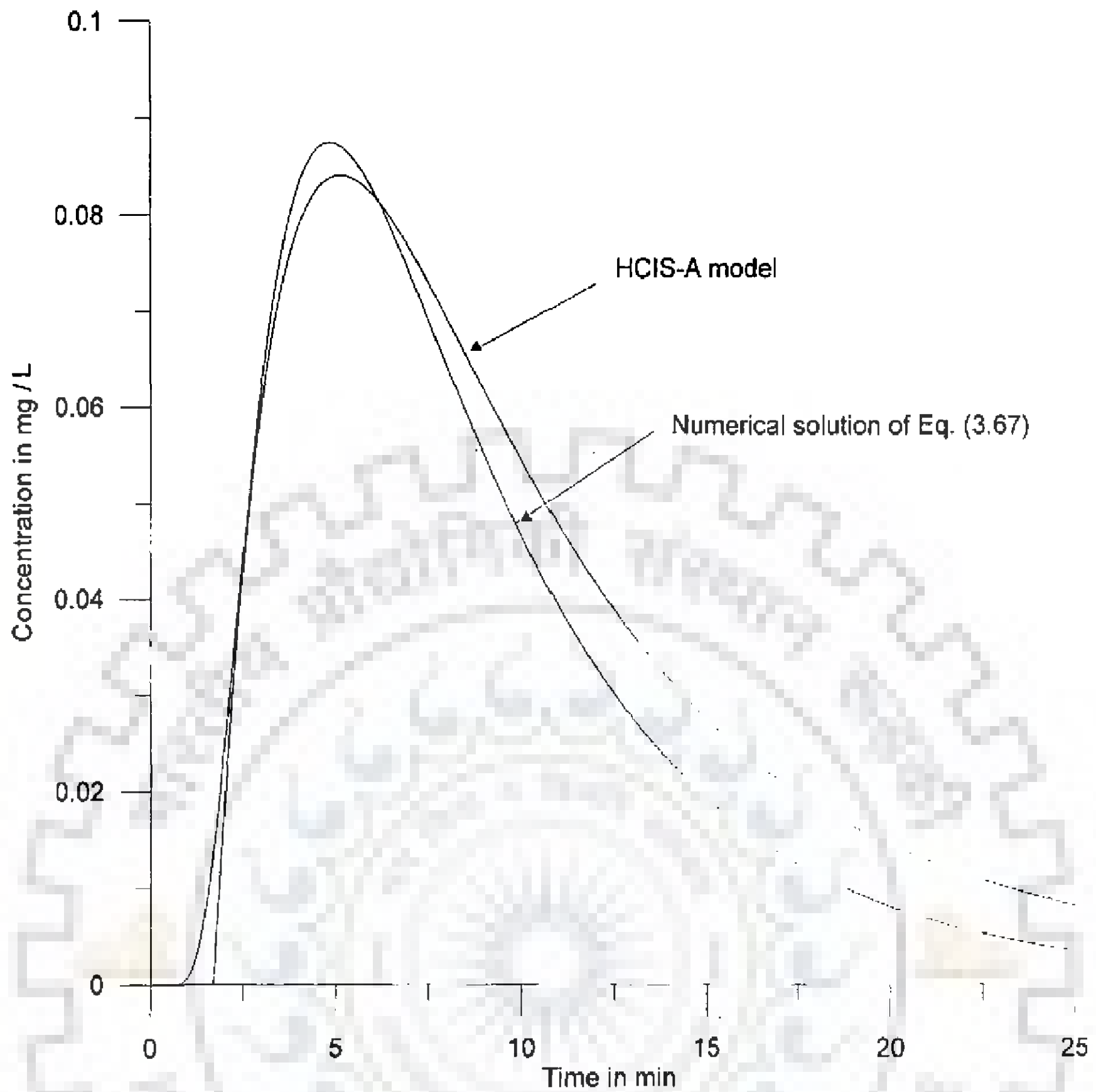


**Fig. 3.6: Impulse response functions of HCIS-A model and numerical solution of Eq. (3.67) at  $x = 200$  m**

### 3.5 RESULTS AND DISCUSSION

The HCIS model simulates the advection-dispersion governed transport of pollutant in a regular channel under uniform flow conditions when the size of the basic process unit,  $\Delta x$ , is equal to or more than  $4 D_L / u$ . This means that, the response of the three-parameter conceptual HCIS model with parameters,  $\alpha$ ,  $T_1$ , and  $T_2$ , which are linked to the flow velocity  $u$  in the stream, is nearly identical to that of the response of the two-parameter ( $u$ ,  $D_L$ ) ADE model at distance  $n\Delta x$ , where  $n$  = an integer, for the same  $u$  and  $D_L$ .

Let the three time parameters,  $\alpha$ ,  $T_1$ , and  $T_2$  of the HCIS model have been predicted from the ADE model for a given value of  $u$  and  $D_L$  satisfying Peclet number,  $P_e \geq 4$ . For  $u = 20 \text{ m / min}$ ,  $D_L = 1000 \text{ m}^2 / \text{min}$ , the HCIS model parameters are:  $\alpha = 1.70 \text{ min}$ ;  $T_1 = 2.3 \text{ min}$ ;  $T_2 = 6.0 \text{ min}$ . Corresponding to the flow velocity  $u=20\text{m/min}$ , the length of the plug flow zone is 34m. To illustrate the adsorption process in the plug flow zone, variation of the solute concentration at the end of plug flow zone with time is presented in Fig. 3.7, which have been computed making use of Eq. (3.32) for different values of  $R_D$  ( $=0, 0.1$  and  $0.25$  per min) for  $\frac{\phi W_p D_B}{A} = 0.1$

At the first arrival time,  $\alpha$ , of the solute at the end of the plug flow zone, the concentration is  $0.948 \text{ mg / L}$  for  $R_D = 0.25$  per min. The reduction in concentration is due to the adsorption in the plug flow zone. With the passage of time, as the rate of adsorbing capacity within the plug flow zone decreases, the concentration of effluent from the plug flow zone increases with time. The solute concentration is nearly equal to the boundary concentration at about 14 min. Fig. 3.7 depicts the unit step response function of the plug flow zone.

The concentration-time distribution in water,  $C(\alpha u, t)$  and soil columns,  $C_s(\alpha u, t)$  at the end of plug flow zone are computed using Eq. (3.32) and Eq. (3.10) for  $R_D = 0.25$  per min and the above set of the parameters and presented in Fig. 3.8.

Making use of the above set of parameters, using Eq. (3.32), the spatial effluent concentration distributions have been computed for different values of  $R_D$  (0.0, 0.1 and

0.25 per min) and presented in Fig. 3.9. In Fig. 3.9, the effluent concentrations at  $x = 34$  are the concentration of pollutant at first arrival time.

The unit step responses of a thoroughly mixed zone are presented in Fig. 3.10 for values of  $R_D$  ( $=0.0, 0.1, 0.2$  and  $0.3$ ) and  $T_I = 2.3$  min. These are exclusively response of an individual unit. In a single thoroughly mixed reservoir in which absorption takes place, the pollutant concentration in the effluent starts from zero and attains boundary concentration at a slower rate than the effluent from a mixed reservoir where adsorption does not take place.

Unit step response functions of a thoroughly mixed zone are presented in Fig 3.11 for residence time equal to 2.3 min and 6.0 min for  $R_D = 0.1$  per min. In case of the reservoir with lesser residence time, effluent attains boundary concentration more rapidly than the effluent from a thoroughly mixed zone with larger residence time.

Unit step response functions, of a hybrid unit computed using Eq. (3.64), are presented in Fig. 3.12 for the following set of data:  $\alpha = 1.70$  min;  $T_I = 2.3$  min;  $T_2 = 6.0$  min;  $\Delta x = 200$  m;  $\frac{\phi W_P D_B}{A} = 0.1$ ;  $u = 20$  m/min;  $D_L = 1000$  m<sup>2</sup>/min and  $R_D = 0, 0.1, 1.0$  per min. The pollutant concentration is zero until time  $t = \alpha$ , and increases with time to attain boundary concentration. For the higher  $R_D$  value, the pollutant gets more adsorbed initially; therefore, the pollutant concentration in the effluent for higher  $R_D$  is less than that for lower  $R_D$ . But as absorption rate in the plug flow zone decreases with time, the solute concentration of the effluent from plug flow zone increases faster at later time to reach the boundary concentration earlier than that of with lesser  $R_D$  value.

Making use of the above set of the parameters, the unit pulse responses, of a hybrid unit computed using Eq. (3.65), are presented in Fig. 3.13 where unit pulse duration has been taken as 0.05 min. The peak concentration decreases and a longer tail in falling limb are exhibited with increasing  $R_D$  value. The time to peak marginally decreases, as  $R_D$  value increases to 0.25 per min. Further increase in  $R_D$ , increases the time to peak.

Unit step and unit pulse response functions of a hybrid unit for  $R_D = 0.0$ ,  $\alpha = 1.70$  min;  $T_1 = 2.3$  min;  $T_2 = 6.0$  min;  $\Delta x = 200$  m;  $\frac{\phi W_P D_B}{A} = 0.1$ ;  $u = 20$  m/min and  $D_L = 1000$  m<sup>2</sup>/min are compared with those obtained from Ogata and Banks' (1961) analytical solution of ADE model at a distance of 200 m from injection point for  $u = 20$  m / min and  $D_L = 1000$  m<sup>2</sup> / min in Figs. 3.14 and 3.15 respectively. There is a marginal difference in peak concentrations in the unit pulse response functions of hybrid model and the ADE model. This difference is due to the space discretization in the hybrid model. The unit step response function obtained from the present study is close to that obtained from Ogata and Banks' (1961) solution.

Making use of the values of above set of parameters ( $\alpha$ ,  $T_1$ ,  $T_2$ ,  $\Delta x$ ,  $\frac{\phi W_P D_B}{A}$ ,  $u$  and  $D_L$ ) the unit pulse response functions have been generated for values of  $R_D = 0.1$  per min and 0 at the end of 2<sup>nd</sup>, 5<sup>th</sup> and 10<sup>th</sup> hybrid units using Eq. (3.66) and are shown in Fig. 3.16. From  $C-t$  profiles shown in Fig. 3.16, it can be seen that, as the pollutants move from the near field to the far field, the  $C-t$  distributions undergoing absorption get more and more attenuated and elongated and the peak concentrations reduces in comparison to those without absorption.

The influence of the dimensionless parameter  $\frac{\phi W_P D_B}{A}$  on effluent concentration is shown in Fig. 3.17. For stream with large width, the dimensionless parameter is nearly equal to porosity  $\phi$ . Higher the porosity means larger dead zone volume interacts with the transport of the solute in the main stream. With larger volume of dead zone, the peak concentration gets reduced, the time to peak is marginally reduced and the falling limb gets elongated. Variations of peak concentration with volume of dead zone at the end of the first and fifth hybrid units are presented in Fig. 3.18. The peak concentration decreases linearly with porosity or dead zone storage volume.

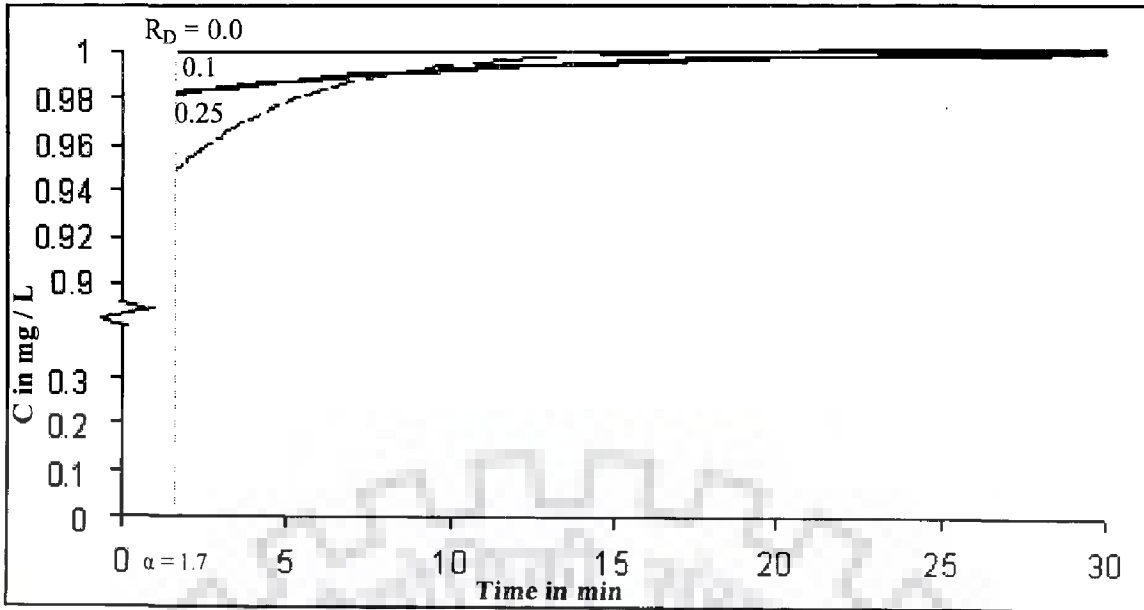


Fig. 3.7: Concentration – time profile at the end of the plug flow zone (34 m) for different values of  $R_D$  and  $\alpha = 1.7$  min;  $u = 20$  m / min;  $\frac{\phi W_P D_B}{A} = 0.1$

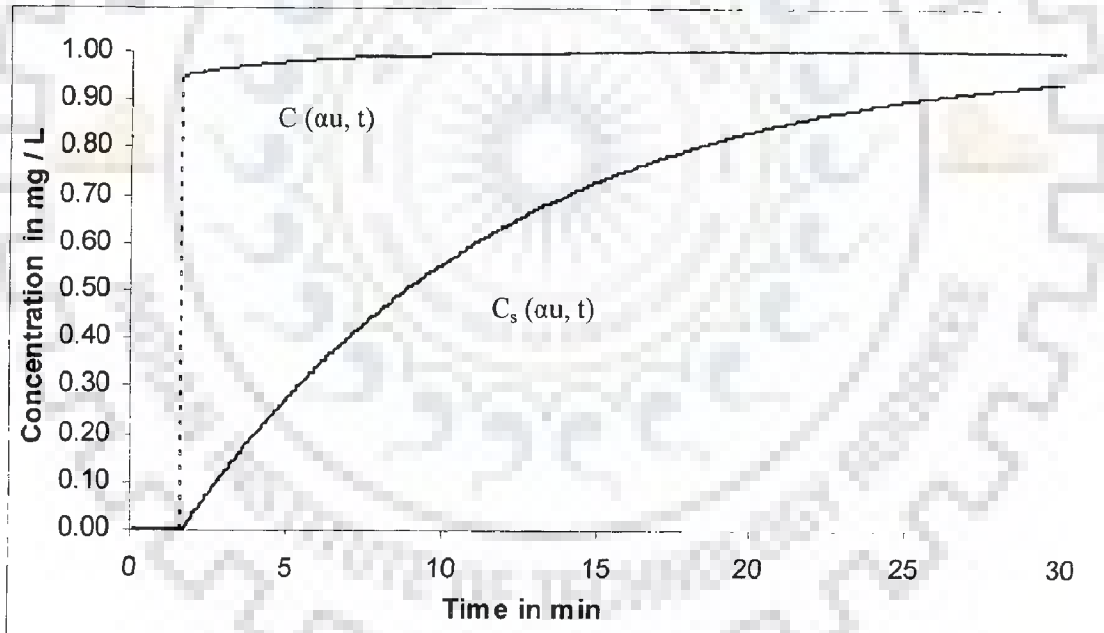


Fig. 3.8: Concentration – time distribution in water and soil column at the end of the plug flow zone (34 m) for  $R_D = 0.25$  per min and  $\alpha = 1.7$  min;  $u = 20$  m / min;  $\frac{\phi W_P D_B}{A} = 0.1$

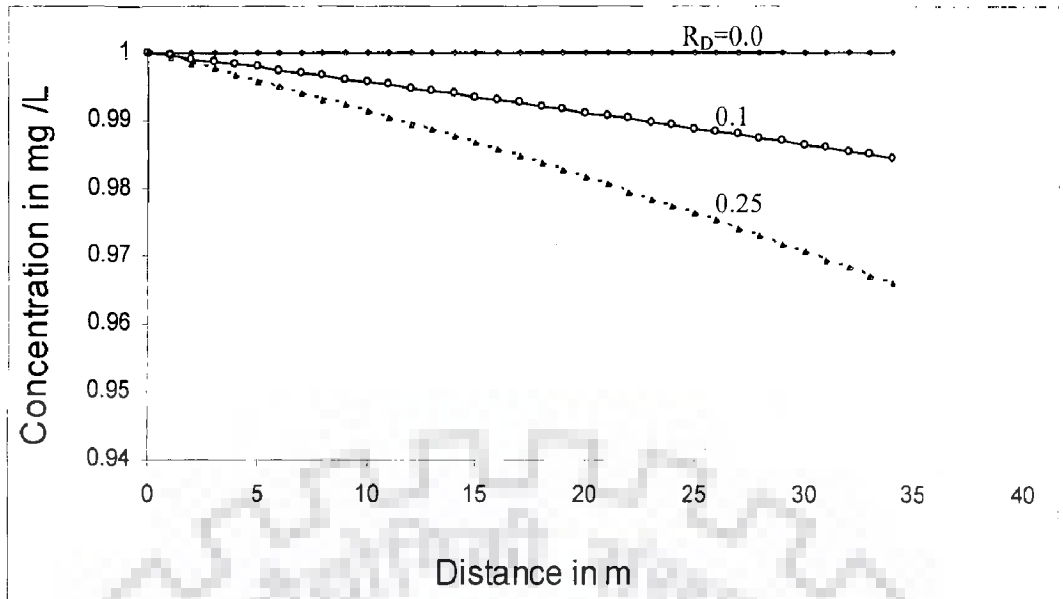


Fig. 3. 9: Spatial distribution of effluent concentration in the plug flow zone for different values of  $R_D$  ( $=0.0, 0.1$  and  $0.25$  per min) and  $\alpha = 1.7$  min;  $u = 20$  m / min;  $\frac{\phi W_p D_B}{A} = 0.1$

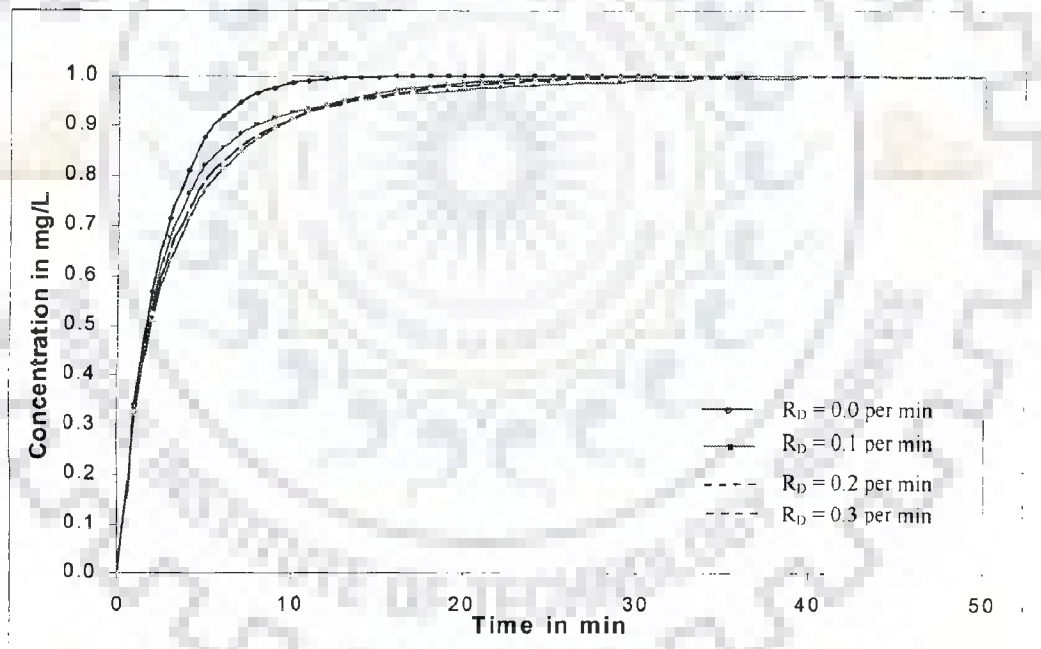
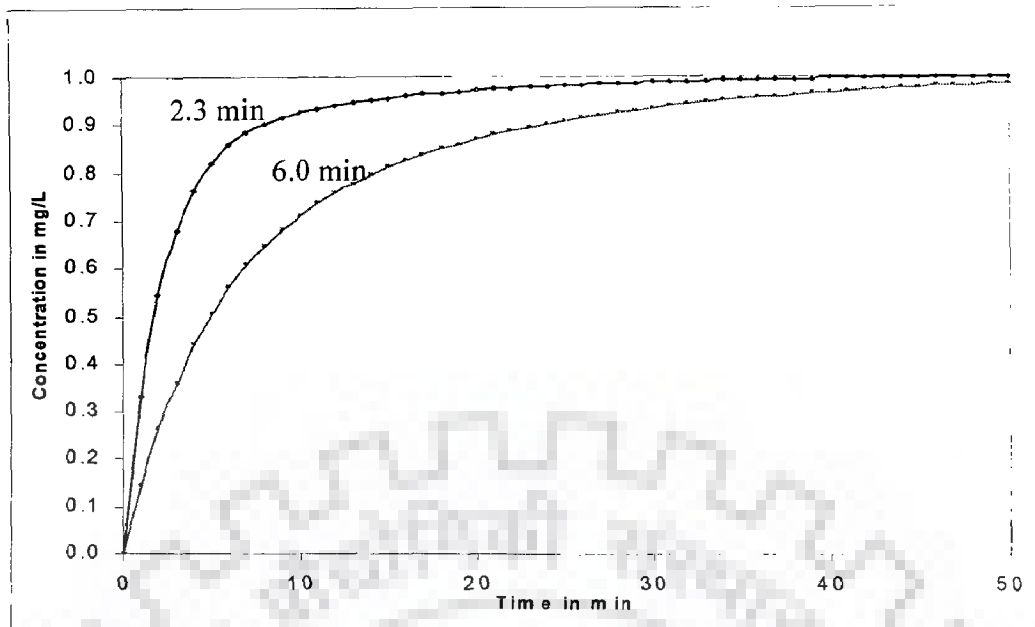
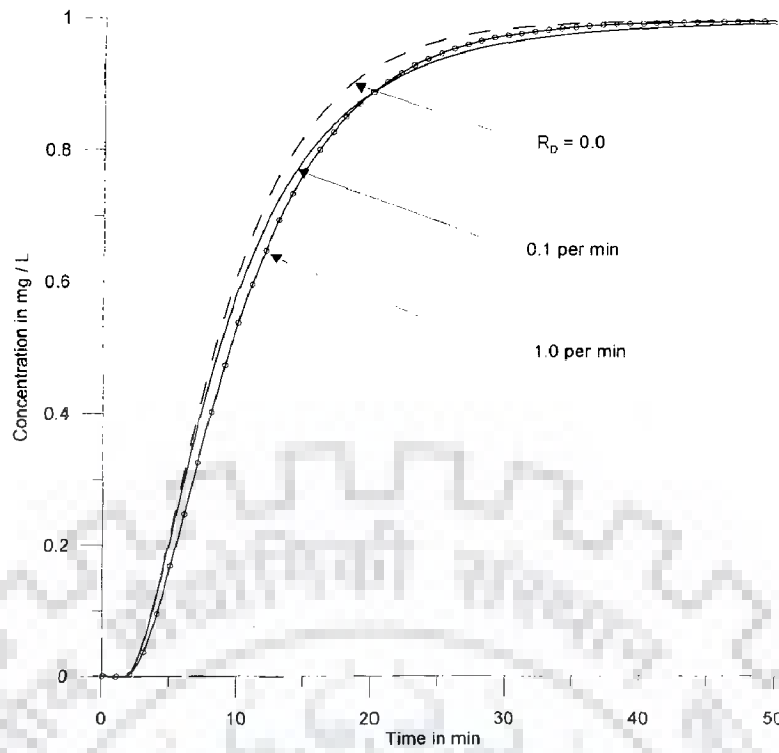


Fig. 3.10: Unit step response function of a thoroughly mixed zone for different values of  $R_D$  and residence time is 2.3 min;  $u = 20$  m / min;  $\frac{\phi W_p D_B}{A} = 0.5$



**Fig. 3.11:** Unit step response function of a thoroughly mixed zone for different values of residence time ( $T$ ), for  $R_D = 0.1$  per min;  $u = 20$  m / min;  $\frac{\phi W_r D_B}{A} = 0.5$





**Fig. 3.12: Unit step responses of HCIS-A model for Adsorption rate  $R_D = 0, 0.1$  and  $1.0$  per min;  $\alpha = 1.7$  min,  $T_1 = 2.3$  min,  $T_2 = 6.0$  min and Porosity  $\phi = 0.2$**

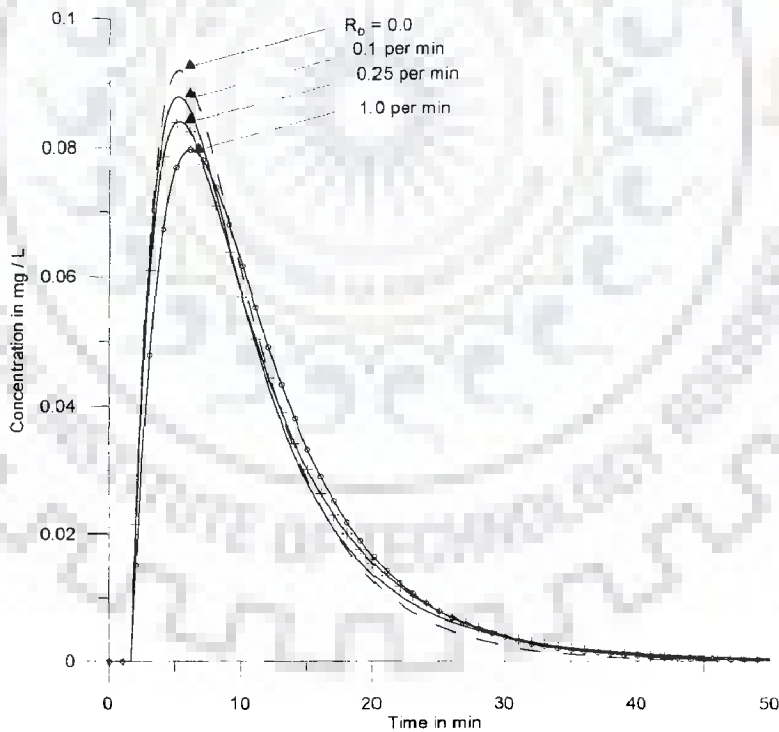


**Fig. 3.13: Unit pulse responses of HCIS-A model for Adsorption rate  $R_D = 0, 0.1$  and  $1.0$  per min;  $\alpha = 1.7$  min,  $T_1 = 2.3$  min,  $T_2 = 6.0$  min and Porosity  $\phi = 0.2$**

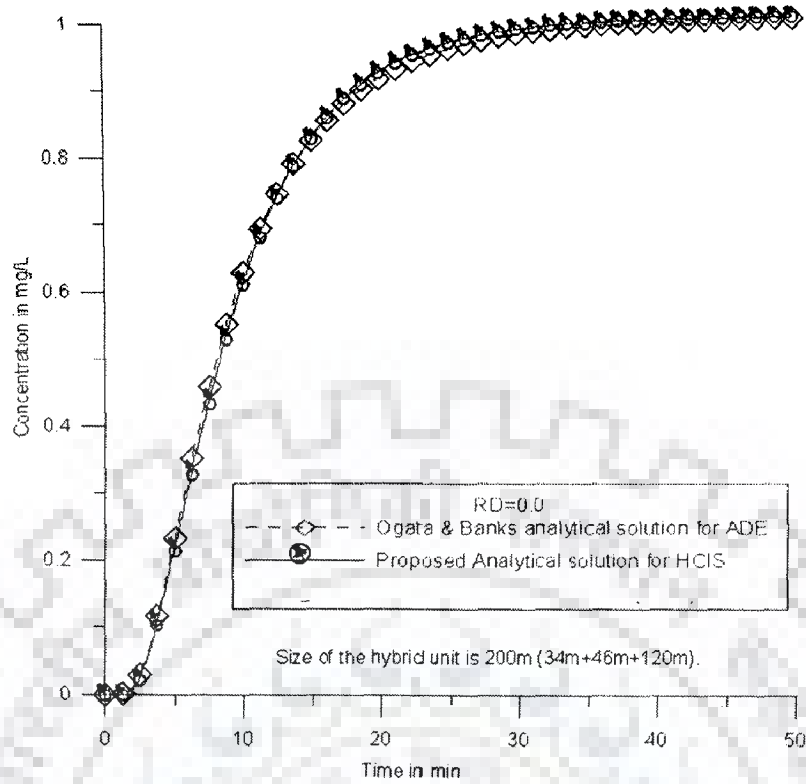


**Fig. 3.14: Step responses of the ADE model ( $u = 20$  m/ min;  $D_L = 1000$  m<sup>2</sup>/min) and the HCIS model in absence of adsorption for  $\alpha = 1.7$  min,  $T_1 = 2.3$  min,  $T_2 = 6.0$  min.**

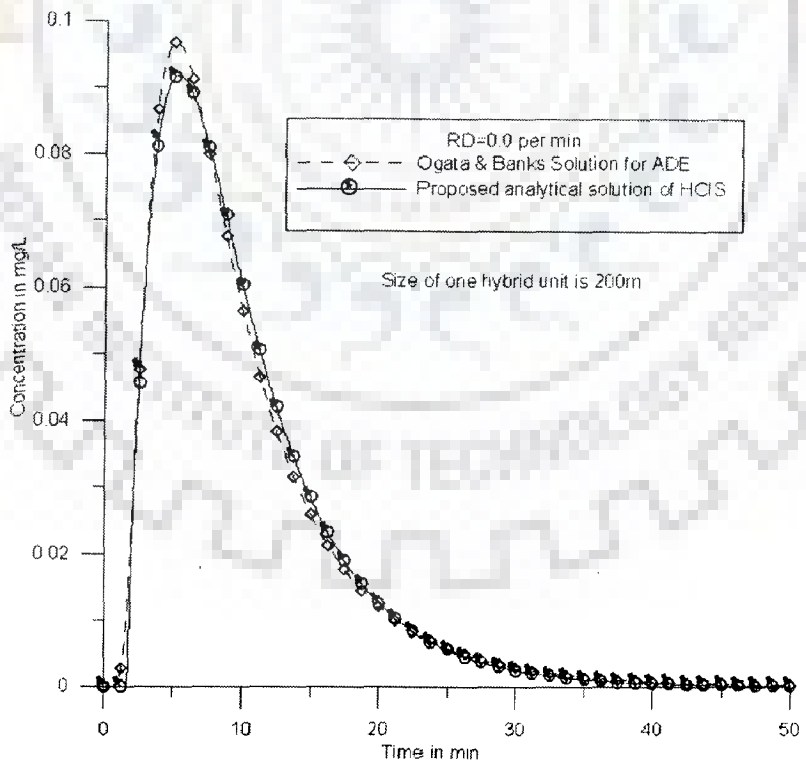


**Fig. 3.15: Unit pulse responses of the ADE model ( $u = 20$  m/ min;  $D_L = 1000$  m<sup>2</sup>/min) and the HCIS model in absence of adsorption for  $\alpha = 1.7$  min,  $T_1 = 2.3$  min,  $T_2 = 6.0$  min**

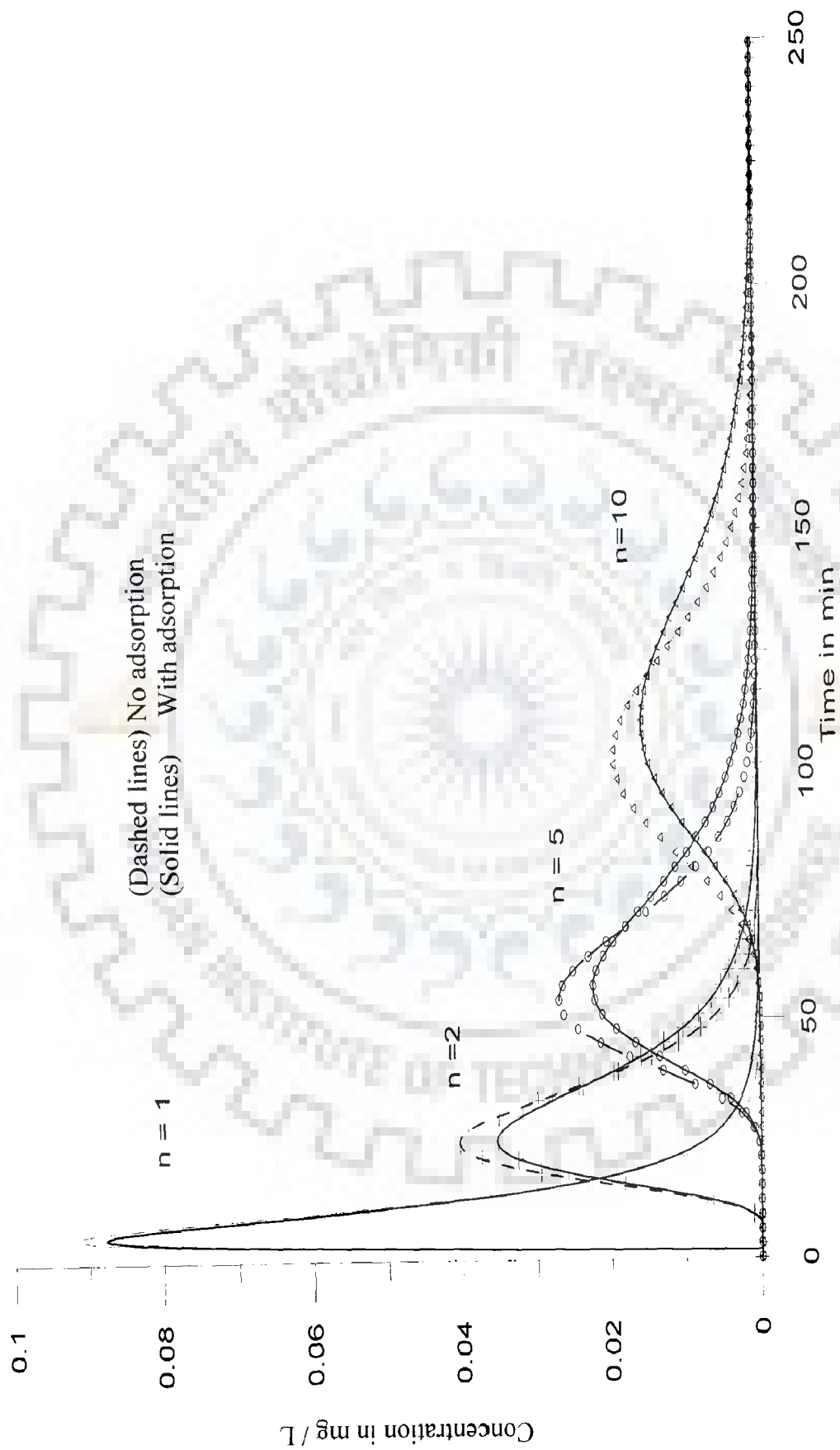


Fig. 3.16: Unit pulse responses of the HCIS-A model, with adsorption rate co-efficient,  $R_D = 0.0$  and  $0.1$  per min, at the end of first ( $n = 1$ ), second ( $n = 2$ ), fifth ( $n = 5$ ) and tenth ( $n = 10$ ) hybrid units for  $\alpha=1.7$  min,  $T_I=2.3$  min,  $T_I=6.0$  min,  $t=20$  m/min and  $\Delta x = 200$  m.

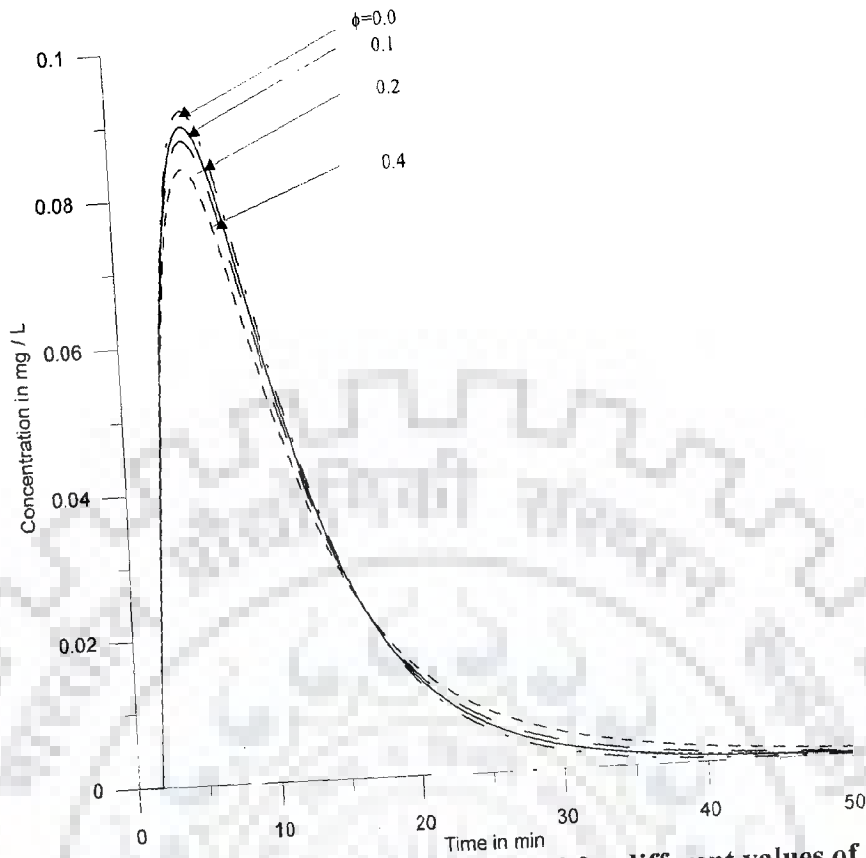


Fig. 3.17: Unit pulse responses of the HCIS-A model for different values of porosity

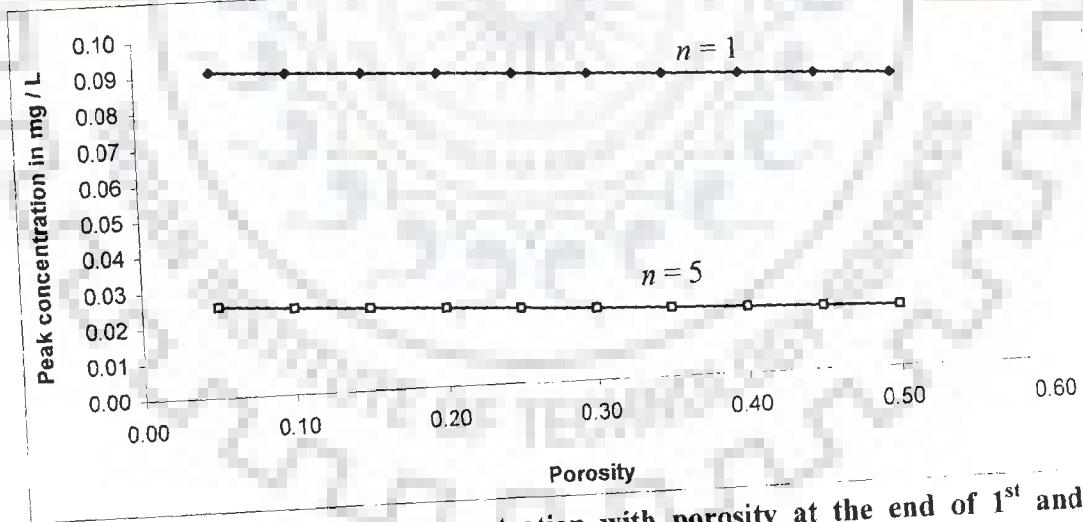


Fig.3.18: Variation of Peak concentration with porosity at the end of 1<sup>st</sup> and 5<sup>th</sup> hybrid units for  $\alpha = 1.7$  min,  $T_1 = 2.3$  min,  $T_2 = 6.0$  min,  $W_P = 10$  m,  $D_B = 1$  m,  $A = 20$  m<sup>2</sup> and size of one hybrid unit,  $\Delta x = 200$  m corresponding to  $P_e = 4$ ,  $u = 20$  m/min,  $D_L = 1000$  m<sup>2</sup>/min

### 3.5 CONCLUSIONS

1. The review on earlier studies of solute transport indicates that the Fickian dispersion models have limitations in the practical applications. Limitations in CIS and ADZ models in simulating time concentration profile with respect to first arrival time of pollutant at sampling site downstream of the injection have been observed. For resolving environmental issues, it is necessary to predict the pollutant transport more accurately by incorporating possible additional processes along with advection and dispersion. By introducing a plug flow zone in cell in series model, HCIS model predicts the first arrival time of pollutant at sampling site.
2. A linear non-equilibrium law for exchange of pollutant between the soil column and the mainstream water has been considered along with advection and dispersion for analyzing solute transport in a stream. Incorporating adsorption in each of the three compartments in the HCIS model, i.e., in the plug flow zone and in the two thoroughly mixed reservoirs of unequal residence time, a conceptual hybrid-cells-in-series model coupled with adsorption (HCIS-A) is developed. The HCIS-A model is a four-parameter model representing three time parameters and one time-reciprocal co-efficient.
3. An analytical solution in continuous time and space domain for transport of solute in a plug flow zone, where adsorption takes place, has been obtained using Laplace transform technique. A Hybrid Cells in Series model comprising a plug flow zone and two thoroughly mixed reservoirs, has been derived to simulate advection-dispersion and adsorption governed solute transport in streams in discrete space domain and continuous time domain.
4. The unit step response and the unit pulse response functions of the HCIS-A model have been derived. The characteristics of the concentration-time profiles generated by the HCIS-A model are comparable to the physical processes of pollutant transport governed by the advection-dispersion-adsorption in a natural stream.
5. Due to the addition of adsorption process with advection and dispersion, peak concentration reduces; falling limb of  $C-t$  profile gets smoothed and long tail is

produced in concentration distribution. These characteristics of the  $C-t$  profiles for a conservative pollutant in a stream with adsorbing stream bed and soil sediments are in the expected lines.

6. Response of the HCIS-A model is closely matching with the finite difference solution of the differential equation governing advection dispersion and non-equilibrium adsorption.



# CHAPTER 4

## POLLUTANTS TRANSPORT WITH FIRST ORDER REACTION KINETICS

---

---

### 4.1 INTRODUCTION

Many organic and inorganic contaminants enter most watercourses each day from domestic, industrial and agricultural sectors. These contaminants / pollutants are either reactive/decaying type or non-reactive type. Pollution control measures are more particular with the non-conservative or reactive type pollutants, such as biochemical oxygen demand and coliform bacteria. Decay of pollutant needs to be considered while quantifying BOD or coliform bacteria in moving water. The decay of pollutant is assumed to be governed by a first order reaction kinetics (Streeter and Phelps, 1944; Rinaldi, et al., 1979; Thomman and Muller, 1987). Streeter and Phelps (1944) gave a generalized equation relating the rate of the biochemical oxidation of pollutants and the remaining concentration of unoxidized pollutants. Considering first order decay, advection, dispersion and decay of a pollutant has been simulated in this chapter.

### 4.2 STATEMENT OF THE PROBLEM

The conceptualized hybrid model, which incorporates decay process, (HCIS-D model) consisting of a plug flow zone and two thoroughly mixed zones with unequal residence time, all connected in series is shown in Fig. 4.1. Let the initial concentration of pollutant in each zone be  $C_i$ . The boundary concentration changes from  $C_i$  to  $C_R$ . In the plug flow zone, the fluid gets replaced in time  $\alpha$ . The pollutant loses some fraction of its concentration due to decay while transported to downstream. In the first thoroughly mixed zone, where in the residence time is  $T_1$ , the fluid gets thoroughly mixed before entering to the second thoroughly mixed zone that has residence time  $T_2$ . Decay of the pollutant follows the first order reaction kinetics and takes place in all the zones of the HCIS model.

The flow rate is  $Q \text{ m}^3 / \text{unit time}$  and is under steady state condition. It is aimed to predict the concentration of the decaying pollutant in the effluent of the hybrid unit.

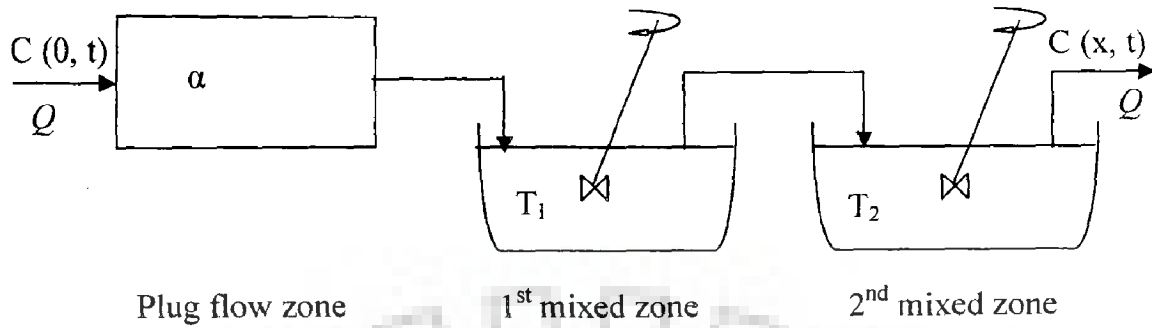


**Fig. 4.1: Conceptualized unit of Hybrid Cells in Series Model**

### 4.3 FORMULATION OF MODEL

#### 4.3.1 Derivation of Concentration of Pollutant in the Plug Flow Zone

In the plug flow zone (Fig. 4.2), within the moving front; the rate of change of total mass in a control volume ( $A \Delta x$ ) is equal to negative of total mass decayed from the control volume. This can be expressed as:

$$A \Delta x \frac{dC(x, t)}{dt} = -k_1 A \Delta x C(x, t) \quad (4.1)$$

where,  $A$  is the cross sectional area of the plug flow zone,  $k_1$  is the first order decay constant.

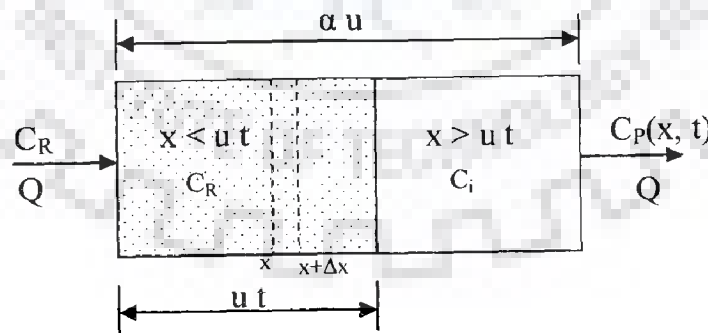


**Fig. 4.2: Pollutant transport through plug flow zone for a unit step input.**

Applying Euler's Equation

$$\frac{dC}{dt} = \frac{\partial C}{\partial t} + u \frac{\partial C}{\partial x} \quad \text{in Eq. (4.1)}$$



$$\frac{\partial C(x,t)}{\partial t} + u \frac{\partial C(x,t)}{\partial x} = -k_1 C(x,t) \quad (4.2)$$

where,  $C(x, t)$  is concentration of pollutant in the water ( $\text{ML}^{-3}$ ),  $t$  is the time (T),  $u$  is the flow velocity ( $\text{LT}^{-1}$ ),  $x$  is the distance (L) from the injection point and  $k_1$  is the decay rate coefficient ( $\text{T}^{-1}$ ).

Initial and boundary conditions for Eq. (4.2) are:

$$C(x,0) = 0; \quad x > 0 \quad (4.3 \text{ a})$$

$$C(0,t) = C_R; \quad t \geq 0 \quad (4.3 \text{ b})$$

$$C(\alpha u, t) = 0; \quad 0 < t < \alpha \quad (4.3 \text{ c})$$

Taking Laplace transform for each terms of Eq. (4.2)

$$\mathcal{L}\left(\frac{\partial C}{\partial t}\right) = sC^* \quad (4.4)$$

$$\mathcal{L}\left(\frac{\partial C}{\partial x}\right) = \frac{dC^*}{dx} \quad (4.5)$$

$$\mathcal{L}(C) = C^* \quad (4.6)$$

and incorporating Eq. (4.4), (4.5) and (4.6) in Eq. (4.2)

$$sC^* + u \frac{dC^*}{dx} = -k_1 C^*$$

$$\text{or} \quad \frac{dC^*}{dx} = -\left(\frac{k_1}{u} + \frac{s}{u}\right) C^* \quad (4.7)$$

$$\text{or} \quad \frac{dC^*}{C^*} = -\left(\frac{k_1}{u} + \frac{s}{u}\right) dx \quad (4.8)$$

Integrating Eq. (4.8),

$$\ln(C^*) = -\left(\frac{k_1}{u} + \frac{s}{u}\right)x + A \quad (4.9)$$

where,  $A$  is the integration constant. At  $x = 0$ ;  $C = C_R$  and  $C^* = C_R/s$ .

Therefore,

$$A = \ln(C_R/s)$$

Substituting  $A$  in Eq. (4.9),

$$\ln \left( \frac{C^*}{C_R/s} \right) = - \left( \frac{k_1}{u} + \frac{s}{u} \right) x$$

or

$$C^* = \frac{C_R}{s} \exp \left[ -k_1 \frac{x}{u} \right] \exp \left( -s \frac{x}{u} \right) \quad (4.10)$$

Taking inverse Laplace transform of Eq. (4.10),

$$C(x, t) = C_R U \left( t - \frac{x}{u} \right) \exp \left( -k_1 \frac{x}{u} \right) \quad (4.11 \text{ a})$$

The concentration at the end of the plug flow zone is,

$$C_p(\alpha u, t) = C_R U(t - \alpha) \exp(-k_1 \alpha) \quad (4.11 \text{ b})$$

which is valid for  $t \geq \alpha$ .  $U(t - \alpha)$  is the step function.

#### 4.3.2 Derivation of Concentration of Pollutant in the First Thoroughly Mixed Zone

Let the first thoroughly mixed zone, shown in Fig. 4.3, has a filling time  $T_1 = V_1 / Q$ , where,  $V_1 =$  volume of the mixed zone. The effluent from the plug flow zone enters the first thoroughly mixed zone. Decay of the pollutant takes place in this zone also. The mass decayed in a duration  $\Delta t$  is equal to  $k_1 V_1 C_{M1} \Delta t$ .  $C_{M1}$  is the concentration in the effluent from the mixed zone, which is also equal to the concentration in the mixed zone. The mass balance is expressed as:

$$V_1 \Delta C_{M1} = C_R U(t - \alpha) e^{-k_1 \alpha} Q \Delta t - C_{M1} Q \Delta t - k_1 V_1 C_{M1} \Delta t \quad (4.12)$$

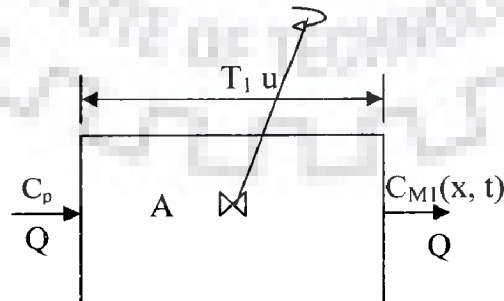


**Fig. 4.3: Pollutant transport through 1<sup>st</sup> thoroughly mixed zone**

Simplifying Eq. (4.12) reduces to

$$\frac{\Delta C_{M1}}{\Delta t} = \frac{C_R U(t-\alpha) e^{-k_1 \alpha}}{T_1} - \frac{C_{M1}}{T_1} - k_1 C_{M1}$$

In differential form,

$$\frac{dC_{M1}}{dt} = \frac{C_R U(t-\alpha) e^{-k_1 \alpha}}{T_1} - \left( \frac{1+k_1 T_1}{T_1} \right) C_{M1} \quad (4.13)$$

Multiplying  $e^{\left(\frac{1+k_1 T_1}{T_1}\right)t}$  on either side

$$\frac{dC_{M1}}{dt} e^{\left(\frac{1+k_1 T_1}{T_1}\right)t} + \left( \frac{1+k_1 T_1}{T_1} \right) C_{M1} e^{\left(\frac{1+k_1 T_1}{T_1}\right)t} = \frac{C_R U(t-\alpha) e^{-k_1 \alpha} e^{\left(\frac{1+k_1 T_1}{T_1}\right)t}}{T_1}$$

or

$$\frac{d \left( C_{M1} e^{\left(\frac{1+k_1 T_1}{T_1}\right)t} \right)}{dt} = \frac{C_R U(t-\alpha) e^{-k_1 \alpha} e^{\left(\frac{1+k_1 T_1}{T_1}\right)t}}{T_1} \quad (4.14)$$

Integrating, Eq. (4.14) reduces to,

$$C_{M1} e^{\left(\frac{1+k_1 T_1}{T_1}\right)t} = \frac{C_R U(t-\alpha) e^{-k_1 \alpha} e^{\left(\frac{1+k_1 T_1}{T_1}\right)t}}{T_1 \left( \frac{1+k_1 T_1}{T_1} \right)} + A \quad (4.15)$$

where,  $A$  is the integration constant. For  $t = \alpha$ ;  $C_{M1} = 0$ .

$$A = - \frac{C_R U(t-\alpha) e^{-k_1 \alpha} e^{\left(\frac{1+k_1 T_1}{T_1}\right)\alpha}}{(1+k_1 T_1)} \quad (4.16)$$

Substituting Eq. (4.16) into Eq. (4.15),

$$C_{M1} e^{\left(\frac{1+k_1 T_1}{T_1}\right)t} = \frac{C_R U(t-\alpha) e^{-k_1 \alpha} e^{\left(\frac{1+k_1 T_1}{T_1}\right)t}}{(1+k_1 T_1)} - \frac{C_R U(t-\alpha) e^{-k_1 \alpha} e^{\left(\frac{1+k_1 T_1}{T_1}\right)\alpha}}{(1+k_1 T_1)}$$

$$C_{M1} = \frac{C_R U(t-\alpha) e^{-k_1 \alpha}}{(1+k_1 T_1)} \left[ 1 - e^{-\left(\frac{1+k_1 T_1}{T_1}\right)[t-\alpha]} \right] \quad (4.17)$$

### 4.3.3 Derivation of Concentration of Pollutant in the Second Thoroughly Mixed Zone

Consider the second thoroughly mixed zone as shown in Fig. 4.4. The outflow from the first thoroughly mixed zone is the inflow to the second thoroughly mixed zone. Performing the mass balance in the second thoroughly mixed zone.

$$V_2 \Delta C_{M2} = \left\{ \frac{C_R U (t-\alpha) e^{-k_1 \alpha}}{(1+k_1 T_1)} \left[ 1 - e^{-\left(\frac{1+k_1 T_1}{T_1}\right)(t-\alpha)} \right] \right\} Q \Delta t - C_{M2} Q \Delta t - k_1 V_2 C_{M2} \Delta t$$

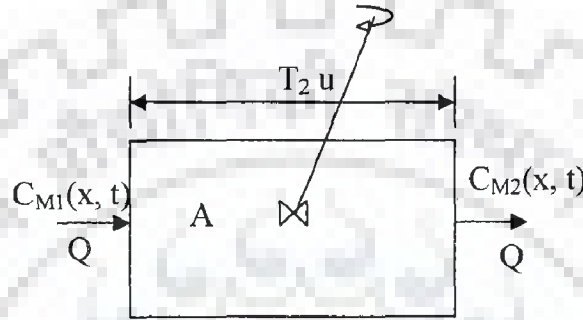


Fig. 4.4: Pollutant transport through 2<sup>nd</sup> thoroughly mixed zone

Rearranging and reducing to differential form,

$$\frac{dC_{M2}}{dt} = \left\{ \frac{C_R U (t-\alpha) e^{-k_1 \alpha}}{T_2 (1+k_1 T_1)} \left[ 1 - e^{-\left(\frac{1+k_1 T_1}{T_1}\right)(t-\alpha)} \right] \right\} - \left( \frac{1+k_1 T_2}{T_2} \right) C_{M2} \quad (4.18)$$

Multiplying  $e^{\left(\frac{1+k_1 T_2}{T_2}\right)t}$

$$\frac{dC_{M2}}{dt} e^{\left(\frac{1+k_1 T_2}{T_2}\right)t} + \left( \frac{1+k_1 T_2}{T_2} \right) C_{M2} e^{\left(\frac{1+k_1 T_2}{T_2}\right)t} = \left\{ \frac{C_R U (t-\alpha) e^{-k_1 \alpha}}{T_2 (1+k_1 T_1)} \left[ 1 - e^{-\left(\frac{1+k_1 T_1}{T_1}\right)(t-\alpha)} \right] \right\} e^{\left(\frac{1+k_1 T_2}{T_2}\right)t}$$

or

$$\frac{d \left( C_{M2} e^{\left(\frac{1+k_1 T_2}{T_2}\right)t} \right)}{dt} = \left\{ \frac{C_R U (t-\alpha) e^{-k_1 \alpha}}{T_2 (1+k_1 T_1)} \left[ 1 - e^{-\left(\frac{1+k_1 T_1}{T_1}\right)(t-\alpha)} \right] \right\} e^{\left(\frac{1+k_1 T_2}{T_2}\right)t} \quad (4.19)$$

Integrating Eq. (4.19)

$$C_{M2} e^{\left(\frac{1+k_1 T_2}{T_2}\right)t} = \frac{C_R U(t-\alpha) e^{-k_1 \alpha}}{T_2 (1+k_1 T_1)} \left\{ \frac{e^{\left(\frac{1+k_1 T_2}{T_2}\right)t}}{\left(\frac{1+k_1 T_2}{T_2}\right)} - \frac{e^{\alpha \left[\frac{1}{T_1} + k_1\right]} e^{\left(\frac{1}{T_2} - \frac{1}{T_1}\right)t}}{\frac{1}{T_2} - \frac{1}{T_1}} \right\} + A \quad (4.20)$$

where,  $A$  is the integration constant. For  $t = \alpha$ ;  $C_{M2} = 0$ , hence,

$$A = - \frac{C_R U(t-\alpha) e^{-k_1 \alpha}}{T_2 (1+k_1 T_1)} \left\{ \frac{e^{\left(\frac{1+k_1 T_2}{T_2}\right)\alpha}}{\frac{1+k_1 T_2}{T_2}} - \frac{e^{\left(\frac{1+k_1 T_1}{T_1}\right)\alpha} e^{\left(\frac{1}{T_2} - \frac{1}{T_1}\right)\alpha}}{\frac{1}{T_2} - \frac{1}{T_1}} \right\} \quad (4.21)$$

Substituting Eq. (4.21) into Eq. (4.20),

$$C_{M2} e^{\left(\frac{1+k_1 T_2}{T_2}\right)t} = \frac{C_R U(t-\alpha) e^{-k_1 \alpha}}{T_2 (1+k_1 T_1)} \left\{ \frac{e^{\left(\frac{1+k_1 T_2}{T_2}\right)t}}{\left(\frac{1+k_1 T_2}{T_2}\right)} - \frac{e^{\alpha \left[\frac{1}{T_1} + k_1\right]} e^{\left(\frac{1}{T_2} - \frac{1}{T_1}\right)t}}{\frac{1}{T_2} - \frac{1}{T_1}} \right\} \\ - \frac{C_R U(t-\alpha) e^{-k_1 \alpha}}{T_2 (1+k_1 T_1)} \left\{ \frac{e^{\left(\frac{1+k_1 T_2}{T_2}\right)\alpha}}{\frac{1+k_1 T_2}{T_2}} - \frac{e^{\left(\frac{1+k_1 T_1}{T_1}\right)\alpha} e^{\left(\frac{1}{T_2} - \frac{1}{T_1}\right)\alpha}}{\frac{1}{T_2} - \frac{1}{T_1}} \right\}$$

or

$$C_{M2} = \frac{C_R U(t-\alpha) e^{-k_1 \alpha}}{T_2 (1+k_1 T_1)} \left\{ \frac{\left[ 1 - e^{-\left(\frac{1+k_1 T_2}{T_2}\right)(t-\alpha)} \right]}{\left(\frac{1+k_1 T_2}{T_2}\right)} - \frac{e^{-\left(\frac{1+k_1 T_1}{T_1}\right)(t-\alpha)} - e^{-\left(\frac{1+k_1 T_2}{T_2}\right)(t-\alpha)}}{\frac{1}{T_2} - \frac{1}{T_1}} \right\} \quad (4.22)$$

The step response function of the HCIS unit is:

$$K_{HCIS-D} = \frac{C_R U(t-\alpha) e^{-k_1 \alpha}}{(1+k_1 T_1)} \left\{ \frac{1 - e^{-\left(\frac{1+k_1 T_2}{T_2}\right)(t-\alpha)}}{1+k_1 T_2} - \frac{T_1 \left[ e^{-\left(\frac{1+k_1 T_1}{T_1}\right)(t-\alpha)} - e^{-\left(\frac{1+k_1 T_2}{T_2}\right)(t-\alpha)} \right]}{T_1 - T_2} \right\} \quad (4.23)$$

which is valid for  $t \geq \alpha$ .

Differentiating with respect to  $t$ ,

$$\frac{d(K_{HCIS-D})}{dt} = k_{HCIS-D} = \frac{C_R U(t-\alpha) e^{-k_1 \alpha}}{(1+k_1 T_1)} \left( \frac{1+k_1 T_1}{T_1-T_2} \right) \left\{ e^{-\left(\frac{1+k_1 T_1}{T_1}\right)[t-\alpha]} - e^{-\left(\frac{1+k_1 T_2}{T_2}\right)[t-\alpha]} \right\} \quad (4.24)$$

where,  $k_{HCIS-D}$  is the unit impulse response function.

Eq. (4.23) and Eq. (4.24) give the responses at the end of the hybrid unit, for the step and unit impulse inputs injected at the entry of the first hybrid unit.

#### 4.4 ESTIMATION OF POLLUTANT CONCENTRATION USING CONVOLUTION TECHNIQUE

Eq. (4.23) predicts the pollutant concentration at the end of a hybrid unit for a step input injected at the entrance of the plug flow zone at time  $t = 0$ . For a unit pulse input, the unit pulse response function  $\delta_{HCIS-D}(n, \Delta t)$  is given by

$$\delta_{HCIS-D}(n, \Delta t) = \frac{K_{HCIS-D}(n\Delta t) - K_{HCIS-D}((n-1)\Delta t)}{\Delta t} \quad (4.25)$$

where,  $K_{HCIS-D}$  is the step response of the first hybrid unit ( $= C_{M2}$ )

Let the stream reach downstream of the injection point of the pollution be composed of a series of equal size hybrid units each having linear dimension  $\Delta x$  and each consisting of a plug flow zone, and two unequal thoroughly mixed reservoirs, as shown in Fig. 4.5 Using the convolution technique, the response of the  $i$ th hybrid unit,  $i \geq 2$ , is expressed as

$$C(i\Delta x, n\Delta t) = \sum_{\gamma=1}^n C((i-1)\Delta x, \gamma) \delta_{HCIS-D}(n-\gamma+1, \Delta t) \quad (4.26)$$

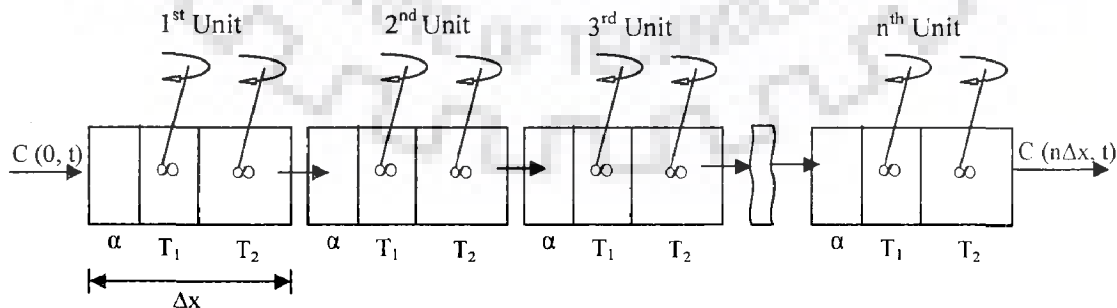


Fig. 4.5: Composed series of hybrid units representing a stream reach of  $n\Delta x$  length

## 4.5 RESULTS AND DISCUSSION

Unit pulse response functions of the first hybrid unit are computed using Eq. (4.24) for  $\alpha = 1.70 \text{ min}$ ,  $T_1 = 2.3 \text{ min}$  and  $T_2 = 6.0 \text{ min}$ ,  $\Delta x = 200 \text{ m}$ ,  $u = 20 \text{ m/min}$ ,  $k_l = 0, 0.1, 1.0$  per min, and compared with analytical solutions of advection dispersion and decay (ADDE) model in Fig. 4.6. There is a marginal difference in peak concentrations in the unit pulse response functions of hybrid model and the ADDE model. This difference is due to the space discretization in the hybrid model. The unit step response function obtained from the present study is close to that obtained from ADDE model. For  $k_l = 0.1$  per min, the peak concentration reduces and time to peak decreases.

Making use of the values of above set of parameters ( $\alpha, T_1, T_2, \Delta x, u$ ) the unit step response functions of HCIS-D model have been generated for values of  $k_l = 0$  and  $0.1$  per min at the end of 1<sup>st</sup>, 2<sup>nd</sup>, 4<sup>th</sup> and 5<sup>th</sup> hybrid units and are shown in Fig. 4.7. From Fig. 4.7, it can be seen that, as the pollutants move from the near field to the far field, the  $C-t$  distributions undergoing first order decay get more and more attenuated and the peak concentrations reduces largely in comparison to those without decay. Comparing those  $C-t$  profiles in Fig. 4.7, the pollution threat to the down stream can be evaluated by fixing norms for pollutant injection.

Unit pulse responses of the HCIS-D model using Eq. (4.24) have been computed with decay rate co-efficient,  $k_l = 0.0$  and  $0.1$  per min, at the end of 1<sup>st</sup>, 2<sup>nd</sup>, 4<sup>th</sup> and 5<sup>th</sup> hybrid units for  $\alpha = 1.7 \text{ min}$ ,  $T_1 = 2.3 \text{ min}$ ,  $T_2 = 6.0 \text{ min}$ ,  $u = 20 \text{ m / min}$  and  $\Delta x = 200 \text{ m}$  and presented in Fig. 4.8. From Fig. 4.8, It can be noted that for  $k_l = 0.1$  per min, the peak concentration enormously reduces and time to peak decreases, as number of hybrid unit increases. At the end of 4<sup>th</sup> and 5<sup>th</sup> hybrid units, the peak concentrations show  $3.35\text{E-}03 \text{ mg / L}$  and  $5.06\text{E-}05 \text{ mg / L}$  respectively for given pulse input ( $=1 \text{ mg / L}$ ) of finite duration ( $\Delta t = 0.05 \text{ min}$ ).

Variations of Peak concentration with number of hybrid units,  $n$  for different values of decay rate co-efficient,  $k_l$  ( $0.0, 0.05, 0.1$  and  $0.25$  per min) have been plotted in Fig. 4.9 for  $\alpha = 1.7 \text{ min}$ ,  $T_1 = 2.3 \text{ min}$ ,  $T_2 = 6.0 \text{ min}$ ,  $W_p = 10 \text{ m}$ ,  $D_B = 1 \text{ m}$ ,  $A = 20 \text{ m}^2$  and  $\Delta x = 200 \text{ m}$  corresponding to  $P_e = 4$ ,  $u = 20 \text{ m/min}$ ,  $D_L = 1000 \text{ m}^2/\text{min}$ . Fig. 4.9 shows that the

pollution threat to downstream, reduces greatly for higher decay rate co-efficient than that for lower one.

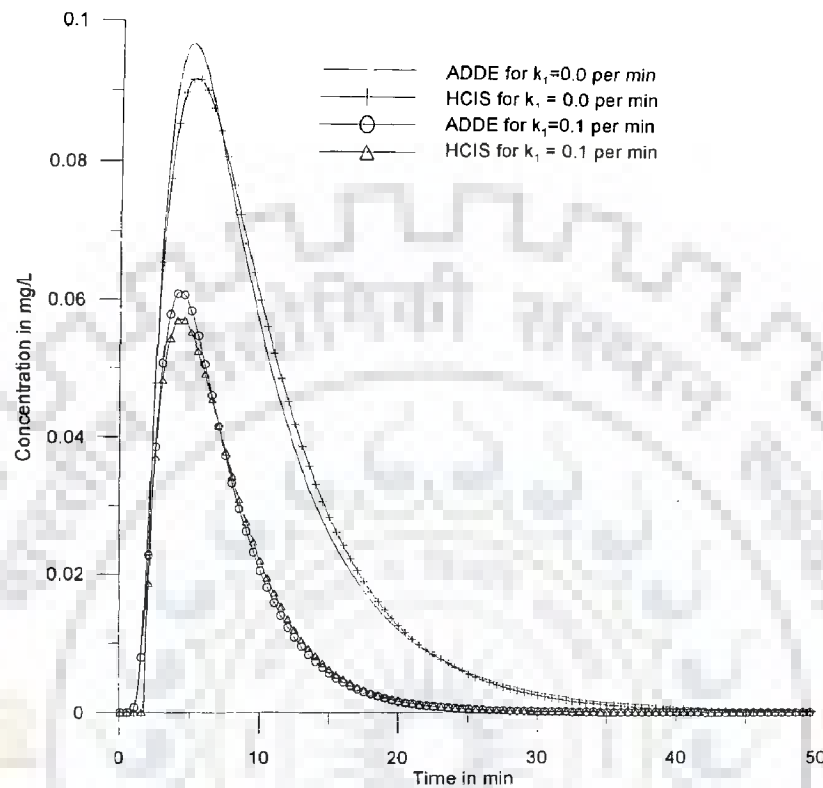


**Fig. 4.6: Unit pulse responses of ADDE model ( $u = 20$  m/ min;  $D_L = 1000$  m<sup>2</sup>/ min and at 200 m) and HCIS-D model ( $\alpha = 1.7$  min;  $T_1 = 2.3$  min;  $T_2 = 6.0$  min;  $\Delta x = 200$  m) for decay rate co-efficient,  $k_1 = 0.0$  and  $0.1$  per min.**



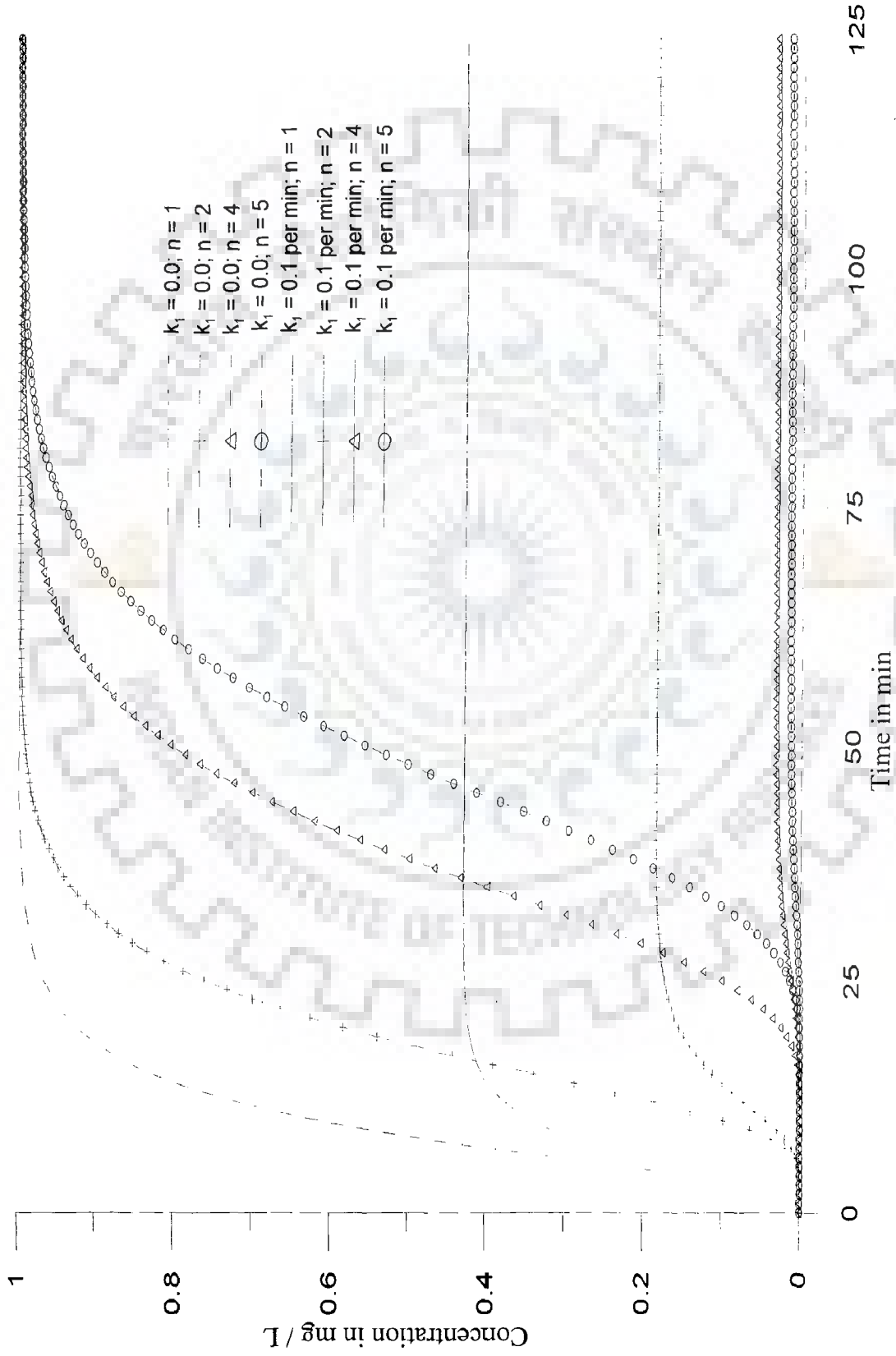


**Fig. 4.7: Unit step responses of the HCIS-D model, with decay rate co-efficient,  $k_1 = 0.0$  and  $0.1$  per min, at the end of first ( $n = 1$ ), second ( $n = 2$ ), fourth ( $n = 4$ ) and fifth ( $n = 5$ ) hybrid units for  $a = 1.7$  min,  $T_1 = 2.3$  min,  $T_2 = 6.0$  min,  $u = 20$  m / min and  $\Delta x = 200$  m**

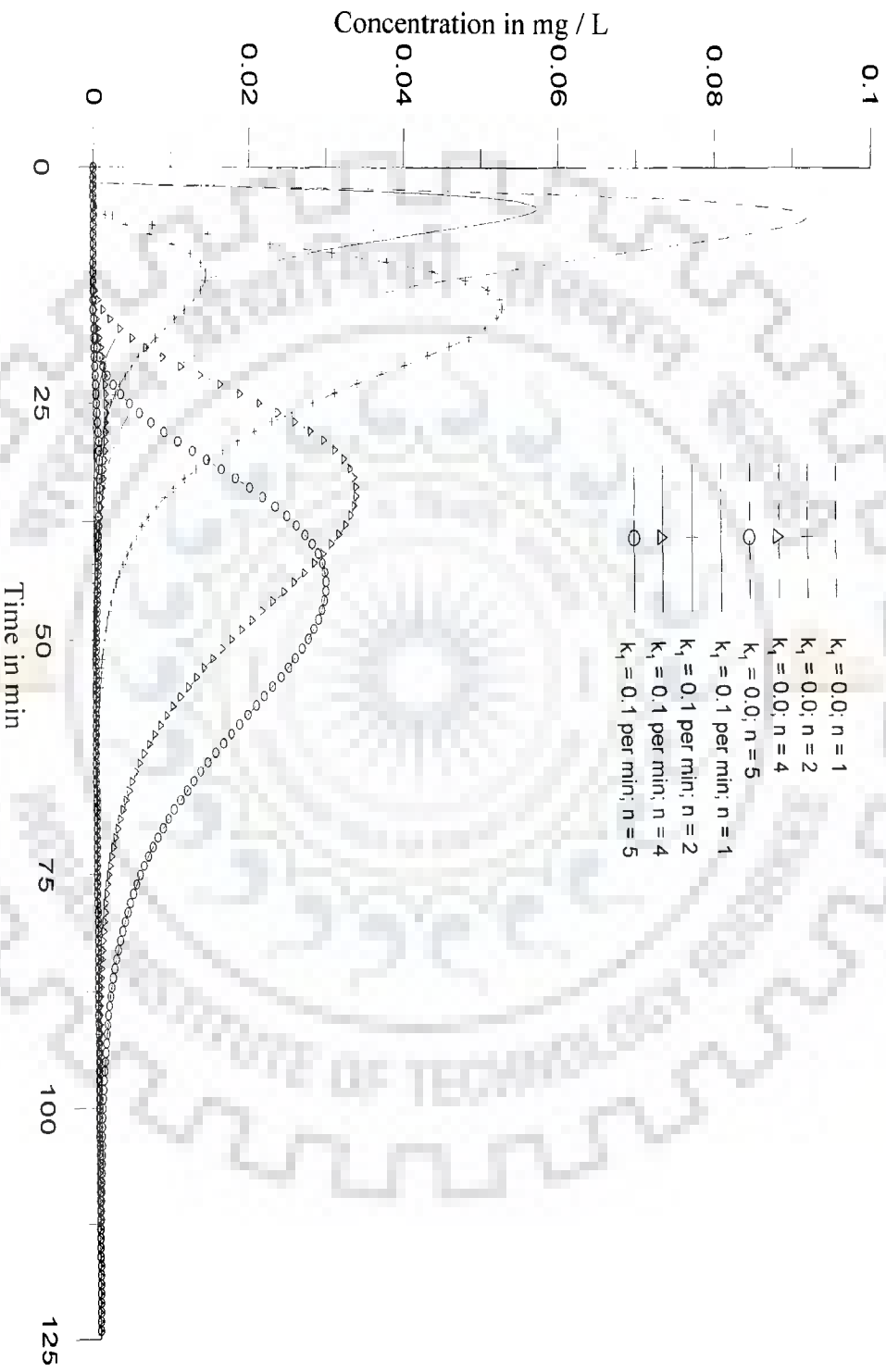


**Fig. 4.8:** Unit pulse responses of the HCIS-D model, with decay rate co-efficient,  $k_1 = 0.0$  and  $0.1$  per min, at the end of first ( $n = 1$ ), second ( $n = 2$ ), fourth ( $n = 4$ ) and fifth ( $n = 5$ ) hybrid units for  $\alpha = 1.7$  min,  $T_1 = 2.3$  min,  $T_2 = 6.0$  min,  $\mu = 20$  m / min and  $\Delta x = 200$  m

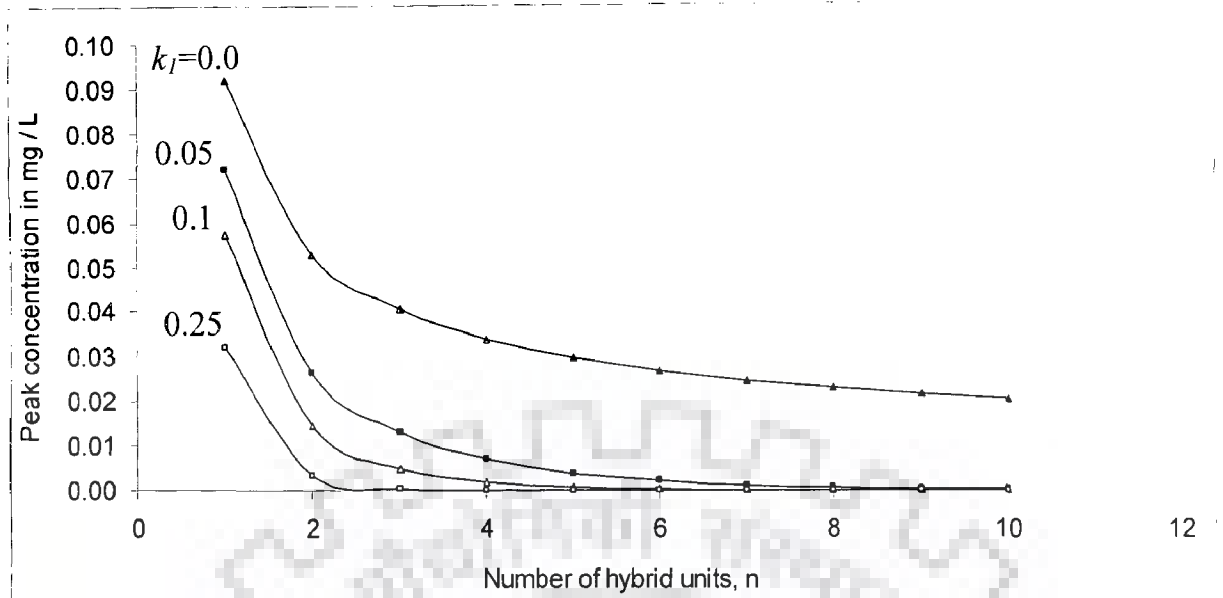


**Fig.4.9: Variation of Peak concentration with number of hybrid units,  $n$  for different values of decay rate co-efficient,  $k_1$  (0.0, 0.05, 0.1 and 0.25 per min) for  $\alpha = 1.7$  min,  $T_1 = 2.3$  min,  $T_2 = 6.0$  min,  $W_P = 10$  m,  $D_B = 1$  m,  $A = 20$  m<sup>2</sup> and  $\Delta x = 200$  m corresponding to  $P_e = 4$ ,  $u = 20$  m/min,  $D_L = 000$  m<sup>2</sup>/min**

#### 4.6 CONCLUSIONS

- 1 A hybrid model is developed adopting first order reaction kinetic along with advection and dispersion of non-conservative pollutant which is injected at the source.
- 2 For the pecllet number greater than 4, the response of the Hybrid Cells in Series model for step and instantaneous input matches with the response of Advection Dispersion Decay Equation (ADDE) model for the same inputs.
- 3 To predict the concentration of non-conservative pollutant, the decay rate co-efficient ( $k_1$ ) for the pollutant load can be determined from the Laboratory experiments.
4. Flexibility of the HCIS model for adopting reaction kinetics along with basic transport processes has been demonstrated



# CHAPTER 5

## POLLUTANT TRANSPORT WITH DE-OXYGENATION AND RE-AERATION

---

---

### 5.1 INTRODUCTION

A stream system gains as well as loses oxygen. It gains oxygen from the atmosphere and from aquatic plants. Running water, because of churning, dissolves more oxygen than still water. Respiration by aquatic lives, decay of pollutants, and various chemical reactions consume oxygen. The decay of pollutant is assumed to be governed by a first order reaction kinetics (Streeter and Phelps, 1944; Rinaldi et al. 1979; Thomman and Muller, 1987). Wastewaters from sewage treatment plants often contain organic materials, which are decomposed by microorganisms using oxygen in the process. Other sources of oxygen-consuming waste include storm water runoff from farmland or urban streets, feedlots, and failing septic systems. Oxygen is measured in its dissolved form as dissolved oxygen (DO). If more oxygen is consumed than is produced, dissolved oxygen levels decline and some sensitive aquatic lives may move away, weaken, or die. DO levels fluctuate seasonally and over a 24-hour period. They vary with water temperature and altitude. Cold water holds more oxygen than warm water and water holds less oxygen at higher altitudes. Thermal discharges, such as cooling water used in a power plant, raise the temperature of water and lower its oxygen content. Aquatic lives are most vulnerable to lowered DO levels. Hence, correct prediction of DO in an aquatic environment is imperative to maintain the ecosystem and control the waste load. Streeter and Phelps (1944) gave a generalized equation relating the rate of the biochemical oxidation of pollutants and the dissolved oxygen concentration. Young and Beck (1974) proposed continuously stirred tank reactor (CSTR) by joining assumptions of hydrology and chemical engineering to account the BOD-DO reactions and the dispersion in the channel. Rinaldi et al (1979) defined the auxiliary variable which relates the dissolved oxygen deficit and BOD load to get the solution for the approximated streeter-Phelps dispersion

model. In this chapter, considering first order decay along with advection and dispersion, DO concentration has been simulated by making use of hybrid cells in series model incorporating de-oxygenation and re-aeration.

## 5.2 STATEMENT OF THE PROBLEM

The conceptualized hybrid model (HCIS-R) consisting of a plug flow zone and two thoroughly mixed zones with unequal residence time, all connected in series is shown in Fig. 5.1.

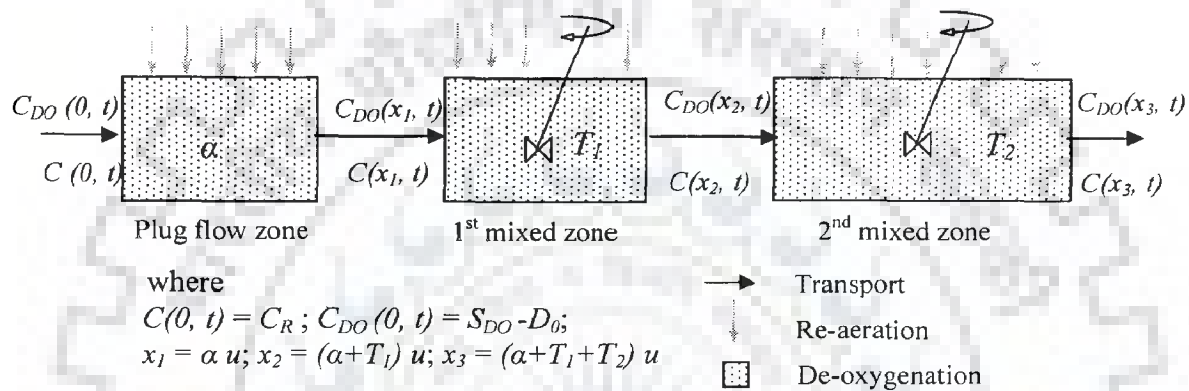


**Fig. 5.1: Conceptual hybrid unit to represent the transport, decay and re-aeration processes.**

Let the initial concentration of pollutant in each zone be  $C_i$ . The boundary concentration changes from  $C_i$  to  $C_R$ . Let initially the DO concentration,  $C_{DO}(x, 0)$  be equal to  $S_{DO}$ , where  $S_{DO}$  is saturated DO concentration. In the plug flow zone, the fluid gets replaced in time  $\alpha$ . The pollutant loses some fraction of its concentration due to decay while transported to downstream by consuming oxygen at a certain rate,  $k_1$ . At the same time, re-aeration takes place depending upon the DO deficit. In the first thoroughly mixed zone, whose filling time is  $T_1$ , the fluid gets thoroughly mixed before entering to the second thoroughly mixed zone that has filling time  $T_2$ . De-oxygenation and re-aeration processes take place in all the zones of the HCIS model, and both follow the first order reaction kinetics. The flow rate is  $Q \text{ m}^3 / \text{unit time}$  and is under steady state condition. It is aimed to predict the DO concentration in the hybrid unit.

### 5.3 FORMULATION OF MODEL

#### 5.3.1 Derivation of DO Concentration in the Plug Flow Zone

Let us consider a plug flow zone of volume,  $V_0$ , through which a non-conservative pollutant is transported. Within the plug flow zone, the concentration of the pollutant in a control volume of size,  $\Delta x$ , is taken as  $C(x, t)$ . Due to the decay process, some fraction of the pollutant concentration is lost, and then the remaining pollutant is replaced by the following plug and moved forward in a time interval  $\Delta t$ . For the decay of pollutant, the dissolved oxygen is consumed from the stream water. At the same time, oxygen gets replenished to the water from atmosphere at a specific rate. Let the concentration of dissolved oxygen be  $C_{DO}$ . Under a steady state flow condition, the mass balance equation for dissolved oxygen (DO) is

$$Q\Delta t C_{DO}(x, t) - k_1 A \Delta x C(x, t) \Delta t + k_2 A \Delta x [S_{DO} - C_{DO}(x, t)] \Delta t = Q\Delta t C_{DO}(x + \Delta x, t + \Delta t) \quad (5.1)$$

where,  $A$  is cross sectional area of the flow,  $C_{DO}(x, t)$  is DO concentration,  $C(x, t)$  is the BOD concentration,  $S_{DO}$  is the saturated DO concentration.

Applying Taylor series of expansion

$$Q\Delta t \left\{ C_{DO}(x, t) + \frac{\partial C_{DO}(x, t)}{\partial t} \Delta t + \frac{\partial C_{DO}(x, t)}{\partial x} \Delta x + \frac{\partial}{\partial x} \left[ \frac{\partial C_{DO}(x, t)}{\partial t} \Delta t \right] \Delta x \right\} - Q\Delta t \{ C_{DO}(x, t) \} \quad (5.2)$$

$$= -k_1 A \Delta x C(x, t) \Delta t + k_2 A \Delta x [S_{DO} - C_{DO}(x, t)] \Delta t$$

Let,  $Q = u A$ .

Simplifying Eq. (5.2) reduces to

$$uA \frac{\partial C_{DO}(x, t)}{\partial t} \Delta t + uA \frac{\partial C_{DO}(x, t)}{\partial x} \Delta x = -k_1 A \Delta x C(x, t) + k_2 A \Delta x [S_{DO} - C_{DO}(x, t)] \quad (5.3)$$

Dividing both sides by  $A u \Delta t$  and equating  $\Delta x / \Delta t = u$

$$\frac{\partial C_{DO}(x, t)}{\partial t} + u \frac{\partial C_{DO}(x, t)}{\partial x} = -k_1 C(x, t) + k_2 [S_{DO} - C_{DO}(x, t)] \quad (5.4)$$

Eq. (5.4) can be alternatively obtained applying Euler's principle.

For the BOD, the following differential equation has been formulated in chapter 4:

$$\frac{\partial C(x,t)}{\partial t} + u \frac{\partial C(x,t)}{\partial x} = -k_1 C(x,t) \quad (5.5)$$

The initial and boundary conditions for Eq. (5.4) and Eq. (5.5) are

$$C(x,0) = 0, \quad x > 0; \quad (5.6 \text{ a})$$

$$C(0,t) = C_R, \quad t \geq 0; \quad (5.6 \text{ b})$$

$$C(\alpha u, t) = 0, \quad 0 < t < \alpha; \quad (5.6 \text{ c})$$

$$C_{DO}(x,0) = S_{DO}, \quad x > 0; \quad (5.6 \text{ d})$$

$$C_{DO}(0,t) = S_{DO} - D_0, \quad t \geq 0. \quad (5.6 \text{ e})$$

where  $D_0$  is the boundary deficit in dissolved oxygen concentration due to the entry of waste water with lesser dissolved oxygen.

Solution for  $C(x, t)$  i.e. for Eq. (5.5) is given in Chapter 4.

i.e.  $C(x, t) = C_R U\left(t - \frac{x}{u}\right) \exp\left(-k_1 \frac{x}{u}\right)$ ; this is the response of the plug flow zone for the

given BOD input,  $C_R$  at the entry.

Considering DO deficit  $D = S_{DO} - C_{DO}$

$$\frac{\partial D}{\partial t} = -\frac{\partial C_{DO}}{\partial t} \quad \text{and} \quad \frac{\partial D}{\partial x} = -\frac{\partial C_{DO}}{\partial x}.$$

Substituting these derivatives in Eq. (5.4)

$$-\left\{\frac{\partial D}{\partial t} + u \frac{\partial D}{\partial x}\right\} = -k_1 C + k_2 D \quad (5.7)$$

Substituting  $C(x, t)$  in Eq. (5.7):

$$\frac{\partial D}{\partial t} + u \frac{\partial D}{\partial x} = k_1 \left\{ C_R U\left(t - \frac{x}{u}\right) \exp\left(-k_1 \frac{x}{u}\right) \right\} - k_2 D \quad (5.8)$$

Taking Laplace transform for each terms of Eq. (5.8)

$$sD^* + u \frac{dD^*}{dx} = k_1 \left\{ C_R \frac{e^{-\frac{sx}{u}}}{s} e^{-k_1 \frac{x}{u}} \right\} - k_2 D^*$$



$$\frac{dD^*}{dx} = \frac{k_1}{u} \left\{ C_R \frac{e^{-\frac{s}{u}x}}{s} e^{-k_1 \frac{x}{u}} \right\} - \left( \frac{s+k_2}{u} \right) D^* \quad (5.9)$$

Multiplying both sides by  $e^{\left(\frac{s+k_2}{u}\right)x}$

$$\frac{dD^*}{dx} e^{\left(\frac{s+k_2}{u}\right)x} + e^{\left(\frac{s+k_2}{u}\right)x} \left( \frac{s+k_2}{u} \right) D^* = \frac{k_1}{u} \left\{ C_R \frac{e^{-\frac{s}{u}x}}{s} e^{-k_1 \frac{x}{u}} \right\} e^{\left(\frac{s+k_2}{u}\right)x}$$

Simplifying

$$\frac{d \left[ D^* e^{\left(\frac{s+k_2}{u}\right)x} \right]}{dx} = \frac{k_1}{u} \left\{ \frac{C_R}{s} e^{\left(\frac{k_2-k_1}{u}\right)x} \right\} \quad (5.10)$$

Integrating Eq. (5.10)

$$D^* e^{\left(\frac{s+k_2}{u}\right)x} = \frac{k_1 C_R}{u s} e^{\left(\frac{k_2-k_1}{u}\right)x} \frac{1}{\left(\frac{k_2-k_1}{u}\right)} + A \quad (5.11)$$

where,  $A$  is the integration constant.

At  $x = 0$ ;  $D = D_0$ , hence  $D^* = D_0 / s$ ,

$$A = \frac{D_0}{s} - \frac{k_1 C_R}{k_2 - k_1} \frac{1}{s}$$

Substituting  $A$  in Eq. (5.11)

$$D^* = \frac{k_1 C_R}{k_2 - k_1} \frac{1}{s} e^{\left(\frac{k_2-k_1}{u}\right)x} e^{-\left(\frac{s+k_2}{u}\right)x} - \frac{k_1 C_R}{k_2 - k_1} \frac{1}{s} e^{-\left(\frac{s+k_2}{u}\right)x} + \frac{D_0}{s} e^{-\left(\frac{s+k_2}{u}\right)x}$$

or

$$D^* = \frac{k_1 C_R}{k_2 - k_1} \left\{ e^{-\frac{k_1}{u}x} - e^{-\frac{k_2}{u}x} \right\} \frac{e^{-\frac{s}{u}x}}{s} + D_0 e^{-\frac{k_2}{u}x} \frac{e^{-\frac{s}{u}x}}{s} \quad (5.12)$$

Taking inverse Laplace transform for Eq. (5.12)

$$D = C_R \left( \frac{k_1}{k_2 - k_1} \right) \left\{ e^{-\frac{k_1}{u}x} - e^{-\frac{k_2}{u}x} \right\} U \left( t - \frac{x}{u} \right) + D_0 e^{-\frac{k_2}{u}x} U \left( t - \frac{x}{u} \right)$$

Hence,

$$C_{DO}(x, t) = S_{DO} - \left\{ C_R \left( \frac{k_1}{k_2 - k_1} \right) \left[ e^{-\frac{k_1 x}{u}} - e^{-\frac{k_2 x}{u}} \right] U \left( t - \frac{x}{u} \right) + D_0 e^{-\frac{k_2 x}{u}} U \left( t - \frac{x}{u} \right) \right\}$$

The dissolved oxygen concentration at the end of plug flow zone is

$$C_{DO}(\alpha u, t) = S_{DO} - \left\{ C_R \left( \frac{k_1}{k_2 - k_1} \right) \left[ e^{-k_1 \alpha} - e^{-k_2 \alpha} \right] U(t - \alpha) + D_0 e^{-k_2 \alpha} U(t - \alpha) \right\} \quad (5.13)$$

where,  $C_{DO}(\alpha u, t)$  is DO concentration at the end of plug flow zone (mg/L).

### 5.3.2 Derivation of DO Concentration in the First Thoroughly Mixed Zone

The effluent from the plug flow zone is the influent to the first thoroughly mixed zone. Decay of the pollutant takes place in the first thoroughly mixed zone. Therefore, dissolved oxygen is consumed. Simultaneously re-aeration takes place. Over a time period  $\Delta t$ , the mass balance for dissolved oxygen is

$$V_1 \Delta C_{DO} = \left\{ S_{DO} - \left\{ C_R \left( \frac{k_1}{k_2 - k_1} \right) \left[ e^{-k_1 \alpha} - e^{-k_2 \alpha} \right] U(t - \alpha) + D_0 e^{-k_2 \alpha} U(t - \alpha) \right\} \right\} Q \Delta t \quad (5.14)$$

$$- C_{DO} Q \Delta t - k_1 V_1 C \Delta t + k_2 V_1 (S_{DO} - C_{DO}) \Delta t$$

where  $V_1$  is the volume of the first thoroughly mixed zone. In Eq. (5.14), the first term in the left hand side is the change in dissolved oxygen storage in the mixed zone over time period  $\Delta t$ , the first term in the right hand side is the DO mass out from the plug flow zone entering to the first thoroughly mixed zone, the second term is the mass leaving the first thoroughly mixed zone, the third term is the consumption of dissolved oxygen and the last term is the replenishment of dissolved oxygen.

Let,  $Q / V_1 = 1 / T_1$ ; then,

$$\frac{\Delta C_{DO}}{\Delta t} = \frac{1}{T_1} \left\{ S_{DO} - \left\{ C_R \left( \frac{k_1}{k_2 - k_1} \right) \left[ e^{-k_1 \alpha} - e^{-k_2 \alpha} \right] U(t - \alpha) + D_0 e^{-k_2 \alpha} U(t - \alpha) \right\} \right\} \quad (5.15)$$

$$- \frac{C_{DO}}{T_1} - k_1 C + k_2 (S_{DO} - C_{DO})$$

In differential form,

$$\frac{dC_{DO}}{dt} = \frac{1}{T_1} \left\{ S_{DO} - \left[ C_R \left( \frac{k_1}{k_2 - k_1} \right) \left[ e^{-k_1 \alpha} - e^{-k_2 \alpha} \right] U(t - \alpha) + D_0 e^{-k_2 \alpha} U(t - \alpha) \right] \right\} - \frac{C_{DO}}{T_1} - k_1 C + k_2 (S_{DO} - C_{DO}) \quad (5.16)$$

Incorporating DO deficit  $D$  as  $S_{DO} - C_{DO}$  and,  $\frac{dD}{dt} = -\frac{dC_{DO}}{dt}$  in Eq. (5.16) and rearranging,

$$\frac{dD}{dt} + \left( \frac{1 + k_2 T_1}{T_1} \right) D = \frac{1}{T_1} \left\{ C_R \left( \frac{k_1}{k_2 - k_1} \right) \left[ e^{-k_1 \alpha} - e^{-k_2 \alpha} \right] U(t - \alpha) + D_0 e^{-k_2 \alpha} U(t - \alpha) \right\} + k_1 C \quad (5.17)$$

Multiplying both sides by  $e^{\left( \frac{1 + k_2 T_1}{T_1} \right) t}$  and simplifying,

$$\frac{d}{dt} \left[ D e^{\left( \frac{1 + k_2 T_1}{T_1} \right) t} \right] = \frac{1}{T_1} \left\{ C_R \left( \frac{k_1}{k_2 - k_1} \right) \left[ e^{-k_1 \alpha} - e^{-k_2 \alpha} \right] U(t - \alpha) + D_0 e^{-k_2 \alpha} U(t - \alpha) \right\} e^{\left( \frac{1 + k_2 T_1}{T_1} \right) t} + k_1 C e^{\left( \frac{1 + k_2 T_1}{T_1} \right) t} \quad (5.18)$$

The BOD concentration  $C$  in the first thoroughly mixed zone has been derived in Chapter 4

$$\text{and it is given by } C_{M1} = C = \frac{C_R e^{-k_1 \alpha}}{(1 + k_1 T_1)} \left[ 1 - e^{-\left( \frac{1 + k_1 T_1}{T_1} \right) [t - \alpha]} \right] U(t - \alpha)$$

Incorporating  $C$  in Eq. (5.18)

$$\frac{d}{dt} \left[ D e^{\left( \frac{1 + k_2 T_1}{T_1} \right) t} \right] = \frac{1}{T_1} \left\{ C_R \left( \frac{k_1}{k_2 - k_1} \right) \left[ e^{-k_1 \alpha} - e^{-k_2 \alpha} \right] U(t - \alpha) + D_0 e^{-k_2 \alpha} U(t - \alpha) \right\} e^{\left( \frac{1 + k_2 T_1}{T_1} \right) t} + k_1 \left\{ \frac{C_R e^{-k_1 \alpha}}{(1 + k_1 T_1)} \left[ 1 - e^{-\left( \frac{1 + k_1 T_1}{T_1} \right) [t - \alpha]} \right] U(t - \alpha) \right\} e^{\left( \frac{1 + k_2 T_1}{T_1} \right) t} \quad (5.19)$$

Rearranging this:

$$d \left[ D e^{\left( \frac{1 + k_2 T_1}{T_1} \right) t} \right] = \frac{1}{T_1} \left\{ C_R \left( \frac{k_1}{k_2 - k_1} \right) \left[ e^{-k_1 \alpha} - e^{-k_2 \alpha} \right] U(t - \alpha) + D_0 e^{-k_2 \alpha} U(t - \alpha) \right\} e^{\left( \frac{1 + k_2 T_1}{T_1} \right) t} dt + k_1 \left\{ \frac{C_R e^{-k_1 \alpha}}{(1 + k_1 T_1)} \left[ e^{\left( \frac{1 + k_2 T_1}{T_1} \right) t} - e^{\left( \frac{1 + k_1 T_1}{T_1} \right) \alpha} e^{(k_2 - k_1)t} \right] U(t - \alpha) \right\} dt \quad (5.20)$$

Integrating Eq. (5.20)

$$\begin{aligned}
De^{\left(\frac{1+k_2T_1}{T_1}\right)t} &= \left\{ C_R \left( \frac{k_1}{k_2-k_1} \right) \left[ e^{-k_1\alpha} - e^{-k_2\alpha} \right] U(t-\alpha) + D_0 e^{-k_2\alpha} U(t-\alpha) \right\} \frac{e^{\left(\frac{1+k_2T_1}{T_1}\right)t}}{(1+k_2T_1)} \\
&+ C_R e^{-k_1\alpha} \left( \frac{k_1}{1+k_1T_1} \right) \left\{ \frac{T_1 e^{\left(\frac{1+k_2T_1}{T_1}\right)t}}{(1+k_2T_1)} - \frac{e^{\left(\frac{1+k_1T_1}{T_1}\right)\alpha} e^{[k_2-k_1]t}}{(k_2-k_1)} \right\} U(t-\alpha) + A
\end{aligned} \tag{5.21}$$

where  $A$  is the integration constant

For  $t = \alpha$ ;  $D = 0$ , hence,

$$\begin{aligned}
A &= - \left\{ C_R \left( \frac{k_1}{k_2-k_1} \right) \left[ e^{-k_1\alpha} - e^{-k_2\alpha} \right] U(t-\alpha) + D_0 e^{-k_2\alpha} U(t-\alpha) \right\} \frac{e^{\left(\frac{1+k_2T_1}{T_1}\right)\alpha}}{(1+k_2T_1)} \\
&- C_R e^{-k_1\alpha} \left( \frac{k_1}{1+k_1T_1} \right) \left\{ \frac{T_1 e^{\left(\frac{1+k_2T_1}{T_1}\right)\alpha}}{(1+k_2T_1)} - \frac{e^{\left(\frac{1+k_1T_1}{T_1}\right)\alpha} e^{(k_2-k_1)\alpha}}{(k_2-k_1)} \right\} U(t-\alpha)
\end{aligned}$$

Substituting  $A$  into Eq. (5.21) and simplifying

$$\begin{aligned}
De^{\left(\frac{1+k_2T_1}{T_1}\right)t} &= C_R U(t-\alpha) \left( \frac{k_1}{k_2-k_1} \right) \left( \frac{1}{1+k_2T_1} \right) (e^{-k_1\alpha} - e^{-k_2\alpha}) e^{\left(\frac{1+k_2T_1}{T_1}\right)t} \\
&+ C_R U(t-\alpha) e^{-k_1\alpha} \left( \frac{T_1 k_1}{1+k_1T_1} \right) \frac{e^{\left(\frac{1+k_2T_1}{T_1}\right)t}}{(1+k_2T_1)} - C_R U(t-\alpha) e^{-k_1\alpha} \left( \frac{k_1}{k_2-k_1} \right) \left( \frac{1}{1+k_1T_1} \right) e^{\left(\frac{1+k_1T_1}{T_1}\right)\alpha} e^{[k_2-k_1]t} \\
&- C_R U(t-\alpha) \left( \frac{k_1}{k_2-k_1} \right) (e^{-k_1\alpha} - e^{-k_2\alpha}) \frac{e^{\left(\frac{1+k_2T_1}{T_1}\right)\alpha}}{(1+k_2T_1)} - C_R U(t-\alpha) e^{-k_1\alpha} \left( \frac{T_1 k_1}{1+k_1T_1} \right) \frac{e^{\left(\frac{1+k_2T_1}{T_1}\right)\alpha}}{(1+k_2T_1)} \\
&+ C_R U(t-\alpha) e^{-k_1\alpha} \left( \frac{k_1}{k_2-k_1} \right) \frac{e^{\left(\frac{1+k_1T_1}{T_1}\right)\alpha} e^{[k_2-k_1]\alpha}}{(1+k_1T_1)} \\
&+ D_0 U(t-\alpha) e^{-k_2\alpha} \left( \frac{1}{1+k_2T_1} \right) e^{\left(\frac{1+k_2T_1}{T_1}\right)t} - D_0 U(t-\alpha) e^{-k_2\alpha} \frac{e^{\left(\frac{1+k_2T_1}{T_1}\right)\alpha}}{(1+k_2T_1)}
\end{aligned} \tag{5.22}$$

Dividing by  $e^{\left(\frac{1+k_2T_1}{T_1}\right)t}$

$$\begin{aligned}
D = & C_R U(t-\alpha) \left( \frac{k_1}{k_2 - k_1} \right) \left( \frac{1}{1 + k_2 T_1} \right) (e^{-k_1 \alpha} - e^{-k_2 \alpha}) \left[ 1 - e^{-\left( \frac{1+k_2 T_1}{T_1} \right) [t-\alpha]} \right] \\
& + C_R U(t-\alpha) e^{-k_1 \alpha} \left( \frac{T_1 k_1}{1 + k_1 T_1} \right) \frac{1}{(1 + k_2 T_1)} \left[ 1 - e^{-\left( \frac{1+k_2 T_1}{T_1} \right) [t-\alpha]} \right] \\
& - C_R U(t-\alpha) e^{-k_1 \alpha} \left( \frac{k_1}{k_2 - k_1} \right) \frac{1}{(1 + k_1 T_1)} \left[ e^{-\left( \frac{1+k_1 T_1}{T_1} \right) [t-\alpha]} - e^{-\left( \frac{1+k_2 T_1}{T_1} \right) [t-\alpha]} \right] \\
& + D_0 U(t-\alpha) e^{-k_2 \alpha} \frac{1}{(1 + k_2 T_1)} \left[ 1 - e^{-\left( \frac{1+k_2 T_1}{T_1} \right) [t-\alpha]} \right]
\end{aligned} \tag{5.23}$$

Hence, DO concentration is

$$C_{DO} = S_{DO} - D$$

The dissolved oxygen concentration of the effluent from the first mixed zone is

$$\begin{aligned}
& C_{DO} [(\alpha + T_1)u, t] \\
= & S_{DO} - \left\{ \begin{aligned}
& C_R U(t-\alpha) \left( \frac{k_1}{k_2 - k_1} \right) \left( \frac{1}{1 + k_2 T_1} \right) (e^{-k_1 \alpha} - e^{-k_2 \alpha}) \left[ 1 - e^{-\left( \frac{1+k_2 T_1}{T_1} \right) [t-\alpha]} \right] \\
& + C_R U(t-\alpha) e^{-k_1 \alpha} \left( \frac{T_1 k_1}{1 + k_1 T_1} \right) \left( \frac{1}{1 + k_2 T_1} \right) \left[ 1 - e^{-\left( \frac{1+k_2 T_1}{T_1} \right) [t-\alpha]} \right] \\
& - C_R U(t-\alpha) e^{-k_1 \alpha} \left( \frac{k_1}{k_2 - k_1} \right) \left( \frac{1}{1 + k_1 T_1} \right) \left[ e^{-\left( \frac{1+k_1 T_1}{T_1} \right) [t-\alpha]} - e^{-\left( \frac{1+k_2 T_1}{T_1} \right) [t-\alpha]} \right] \\
& + D_0 U(t-\alpha) e^{-k_2 \alpha} \left( \frac{1}{1 + k_2 T_1} \right) \left[ 1 - e^{-\left( \frac{1+k_2 T_1}{T_1} \right) [t-\alpha]} \right]
\end{aligned} \right\} \tag{5.24}
\end{aligned}$$

### 5.3.3 Derivation of DO Concentration in the Second Thoroughly Mixed Zone

The effluent from the first thoroughly mixed zone is the influent to the second thoroughly mixed zone. Decay of the pollutant takes place in the second thoroughly mixed zone. Therefore dissolved oxygen is consumed. Simultaneously re-aeration takes place. Over a time period  $\Delta t$ , the mass balance for dissolved oxygen is

$$V_2 \Delta C_{DO} = \left\{ \begin{aligned} & S_{DO} - \left[ C_R U(t-\alpha) \left( \frac{k_1}{k_2 - k_1} \right) \left( \frac{1}{1 + k_2 T_1} \right) (e^{-k_1 \alpha} - e^{-k_2 \alpha}) \left[ 1 - e^{-\left( \frac{1+k_2 T_1}{T_1} \right) [t-\alpha]} \right] \right] \\ & + C_R U(t-\alpha) e^{-k_1 \alpha} \left( \frac{T_1 k_1}{1 + k_1 T_1} \right) \left( \frac{1}{1 + k_2 T_1} \right) \left[ 1 - e^{-\left( \frac{1+k_2 T_1}{T_1} \right) [t-\alpha]} \right] \\ & - C_R U(t-\alpha) e^{-k_1 \alpha} \left( \frac{k_1}{k_2 - k_1} \right) \left( \frac{1}{1 + k_1 T_1} \right) \left[ e^{-\left( \frac{1+k_1 T_1}{T_1} \right) [t-\alpha]} - e^{-\left( \frac{1+k_2 T_1}{T_1} \right) [t-\alpha]} \right] \\ & + D_0 U(t-\alpha) e^{-k_2 \alpha} \left( \frac{1}{1 + k_2 T_1} \right) \left[ 1 - e^{-\left( \frac{1+k_2 T_1}{T_1} \right) [t-\alpha]} \right] \end{aligned} \right\} Q \Delta t \quad (5.25)$$

$$- C_{DO} Q \Delta t - k_1 V_2 C \Delta t + k_2 V_2 (S_{DO} - C_{DO}) \Delta t$$

where  $V_2$  is the volume of the second thoroughly mixed zone. In Eq. (5.25) the first term in right hand side within  $\{ \}$  bracket is the DO mass out from 1<sup>st</sup> mixed zone or inflow to the second thoroughly mixed zone.

Let,  $Q / V_2 = 1 / T_2$ ;

In differential form

$$\frac{dC_{DO}}{dt} = \left\{ \begin{aligned} & \frac{S_{DO}}{T_2} - \frac{1}{T_2} \left[ C_R U(t-\alpha) \left( \frac{k_1}{k_2 - k_1} \right) \left( \frac{1}{1 + k_2 T_1} \right) (e^{-k_1 \alpha} - e^{-k_2 \alpha}) \left[ 1 - e^{-\left( \frac{1+k_2 T_1}{T_1} \right) [t-\alpha]} \right] \right] \\ & + C_R U(t-\alpha) e^{-k_1 \alpha} \left( \frac{T_1 k_1}{1 + k_1 T_1} \right) \left( \frac{1}{1 + k_2 T_1} \right) \left[ 1 - e^{-\left( \frac{1+k_2 T_1}{T_1} \right) [t-\alpha]} \right] \\ & - C_R U(t-\alpha) e^{-k_1 \alpha} \left( \frac{k_1}{k_2 - k_1} \right) \left( \frac{1}{1 + k_1 T_1} \right) \left[ e^{-\left( \frac{1+k_1 T_1}{T_1} \right) [t-\alpha]} - e^{-\left( \frac{1+k_2 T_1}{T_1} \right) [t-\alpha]} \right] \\ & + D_0 U(t-\alpha) e^{-k_2 \alpha} \left( \frac{1}{1 + k_2 T_1} \right) \left[ 1 - e^{-\left( \frac{1+k_2 T_1}{T_1} \right) [t-\alpha]} \right] \end{aligned} \right\} \quad (5.26)$$

$$- \frac{C_{DO}}{T_2} - k_1 C + k_2 (S_{DO} - C_{DO})$$

Incorporating DO deficit,  $D$  as  $S_{DO} - C_{DO}$  and  $\frac{dD}{dt} = -\frac{dC_{DO}}{dt}$  in Eq. (5.26) and rearranging,

$$\frac{dD}{dt} + \left( \frac{1+k_2 T_2}{T_2} \right) D = \left\{ \begin{array}{l} \frac{1}{T_2} \left\{ C_R U(t-\alpha) \left( \frac{k_1}{k_2 - k_1} \right) \left( \frac{1}{1+k_2 T_1} \right) (e^{-k_1 \alpha} - e^{-k_2 \alpha}) \left[ 1 - e^{-\left( \frac{1+k_2 T_1}{T_1} \right) [t-\alpha]} \right] \right\} \\ + C_R U(t-\alpha) e^{-k_1 \alpha} \left( \frac{T_1 k_1}{1+k_1 T_1} \right) \frac{1}{(1+k_2 T_1)} \left[ 1 - e^{-\left( \frac{1+k_2 T_1}{T_1} \right) [t-\alpha]} \right] \\ - C_R U(t-\alpha) e^{-k_1 \alpha} \left( \frac{k_1}{k_2 - k_1} \right) \left( \frac{1}{1+k_1 T_1} \right) \left[ e^{-\left( \frac{1+k_1 T_1}{T_1} \right) [t-\alpha]} - e^{-\left( \frac{1+k_2 T_1}{T_1} \right) [t-\alpha]} \right] \\ + D_0 U(t-\alpha) e^{-k_2 \alpha} \left( \frac{1}{1+k_2 T_1} \right) \left[ 1 - e^{-\left( \frac{1+k_2 T_1}{T_1} \right) [t-\alpha]} \right] \right\} \\ + k_1 C \end{array} \right\} \quad (5.27)$$

Multiplying both sides by  $e^{\left( \frac{1+k_2 T_2}{T_2} \right) t}$  and simplifying

$$\frac{d}{dt} \left[ D e^{\left( \frac{1+k_2 T_2}{T_2} \right) t} \right] = \left\{ \begin{array}{l} \frac{1}{T_2} \left\{ C_R U(t-\alpha) \left( \frac{k_1}{k_2 - k_1} \right) \left( \frac{1}{1+k_2 T_1} \right) (e^{-k_1 \alpha} - e^{-k_2 \alpha}) \left[ 1 - e^{-\left( \frac{1+k_2 T_1}{T_1} \right) [t-\alpha]} \right] \right\} \\ + C_R U(t-\alpha) e^{-k_1 \alpha} \left( \frac{T_1 k_1}{1+k_1 T_1} \right) \frac{1}{(1+k_2 T_1)} \left[ 1 - e^{-\left( \frac{1+k_2 T_1}{T_1} \right) [t-\alpha]} \right] \\ - C_R U(t-\alpha) e^{-k_1 \alpha} \left( \frac{k_1}{k_2 - k_1} \right) \left( \frac{1}{1+k_1 T_1} \right) \left[ e^{-\left( \frac{1+k_1 T_1}{T_1} \right) [t-\alpha]} - e^{-\left( \frac{1+k_2 T_1}{T_1} \right) [t-\alpha]} \right] \\ + D_0 U(t-\alpha) e^{-k_2 \alpha} \left( \frac{1}{1+k_2 T_1} \right) \left[ 1 - e^{-\left( \frac{1+k_2 T_1}{T_1} \right) [t-\alpha]} \right] \right\} \\ + k_1 C e^{\left( \frac{1+k_2 T_2}{T_2} \right) t} \end{array} \right\} e^{\left( \frac{1+k_2 T_2}{T_2} \right) t} \quad (5.28)$$

The BOD concentration  $C$  in the second thoroughly mixed zone has been derived in Chapter 4 and it is given by

$$C_{M2} = C = \frac{C_R U(t-\alpha) e^{-k_1 \alpha}}{(1+k_1 T_1)} \left\{ \frac{\left( 1 - e^{-\left( \frac{1+k_1 T_2}{T_2} \right) [t-\alpha]} \right)}{1+k_1 T_2} - \frac{T_1 \left( e^{-\left( \frac{1+k_1 T_1}{T_1} \right) [t-\alpha]} - e^{-\left( \frac{1+k_2 T_2}{T_2} \right) [t-\alpha]} \right)}{T_1 - T_2} \right\}$$

Incorporating  $C$  in Eq. (5.28)

$$\frac{d}{dt} \left[ De^{\left(\frac{1+k_2 T_2}{T_2}\right)t} \right] = \left\{ \begin{aligned} & \frac{1}{T_2} \left[ C_R U(t-\alpha) \left( \frac{k_1}{k_2 - k_1} \right) \left( \frac{1}{1+k_2 T_1} \right) (e^{-k_1 \alpha} - e^{-k_2 \alpha}) \left[ 1 - e^{-\left(\frac{1+k_2 T_1}{T_1}\right)(t-\alpha)} \right] \right. \\ & + C_R U(t-\alpha) e^{-k_1 \alpha} \left( \frac{T_1 k_1}{1+k_1 T_1} \right) \frac{1}{(1+k_2 T_1)} \left[ 1 - e^{-\left(\frac{1+k_2 T_1}{T_1}\right)(t-\alpha)} \right] \\ & - C_R U(t-\alpha) e^{-k_1 \alpha} \left( \frac{k_1}{k_2 - k_1} \right) \frac{1}{(1+k_1 T_1)} \left[ e^{-\left(\frac{1+k_1 T_1}{T_1}\right)(t-\alpha)} - e^{-\left(\frac{1+k_2 T_1}{T_1}\right)(t-\alpha)} \right] \\ & \left. + D_0 U(t-\alpha) e^{-k_2 \alpha} \frac{1}{(1+k_2 T_1)} \left[ 1 - e^{-\left(\frac{1+k_2 T_1}{T_1}\right)(t-\alpha)} \right] \right] \right\} e^{\left(\frac{1+k_2 T_2}{T_2}\right)t} \\ & + \left[ C_R U(t-\alpha) e^{-k_1 \alpha} \frac{k_1}{(1+k_1 T_1)(1+k_1 T_2)} \left( 1 - e^{-\left(\frac{1+k_1 T_2}{T_2}\right)(t-\alpha)} \right) \right] e^{\left(\frac{1+k_2 T_2}{T_2}\right)t} \\ & - \left[ C_R U(t-\alpha) e^{-k_1 \alpha} \frac{k_1}{(1+k_1 T_1)(T_1 - T_2)} \left( e^{-\left(\frac{1+k_1 T_1}{T_1}\right)(t-\alpha)} - e^{-\left(\frac{1+k_1 T_2}{T_2}\right)(t-\alpha)} \right) \right] e^{\left(\frac{1+k_2 T_2}{T_2}\right)t} \quad (5.29) \end{aligned} \right.$$

Integrating Eq. (5.29)

$$De^{\left(\frac{1+k_2 T_2}{T_2}\right)t} = \left\{ \begin{aligned} & \left[ \begin{aligned} & C_R U(t-\alpha) \left( \frac{k_1}{k_2 - k_1} \right) \left( \frac{1}{1+k_2 T_1} \right) (e^{-k_1 \alpha} - e^{-k_2 \alpha}) \left[ \frac{e^{\left(\frac{1+k_2 T_2}{T_2}\right)t}}{1+k_2 T_2} - \frac{T_1 e^{\left(\frac{1+k_2 T_1}{T_1}\right)\alpha} e^{\left(\frac{T_1 - T_2}{T_1 T_2}\right)t}}{T_1 - T_2} \right] \right. \\ & + C_R U(t-\alpha) e^{-k_1 \alpha} \left( \frac{T_1 k_1}{1+k_1 T_1} \right) \frac{1}{(1+k_2 T_1)} \left[ \frac{e^{\left(\frac{1+k_2 T_2}{T_2}\right)t}}{1+k_2 T_2} - \frac{T_1 e^{\left(\frac{1+k_2 T_1}{T_1}\right)\alpha} e^{\left(\frac{T_1 - T_2}{T_1 T_2}\right)t}}{T_1 - T_2} \right] \right. \\ & - C_R U(t-\alpha) e^{-k_1 \alpha} \left( \frac{k_1}{k_2 - k_1} \right) \frac{1}{(1+k_1 T_1)} \left[ \frac{T_1 e^{\left(\frac{1+k_1 T_1}{T_1}\right)\alpha} e^{\left[\left(\frac{1+k_2 T_2}{T_2}\right)t - \left(\frac{1+k_1 T_1}{T_1}\right)t\right]}}{T_1(1+k_2 T_2) - T_2(1+k_1 T_1)} - \frac{T_1 e^{\left(\frac{1+k_1 T_1}{T_1}\right)\alpha} e^{\left(\frac{T_1 - T_2}{T_1 T_2}\right)t}}{T_1 - T_2} \right] \right. \\ & \left. + D_0 U(t-\alpha) e^{-k_2 \alpha} \frac{1}{(1+k_2 T_1)} \left[ \frac{e^{\left(\frac{1+k_2 T_2}{T_2}\right)t}}{1+k_2 T_2} - \frac{T_1 e^{\left(\frac{1+k_2 T_1}{T_1}\right)\alpha} e^{\left(\frac{T_1 - T_2}{T_1 T_2}\right)t}}{T_1 - T_2} \right] \right] \right\} \\ & + \left[ C_R U(t-\alpha) e^{-k_1 \alpha} \frac{k_1}{(1+k_1 T_1)(1+k_1 T_2)} \left( \frac{T_2 e^{\left(\frac{1+k_2 T_2}{T_2}\right)t}}{1+k_2 T_2} - \frac{e^{\left(\frac{1+k_1 T_2}{T_2}\right)\alpha} e^{(k_2 - k_1)t}}{k_2 - k_1} \right) \right] \\ & - \left[ C_R U(t-\alpha) e^{-k_1 \alpha} \frac{k_1}{(1+k_1 T_1)(T_1 - T_2)} \left( \frac{T_1 T_2 e^{\left(\frac{1+k_1 T_1}{T_1}\right)\alpha} e^{\left[\left(\frac{1+k_2 T_2}{T_2}\right)t - \left(\frac{1+k_1 T_1}{T_1}\right)t\right]}}{T_1(1+k_2 T_2) - T_2(1+k_1 T_1)} - \frac{e^{\left(\frac{1+k_1 T_2}{T_2}\right)\alpha} e^{(k_2 - k_1)t}}{k_2 - k_1} \right) \right] + A \quad (5.30) \end{aligned} \right.$$

where  $A$  is the integration constant.





$$\begin{aligned}
De^{\left(\frac{1+k_2T_2}{T_2}\right)t} = & \left\{ \begin{aligned} & C_R U(t-\alpha) \left( \frac{k_1}{k_2-k_1} \right) \left( \frac{1}{1+k_2T_1} \right) (e^{-k_1\alpha} - e^{-k_2\alpha}) \left[ \frac{e^{\left(\frac{1+k_2T_2}{T_2}\right)t}}{1+k_2T_2} \frac{1+k_2T_2}{1+k_2T_2} + \frac{T_1 e^{\left(\frac{1+k_2T_2}{T_2}\right)t}}{T_1 - T_2} + \frac{T_1 e^{\left(\frac{1+k_2T_2}{T_2}\right)t}}{T_1 - T_2} \right] \\ & + C_R U(t-\alpha) e^{-k_1\alpha} \left( \frac{T_1 k_1}{1+k_1T_1} \right) \left( \frac{1}{1+k_2T_1} \right) \left[ \frac{e^{\left(\frac{1+k_2T_2}{T_2}\right)t}}{1+k_2T_2} \frac{1+k_2T_2}{1+k_2T_2} + \frac{T_1 e^{\left(\frac{1+k_2T_2}{T_2}\right)t}}{T_1 - T_2} + \frac{T_1 e^{\left(\frac{1+k_2T_2}{T_2}\right)t}}{T_1 - T_2} \right] \end{aligned} \right\} \\
& - \left\{ \begin{aligned} & C_R U(t-\alpha) e^{-k_2\alpha} \left( \frac{k_1}{k_2-k_1} \right) \left( \frac{1}{1+k_1T_1} \right) \left[ \frac{T_1 e^{\left(\frac{1+k_2T_2}{T_2}\right)t}}{T_1(1+k_2T_2) - T_2(1+k_1T_1)} + \frac{T_1 e^{\left(\frac{1+k_2T_2}{T_2}\right)t}}{T_1(1+k_2T_2) - T_2(1+k_1T_1)} + \frac{T_1 e^{\left(\frac{1+k_2T_2}{T_2}\right)t}}{T_1 - T_2} \right] \\ & + C_R U(t-\alpha) e^{-k_1\alpha} \left( \frac{k_1}{1+k_1T_1} \right) \left( \frac{1}{1+k_1T_2} \right) \left[ \frac{T_2 e^{\left(\frac{1+k_2T_2}{T_2}\right)t}}{1+k_2T_2} + \frac{T_2 e^{\left(\frac{1+k_2T_2}{T_2}\right)t}}{1+k_2T_2} + \frac{T_2 e^{\left(\frac{1+k_2T_2}{T_2}\right)t}}{1+k_2T_2} \right] \\ & - C_R U(t-\alpha) e^{-k_1\alpha} \left( \frac{k_1}{1+k_1T_1} \right) \left( \frac{T_1}{T_1 - T_2} \right) \left[ \frac{T_1 T_2 e^{\left(\frac{1+k_2T_2}{T_2}\right)t}}{T_1(1+k_2T_2) - T_2(1+k_1T_1)} + \frac{T_1 T_2 e^{\left(\frac{1+k_2T_2}{T_2}\right)t}}{T_1(1+k_2T_2) - T_2(1+k_1T_1)} + \frac{T_1 T_2 e^{\left(\frac{1+k_2T_2}{T_2}\right)t}}{k_2 - k_1} \right] \end{aligned} \right\} \\
& + D_0 e^{-k_2\alpha} \frac{U(t-\alpha)}{(1+k_2T_1)} \left( \frac{e^{\left(\frac{1+k_2T_2}{T_2}\right)t}}{1+k_2T_2} \frac{1+k_2T_2}{1+k_2T_2} + \frac{T_1 e^{\left(\frac{1+k_2T_2}{T_2}\right)t}}{T_1 - T_2} + \frac{T_1 e^{\left(\frac{1+k_2T_2}{T_2}\right)t}}{T_1 - T_2} \right)
\end{aligned} \tag{5.31}$$

Dividing by  $e^{\left(\frac{1+k_2T_2}{T_2}\right)t}$

$$\begin{aligned}
D = & \left\{ \left[ C_R U(t-\alpha) \left( \frac{k_1}{k_2 - k_1} \right) \left( \frac{1}{1 + k_2 T_1} \right) (e^{-k_1 \alpha} - e^{-k_2 \alpha}) \right] \left[ \frac{1}{1 + k_2 T_2} \left( 1 - e^{-\left( \frac{1+k_2 T_2}{T_2} \right) [t-\alpha]} \right) - \frac{T_1}{T_1 - T_2} \left( e^{-\left( \frac{1+k_2 T_1}{T_1} \right) [t-\alpha]} - e^{-\left( \frac{1+k_2 T_2}{T_2} \right) [t-\alpha]} \right) \right] \right\} \\
& + C_R U(t-\alpha) e^{-k_1 \alpha} \left( \frac{T_1 k_1}{1 + k_1 T_1} \right) \left( \frac{1}{1 + k_2 T_1} \right) \\
& - C_R U(t-\alpha) e^{-k_1 \alpha} \left( \frac{k_1}{k_2 - k_1} \right) \frac{1}{(1 + k_1 T_1)} \left[ \frac{T_1}{T_1 (1 + k_2 T_2) - T_2 (1 + k_1 T_1)} \right] \left\{ e^{-\left( \frac{1+k_1 T_1}{T_1} \right) [t-\alpha]} - e^{-\left( \frac{1+k_2 T_2}{T_2} \right) [t-\alpha]} \right\} - \frac{T_1}{T_1 - T_2} \left\{ e^{-\left( \frac{1+k_2 T_1}{T_1} \right) [t-\alpha]} - e^{-\left( \frac{1+k_2 T_2}{T_2} \right) [t-\alpha]} \right\} \right\} \\
& + C_R U(t-\alpha) e^{-k_1 \alpha} \frac{k_1}{(1 + k_1 T_1) (1 + k_2 T_2)} \frac{1}{1 + k_2 T_2} \left[ \frac{T_2}{1 + k_2 T_2} \left( 1 - e^{-\left( \frac{1+k_2 T_2}{T_2} \right) [t-\alpha]} \right) - \frac{1}{k_2 - k_1} \left( e^{-\left( \frac{1+k_2 T_1}{T_1} \right) [t-\alpha]} - e^{-\left( \frac{1+k_2 T_2}{T_2} \right) [t-\alpha]} \right) \right] \\
& - C_R U(t-\alpha) e^{-k_1 \alpha} \frac{k_1}{(1 + k_1 T_1) (T_1 - T_2)} \frac{T_1}{T_1 (1 + k_2 T_2) - T_2 (1 + k_1 T_1)} \left\{ e^{-\left( \frac{1+k_1 T_1}{T_1} \right) [t-\alpha]} - e^{-\left( \frac{1+k_2 T_2}{T_2} \right) [t-\alpha]} \right\} - \frac{1}{k_2 - k_1} \left\{ e^{-\left( \frac{1+k_2 T_1}{T_1} \right) [t-\alpha]} - e^{-\left( \frac{1+k_2 T_2}{T_2} \right) [t-\alpha]} \right\} \right\} \\
& + D_0 U(t-\alpha) e^{-k_2 \alpha} \frac{1}{(1 + k_2 T_1)} \left[ \frac{1}{1 + k_2 T_2} \left( 1 - e^{-\left( \frac{1+k_2 T_2}{T_2} \right) [t-\alpha]} \right) - \frac{T_1}{T_1 - T_2} \left( e^{-\left( \frac{1+k_2 T_1}{T_1} \right) [t-\alpha]} - e^{-\left( \frac{1+k_2 T_2}{T_2} \right) [t-\alpha]} \right) \right]
\end{aligned} \tag{5.32}$$

Eq. (5.32) is the step response function at the exit of first hybrid unit comprising the response to boundary step pollutant perturbation  $C_R$  and boundary step deficit perturbation  $D_0$ . The response can be decomposed into two parts. Let for  $D_0 = 0$ , the step response function be represented by  $K_{D-CR}(t)$ . A unit step response function,  $K_{D-CRU}(t)$  is defined by substituting  $C_R = 1$  and  $D_0 = 0$  in Eq. (5.32).

Differentiating  $K_{D-CR}(t)$  with respect to  $t$ , the impulse response function,  $k_{D-CR}(t)$  in respect of deficit owing to an impulse pollutant perturbation

$C_R$  is

$$\begin{aligned}
 k_{D-CR}(t) = & \left[ \begin{aligned} & C_R U(t-\alpha) \left( \frac{k_1}{k_2 - k_1} \right) \left( \frac{1}{1 + k_2 T_1} \right) (e^{-k_1 \alpha} - e^{-k_2 \alpha}) \\ & + C_R U(t-\alpha) e^{-k_1 \alpha} \left( \frac{T_1 k_1}{1 + k_1 T_1} \right) \left( \frac{1}{1 + k_2 T_1} \right) \end{aligned} \right] \left[ \begin{aligned} & \left( \frac{1}{T_2} e^{-\left(\frac{1+k_2 T_2}{T_2}\right) [t-\alpha]} \right) - \frac{T_1}{T_1 - T_2} \left( \frac{1 + k_2 T_2}{T_2} e^{-\left(\frac{1+k_2 T_2}{T_2}\right) [t-\alpha]} \right) - \frac{1 + k_2 T_1}{T_1} e^{-\left(\frac{1+k_2 T_1}{T_1}\right) [t-\alpha]} \\ & \left[ \frac{T_1 (1 + k_2 T_2) - T_2 (1 + k_1 T_1)}{T_1} \right] \left( \frac{1 + k_2 T_2}{T_2} e^{-\left(\frac{1+k_2 T_2}{T_2}\right) [t-\alpha]} \right) - \frac{1 + k_1 T_1}{T_1} e^{-\left(\frac{1+k_1 T_1}{T_1}\right) [t-\alpha]} \end{aligned} \right] \\
 & - C_R U(t-\alpha) e^{-k_1 \alpha} \left( \frac{k_1}{k_2 - k_1} \right) \left( \frac{1}{1 + k_1 T_1} \right) \left[ \frac{T_1 (1 + k_2 T_2) - T_2 (1 + k_1 T_1)}{T_1} \right] \left( \frac{1 + k_2 T_2}{T_2} e^{-\left(\frac{1+k_2 T_2}{T_2}\right) [t-\alpha]} \right) - \frac{1 + k_1 T_1}{T_1} e^{-\left(\frac{1+k_1 T_1}{T_1}\right) [t-\alpha]} \\
 & + C_R U(t-\alpha) e^{-k_1 \alpha} \left( \frac{k_1}{1 + k_1 T_1} \right) \left( \frac{1}{1 + k_1 T_2} \right) \left[ \left( \frac{1}{e^{-\left(\frac{1+k_2 T_2}{T_2}\right) [t-\alpha]}} \right) - \frac{1}{k_2 - k_1} \left( \frac{1 + k_2 T_2}{T_2} e^{-\left(\frac{1+k_2 T_2}{T_2}\right) [t-\alpha]} \right) - \frac{1 + k_1 T_2}{T_2} e^{-\left(\frac{1+k_1 T_2}{T_2}\right) [t-\alpha]} \right] \\
 & - C_R U(t-\alpha) e^{-k_1 \alpha} \left( \frac{k_1}{1 + k_1 T_1} \right) \left( \frac{T_1}{T_1 - T_2} \right) \left[ \frac{T_1 T_2}{T_1 (1 + k_2 T_2) - T_2 (1 + k_1 T_1)} \right] \left( \frac{1 + k_2 T_2}{T_2} e^{-\left(\frac{1+k_2 T_2}{T_2}\right) [t-\alpha]} \right) - \frac{1 + k_1 T_1}{T_1} e^{-\left(\frac{1+k_1 T_1}{T_1}\right) [t-\alpha]} \right] \\
 & - \left[ \frac{1}{k_2 - k_1} \left( \frac{1 + k_2 T_2}{T_2} e^{-\left(\frac{1+k_2 T_2}{T_2}\right) [t-\alpha]} \right) - \frac{1 + k_1 T_2}{T_2} e^{-\left(\frac{1+k_1 T_2}{T_2}\right) [t-\alpha]} \right] \left[ \frac{1 + k_2 T_2}{T_2} e^{-\left(\frac{1+k_2 T_2}{T_2}\right) [t-\alpha]} \right] - \frac{1 + k_1 T_1}{T_1} e^{-\left(\frac{1+k_1 T_1}{T_1}\right) [t-\alpha]} \right] \\
 & \left. \right] \quad (5.33)
 \end{aligned}$$

A unit impulse response function  $k_{D-CRU}(t)$  is defined by assigning  $C_R = 1$  in Eq. (5.33)

Let the step response corresponding to the boundary deficit oxygen perturbation be designated by  $K_{D-D0}(t)$ .

From Eq. (5.32)

$$K_{D-D0}(t) = D_0 U(t-\alpha) e^{-k_2 \alpha} \frac{1}{(1+k_2 T_1)} \left[ \frac{1}{1+k_2 T_2} \left( 1 - e^{-\left(\frac{1+k_2 T_2}{T_2}\right)(t-\alpha)} \right) - \frac{T_1}{T_1 - T_2} \left( e^{-\left(\frac{1+k_2 T_1}{T_1}\right)(t-\alpha)} - e^{-\left(\frac{1+k_2 T_2}{T_2}\right)(t-\alpha)} \right) \right] \quad (5.34)$$

A unit step response function  $K_{D-D0} U(t)$  can be defined by substituting  $D_0 = 1$  in Eq. (5.34). Differentiating  $K_{D-D0}(t)$  with respect to  $t$ , the impulse response pertaining a boundary impulse deficit  $D_0$  is obtained as:

$$k_{D-D0}(t) = D_0 U(t-\alpha) \frac{e^{-k_2 \alpha}}{(1+k_2 T_1)} \left[ \frac{1}{T_2} \left( e^{-\left(\frac{1+k_2 T_2}{T_2}\right)(t-\alpha)} \right) - \frac{T_1}{T_1 - T_2} \left( \frac{1+k_2 T_2}{T_2} e^{-\left(\frac{1+k_2 T_2}{T_2}\right)(t-\alpha)} - \frac{1+k_2 T_1}{T_1} e^{-\left(\frac{1+k_2 T_1}{T_1}\right)(t-\alpha)} \right) \right] \quad (5.35)$$

A unit impulse response function  $k_{D-D0} U(t)$  is obtained by putting  $D_0 = 1$  in Eq. (5.35).

#### 5.4 DERIVATION OF DO DEFICIT AT SECOND AND SUBSEQUENT HYBRID UNITS

The oxygen deficit, due to the transport of pollutant, at the end of the  $n^{\text{th}}$  hybrid unit can be obtained using successive convolution. Let the pollutant concentration at the end of  $(n-1)^{\text{th}}$  hybrid unit be designated as  $C(n-1, t)$ . Method for computation of  $C(n-1, t)$  has been explained in chapter 4. Let the time span be discretised into  $m$  equal interval. Applying convolution technique, the dissolved oxygen deficit

$$\begin{aligned} D_{C_R}(n, t) &= \int_0^t C(n-1, \tau) k_{D-C_R U}(t-\tau) d\tau = \int_0^{m\Delta t} C(n-1, \tau) k_{D-C_R U}(m\Delta t - \tau) d\tau \\ &= \int_0^{\Delta t} C(n-1, \tau) k_{D-C_R U}(m\Delta t - \tau) d\tau + \int_{\Delta t}^{2\Delta t} C(n-1, \tau) k_{D-C_R U}(m\Delta t - \tau) d\tau \\ &\quad + \dots + \int_{(m-1)\Delta t}^{m\Delta t} C(n-1, \tau) k_{D-C_R U}(m\Delta t - \tau) d\tau \end{aligned} \quad (5.36)$$

where  $\Delta t$  is step size and  $t = m \Delta t$ . Between an interval  $(\gamma-1) \Delta t$  to  $\gamma \Delta t$ , an average rate of perturbation is

$$\bar{C}(n-1, \tau) = \frac{C[n-1, (\gamma-1)\Delta t] + C[n-1, \gamma\Delta t]}{2}, \quad (\gamma-1)\Delta t < \tau < \gamma\Delta t \quad (5.37)$$

Let  $\int_0^{\Delta t} k_{D-C_R U}(M\Delta t - \tau) d\tau$  be designated as  $\delta_{D-C_R U}(M, \Delta t)$

$$\delta_{D-C_R U}(M, \Delta t) = K_{D-C_R U}(M\Delta t) - K_{D-C_R U}((M-1)\Delta t) \quad (5.38)$$

Selecting a time step size  $\Delta t$ ,  $\delta_{D-C_R U}(M, \Delta t)$  can be generated for different integer value of  $M$ .

Then,

$$D_{C_R}(n, m\Delta t) = \sum_{\gamma=1}^m \bar{C}(n-1, \gamma\Delta t) \delta_{D-C_R U}(m-\gamma+1, \Delta t), \quad n \geq 2 \quad (5.39)$$

Similarly, the oxygen deficit, due to the boundary deficit, at the end of the  $n^{\text{th}}$  hybrid unit can be obtained using successive convolution. Let the response at the end of  $(n-1)^{\text{th}}$  hybrid unit be designated as  $D_0(n-1, t)$ . Let the time span be discretised into  $m$  equal interval. Applying convolution technique

$$\begin{aligned} D_{D_0}(n, t) &= \int_0^t D_0(n-1, \tau) k_{D-D_0 U}(t-\tau) d\tau = \int_0^{m\Delta t} D_0(n-1, \tau) k_{D-D_0 U}(m\Delta t - \tau) d\tau \\ &= \int_0^{\Delta t} D_0(n-1, \tau) k_{D-D_0 U}(m\Delta t - \tau) d\tau + \int_{\Delta t}^{2\Delta t} D_0(n-1, \tau) k_{D-D_0 U}(m\Delta t - \tau) d\tau \\ &\quad + \dots + \int_{(m-1)\Delta t}^{m\Delta t} D_0(n-1, \tau) k_{D-D_0 U}(m\Delta t - \tau) d\tau \end{aligned} \quad (5.40)$$

Between an interval  $(\gamma-1) \Delta t$  to  $\gamma \Delta t$ , an average  $D_0$  is

$$\bar{D}_0(n-1, \tau) = \frac{D_0[n-1, (\gamma-1)\Delta t] + D_0[n-1, \gamma\Delta t]}{2}, \quad (\gamma-1)\Delta t < \tau < \gamma\Delta t \quad (5.41)$$

Let  $\int_0^{\Delta t} k_{D-D_0 U}(M\Delta t - \tau) d\tau$  be designated as  $\delta_{D-D_0 U}(M, \Delta t)$

$$\delta_{D-D_0 U}(M, \Delta t) = K_{D-D_0 U}[M\Delta t] - K_{D-D_0 U}[(M-1)\Delta t] \quad (5.42)$$

Then,

$$D_{D_0}(n, m \Delta t) = \sum_{\gamma=1}^m \bar{D}_0(n-1, \gamma \Delta t) \delta_{D-D_0 U}(m-\gamma+1, \Delta t), \quad n \geq 2 \quad (5.43)$$

The total deficit,  $D(n, m \Delta t)$ , at the end of the  $n^{\text{th}}$  hybrid unit is obtained by adding Eq. (5.39) and (5.43). At the end of the  $n^{\text{th}}$  hybrid unit, the dissolved oxygen concentration is then obtained by:

$$C_{DO}(n, m \Delta t) = S_{DO} - D(n, m \Delta t) = S_{DO} - \{D_{CR}(n, m \Delta t) + D_{D_0}(n, m \Delta t)\} \quad (5.44)$$

## 5.5 COMPARISON OF HCIS-R MODEL WITH STREETER-PHELPS DISPERSION MODEL

Streeter-Phelps model for BOD-DO which incorporates dispersion component is described in the form (Source: Rinaldi et al., 1979)

$$\frac{\partial C}{\partial t} = -u \frac{\partial C}{\partial x} + D_L \frac{\partial^2 C}{\partial x^2} - k_1 C \quad (5.45)$$

$$\frac{\partial D}{\partial t} = -u \frac{\partial D}{\partial x} + D_L \frac{\partial^2 D}{\partial x^2} + k_1 C - k_2 D \quad (5.46)$$

where  $C$  is the concentration of the pollutant ( $\text{ML}^{-3}$ ),  $D$  is the DO deficit ( $\text{ML}^{-3}$ ),  $u$  is the flow velocity ( $\text{LT}^{-1}$ ),  $D_L$  is the longitudinal dispersion co-efficient ( $\text{L}^2\text{T}^{-1}$ ),  $k_1$  is the decay rate constant ( $\text{T}^{-1}$ ),  $k_2$  is the re-aeration rate constant ( $\text{T}^{-1}$ ),  $x$  is the distance (L), and  $t$  is the time (T).

The initial and boundary conditions for Eq. (5.45) and Eq. (5.56) are:

$$C(x, 0) = 0, \quad x > 0;$$

$$C(0, t) = C_R, \quad t \geq 0;$$

$$C_{DO}(x, 0) = S_{DO}, \quad x > 0;$$

$$C_{DO}(0, t) = S_{DO} - D_0, \quad t \geq 0.$$

Rinaldi et al. (1979) incorporated an auxiliary variable,  $a$  in terms of  $C$  and  $D$  as follows:

$$a = D + \frac{k_1}{k_1 - k_2} C \quad (5.47 \text{ a})$$

$$\text{or } D = a - \frac{k_1}{k_1 - k_2} C \quad (5.47 \text{ b})$$

Differentiating Eq. (5.47 b)

$$\frac{\partial D}{\partial t} = \frac{\partial a}{\partial t} - \frac{k_1}{k_1 - k_2} \frac{\partial C}{\partial t}$$

$$\frac{\partial D}{\partial x} = \frac{\partial a}{\partial x} - \frac{k_1}{k_1 - k_2} \frac{\partial C}{\partial x}$$

$$\frac{\partial^2 D}{\partial x^2} = \frac{\partial^2 a}{\partial x^2} - \frac{k_1}{k_1 - k_2} \frac{\partial^2 C}{\partial x^2}$$

Substituting D and its derivatives in Eq. (5.46) and incorporating Eq. (5.45), one gets

$$\frac{\partial a}{\partial t} = -u \frac{\partial a}{\partial x} + D_L \frac{\partial^2 a}{\partial x^2} - k_2 a \quad (5.48)$$

Thus Eq. (5.45) and (5.48) are similar.

Solution to Eq. (5.45) has been given (Source: Rinaldi et al., 1979) as:

$$k(x, t) = \frac{C_R x}{2t \sqrt{\pi D_L t}} \exp \left\{ - \left[ \frac{(x - ut)^2}{4D_L t} \right] - k_1 t \right\} \quad (5.49)$$

where  $k(x, t)$  is an impulse response function.

Therefore, the solution for Eq. (5.48) can be obtained by replacing  $k_1$  by  $k_2$  and  $C$  by  $a$ . The

solution of DO deficit equation can be deduced from Eq. (5.47 b), as:

$$D(x, t) = \frac{C_R x}{2t \sqrt{\pi D_L t}} \exp \left\{ - \left[ \frac{(x - ut)^2}{4D_L t} \right] \right\} \left[ \frac{k_1}{k_1 - k_2} \exp(-k_1 t) - \exp(-k_2 t) \right] \quad (5.50)$$

The DO concentration can be obtained by subtracting  $D(x, t)$  from saturated DO concentration ( $S_{DO}$ ).



One can conveniently solve Eq. (5.46) numerically using any scheme. For the purpose of demonstration, Eq. (5.46) as been solved numerically by explicit finite difference scheme of forward and central differences in time and space respectively.

The finite difference form of Eq. (5.45) is

$$\frac{C(x, t + \Delta t) - C(x, t)}{\Delta t} = -u \frac{C(x + \Delta x, t) - C(x - \Delta x, t)}{2\Delta x} + D_L \frac{C(x + \Delta x, t) - 2C(x, t) + C(x - \Delta x, t)}{(\Delta x)^2} - k_1 C(x, t) \quad (5.51)$$

The finite difference form of Eq. (5.46) is

$$\frac{D(x, t + \Delta t) - D(x, t)}{\Delta t} = -u \frac{D(x + \Delta x, t) - D(x - \Delta x, t)}{2\Delta x} + D_L \frac{D(x + \Delta x, t) - 2D(x, t) + D(x - \Delta x, t)}{(\Delta x)^2} + k_1 C(x, t) - k_2 D(x, t) \quad (5.52)$$

or

$$D(x, t + \Delta t) = D(x, t) \left[ 1 - \frac{2D_L \Delta t}{(\Delta x)^2} - k_2 \Delta t \right] + D(x + \Delta x, t) \left[ -\frac{u \Delta t}{2\Delta x} + \frac{D_L \Delta t}{(\Delta x)^2} \right] + D(x - \Delta x, t) \left[ \frac{u \Delta t}{2\Delta x} + \frac{D_L \Delta t}{(\Delta x)^2} \right] + k_1 C(x, t) \Delta t \quad (5.53)$$

where  $C(x, t)$  is the analytical solution of Eq. (5.45).

Letting  $x = i \Delta x, t = j \Delta t$

$$D(i, j + 1) = D(i, j) \left[ 1 - \frac{2D_L \Delta t}{(\Delta x)^2} - k_2 \Delta t \right] + D(i + 1, j) \left[ -\frac{u \Delta t}{2\Delta x} + \frac{D_L \Delta t}{(\Delta x)^2} \right] + D(i - 1, j) \left[ \frac{u \Delta t}{2\Delta x} + \frac{D_L \Delta t}{(\Delta x)^2} \right] + k_1 C(i, j) \Delta t \quad (5.54)$$

where  $i = 1, 2, \dots, I_{max}$  and  $j = 0, 1, \dots, J_{max}; D(0, j) = D_0$

Unit impulse response function is given by

$$k_D(i, j) = \frac{D(i, j + 1) - D(i, j)}{\Delta t} \quad (5.55)$$

The impulse response functions computed using the HCIS-R model, by Rinaldi approach, and explicit finite difference scheme are compared in Fig. 5.2 for the following set of data at a distance,  $x = 200$  m:  $\alpha = 1.7$  min,  $T_I = 2.3$  min,  $T_2 = 6.0$  min,  $k_1 = 0.1$  per min,  $k_2 = 0.3$  per min,  $D_0 = 0$ ,  $C_R = 50$  mg / L,  $u = 20$  m / min,  $D_L = 1000$  m<sup>2</sup> / min. The space and time grid size have been chosen as 20 m and 0.05 min in such a way that  $u\Delta t > \Delta x / 10$ , to avoid numerical oscillation. From Fig. 5.2, it can be noted that the response of the HCIS-R model is closely matching the numerical solution of Streeter-Phelps dispersion model. The results obtained from Rinaldi approach does not match with numerical solution.

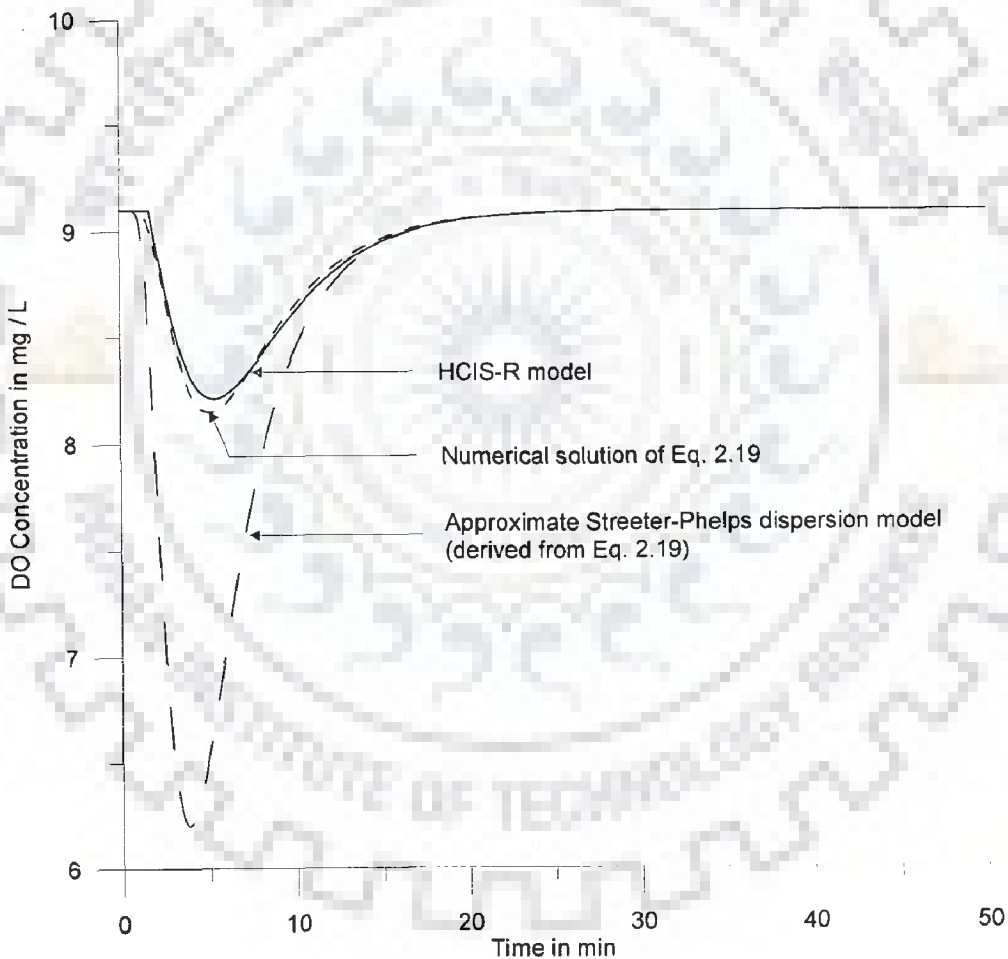


**Fig. 5.2: Impulse responses of HCIS-R model, Numerical solution of BOD-DO Equation with dispersion (Eq. 2.19), approximate Streeter-Phelps model with dispersion (approximated from Eq. 2.19)**

## 5.6 RESULTS AND DISCUSSION

The temporal variations of dissolved oxygen concentrations ( $C_{DO}$ ) at the end of 1<sup>st</sup> hybrid unit of size,  $\Delta x = 200$  m are presented in Fig. 5.3 for  $D_0 = 0$ ,  $\alpha = 1.7$  min,  $T_1 = 2.3$  min,  $T_2 = 6.0$  min,  $k_1 = 0.3$  per min and  $k_2 = 0.1$  per min for impulse inputs of non-conservative pollutant (BOD = 50, 100, 170 mg / L), which consume the dissolved oxygen. The dissolved oxygen concentration at saturated level,  $S_{DO}$  is taken as 9.1 mg / L. From the figure, it is seen that  $C_{DO}$  attains minimum value between 5 to 6 min resumes the saturation level after 20 min. For a higher BOD of 170 mg / L, the minimum  $C_{DO}$  becomes nearly zero. BOD load more than 170 mg / L would result in septic condition.

For  $k_1 = 0.1$  per min and  $k_2 = 0.3$  per min, all other parameters remaining the same the DO concentration – time profiles have been plotted in Fig. 5.4. This shows quick recovery in oxygen level even for higher BOD load (170 mg / L) due to the higher re-aeration rate co-efficient (0.3 per min). Comparing Fig. 5.3 with Fig. 5.4, it could be seen that the oxygen sag curves are flatter for higher re-aeration rate co-efficient.

A Situation has been assumed with no decay and no re-aeration by considering, very small value of  $k_1$  and  $k_2$ . Fig. 5.5 shows the DO concentration is equal to the saturated DO ( $S_{DO} = 9.1$  mg / L). For lower values of  $k_1$  and  $k_2$ , it shows minimal dissolved oxygen deficit.

Step response functions (Cumulative DO curve) of a hybrid unit computed using Eq. (5.33) are presented in Fig. 5.6 for the following set of data:  $D_0 = 0$ ;  $\alpha = 1.70$  min;  $T_1 = 2.3$  min;  $T_2 = 6.0$  min;  $\Delta x = 200$  m;  $k_1 = 0.1$  per min;  $k_2 = 0.3$  per min;  $C_R = 50$  mg / L; The Dissolved oxygen concentration is equal to saturated level until time  $t = \alpha$ , and decreases with time and reaches 2 mg / L at 18 min, then after the variation with time is very minimum. Fig. 5.6 also shows the impulse response function (Oxygen sag curve) and DO deficits. It can be noted that the critical low dissolved oxygen, about 8.1 mg / L, is shown at 5 min in DO sag curve; however this is within the allowable limit.

The impulse response functions for  $k_1 = 0.1$  and 1.5 per min with BOD load of 100 mg / L have been computed and presented in Fig. 5.7 for the following set of parameters:  $D_0 = 0$ ;  $\alpha = 1.70$  min;  $T_1 = 2.3$  min;  $T_2 = 6.0$  min;  $\Delta x = 200$  m;  $k_2 = 0.3$  per min. From this

figure, it can be noted that the DO concentration reaches to saturation level at 14 min when  $k_1$  is 1.5 per min where as, it takes more than 20 min when  $k_1 = 0.1$  per min. This is because for higher decay rate co-efficient, higher amount of dissolved oxygen has been consumed and for the same value of  $k_2$  higher amount of DO aerated.

For a constant value of  $k_1$  ( $= 0.1$  per min) and  $k_2 = 0.3$  and  $1.2$  per min, the impulse response functions have been computed and presented in Fig. 5.8 with the following set of parameters:  $D_0 = 0$ ;  $\alpha = 1.70$  min;  $T_1 = 2.3$  min;  $T_2 = 6.0$  min;  $\Delta x = 200$  m. It shows very quick recovery of dissolved oxygen level for the higher value of  $k_2$  than for the lower value of  $k_2$ .

The impulse response functions at distances 200, 400 and 600 m from the point of injection of BOD load (150 mg / L) have been computed using Eq. (5.44) and are presented in Fig. 5.9 for the following set of parameters:  $D_0 = 0$ ;  $\alpha = 1.70$  min;  $T_1 = 2.3$  min;  $T_2 = 6.0$  min;  $\Delta x = 200$  m;  $k_1 = 0.3$  per min and  $k_2 = 0.1$  per min. It shows the DO concentration at 400 m is within allowable limit for bathing, recreational purposes and it shows slight risk for drinking purpose, where as the critical low DO at 600 m is about 8 mg / L. Having  $k_1 = 0.15$  per min and  $k_2 = 0.1$  per min and keeping other parameters same as mentioned above, the impulse response functions have been computed and presented in Fig. 5.9. It shows at 200 m, minimum DO concentration about 3.2 mg / L and DO concentration at 400 m is within allowable limit for drinking purpose.

The variations of dissolved oxygen concentration,  $C_{DO}$ , and deficit,  $D$ , with time for different values of boundary deficit ( $D_0 = 1, 2$  and  $5$  mg / L) in the first hybrid unit have been presented in Fig. 5.10 for the following set of parameters:  $\alpha = 3.6$  min;  $T_1 = 4.5$  min;  $T_2 = 6.9$  min;  $\Delta x = 300$  m;  $k_2 = 0.3$  per min, BOD input,  $C_R = 0$ . From the plots, it can be noted that the variation of  $C_{DO}$  and  $D$  occurs linearly with respect to values of  $D_0$ .

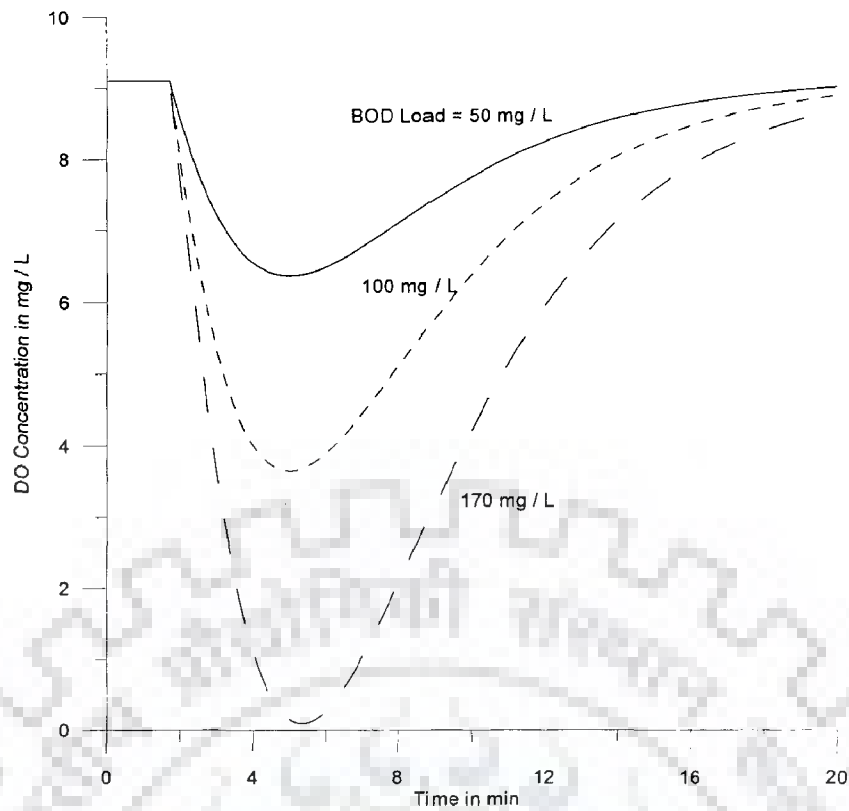


**Fig. 5.3: DO concentration - time profile for different BOD load ( $C_R$ ) with  $k_1 = 0.3$  per min and  $k_2 = 0.1$  per min ( $\alpha = 1.7$  min,  $T_1 = 2.3$  min and  $T_2 = 6.0$  min) at  $x = 200$  m.**

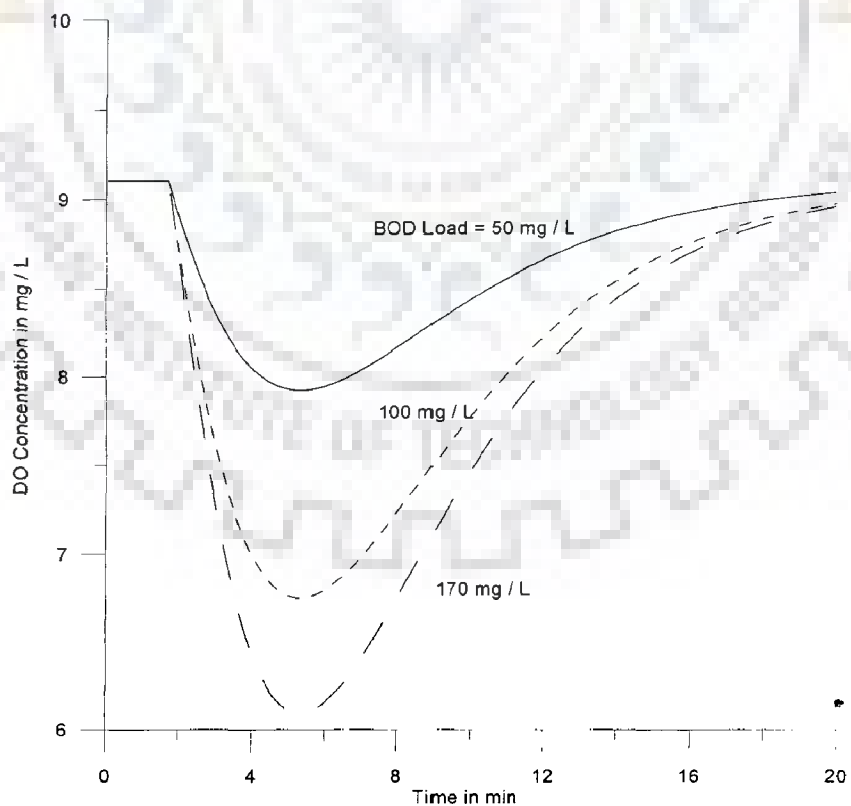


**Fig. 5.4: DO concentration - time profile for different BOD load ( $C_R$ ) with  $k_1 = 0.1$  per min and  $k_2 = 0.3$  per min ( $\alpha = 1.7$  min,  $T_1 = 2.3$  min and  $T_2 = 6.0$  min) at  $x = 200$  m.**

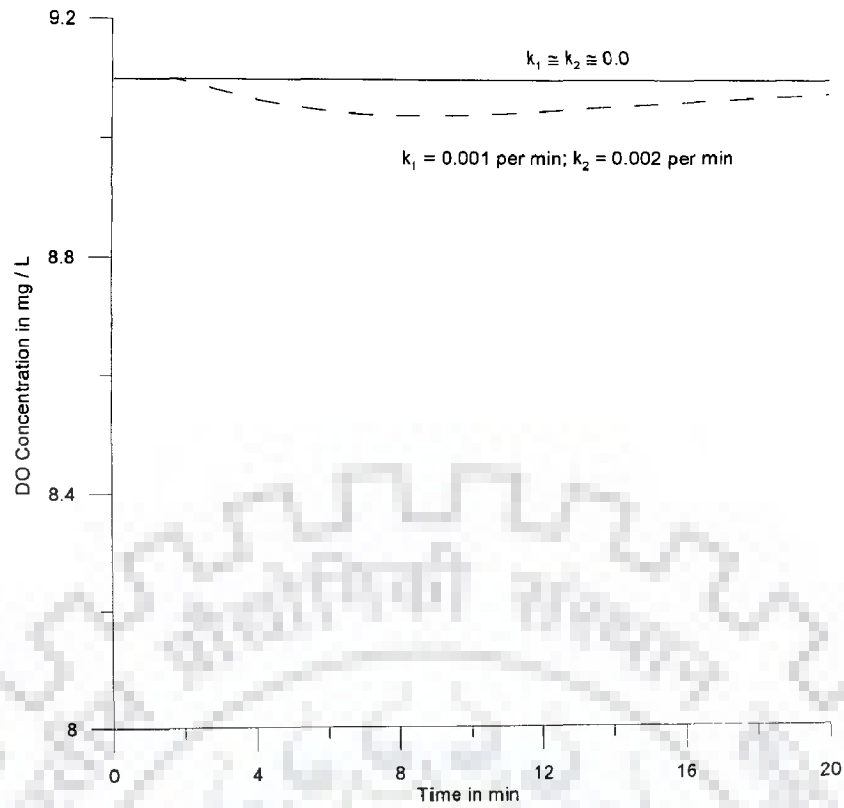


**Fig. 5.5: DO Concentration for very low values of  $k_1$  and  $k_2$**

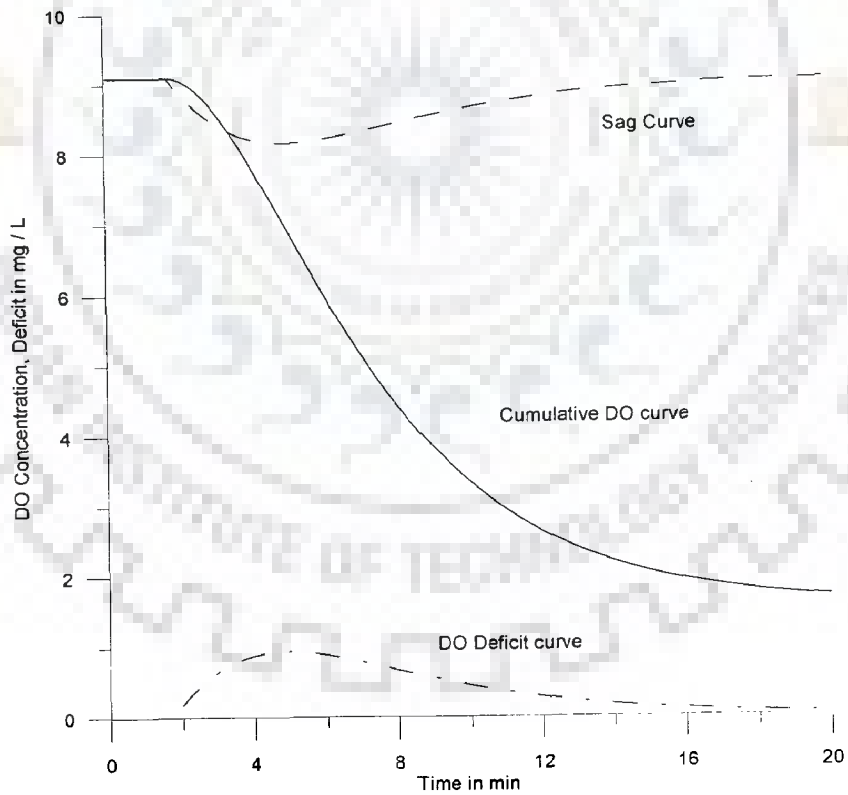


**Fig. 5.6: Step and Impulse response functions for DO concentration and impulse response for DO Deficit**

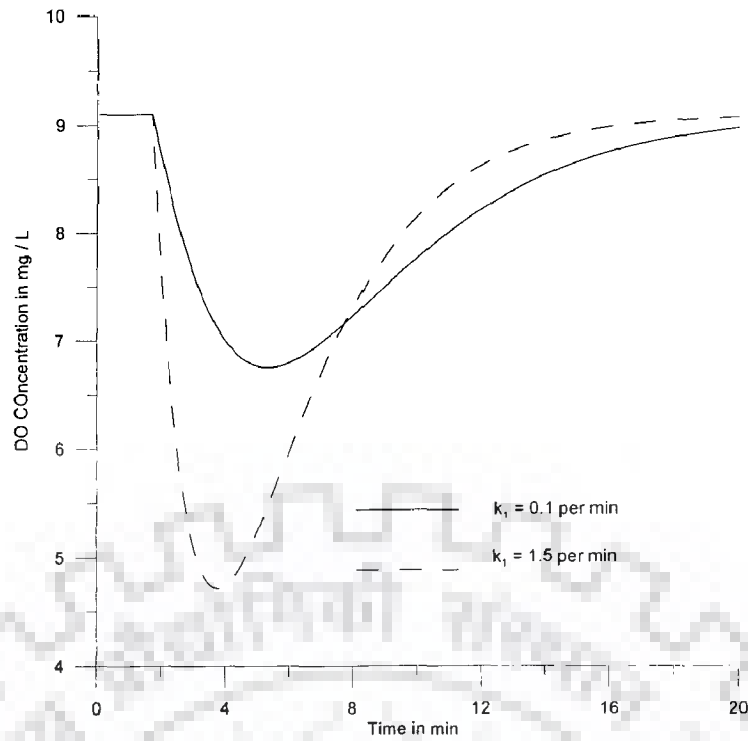


**Fig. 5.7: DO concentration for different values of  $k_1$  (0.1, 1.5 per min) and  $k_2 = 0.2$  per min; BOD load,  $C_R = 100$  mg / L; DO at Saturation = 9.1 mg / L;  $\alpha = 1.7$  min,  $T_1 = 2.3$  min and  $T_2 = 6.0$  min.**

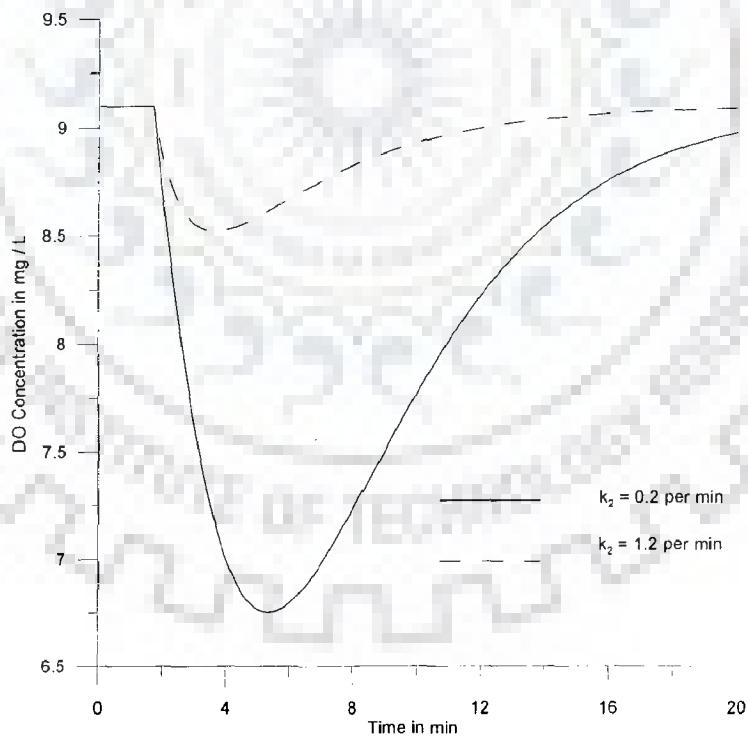


**Fig. 5.8: DO concentration for different values of  $k_2$  (0.2, 1.2 per min) and  $k_1 = 0.1$  per min; BOD load,  $C_R = 100$  mg / L; DO at Saturation = 9.1 mg / L;  $\alpha = 1.7$  min,  $T_1 = 2.3$  min and  $T_2 = 6.0$  min.**

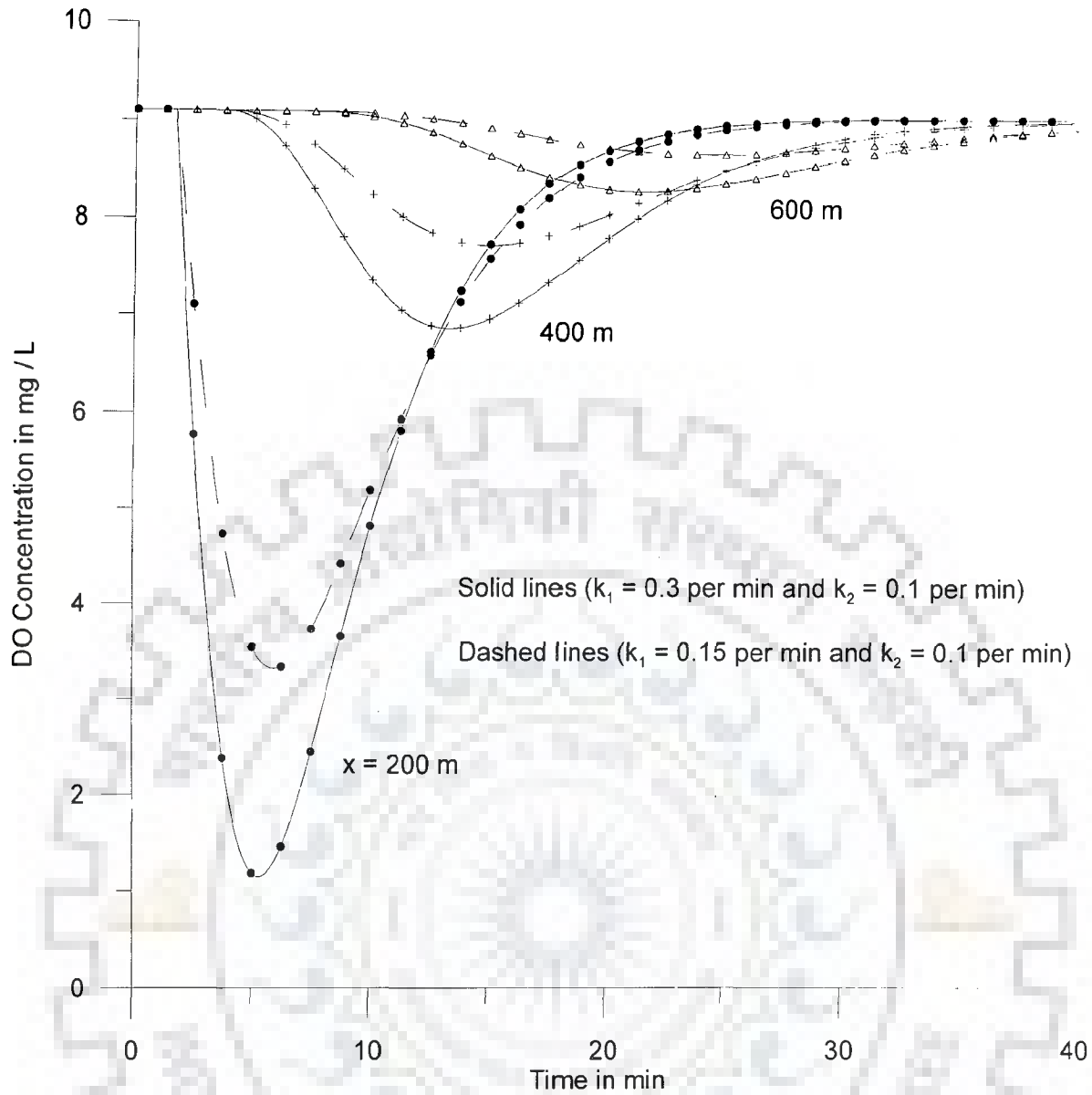


**Fig. 5.9:** DO concentration at different locations ( $x = 200, 400$  and  $600$  m) down stream of point of injection and BOD load,  $C_R = 150$  mg / L; DO at Saturation =  $9.1$  mg / L;  $\alpha = 1.7$  min,  $T_1 = 2.3$  min and  $T_2 = 6.0$  min



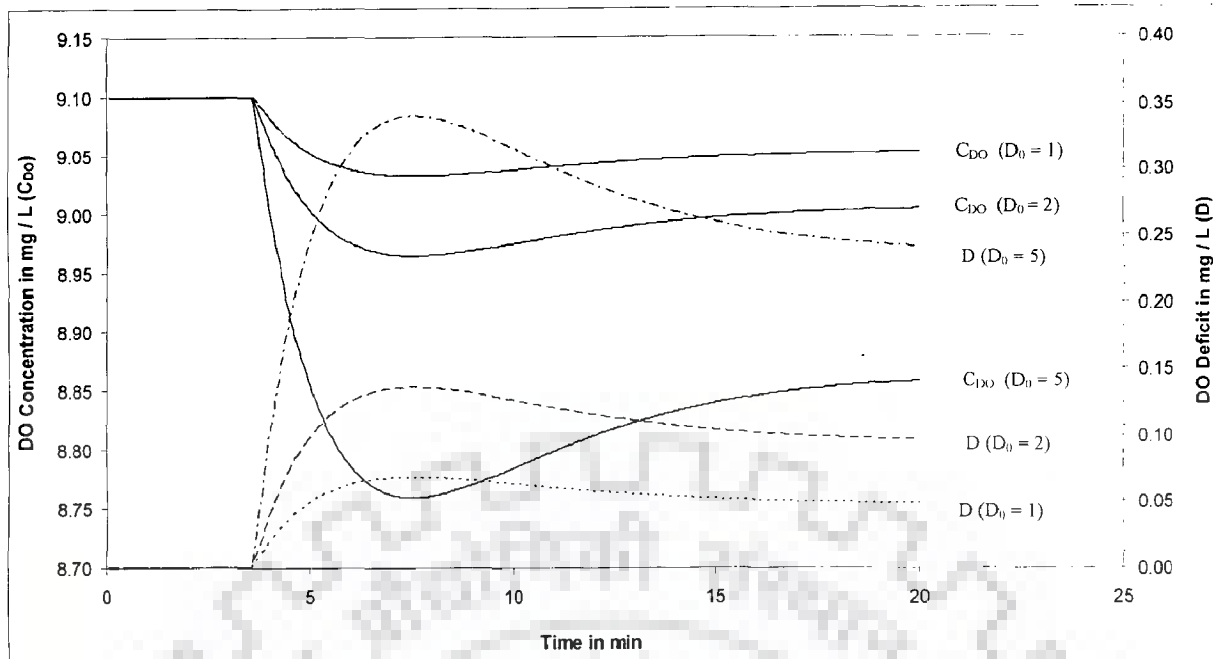


**Fig. 5.10: Variation of  $C_{DO}$  and  $D$  with time in the first hybrid unit for BOD input,  $C_R = 0$  and different values of boundary deficit ( $D_0 = 1, 2$  and  $5$  mg / L)**

## 5.7 CONCLUSIONS

A hybrid model is developed adopting first order reaction kinetic along with advection and dispersion of pollutant and first order re-aeration to predict the DO concentration where as the classical Streeter and Phelps (1944) model incorporates first order de-oxygenation and re-aeration only. For the pecllet number greater than 4, the dissolved oxygen deficit and DO sag curves has been plotted for different BOD load at the entry. To predict the concentration of DO for the given BOD load, the decay rate co-efficient ( $k_1$ ) for the pollutant load can be determined from the Laboratory experiments and re-aeration rate co-efficient ( $k_2$ ) can be estimated from any suitable empirical equations. Flexibility of the HCIS model for adopting reaction kinetics and first order re-aeration along with basic transport processes has been demonstrated. The response of the HCIS-R model is closely matching the numerical solution of Streeter-Phelps dispersion model. The results obtained from Rinaldi approach does not match with numerical solution.



## CHAPTER 6

### PARAMETER ESTIMATION OF HYBRID MODELS

---

#### 6.1 INTRODUCTION

Parameter estimation of a model is an inverse problem. An inverse problem can be solved if the direct problem has been solved a priori. Basically the HCIS model is a three parameters model. These parameters are:  $\alpha$ ,  $T_1$  and  $T_2$ , i.e. time taken by the flowing fluid to fill the plug flow zone and the first and the second thoroughly mixed zones respectively. The HCIS model is a promising one to simulate advection dispersion governed pollutant transport in natural streams. The HCIS model has the flexibility to incorporate additional processes like adsorption, retardation or decay and growth of pollutants along with advection and dispersion. In chapter 3 the HCIS model has been used to simulate the pollutant concentration incorporating adsorption of a conservative pollutant. Due to inclusion of this additional process, the HCIS model becomes a four parameters model. The parameters are:  $\alpha$ ,  $T_1$ ,  $T_2$  and  $R_D$  when sorption of pollutant is considered with advection and dispersion. Among these parameters,  $\alpha$ ,  $T_1$ ,  $T_2$  are the time parameters,  $R_D$  is adsorption rate co-efficient. Estimation of these parameters of the HCIS model holds importance in the simulation of concentration time profile of a particular pollutant in natural streams. The unit impulse response function has distinct characteristics such as: time to peak, a peak concentration, a rising limb, and a falling limb. The characteristic of the unit impulse response function, which could be used for identification of parameters are: time to peak, and peak concentration. Time to peak is obtained from the relation corresponding to:

$$\left. \frac{dk}{dt} \right|_{t=t_p} = 0 \quad (6.1)$$

where,  $k$  is the unit impulse response and  $t_p$  is time to peak.

Differentiating Eq. A3 with respect to  $t$  and equating the differential at  $t_p$  to zero, time to peak is obtained as:

$$t_p = \left( \frac{T_1 T_2}{T_1 - T_2} \right) \ln \left( \frac{T_1}{T_2} \right) + \alpha \quad (6.2)$$

The peak concentration, which occurs at time to peak ( $t_p$ ), is given by:

$$k(t_p) = \left( \frac{1}{T_1 - T_2} \right) \left[ e^{-\left( \frac{T_2 \ln \left( \frac{T_1}{T_2} \right)}{T_1 - T_2} \right)} - e^{-\left( \frac{T_2 \ln \left( \frac{T_1}{T_2} \right)}{T_1 - T_2} \right)} \right] \quad (6.3)$$

Time to peak and peak concentration of the HCIS model simulating adsorption can be obtained numerically from a given  $C-t$  profile. The parameters of a conceptual model can be determined by many methods, viz., i) method of moments, ii) method using first moment, time to peak and peak concentration, iii) Least squares optimization, etc. Among these methods, least squares optimization has been found to be most effective method.

## 6.2 LEAST SQUARES OPTIMIZATION

The least squares optimization method has been used by many investigators (Jones, 1971; Synder, 1972) for identification of parameters of linear or non-linear hydrological models. The least squares optimization method requires observed response at some sampling site downstream of the injection point for finding the parameters of the system. It involves minimization of squares of difference between observed and computed responses obtained with an initial guess of the parameters. The well known Marquardt Algorithm is a technique in which parameters of a model are estimated by performing minimization of the squares of the error.

The least square optimization technique has been used to estimate the parameters of the following models; the basic HCIS model and the HCIS model for simulating adsorption of pollutants.

### 6.2.1 The HCIS Model

The unit impulse response function obtained from the HCIS model representing only advection and dispersion of pollutant over time is given by:

$$k(t) = \frac{U(t-\alpha)}{T_1 - T_2} \left[ \exp\left\{-\frac{(t-\alpha)}{T_1}\right\} - \exp\left\{-\frac{(t-\alpha)}{T_2}\right\} \right] \quad (6.4)$$

where,  $k(t)$  is the unit impulse response function,  $U(t-\alpha)$  is a unit step function,  $\alpha$  is the filling time of the plug flow zone,  $T_1$  is the filling time of first mixed zone and  $T_2$  is the filling time of second mixed zone.

Let  $k_o(i\Delta t)$  be the observed concentration at any section of stream over time. Choosing any guess value of the parameters as  $\alpha^*$ ,  $T_1^*$  and  $T_2^*$ , the response can be computed as  $k_c(\alpha^*, T_1^*, T_2^*, i\Delta t)$ . Using Taylor series of expansion and neglecting higher order term, the concentration for values of parameters  $\alpha = \alpha^* + \Delta\alpha$ ;  $T_1 = T_1^* + \Delta T_1$ ; and  $T_2 = T_2^* + \Delta T_2$  can be written as:

$$k_c(\alpha^* + \Delta\alpha, T_1^* + \Delta T_1, T_2^* + \Delta T_2, i\Delta t) = \left\{ \begin{array}{l} k_c(i\Delta t) + \frac{\partial k_c}{\partial \alpha} \Delta\alpha \\ + \frac{\partial k_c}{\partial T_1} \Delta T_1 + \frac{\partial k_c}{\partial T_2} \Delta T_2 \end{array} \right\}_{\alpha^*, T_1^*, T_2^*} \quad (6.5)$$

The sum of the squares of the error,  $\varepsilon$ , corresponding to the new values of parameters is:

$$\varepsilon = \sum_{i=1}^n \left[ k_o(i\Delta t) - \left\{ \begin{array}{l} k_c(i\Delta t) + \frac{\partial k_c}{\partial \alpha} \Delta\alpha \\ + \frac{\partial k_c}{\partial T_1} \Delta T_1 + \frac{\partial k_c}{\partial T_2} \Delta T_2 \end{array} \right\}_{\alpha^*, T_1^*, T_2^*} \right]^2 \quad (6.6)$$

Since  $\Delta\alpha = \alpha - \alpha^*$ ;  $\Delta T_1 = T_1 - T_1^*$ ; and  $\Delta T_2 = T_2 - T_2^*$

$$\varepsilon = \sum_{i=1}^n \left[ k_o(i\Delta t) - \left\{ \begin{array}{l} k_c(i\Delta t) + \frac{\partial k_c}{\partial \alpha} (\alpha - \alpha^*) \\ + \frac{\partial k_c}{\partial T_1} (T_1 - T_1^*) + \frac{\partial k_c}{\partial T_2} (T_2 - T_2^*) \end{array} \right\}_{\alpha^*, T_1^*, T_2^*} \right]^2 \quad (6.7)$$

The square of the error will be zero or minimum, when the values of parameters are exact values, i.e. derivatives of  $\varepsilon$  with respect to the parameters equal to 0. Differentiating Eq. (6.7) with respect to  $\alpha$ ,  $T_1$ , and  $T_2$  and equating to 0, three equations are obtained. These can be expressed in matrix form as follows,

$$\begin{bmatrix} A(1,1) & A(1,2) & A(1,3) \\ A(2,1) & A(2,2) & A(2,3) \\ A(3,1) & A(3,2) & A(3,3) \end{bmatrix} \begin{bmatrix} \Delta\alpha \\ \Delta T_1 \\ \Delta T_2 \end{bmatrix} = \begin{bmatrix} B(1,1) \\ B(2,1) \\ B(3,1) \end{bmatrix} \quad (6.8)$$

where, the elements of the matrices are been given in Appendix C.

Applying matrix inversion, the values of  $\Delta\alpha$ ,  $\Delta T_1$  and  $\Delta T_2$  are:

$$\begin{bmatrix} \Delta\alpha \\ \Delta T_1 \\ \Delta T_2 \end{bmatrix} = \begin{bmatrix} A(1,1) & A(1,2) & A(1,3) \\ A(2,1) & A(2,2) & A(2,3) \\ A(3,1) & A(3,2) & A(3,3) \end{bmatrix}^{-1} \begin{bmatrix} B(1,1) \\ B(2,1) \\ B(3,1) \end{bmatrix} \quad (6.9)$$

The new values of  $\alpha$ ,  $T_1$  and  $T_2$  are then obtained by adding the  $\Delta\alpha$ ,  $\Delta T_1$  and  $\Delta T_2$  with the earlier values of  $\alpha^*$ ,  $T_1^*$  and  $T_2^*$ . By iterative manner, the parameters are being updated until the modulus of the difference between two successive iterated values for each parameter is less than the accuracy limit chosen.

### 6.2.2 The HCIS Model with Adsorption (HCIS-A)

The unit impulse response function, which describes the temporal variation in concentration of the pollutant predicted by the HCIS-A model, represents the adsorption along with advection and dispersion, is given by Eq. (3.65). Though the unit impulse responses function (Eq. 3.65) is not in functional form, its partial derivatives with respect to parameters can be found numerically and Eq. 3.65 can be considered to determine the model parameters.

Let  $k_O(i\Delta t)$  be the observed concentration at any section of stream down stream of the point of injection. Choosing any guess value of the parameters as  $\alpha^*$ ,  $T_1^*$ ,  $T_2^*$  and  $R_D^*$  the response can be computed as  $k_C(\alpha^*, T_1^*, T_2^*, R_D^*, i\Delta t)$ . Using Taylor series of expansion and

neglecting higher order term, the concentration for values of parameters  $\alpha = \alpha^* + \Delta \alpha$ ;  $T_1 = T_1^* + \Delta T_1$ ;  $T_2 = T_2^* + \Delta T_2$ ;  $R_D = R_D^* + \Delta R_D$  can be written as:

$$k_c(\alpha^* + \Delta \alpha, T_1^* + \Delta T_1, T_2^* + \Delta T_2, R_D, i\Delta t) = \left. \left\{ \begin{array}{l} k_c(i\Delta t) + \frac{\partial k_c}{\partial \alpha} \Delta \alpha + \frac{\partial k_c}{\partial T_1} \Delta T_1 \\ + \frac{\partial k_c}{\partial T_2} \Delta T_2 + \frac{\partial k_c}{\partial R_D} \Delta R_D \end{array} \right\} \right|_{\alpha^*, T_1^*, T_2^*, R_D^*} \quad (6.10)$$

The sum of the squares of the error,  $\varepsilon$ , corresponding to the new set of parameters is:

$$\varepsilon = \sum_{i=1}^n \left[ k_o(i\Delta t) - \left. \left\{ \begin{array}{l} k_c(i\Delta t) + \frac{\partial k_c}{\partial \alpha} \Delta \alpha + \frac{\partial k_c}{\partial T_1} \Delta T_1 \\ + \frac{\partial k_c}{\partial T_2} \Delta T_2 + \frac{\partial k_c}{\partial R_D} \Delta R_D \end{array} \right\} \right|_{\alpha^*, T_1^*, T_2^*, R_D^*} \right]^2 \quad (6.11)$$

Since  $\Delta \alpha = \alpha - \alpha^*$ ;  $\Delta T_1 = T_1 - T_1^*$ ;  $\Delta T_2 = T_2 - T_2^*$  and  $\Delta R_D = R_D - R_D^*$

$$\varepsilon = \sum_{i=1}^n \left[ k_o(i\Delta t) - \left. \left\{ \begin{array}{l} k_c(i\Delta t) + \frac{\partial k_c}{\partial \alpha} (\alpha - \alpha^*) + \frac{\partial k_c}{\partial T_1} (T_1 - T_1^*) \\ + \frac{\partial k_c}{\partial T_2} (T_2 - T_2^*) + \frac{\partial k_c}{\partial R_D} (R_D - R_D^*) \end{array} \right\} \right|_{\alpha^*, T_1^*, T_2^*, R_D^*} \right]^2 \quad (6.12)$$

The square of the error will be zero or minimum, when the values of parameters are exact values, i.e. derivatives of  $\varepsilon$  with respect to the parameters equal to 0. Differentiating Eq. (6.12) with respect to  $\alpha$ ,  $T_1$ ,  $T_2$  and  $R_D$  and equating to 0, four equations are obtained. These can be expressed in matrix form as:

$$\begin{bmatrix} A(1,1) & A(1,2) & A(1,3) & A(1,4) \\ A(2,1) & A(2,2) & A(2,3) & A(2,4) \\ A(3,1) & A(3,2) & A(3,3) & A(3,4) \\ A(4,1) & A(4,2) & A(4,3) & A(4,4) \end{bmatrix} \begin{bmatrix} \Delta \alpha \\ \Delta T_1 \\ \Delta T_2 \\ \Delta R_D \end{bmatrix} = \begin{bmatrix} B(1,1) \\ B(2,1) \\ B(3,1) \\ B(4,1) \end{bmatrix} \quad (6.13)$$

The elements of the matrices are given in Appendix C. the matrix in the left is the Jacobian matrix. Applying matrix inversion, the values of  $\Delta \alpha$ ,  $\Delta T_1$ ,  $\Delta T_2$  and  $\Delta R_D$  are

$$\begin{bmatrix} \Delta\alpha \\ \Delta T_1 \\ \Delta T_2 \\ \Delta R_D \end{bmatrix} = \begin{bmatrix} A(1,1) & A(1,2) & A(1,3) & A(1,4) \\ A(2,1) & A(2,2) & A(2,3) & A(2,4) \\ A(3,1) & A(3,2) & A(3,3) & A(3,4) \\ A(4,1) & A(4,2) & A(4,3) & A(4,4) \end{bmatrix}^{-1} \begin{bmatrix} B(1,1) \\ B(2,1) \\ B(3,1) \\ B(4,1) \end{bmatrix} \quad (6.14)$$

The new values of  $\alpha$ ,  $T_1$ ,  $T_2$  and  $R_D$  are then obtained by adding the  $\Delta\alpha$ ,  $\Delta T_1$ ,  $\Delta T_2$ ,  $\Delta R_D$  with the initial guess values of  $\alpha^*$ ,  $T_1^*$ ,  $T_2^*$  and  $R_D^*$ . The parameters are updated until the modulus of the difference between two successive iterated values for each parameter is less than the accuracy limit chosen.

### 6.3 OBSERVED DATA

Synthetic data are used for testing the efficacy of the least square optimization method suggested here. Moreover synthetic data should be used for checking the efficacy of a model (Mishra and Jain, 1999). For an assumed set of parameters, the response of the system is computed using the suggested model. The mean and standard deviation ( $S_d$ ) of the computed response are found. Random error with zero mean and certain percentage of  $S_d$  as standard deviation is added to the response. These responses containing the random errors are considered as the synthetic observed data to solve the inverse problem by least square optimization.

To investigate the robustness of least squares optimization method, random error with higher percentage of standard deviation ranging from 0 to 20 % of  $S_d$  are added for generating synthetic observation data. Using these synthetic observation data, the parameters of respective models are estimated and compared with original values of the parameters, which had been used to generate the synthetic observation data. The comparison is made in Tables 6.1 and 6.2 for HCIS and HCISA models respectively.



**Table 6.1: Comparison of the estimated parameters with the true parameters ( $\alpha = 1.7m$  in,  $T_1 = 2.3$  min,  $T_2 = 6.0$  min) for different % of  $S_d$  for HCIS model**

S. No	% of $S_d$ in synthetic observed data	$\alpha^*$ (min)	$T_1^*$ (min)	$T_2^*$ (min)	Accuracy level
1	0 %	1.701	2.281	5.999	0.00001
2	5 %	1.704	2.272	6.03	0.00001
3	10 %	1.694	2.32	5.879	0.00005
4	15 %	1.721	2.253	6.1	0.0001
5	20 %	1.75	2.199	5.897	0.0001

**Table 6.2: Comparison of the estimated parameters with the true parameters ( $\alpha = 1.7m$  in,  $T_1 = 2.3$  min,  $T_2 = 6.0$  min,  $R_D = 0.1$  per min) for different % of  $S_d$  for HCIS-A model**

S. No	% of $S_d$ in synthetic observed data	$\alpha^*$ (min)	$T_1^*$ (min)	$T_2^*$ (min)	$R_D^*$ (per min)	Accuracy level
1	0 %	1.7105	2.3002	5.9967	0.0996	0.00001
2	5 %	1.704	2.27	6.01	0.103	0.0001
3	10 %	1.742	2.255	5.937	0.105	0.0001
4	15 %	1.712	2.31	6.058	0.099	0.0001
5	20 %	1.735	2.139	6.021	0.109	0.0001

The parameters are estimated with reasonable accuracy by least square optimization method. Using synthetic data containing random error with standard deviation of 20 % of  $S_d$  the parameters could be estimated closely to the true value.

## 6.4 SELECTION OF APPROPRIATE MODEL

The zero<sup>th</sup> and 1<sup>st</sup> moment of the unit impulse response, observed at a sampling site downstream of the point of injection, or synthetically generated, can be determined numerically (Kafarov, 1976) as follows, by taking  $r = 0$  and 1 respectively:

$$M_r = \frac{\sum_{i=1}^n \left( \frac{k(t_i)}{r+1} \right) (t_{i+1}^{r+1} - t_i^{r+1})}{\sum_{i=1}^n k(t_i) \Delta t} \quad (6.15)$$

where,  $M_r$  is the  $r^{\text{th}}$  moment,  $k(t_i)$  is the unit impulse response.

If the zero<sup>th</sup> moment is approximately equal to 1, then there is no loss of pollutant, i.e. the pollutant mass is conserved. For this case, there may be either i) advection - dispersion or ii) advection - dispersion - adsorption of pollutants.

For a given  $C-t$  profile (observed or synthetically generated), using least squares optimization, the parameters of the model can be estimated from steps explained either in section (6.2.1) or (6.2.2). Solving the inverse problem by the HCIS model for a given  $C-t$  profile, tracer velocity ( $\hat{u}$ ) can be estimated using the relation:

$$\hat{u} = \frac{\Delta x}{\alpha + T_1 + T_2} \quad (6.16)$$

where,  $\Delta x$  is the size of the hybrid unit,  $\alpha$ ,  $T_1$ ,  $T_2$  are estimated parameters of the HCIS model.

If the tracer velocity ( $\hat{u}$ ) and the mean flow velocity ( $\bar{u}$ ) are approximately same, then pollutant transport is governed by advection and dispersion only and the parameters estimated by the HCIS model are correct. It is found that the HCIS-A model fails to estimate the parameters from the synthetically  $C-t$  profile that has been generated using HCIS, because some of the elements of inverse matrix (Eq. 6.14) become very large during the matrix inversion. The least square procedure yields results if the accuracy level is low of the order 0.01. But in that case the tracer velocity and the mean flow velocity do not match.

For another set of data, if the tracer velocity, found from the estimated parameters using HCIS, and mean flow velocity are not equal, then it can be concluded that there are

some additional processes taking place along with advection and dispersion of pollutant. One of the additional processes may be adsorption of pollutants. In that case, both the HCIS model and the HCIS-A model estimate their parameters. Between these two models, the appropriate model is to be chosen using the following procedure:

- 1) Estimate the mean of the distribution  $M_I^*$  ( $= \alpha + T_1 + T_2$ ) using parameters of the HCIS model. If the first moment ( $M_I$ ), from Eq. (6.15), is greater than mean of the distribution ( $M_I^*$ ), then there is an additional processes taking place along with advection and dispersion. Therefore, the estimated parameters of the HCIS model are not pertinent.
- 2) As an additional check, tracer velocity  $\hat{u}$  ( $= \Delta x / (\alpha + T_1 + T_2)$ ) can be compared with mean flow velocity. If  $\hat{u}$  and  $\bar{u}$  are not equal, then the adsorption is taking place. Therefore, the estimated parameters of HCIS-A model are pertinent.

Fig. 6.1 shows the procedure in a flow chart for identifying the appropriate model and the model parameters while solving the inverse problem from one  $C-t$  profile.

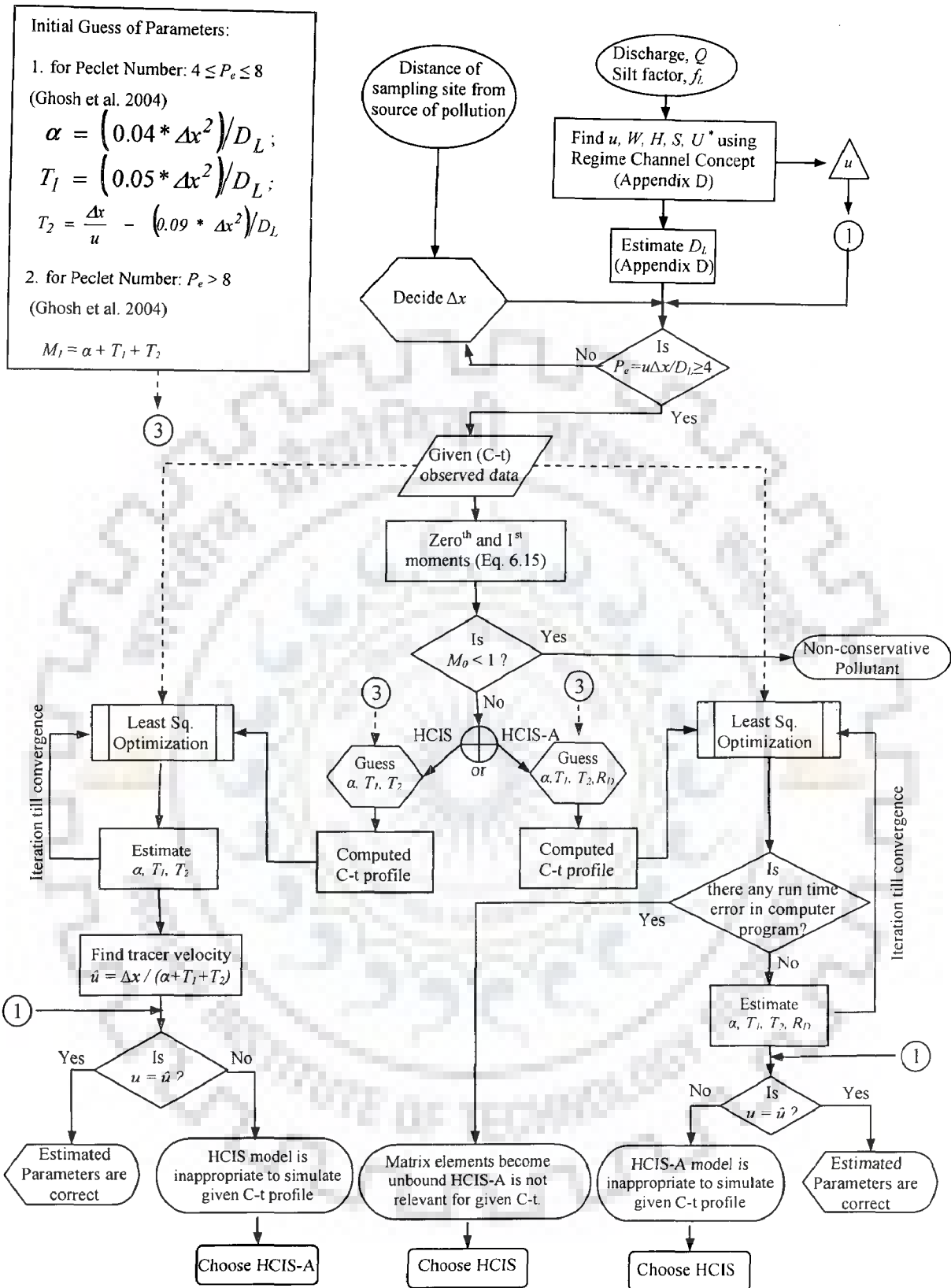


**Fig. 6.1** Flow chart showing the procedure to select an appropriate model and estimation of its parameters to simulate given observed data (C-t profile)

## 6.5 RESULTS AND DISCUSSION

Efficacy of the procedure for solving the inverse problem as described above is shown considering the following two sets of synthetic observation data. One set of data are generated making use of HCIS model ( $\Delta x = 200\text{m}$ ,  $\alpha = 1.7\text{ min}$ ,  $T_1 = 2.3\text{ min}$  and  $T_2 = 6.0\text{ min}$ ) and the other set of data are generated making use of HCIS-A model ( $\Delta x = 200\text{m}$ ,  $\alpha = 1.7\text{ min}$ ,  $T_1 = 2.3\text{ min}$ ,  $T_2 = 6.0\text{ min}$ , and  $R_D = 0.1$ ). The observation data are generated at two sampling sites, which are located at a distance of 200m 1000 m and 2000m downstream from the point of injection. The flow velocity,  $u$ , in the stream is 20m/min. Random errors, with zero mean and standard deviation 5% of  $S_d$ , are added to obtain the synthetic observation data.

The synthetic  $C-t$  profiles, generated using HCIS model have the following characteristics: at  $x = 200\text{m}$ , the time to peak ( $t_p$ ) = 5.276 min and peak concentration ( $k_{t_p}$ ) = 0.0918.

The synthetic  $C-t$  profiles, generated using HCIS-A model have the following characteristics: at  $x = 200\text{m}$ , the time to peak ( $t_p$ ) = 4.954 min and peak concentration ( $k_{t_p}$ ) = 0.0842.

Let us consider the first  $C-t$  profile. The zero<sup>th</sup> moment ( $M_0$ ) of the profile is found to be equal to 1. Using least squares optimization, the parameters of the HCIS model are estimated with an accuracy of 0.00001 as:  $\alpha = 1.704\text{ min}$ ,  $T_1 = 2.272\text{ min}$  and  $T_2 = 6.03\text{ min}$ . Hence, from Eq. (6.16), the corresponding tracer velocity is 19.988 m / min, which is approximately equal to the mean flow velocity (20 m / min). This implies that advection and dispersion processes govern the pollutant transport and the parameters, estimated using the HCIS model, are pertinent.

Let us use the same set of data (the first set) and apply the HCIS-A model for solving the inverse problem. For the accuracy 0.00001, the iteration procedure does not converge. The elements of the inverse matrix diverge and become unbounded. However, for a lower accuracy of 0.01, the iteration converges and the parameters of HCIS-A model are estimated as:  $\alpha = 1.671\text{ min}$ ,  $T_1 = 2.918\text{ min}$ ,  $T_2 = 4.428\text{ min}$  and  $R_D = 0.266\text{ per min}$ .

The corresponding tracer velocity is 22.18 m / min, which differs from the mean flow velocity (= 20 m / min). The tracer velocity is over estimated. The  $C-t$  profiles at 1000 m and 2000 m down stream computed with the estimated parameters are compared with the observed  $C-t$  profiles and presented in Fig. 6.2. It can be noted that responses of the HCIS and HCIS-A models reasonably match with observed  $C-t$  profiles. However, HCIS-A doesn't give tracer velocity equivalent to the mean flow velocity. Hence, the HCIS-A model is not an appropriate model to simulate the given  $C-t$  profile.

For the second  $C-t$  profile generated with HCIS-A, the zero<sup>th</sup> moment ( $M_0$ ) is found to be 1. Applying the HCIS model for solving the inverse problem, the parameters are estimated as:  $\alpha = 1.724$  min,  $T_1 = 1.882$  min and  $T_2 = 7.012$  min. The corresponding tracer velocity from Eq. (6.16) is 18.18 m / min, which is not equal to the mean flow velocity (20 m / min). The tracer velocity is under estimated. This implies that the adsorption process is taking place along with advection and dispersion and selection of the HCIS model for solving the inverse problem is not pertinent.

The HCIS-A model is next applied to estimate the parameters from the second  $C-t$  profile. The parameters are estimated as  $\alpha = 1.704$  min,  $T_1 = 2.27$  min,  $T_2 = 6.01$  min and  $R_D = 0.103$  per min with an accuracy tag of 0.0001. The corresponding tracer velocity is found to be 20.03 m / min, which matches with the mean flow velocity (= 20 m / min). Hence, the HCIS-A model is identified as the appropriate model to simulate the parameter.  $C-t$  profiles at 1000 m and 2000 m down stream are computed with estimated parameters are compared with the second set of observed  $C-t$  profiles. It can be noted that, from Fig. 6.3, responses of the HCIS model shows moderate difference with observed data where as HCIS-A models reasonably matches with observed second set of  $C-t$  profiles. Also, parameters estimated using HCIS do not yield tracer velocity matching with the mean flow velocity. Hence, the HCIS model is not simulating the given  $C-t$  profile.

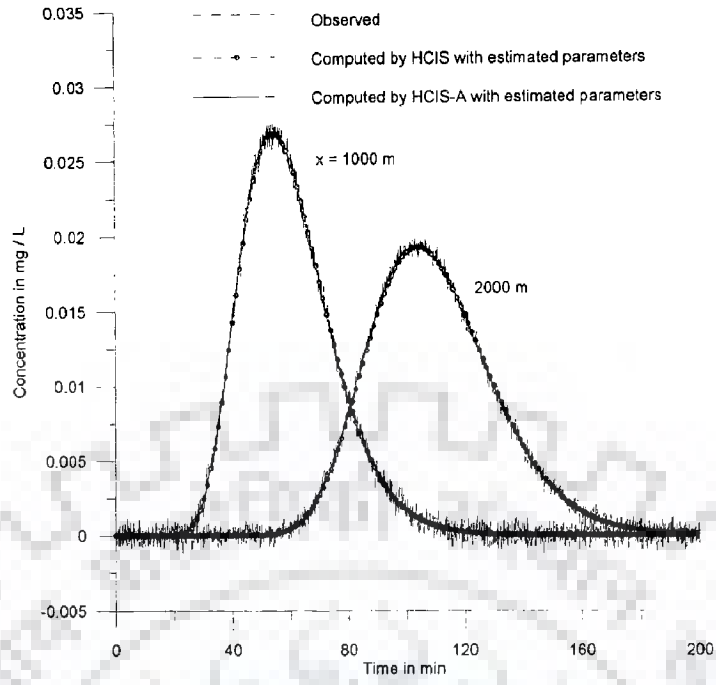


**Fig. 6.2: Observed and Computed C-t profiles by HCIS ( $\alpha = 1.704$  min,  $T_1 = 2.272$  min,  $T_2 = 6.03$  min) and HCIS-A ( $\alpha = 1.671$  min,  $T_1 = 2.918$  min,  $T_2 = 4.428$  min,  $R_D = 0.266$  per min) models with estimated parameters at  $x = 1000$  m and  $2000$  m down stream.**

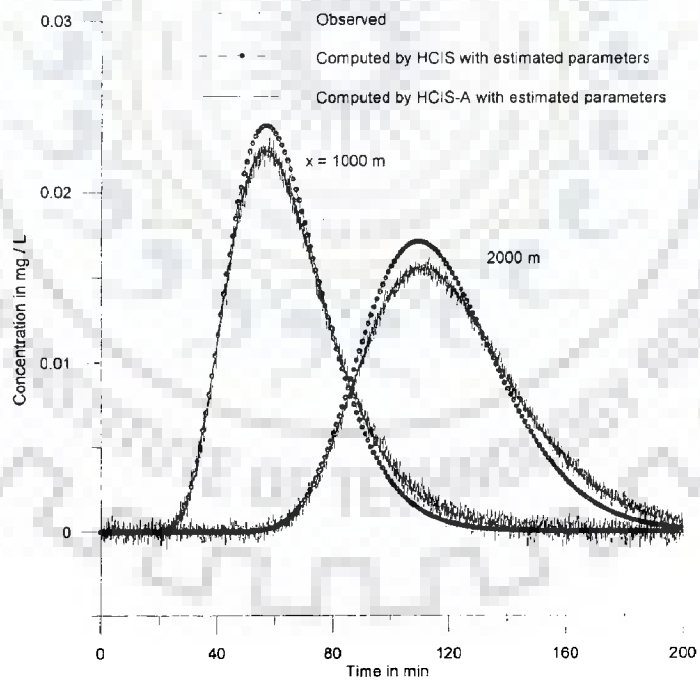
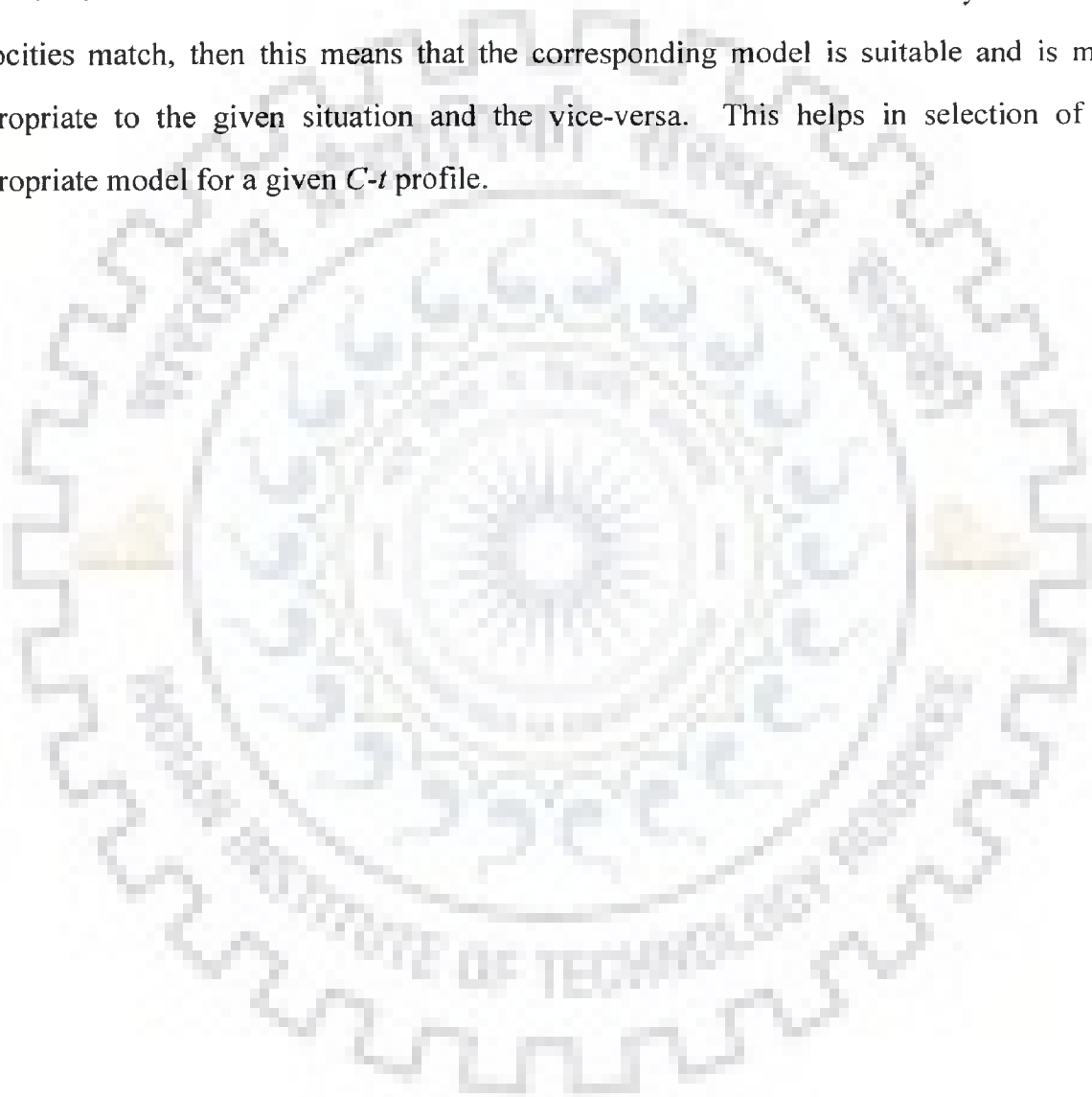


**Fig. 6.3: Observed and Computed C-t profiles by HCIS ( $\alpha = 1.724$  min,  $T_1 = 1.882$  min,  $T_2 = 7.012$  min) and HCIS-A ( $\alpha = 1.704$  min,  $T_1 = 2.27$  min,  $T_2 = 6.01$  min,  $R_D = 0.103$  per min) models with estimated parameters at  $x = 1000$  m and  $2000$  m down stream.**

## 6.6 CONCLUSIONS

In order to identify the suitability of the HCIS or HCIS-A model for a particular  $C-t$  profile, it is required to know the corresponding parameters of the HCIS and HCIS-A models. In this chapter, the parameters of the HCIS and the HCIS-A models are estimated using least squares optimization method for a given sets of observed  $C-t$  profile. The suitability of the model is identified by comparing the tracer velocities estimated using the parameters of the HCIS and the HCIS-A models with the mean flow velocity. If the two velocities match, then this means that the corresponding model is suitable and is more appropriate to the given situation and the vice-versa. This helps in selection of the appropriate model for a given  $C-t$  profile.





# CHAPTER 7

## PERFORMANCE EVALUATION OF HYBRID MODELS USING FIELD DATA

---

---

### 7.1 INTRODUCTION AND STUDY AREA DESCRIPTION

In recent years, the growing industrialization and urbanization are the main reasons of increasing pollution threats and public concerns towards health related issues. With the advent of sophisticated computational tools and investigation technologies, much attention is being paid to derive pollutant's transport phenomena more close to reality. Rivers are uncontrollably used as a sink to the pollutants. This in turn deteriorates the water quality and spoils the eco-system maintained by the rivers. Rivers have limited assimilation capacity to the pollutants. Disposal of pollutants in excess to the assimilating capacity of the river would not only affect the health of water but would also damage the aquatic life marinated by the river. Thus, study of pollutant's transport in a stream/river is essential to correctly evaluate the state of pollution threat at downstream locations from the source and for regulating disposal of pollutants in rivers such that the eco-system remains safe from any incoming threat.

The river Brahmani is one of the major rivers in India. Many stretches of river runs in Orissa state where a numerous industries located near the river are discharging their effluents to the river as on today. The consequence is that, many stretches of the river are under the grim of pollution exceeding the limiting level of BOD load. As per National Water Commission's survey (NWC report, 2000), the stretch of 310 km down below Rengali dam is most polluted due to, the effluents from aluminum, steel and fertilizer industries and due to the mining and urban activities. The pollutants are discharged to the River Brahmani through its tributaries; Tikira, at 25 km, Nandira at 75 km and Bangura at 95 km down below the Rengali Dam. In this Chapter, the river stretch (57 km) from Rengali dam to Talcher has been chosen for study. Talcher is affected seriously by the

waste water discharged by river Tikira, main tributary of river Brahmani. This stretch is reported by central pollution control board as D class, i.e., it is designated to use for propagation of wild life and fisheries, which has the following criteria: 1) pH 6.5 to 8.5, 2) Dissolved Oxygen 4mg/l or more, 3) Biochemical Oxygen Demand 5 days 20°C 3 mg/l or less. Due to increasing quantum of pollutants, water quality of this stretch deteriorates. Hence it is imperative to predict the fate of pollutant and to regulate the pollutant disposal. The catchment area of the river at upstream and down below Rengali dam receives 890 to 2850 mm / year rainfall. The study stretch between two locations Rengali Dam and Talcher having lat-long, 85°02' E - 21°17' N and 85°13' E - 20°57' N respectively, is presented in Fig. 7.1.

## **7.2 DATA REQUIREMENT**

In order to evaluate the performance of hybrid model, various data, collected from the river stretch of 57 km, have been used, viz. flow data, river bed soil sediments and water quality/pollution data. Most of the data are collected from a dissertation report (Palo, 2002) and central pollution control board (CPCB) web site.

## **7.3 FLOW DATA AND ROUTING**

Daily released flow from Rengali reservoir and flow in Brahmani River observed at Talcher have been used in this study. The release from the reservoir varies between 500 m<sup>3</sup>/s and 2500 m<sup>3</sup>/s during monsoon months (June to October). During non-monsoon months (November to May), the flow reduces and it varies between 125 m<sup>3</sup>/s and 500 m<sup>3</sup>/s. The study reach of the river has a general bed slope of 1 in 5600. The flow from Rengali dam has been routed through various sections of the reach using Muskingum-Cunge method (Appendix E) up to the location where Tikira joins, and the flow hydrographs of Tikira is added and routing is proceeded up to Talcher. The observed flow data at Talcher is compared with the computed flow data at Talcher. Some difference of flow between computed and observed hydrographs during monsoon period is found. This is because of the unaccounted contribution of intermediate catchments during rainy season. A correction

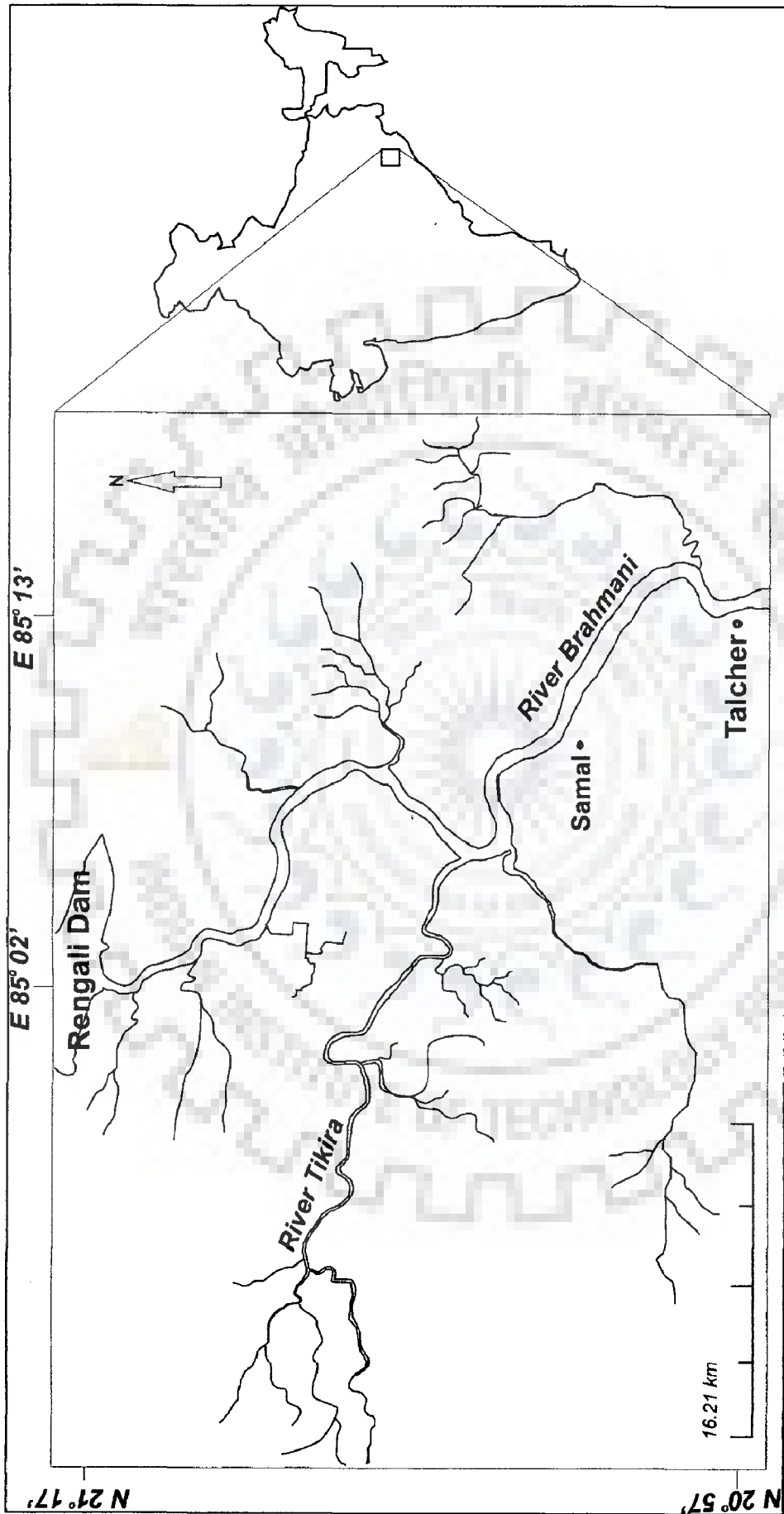


**Fig. 7.1:** Location map showing River Brahmani and its tributary Tikira (Digitized from Google Earth)

in flow is therefore necessary. Some fraction of Tikira's flow is assumed to be the catchments' contribution. Adding this, again the routing is done to get corrected flow hydrograph at various sections up to Talcher. Fig. 7.2 shows the flow hydrograph of various sections before and after correction. The computed and corrected flow data of various sections have been categorized in to two segments, viz. monsoon and non-monsoon periods by considering moving average approximation over a season. Due to the low flow during non-monsoon period, assimilating capacity of the river is limited. Hence, analysis of flow and pollutants' transport during this period is imperative.

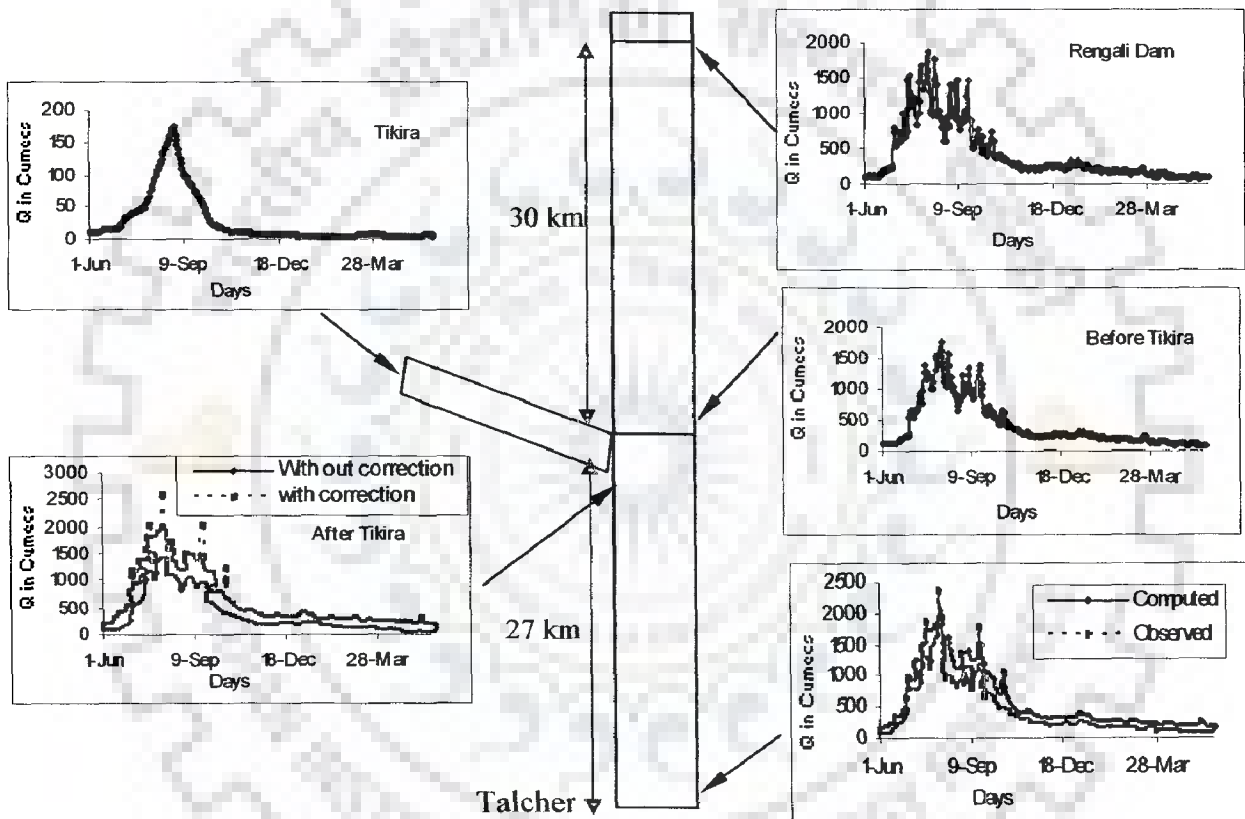


**Fig. 7.2: Computed Flow Rate of River Brahmani and Tikira at specific locations**

The flow rate with out and with correction just after Tikira is shown Fig. 7.3. Observed and computed flow rate at Talcher before and after correction are shown in Fig. 7.4 and 7.5.

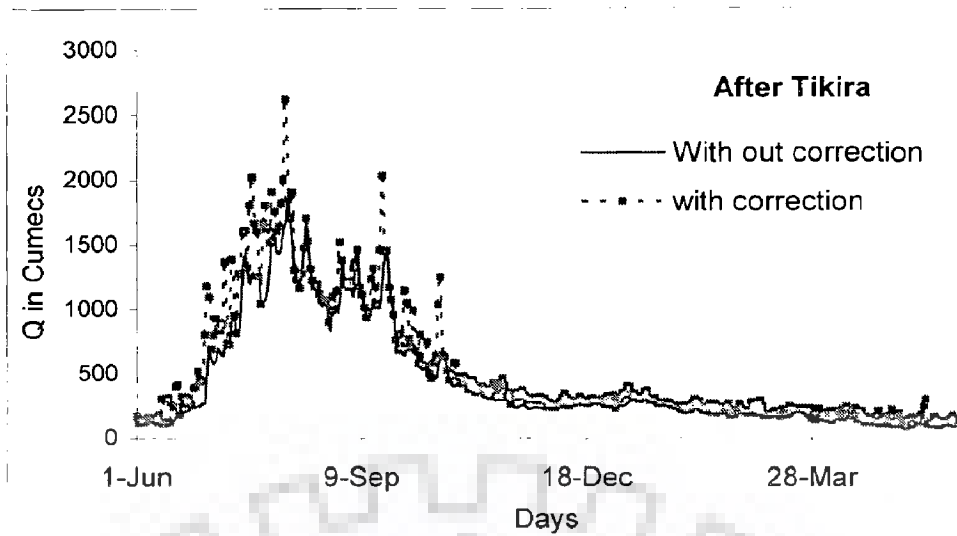


**Fig. 7.3: Flow hydrograph with out and with correction at a location after Tikira**

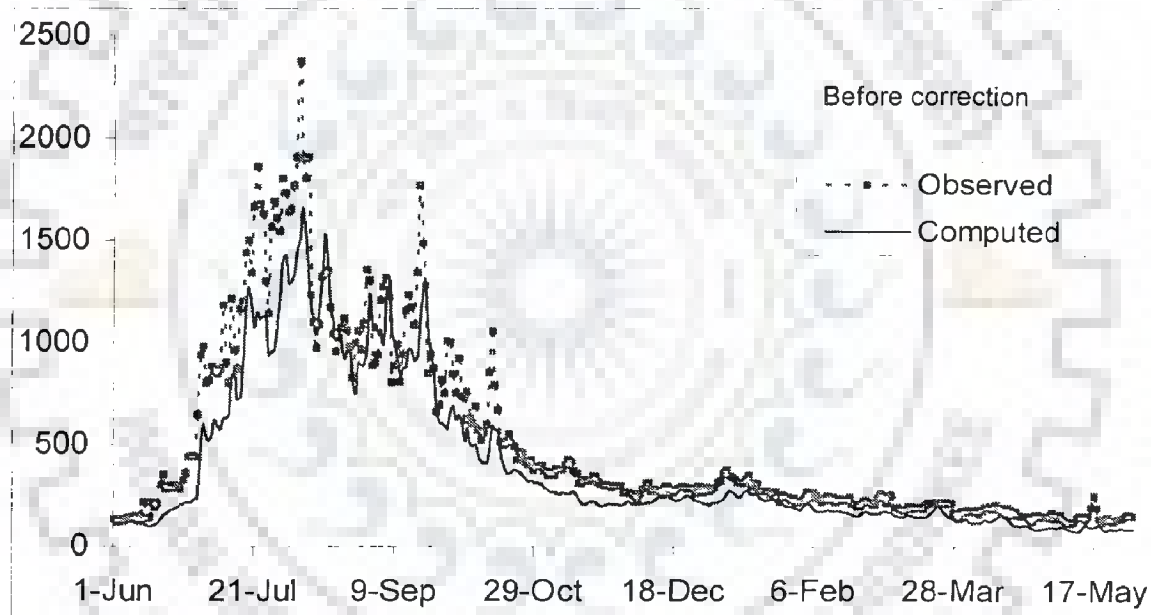


**Fig. 7.4: Observed and computed flow rates before correction at Talcher**

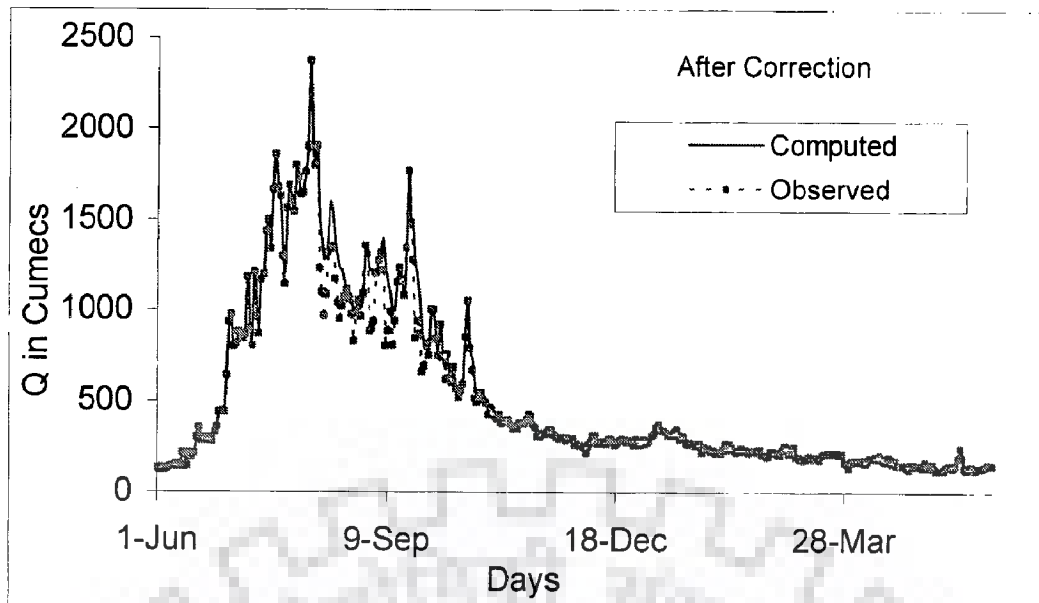


**Fig. 7.5: Observed and computed flow rates after correction at Talcher**

The average flow rate during high and low flow period at Talcher is presented in Fig 7.6.

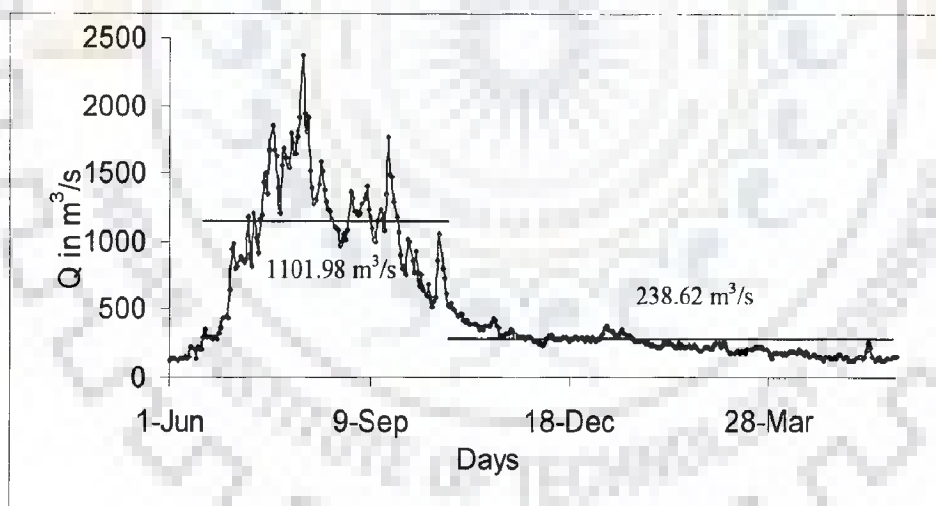


**Fig. 7.6: Seasonal average computed flow rate at Talcher**

The average flow rates at various sections in each season computed by Muskingum-Cunge Method are presented in Table 7.1.

**Table 7.1: Average flow rates at various sections of River Brahmani**

Locations	Flow Rate in m <sup>3</sup> /s	
	Monsoon period	Non-monsoon period
Rengali Dam	951	196.55
Location before Tikira joins	940.8	195.98
Location after Tikira joins	1153.69	239.72
Talcher	1101.98	238.62

#### 7.4 PARTICLE SIZE ANALYSIS FOR THE BED MATERIALS OF RIVER BRAHMANI AND SILT FACTOR

Bed samples from pre-decided locations along the length have been collected and analyzed in the laboratory to obtain the grain size distribution. Sieve analysis (dry test) and Hydrometer analysis (wet test) were carried out to obtain grain size distribution. The plot of particle size versus percent of finer is shown in Fig.7.7. The mean grain size estimated using the Eq. (D7) is found to be 0.149 mm. The silt factor ( $f_L$ ) corresponding to this grain size estimated as 0.6141.

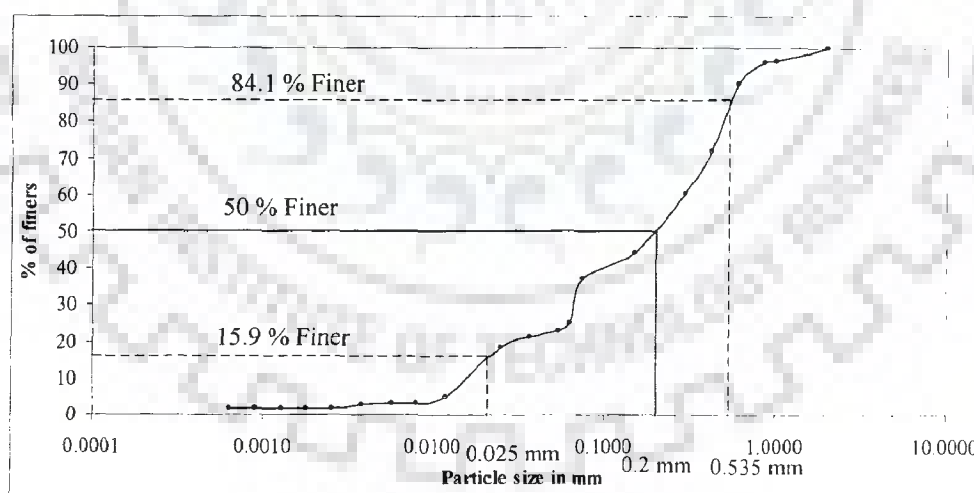


**Fig. 7.7: Grain size distribution curve of bed sediment samples collected from Brahmani.**

## 7.5 REGIME CHANNEL CONCEPT

Considering the flow rate and silt factor the channel geometry has been estimated using regime channel concept (Eq. D2 to Eq. D6) and presented in Table 7.2 and 7.3 for non-monsoon and monsoon seasons respectively.

**Table 7.2: Channel geometry estimation corresponding to average flow rate (Non-monsoon) and silt factor**

Location	<i>Average</i> $Q$ (m <sup>3</sup> /s)	<i>Average</i> $U$ (m/s)	$A$ (m <sup>2</sup> )	$H$ (m)	$W$ (m)	$S$
Rengali Dam	196.55	0.8977	218.6499	3.2150	68.01	5.52E-05
before Tikira joins	195.98	0.8973	218.1214	3.2119	67.91	5.52E-05
after Tikira joins	239.72	0.9279	257.9935	3.4349	75.10	5.34E-05
Talcher	238.62	0.9272	257.0065	3.4297	74.93	5.34E-05

**Table 7.3: Channel geometry estimation corresponding to average flow rate (Monsoon) and silt factor**

Location	<i>Average</i> $Q$ (m <sup>3</sup> /s)	<i>Average</i> $U$ (m/s)	$A$ (m <sup>2</sup> )	$H$ (m)	$W$ (m)	$S$
Rengali Dam	951	1.1675	813.4651	5.4377	149.5985	4.24E-05
before Tikira joins	940.8	1.1654	806.1878	5.4181	148.7941	4.25E-05
after Tikira joins	1153.69	1.2057	955.5705	5.7994	164.7713	4.109E-05
Talcher	1101.98	1.1965	919.7432	5.7114	161.0363	4.14E-05

The above stream geometry has been estimated by regime channel concept. Regime channel width corresponding to flow rate,  $Q = 2500 \text{ m}^3 / \text{s}$  which occurs during monsoon



period is computed as 242.37 m. From satellite image (Google Earth) the average width at three cross sections during monsoon period near Talcher is measured and found to be 250 m. The regime channel depth could not be compared with the actual depth of flow due to absence of observations. For the purpose of analysis of pollutant transport, the regime channel width and depth computed for different flow are assumed to be appropriate.

## 7.6 DETERMINATION OF LONGITUDINAL DISPERSION CO-EFFICIENT

Adopting the empirical equation proposed by Seo & Cheong (1998), the longitudinal dispersion co-efficient has been estimated and tabulated in Table 7.4 & 7.5.  $D_L$  changes between source and Talcher due to the change in channel geometry for a particular season due to the inflow from external sources.

**Table 7.4: Estimated longitudinal dispersion co-efficient during non-monsoon period**

$U_*$ (m/s)	$U$ (m/s)	$W$ (m)	$H$ (m)	$D_L$ (m <sup>2</sup> /s)
0.0417	0.8977	68.01	3.2150	431.5445
0.0417	0.8973	67.91	3.2119	430.7427
0.0424	0.9279	75.10	3.4349	490.0522
0.0424	0.9272	74.93	3.4297	488.611
Average				460.24 m <sup>2</sup> /s

**Table 7.5: Estimated longitudinal dispersion co-efficient during monsoon period**

$U_*$ (m/s)	$U$ (m/s)	$W$ (m)	$H$ (m)	$D_L$ (m <sup>2</sup> /s)
0.0476	1.1675	149.5985	5.4377	1184.3133
0.0475	1.1654	148.7941	5.4181	1176.1638
0.0484	1.2057	164.7713	5.7994	1340.2817
0.0482	1.1965	161.0363	5.7114	1301.4983
Average				1250.56 m <sup>2</sup> /s

## 7.7 RIVER REACH DISCRETIZATION AND PARAMETER ESTIMATION

The river stretch between Rengali dam and Talcher of length 57 km has been used for the study. In order to use hybrid model to predict the pollutants transport, the hybrid unit size ( $\Delta x$ ) has to be chosen such a way that the pecelet number should be equal to or more than 4. By having estimated  $u$  and  $D_L$ ,  $\Delta x$  is chosen as 3000 m in the reach between Rengali dam and Tikira confluent site, and 3857 m in the remaining reach up to Talcher.

Having estimated values of  $u$  (55.65 m / min),  $D_L$  (29359.92 m<sup>2</sup> / min) corresponding to the average lean flow rate, 239.17 m<sup>3</sup> / s, the parameters of the hybrid model ( $\alpha$ ,  $T_1$  and  $T_2$ ) are estimated using the relationships, given in flow chart (Fig. 6.1), as:  $\alpha = 20.267$  min,  $T_1 = 25.335$  min and  $T_2 = 23.706$  min. The reach length of 27 km (from Tikira confluence up to Talcher) is covered with 7 hybrid units of size 3857 m.

## 7.8 POLLUTION DATA

Water quality data at different locations in river Brahmani and its tributary, Tikira, are collected which include pH, Temperature, BOD, DO, Coliform. In the study reach a point load of pollution is discharged by river Tikira into the river Brahmani at 30 km down stream from Rengali dam. According to CPCB survey, 2980000 m<sup>3</sup> / day of waste water due to industrial, domestic and mining activities are discharged. The water quality data of the reach in river Brahmani before Tikira joins have been given in Table 7.6 as:

**Table 7.6: Water quality data in river Brahmani**

Locations	pH	Temperature (°C)	BOD (mg / L)	DO (mg / L)
Rengali dam	7.9	27.6	13.6	7.7
Before Tikira joins	7.8	27.7	12.6	7.3

The rate of discharge of waste water and chemical constituents for the months from November to May are presented in Table 7.7, it can be noted that the BOD load through Tikira is nearly steady.

**Table 7.7: Water quality data in river Tikira**

Month	Discharge (m <sup>3</sup> / s)	BOD (mg / L)	DO (mg / L)
November	18.1	216.8	3.4
December	15.4	218.9	3.3
January	13.7	221.6	2.9
February	13.5	223.5	1.5
March	13.2	225.6	1.5
April	12.5	228.6	1.2
May	13.3	229.5	0.9

The waste water with the above chemical constituents is discharged in to river Brahmani at 30 km down from the Rengali dam. Using the dilution equation the boundary deficit of DO in river Brahmani down stream of confluence is found as 1.76 mg / L (assuming DO at saturation as 9.1 mg / L) and the BOD is 24.03 mg / L. The decay rate and re-aeration rate constants are adopted as 0.23 and 4 per day respectively from Palo, 2002.

## **7.9 SIMULATION OF BOD**

The parameters of the hybrid cells in series model ( $\alpha$ ,  $T_1$  and  $T_2$ ) are ascertained for corresponding flow. The decay rate constant,  $k_1$  has been taken as 0.23 per day (Palo, 2002). Temporal variation of the BOD concentration at the end of first hybrid unit of size, 3857 m is simulated using HCIS-D model. The impulse response is compared with the response of ADDE model in Fig. 7.8. The impulse response simulated by HCIS-D model matches with the impulse response generated by ADDE model.

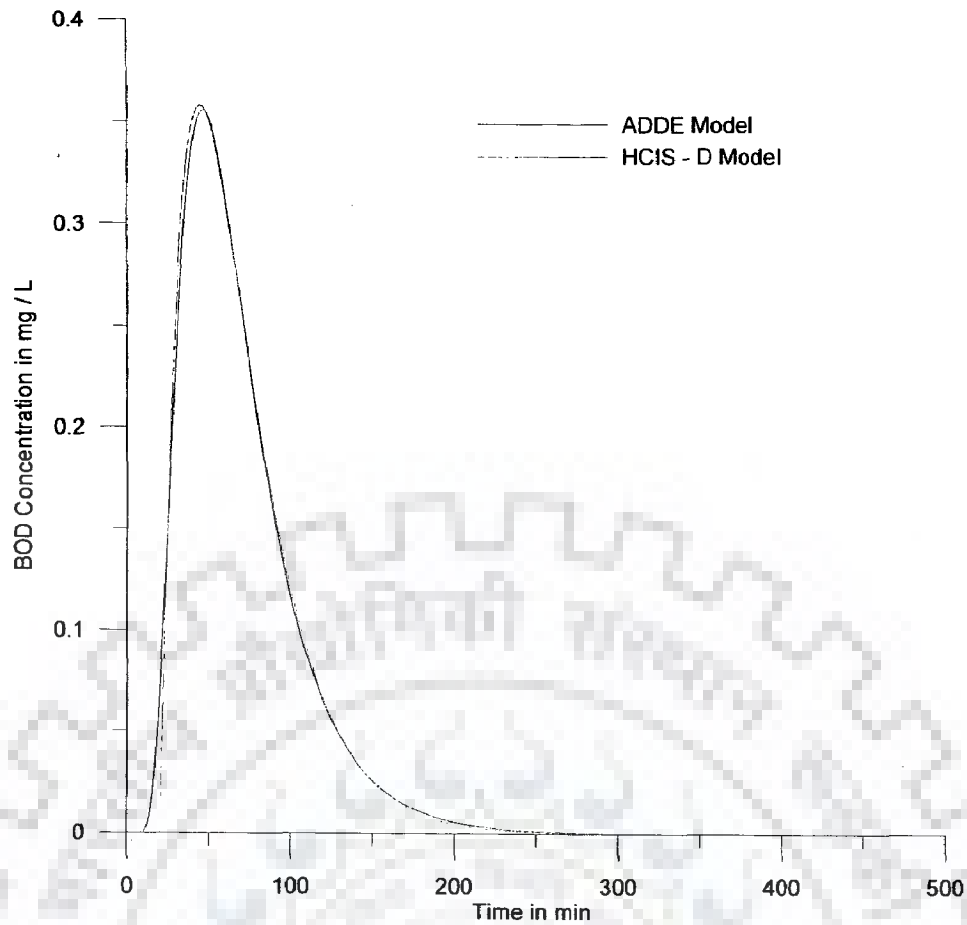


**Fig. 7.8: Impulse response functions of HCIS-D and ADDE models at 3.857 km from Tikira confluence for  $Q = 239.17 \text{ m}^3 / \text{s}$ ,  $C_R = 24.03 \text{ mg} / \text{L}$ ;  $u = 55.65 \text{ m} / \text{min}$   $D_L = 29359.92 \text{ m}^2 / \text{min}$ ,  $\Delta x = 3857 \text{ m}$ ,  $\alpha = 20.267 \text{ min}$ ;  $T_1 = 25.335 \text{ min}$ ;  $T_2 = 23.706 \text{ min}$  and  $k_1 = 0.23 \text{ per day}$**

The river reach, between Tikira confluence and Talcher, is discretized into 7 hybrid units. By convoluting, the state of BOD concentration (impulse and step responses) at Talcher are predicted and presented in Fig. 7.9 and 7.10.

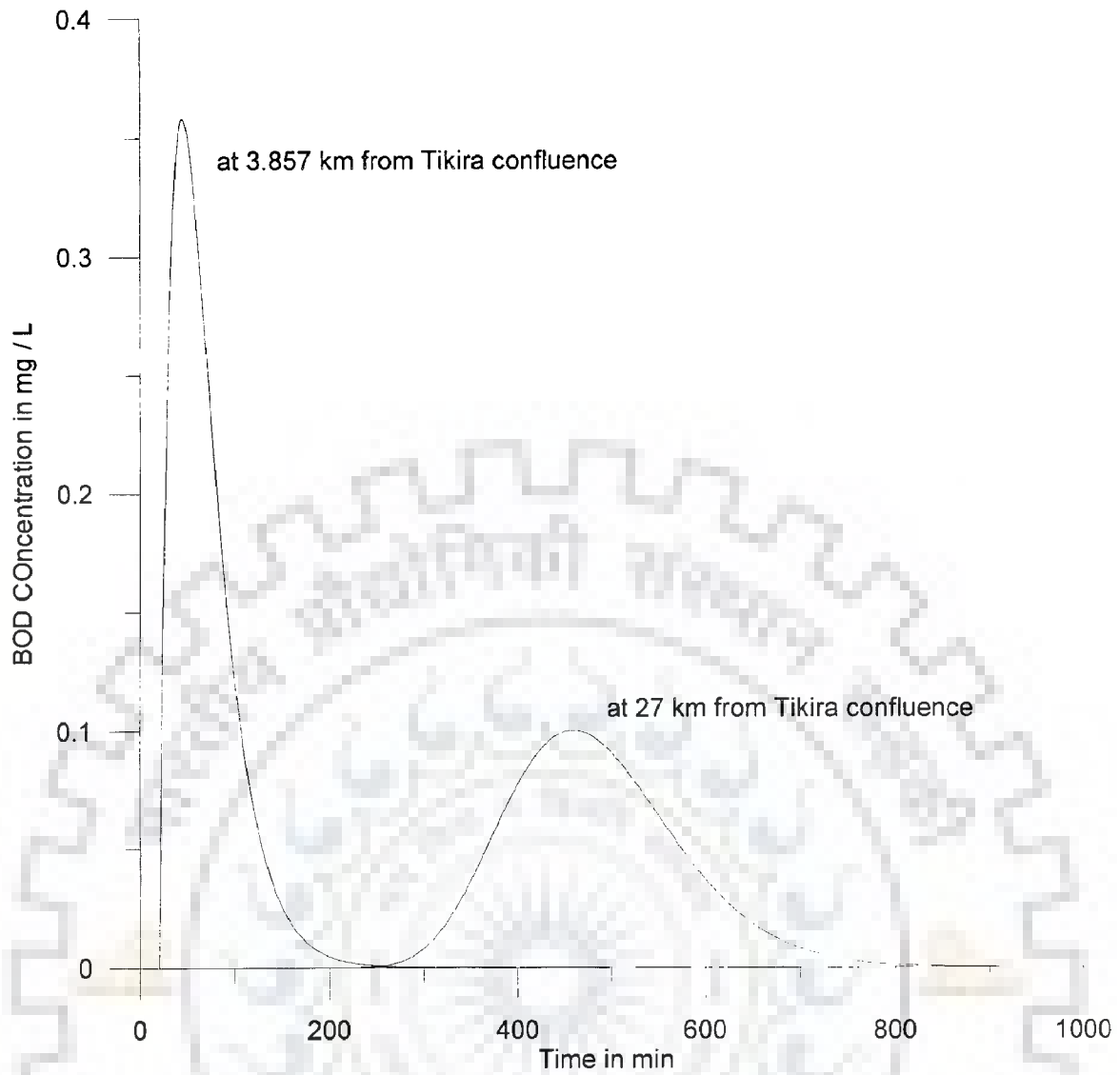


**Fig 7.9: Impulse response functions of HCIS-D model at different locations from Tikira confluence for  $C_R = 24.03 \text{ mg / L}$ ,  $k_l = 0.23 \text{ per day}$ ,  $Q = 239.17 \text{ m}^3 / \text{s}$ ,  $a = 20.267 \text{ min}$ ;  $T_1 = 25.335 \text{ min}$  and  $T_2 = 23.706 \text{ min}$ ,  $u = 55.65 \text{ m / min}$  and  $\Delta x = 3857 \text{ m}$ .**

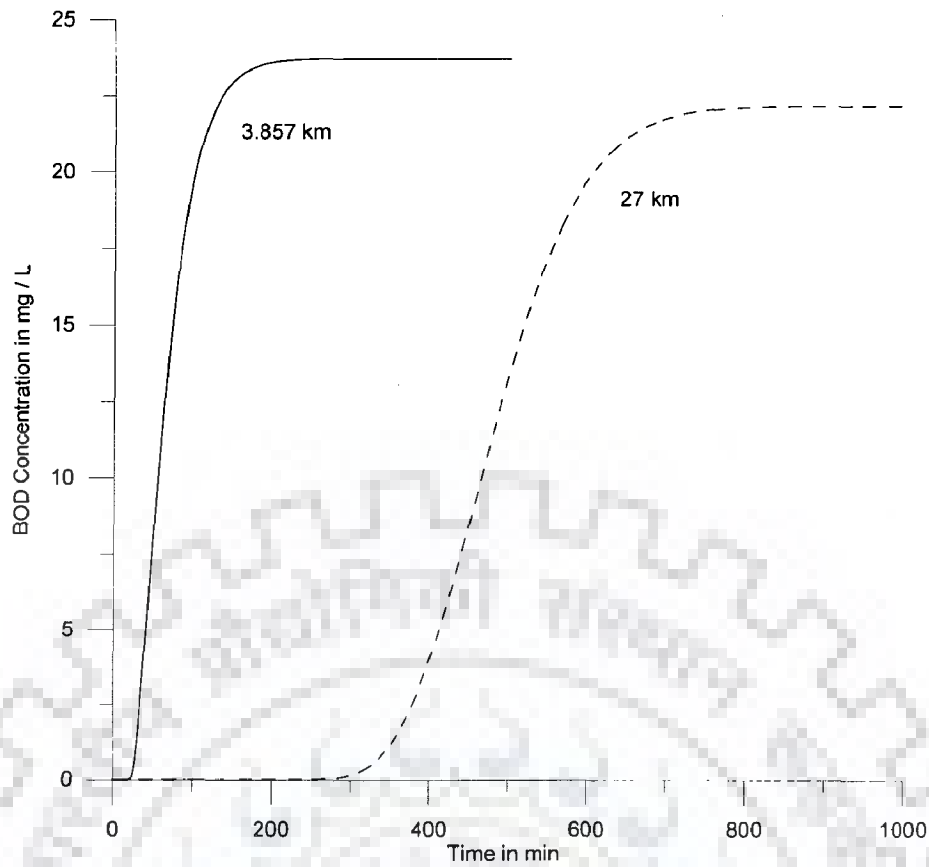


**Fig 7.10: Step response functions of HCIS-D model at different locations for  $C_R = 24.03 \text{ mg / L}$ ,  $k_1 = 0.23 \text{ per day}$ ,  $Q = 239.17 \text{ m}^3 / \text{s}$ ,  $\alpha = 20.267 \text{ min}$ ;  $T_1 = 25.335 \text{ min}$  and  $T_2 = 23.706 \text{ min}$ .**

As seen from Fig 7.9, due to the impulse injection ( $C_R = 24.03 \text{ mg / L}$ ) at Tikira, the peak concentration of BOD at Talcher is approximately  $0.1 \text{ mg / L}$  which is observed at  $t = 450 \text{ min}$ . The concentration of BOD at Talcher is presented in Fig. 7.10. The maximum concentration at Talcher is about  $22.5 \text{ mg / L}$  due to continuous discharge of waste at Tikira. At Talcher the concentration attains its maximum level in  $800 \text{ min}$  after waste disposal. It is observed, the BOD concentration in river Brahmani down stream of Rengali dam site and prior to the waste disposal site at Tikira is already  $12.6 \text{ mg / L}$ . Thus to satisfy the water quality requirement of  $3 \text{ mg / L}$  as BOD at Talcher, the effluent dumped to river Brahmani between Rengali and Talcher including that of Tikira requires prior treatment.

In order to analysis the effect of reduction in flow rate on BOD concentration,  $1/3$  of average lean flow rate ( $79.72 \text{ m}^3 / \text{s}$ ) is considered. Corresponding  $u$  and  $D_L$  are estimated as  $46.34 \text{ m / min}$  and  $14528.69 \text{ m}^2 / \text{min}$  respectively. The  $\Delta x$ , that satisfies  $P_e \geq 4$ , is  $2450 \text{ m}$ . The corresponding parameters of the HCIS model are estimated as:  $\alpha = 16.53$

min,  $T_1 = 20.657$  min and  $T_2 = 15.687$  min. The reach length of 27 km is represented by 11 hybrid units. Using, this set of parameters, the BOD concentrations (impulse and step responses) at Talcher are predicted using convolution technique. The variations in BOD concentration are presented in Fig. 7.11 and 7.12.

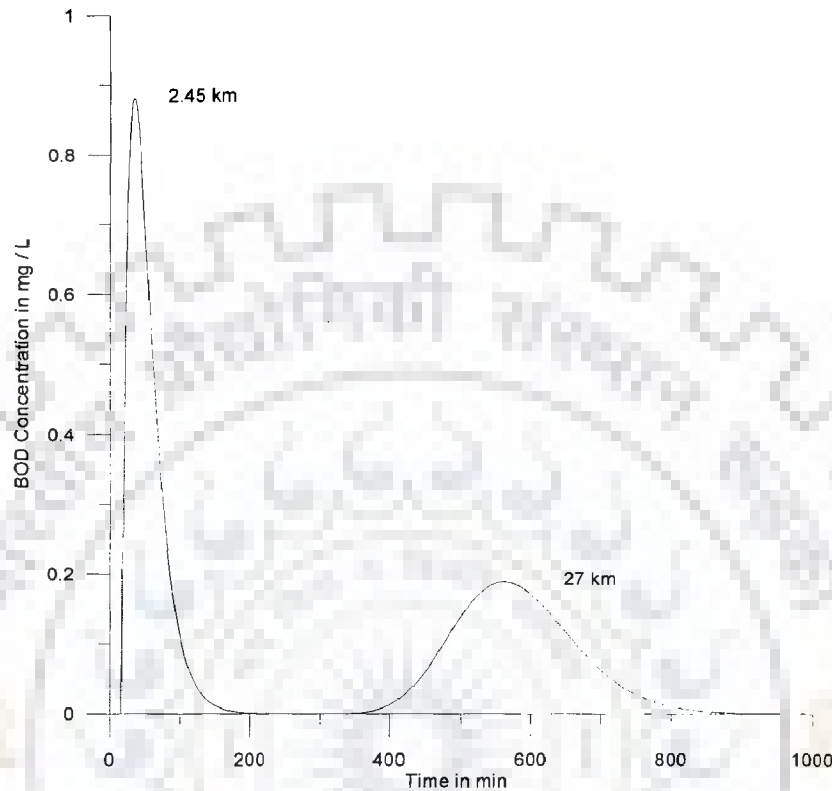


**Fig 7.11: Impulse response functions of HCIS-D model at different locations from Tikira confluence for  $C_R = 43.61$  mg / L,  $k_I = 0.23$  per day for flow rate,  $Q = 79.72$  m<sup>3</sup> / s and corresponding parameters:  $\alpha = 16.53$  min;  $T_1 = 20.657$  min,  $T_2 = 15.687$  min,  $u = 46.34$  m / min and  $\Delta x = 2450$  m.**

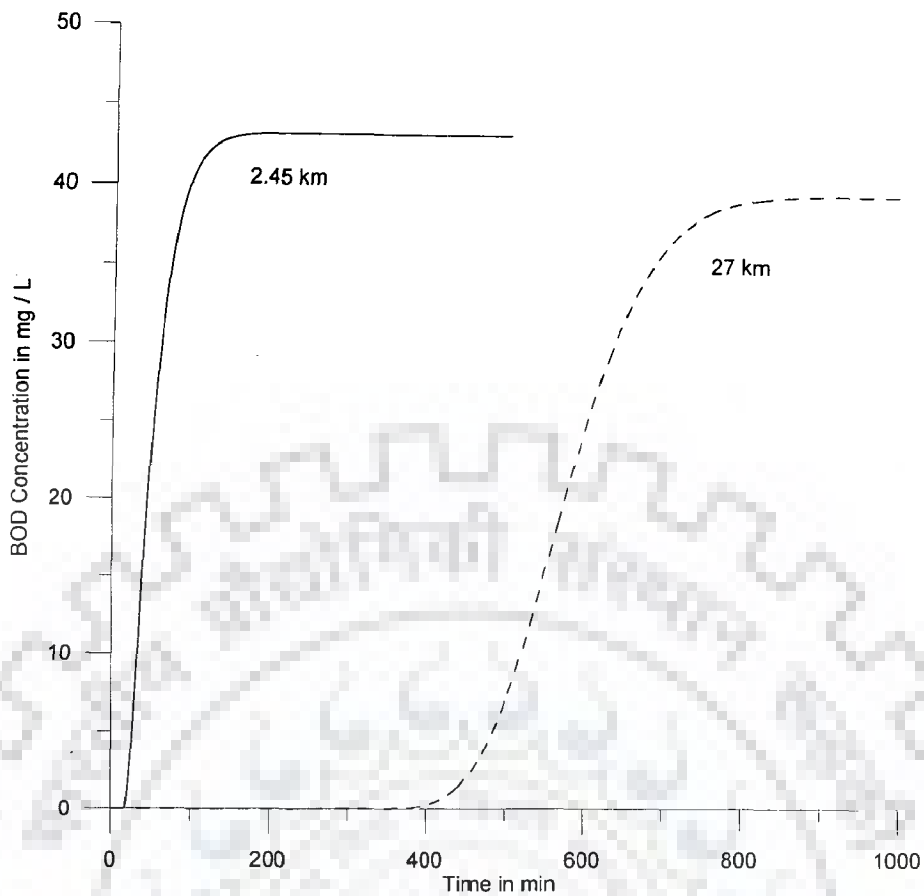


**Fig 7.12: Step response functions of HCIS-D model at different locations from Tikira confluence for  $C_R = 43.61 \text{ mg / L}$ ,  $k_1 = 0.23$  per day for flow rate,  $Q = 79.72 \text{ m}^3 / \text{s}$  and corresponding parameters:  $\alpha = 16.53 \text{ min}$ ;  $T_1 = 20.657 \text{ min}$ ,  $T_2 = 15.687 \text{ min}$   $u = 46.34 \text{ m / min}$  and  $\Delta x = 2450 \text{ m}$ .**

Due to an impulse injection of BOD ( $43.61 \text{ mg / L}$ ) at Tikira, the maximum BOD concentration at Talcher is  $0.2 \text{ mg / L}$ . For continuous disposal of BOD load at Tikira, the maximum BOD at Talcher is about  $40 \text{ mg / L}$ . Thus with reduction of flow, the water quality will further deteriorate. Therefore, the industrial effluent at Tikira needs prior treatment before it is dumped to the stream.

The state of water quality during peak flow period is analyzed by considering average high flow rate ( $1127.84 \text{ m}^3 / \text{s}$ ) during monsoon period. Corresponding  $u$  and  $D_L$  are estimated as  $72.07 \text{ m / min}$  and  $79258.42 \text{ m}^2 / \text{min}$  respectively, and the corresponding parameters of the HCIS model are estimated as:  $\alpha = 22.99 \text{ min}$ ,  $T_1 = 28.74 \text{ min}$  and  $T_2 = 41.92 \text{ min}$  for the size of the hybrid unit,  $\Delta x = 6750 \text{ m}$ . The reach length of  $27 \text{ km}$  is represented by 4



hybrid units. Using, this set of parameters, the BOD concentrations (impulse and step responses) at Talcher are predicted using convolution technique. The variations in BOD concentrations are presented in Fig. 7.13 and 7.14.

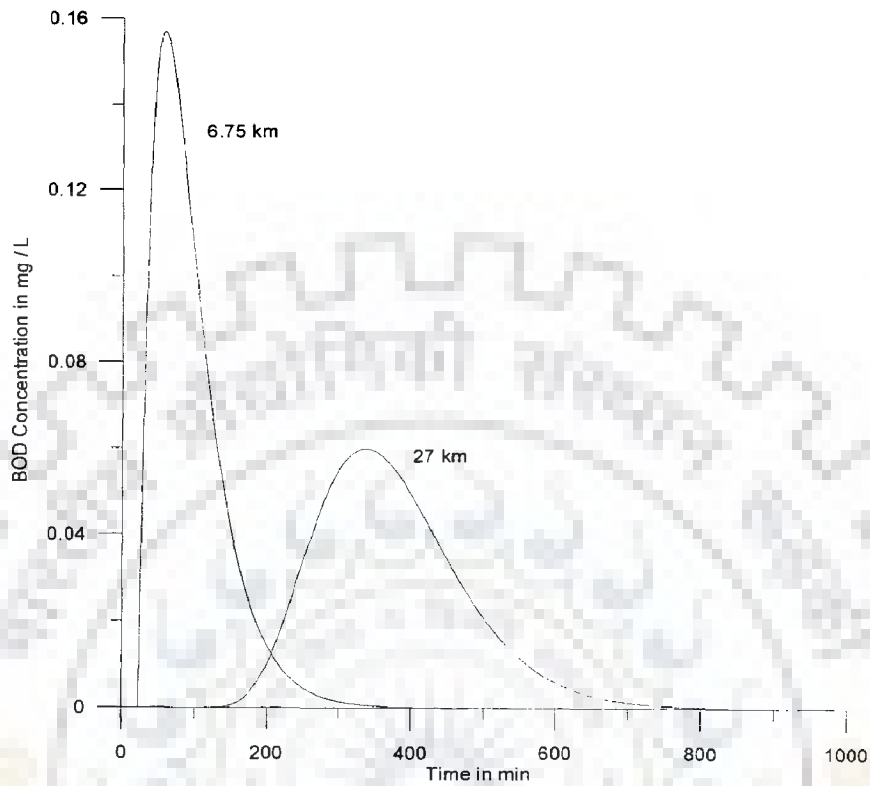


**Fig 7.13: Impulse response functions of HCIS-D model at different locations from Tikira confluence for  $C_R = 15.13 \text{ mg / L}$ ,  $k_I = 0.23$  per day for flow rate,  $Q = 1127.84 \text{ m}^3 / \text{s}$  and corresponding parameters:  $\alpha = 22.99 \text{ min}$ ;  $T_1 = 28.74 \text{ min}$ ,  $T_2 = 41.92 \text{ min}$ ,  $u = 72.07 \text{ m / min}$  and  $\Delta x = 6750 \text{ m}$ .**

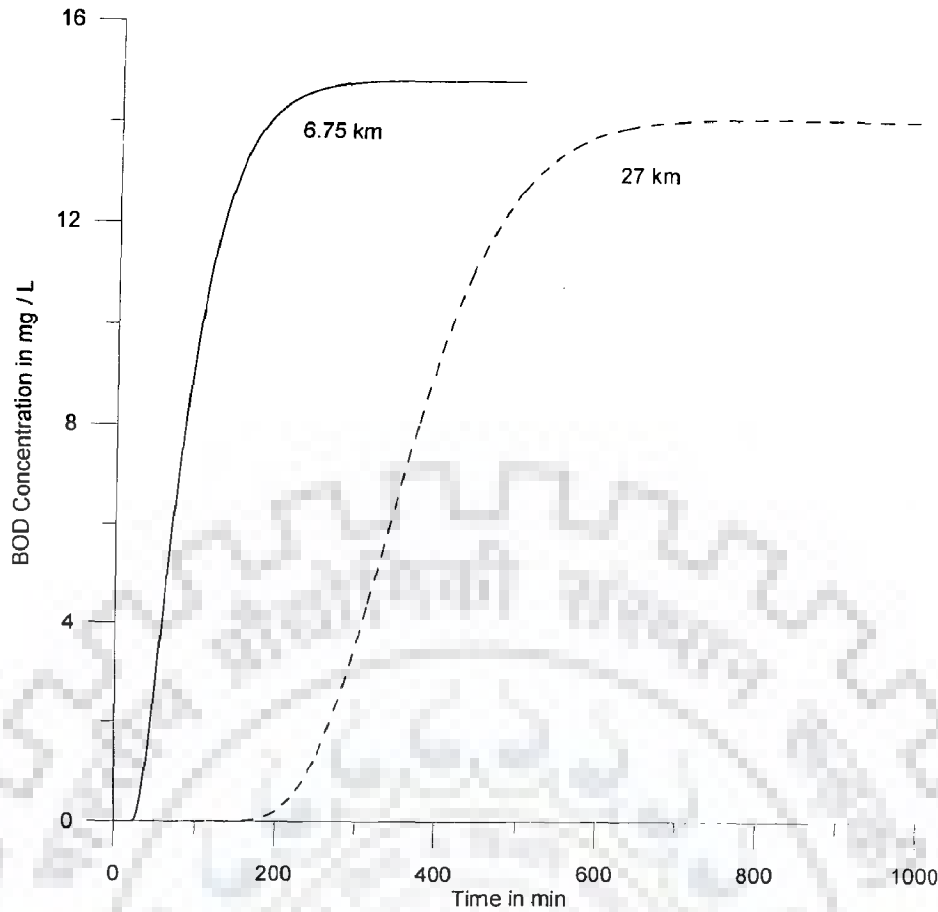


**Fig 7.14: Step response functions of HCIS-D model at different locations from Tikira confluence for  $C_R = 15.13$  mg / L,  $k_I = 0.23$  per day for flow rate,  $Q = 1127.84$   $m^3 / s$  and corresponding parameters:  $\alpha = 22.99$  min;  $T_1 = 28.74$  min,  $T_2 = 41.92$  min,  $u = 72.07$  m / min and  $\Delta x = 6750$  m.**

Corresponding to an impulse injection of BOD (15.13 mg / L) at Tikira, the maximum BOD concentration at Talcher is 0.05 mg / L. For continuous disposal of BOD load at Tikira, the maximum BOD at Talcher is about 14 mg / L. Degradation of pollutant within the reach is very low even for high flow, due to very small value of  $k_I$ . Therefore, such BOD load for which  $k_I$  is small is to be treated prior to its disposal to Tikira.

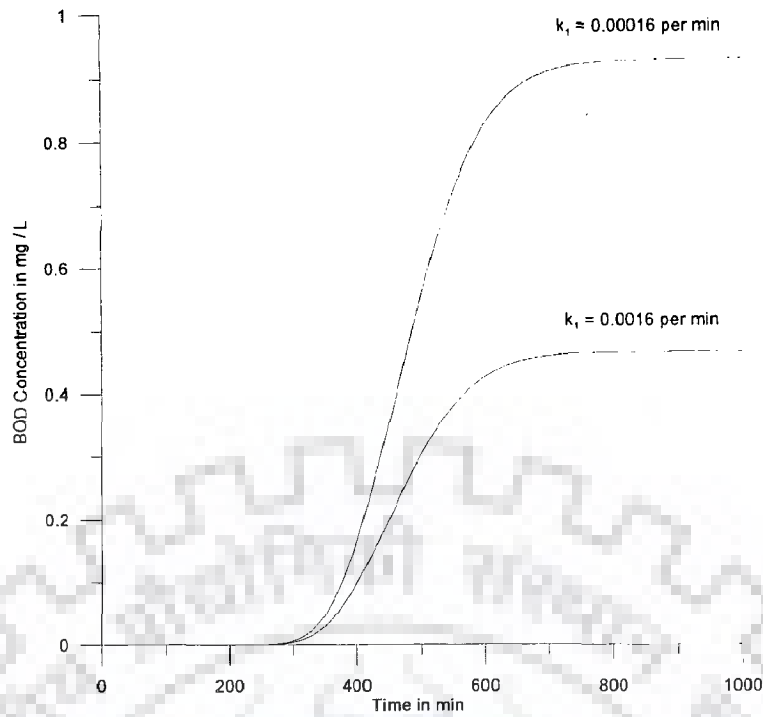


**Fig. 7.15: Unit step response functions for different values of  $k_1$  during lean flow ( $Q = 239.17 \text{ m}^3 / \text{s}$ )**

In Fig. 7.15, the influence of parameter,  $k_1$  on unit step response function is compared. Low value of  $k_1$  means less bio-degradable. Therefore the step response BOD load attains higher values in comparison to that for higher  $k_1$  values.

### 7.10 SIMULATION OF DO

Having the estimated values of hybrid model parameters ( $\alpha$ ,  $T_1$  and  $T_2$ ), BOD load corresponding to the decay rate constant,  $k_1$ , assuming re-aeration rate constant,  $k_2$ , and boundary DO deficit,  $D_0$ , the impulse response function for DO concentrations are simulated using HCIS-R model at 3.857 and 27 km from Tikira confluence point. The variations of DO concentrations are presented in Fig. 7.16.

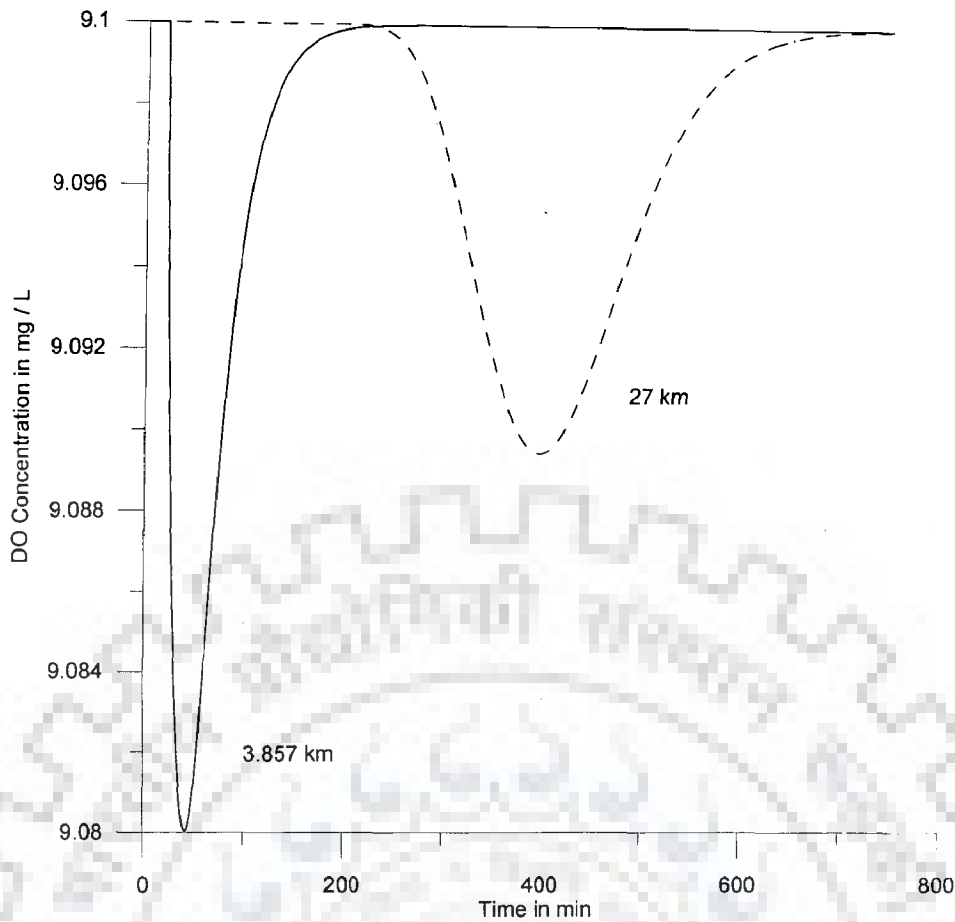


**Fig. 7.16: Impulse response functions of HCIS-R model at different locations from Tikira confluence for  $C_R = 24.03 \text{ mg / L}$ , boundary deficit,  $D_0 = 1.76 \text{ mg / L}$ ,  $k_1 = 0.23 \text{ per day}$ ,  $k_2 = 4 \text{ per day}$ ,  $Q = 239.17 \text{ m}^3 / \text{s}$ ,  $\alpha = 20.267 \text{ min}$ ;  $T_1 = 25.335 \text{ min}$ ,  $T_2 = 23.706 \text{ min}$ ,  $u = 55.65 \text{ m / min}$  and  $\Delta x = 3857 \text{ m}$ .**

For continuous BOD input of  $24.03 \text{ mg / L}$  injected at Tikira confluence point with boundary deficit,  $D_0 = 1.76 \text{ mg / L}$  and  $k_1 = 0.23 \text{ per day}$ ,  $k_2 = 4 \text{ per day}$   $\alpha = 20.267 \text{ min}$ ;  $T_1 = 25.335 \text{ min}$  and  $T_2 = 23.706 \text{ min}$ ., the step response function at Talcher is simulated and presented in Fig. 7.17.

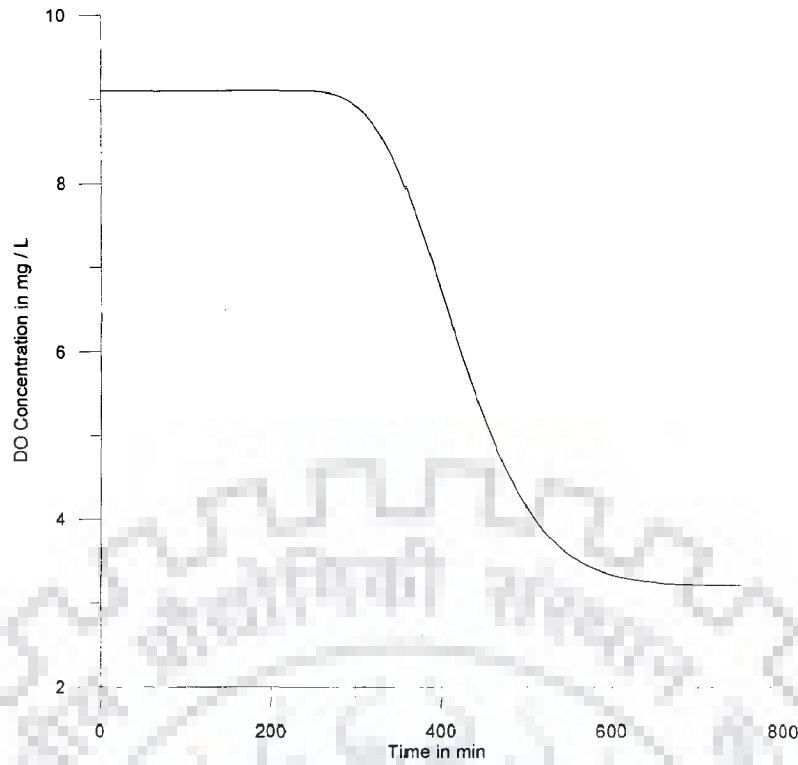


**Fig. 7.17: Step response function of HCIS-R model at Talcher for  $C_R = 24.03$  mg / L, boundary deficit,  $D_0 = 1.76$  mg / L,  $k_1 = 0.23$  per day,  $k_2 = 4$  per day,  $Q = 239.17$  m<sup>3</sup> / s,  $\alpha = 20.267$  min;  $T_1 = 25.335$  min,  $T_2 = 23.706$  min,  $u = 55.65$  m / min and  $\Delta x = 3857$  m.**

For analyzing the effect of low and high flow on DO concentration, the low flow rate is considered as 79.72 m<sup>3</sup> / s (1/3 of lean flow) and the high flow rate as 1127 m<sup>3</sup> / s (average flow in monsoon period). The BOD inputs, boundary deficits, flow characteristics, longitudinal dispersion co-efficient and parameters of hybrid model corresponding to the flow rates are given in Table 7.8.

**Table 7.8: Parameters estimated corresponding to the low and high flow rates of river Brahmani**

$Q$ (m <sup>3</sup> /s)	$u$ (m / s)	$D_L$ (m <sup>2</sup> / s)	$C_R$ (mg/L)	$D_0$ (mg/L)	Parameters of hybrid model			$\Delta x$ (m)
					$\alpha$ (min)	$T_1$ (min)	$T_2$ (min)	
79.72	0.77	242.14	43.61	2.4	16.53	20.657	15.687	2450
1127.84	1.20	1320.9	15.13	1.48	22.99	28.74	41.92	6750

Making use of these sets of data for low flow, impulse and step responses of HCIS-R model are simulated and presented in Fig. 7.18 and 7.19 respectively for  $k_1 = 0.23$  per day and  $k_2 = 4$  per day. For high flow, impulse and step responses of HCIS-R model are simulated and presented in Fig. 7.20 and 7.21 respectively.

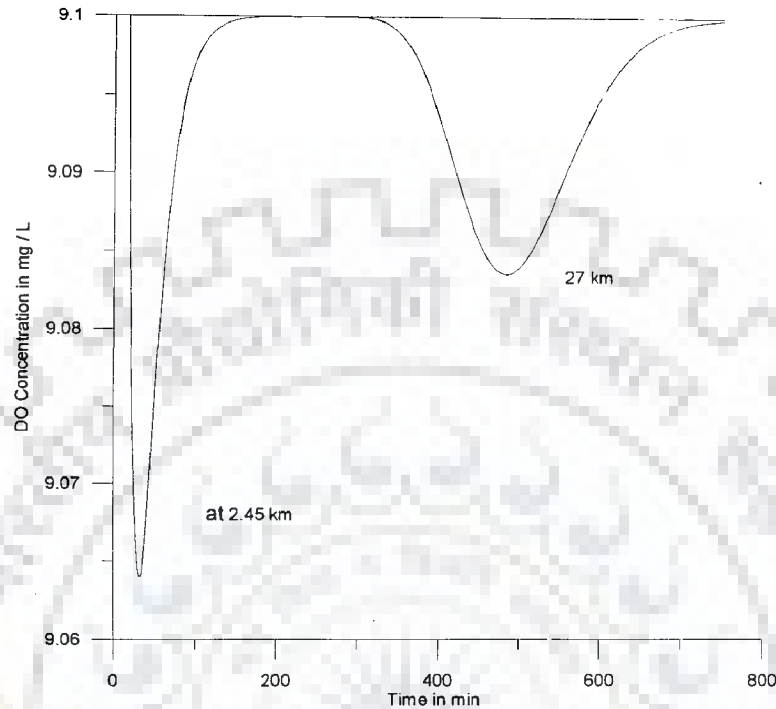


**Fig. 7.18: Impulse response functions of HCIS-R model at different locations from Tikira confluence for  $C_R = 43.61$  mg / L, boundary deficit,  $D_0 = 2.4$  mg / L,  $k_1 = 0.23$  per day,  $k_2 = 4$  per day,  $Q = 79.72$  m<sup>3</sup> / s,  $\alpha = 16.53$  min;  $T_1 = 20.657$  min,  $T_2 = 15.687$  min,  $u = 46.34$  m / min and  $\Delta x = 2450$  m.**

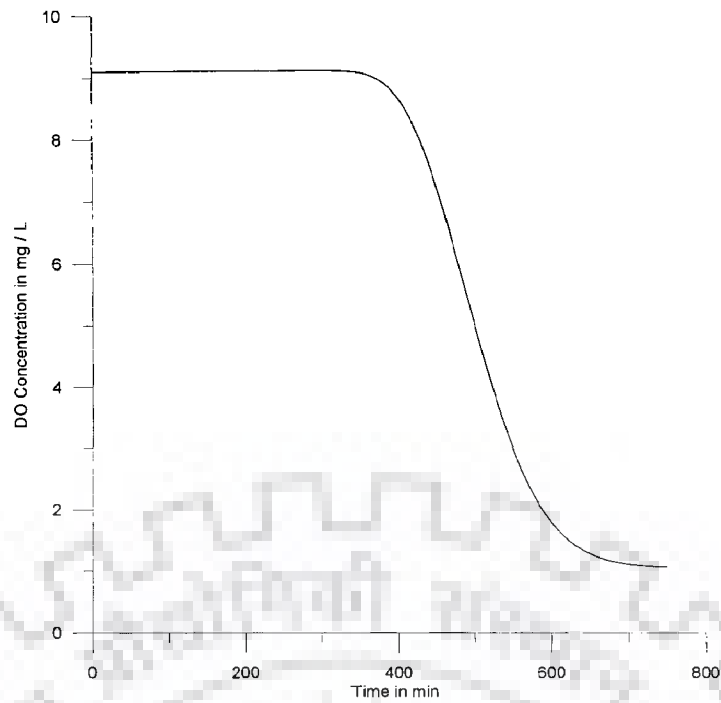


**Fig. 7.19: Step response function of HCIS-R model at Talcher for  $C_R = 43.61$  mg / L, boundary deficit,  $D_0 = 2.4$  mg / L,  $k_1 = 0.23$  per day,  $k_2 = 4$  per day,  $Q = 79.72$  m<sup>3</sup> / s,  $\alpha = 16.53$  min;  $T_1 = 20.657$  min,  $T_2 = 15.687$  min,  $u = 46.34$  m / min and  $\Delta x = 2450$  m.**

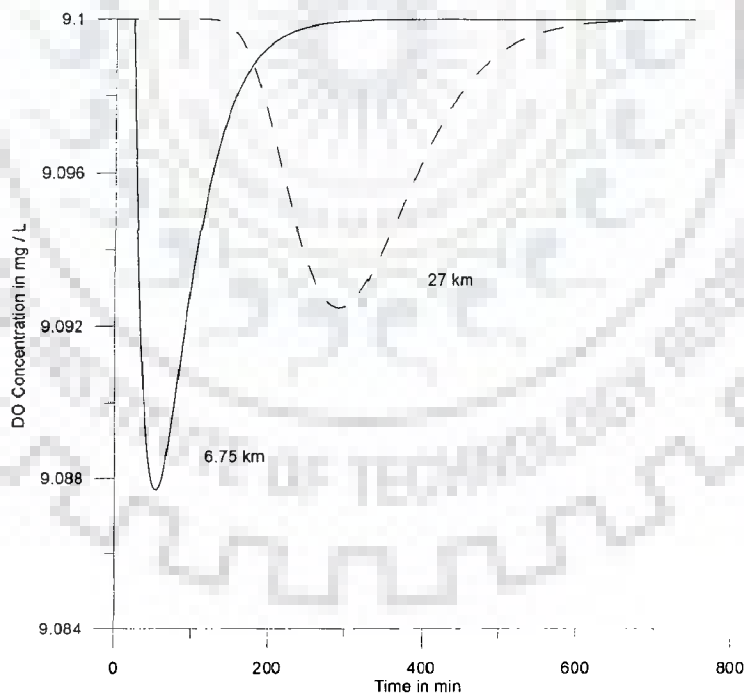


**Fig. 7.20: Impulse response functions of HCIS-R model at different locations from Tikira confluence for  $C_R = 15.13$  mg / L, boundary deficit,  $D_0 = 1.48$  mg / L,  $k_1 = 0.23$  per day,  $k_2 = 4$  per day,  $Q = 1127.84$  m<sup>3</sup> / s,  $\alpha = 22.99$  min;  $T_1 = 28.74$  min,  $T_2 = 41.92$  min,  $u = 72.07$  m / min and  $\Delta x = 6750$  m.**

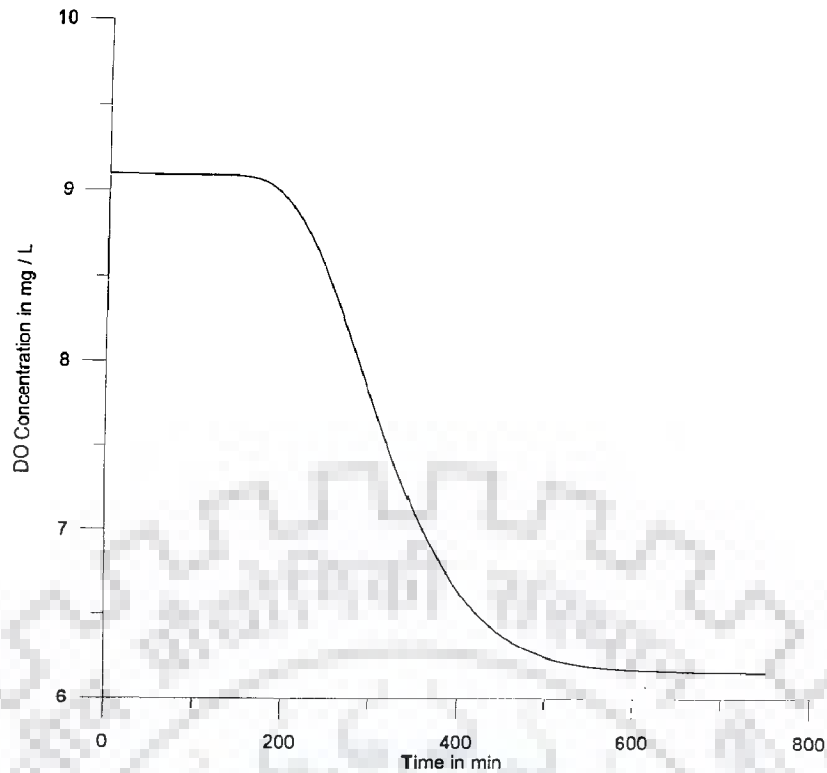


**Fig. 7.21: Step response function of HCIS-R model at Talcher for  $C_R = 15.13$  mg / L, boundary deficit,  $D_0 = 1.48$  mg / L,  $k_1 = 0.23$  per day,  $k_2 = 4$  per day,  $Q = 1127.84$  m<sup>3</sup> / s,  $\alpha = 22.99$  min;  $T_1 = 28.74$  min,  $T_2 = 41.92$  min,  $u = 72.07$  m / min and  $\Delta x = 6750$  m.**

As seen from Fig. 7.21, the DO concentration during monsoon period is above 6 mg / L which is required DO concentration for class - C type river reach.

## 7.11 CONCLUSIONS

1. River width computed using regime channel theory for high flow matches with actual river width observed from satellite data. The Longitudinal dispersion co-efficient can be ascertained from the river geometry predicted using regime channel theory.
2. A hybrid CIS model can be used successfully to predict stream water quality downstream of the pollutant disposal site.
3. Consequent to BOD load disposal at Tikira, the minimum DO level during lean flow period at Talcher is about 3 mg / L. During high flow period, the minimum DO level is 6 mg / L.



4. The BOD concentration (which has very small  $k_1$  values) at Talcher during lean flow period is 40 mg / L, and during high flow period is 14 mg / L. The BOD at Talcher exceeds the limiting value. Hence the waste needs treatment prior to its disposal.





## CHAPTER 8

### SUMMARY AND CONCLUSIONS

---

#### 8.1 GENERAL

The applications of conceptual potential alternatives to the ADE model, namely the CIS and the ADZ models have their own limitations. The CIS model has limitation toward simulating advection component, while the ADZ model faces complexity in selecting the model order. The HCIS model simulates advection-dispersion governed solute transport as depicted by the ADE model under steady and uniform flow conditions closely when size of the basic process unit of the HCIS model is equal to or greater than  $4D_L / u$  or when the size of the basic process unit is chosen satisfying the condition Peclet number,  $P_e = (\Delta x u) / D_L \geq 4$ . The parameters ( $\alpha$ ,  $T_1$  and  $T_2$ ) of the HCIS model have been determined from the measurement of single  $C-t$  profile without invoking measurements of  $u$  and  $D_L$ . In the HCIS model, pure advection is represented by an explicitly derived time parameter, and the model also represents the advection and dispersion components implicitly by two time parameters, whereas, in the ADE model, both advection and dispersion are represented implicitly by  $u$  and  $D_L$ . The HCIS is a simple semi-analytical model and can accommodate non-homogeneity character of the system.

#### 8.2 CONCLUSIONS FROM PRESENT STUDY

Alike in the ADE model, natural adsorption and desorption, transient storage, growth and decay components can be incorporated into the HCIS model. Thus, the HCIS model seems to have overcome the weaknesses of the ADE, the CIS, and the ADZ model. For resolving environmental issues, it is necessary to predict the pollutant transport more accurately by incorporating possible additional processes along with advection and dispersion. Considering the strength and the flexibility of the HCIS model, it has been extended to the study of solute transport in streams for resolving the model complexities of various processes like adsorption/desorption, and non-conservative nature of the pollutants.

In the present study, the adsorption/desorption mechanism for a conservative as well as non-conservative substance have been analyzed using the HCIS model. A linear non-equilibrium isotherm for exchange of pollutant between the soil column and the mainstream water has been considered along with advection and dispersion. Incorporating an adsorption rate co-efficient in each of the three compartments in the HCIS model, i.e., the plug flow zone and two thoroughly mixed reservoirs of unequal residence time, a conceptual hybrid-cells-in-series model coupled with adsorption (HCIS-A) is developed. The HCIS-A model is a four-parameter model representing three time parameters and one time-reciprocal co-efficient. An analytical solution in continuous time and space domain for transport of solute in a plug flow zone, where adsorption takes place, has been obtained using Laplace transform technique. A Hybrid Cells in Series model comprising a plug flow zone and two thoroughly mixed reservoirs has been derived to simulate advection-dispersion and adsorption governed solute transport in streams in discrete space domain and continuous time domain. The unit step response and the unit pulse response functions of the HCIS-A model have been derived. Due to the addition of the adsorption process with advection and dispersion, peak concentration reduces, falling limb of  $C-t$  profile smoothed and long tail produced in concentration distribution. These characteristics of the  $C-t$  profiles for a conservative pollutant in a stream with adsorbing stream bed and soil sediments are in the expected lines. The characteristics of the concentration-time profiles generated by the HCIS-A model have been compared with explicit finite difference numerical solution of ADE with non-equilibrium adsorption.

A hybrid model is developed adopting first order reaction kinetic along with advection and dispersion of non-conservative pollutant which is injected at the source. For the pecllet number greater than 4, the response of the Hybrid Cells in Series model for step and instantaneous input matches with the response of Advection Dispersion Decay Equation (ADDE) model for the same inputs. Flexibility of the HCIS model for adopting reaction kinetics along with basic transport processes has been demonstrated.

A hybrid model is developed adopting first order reaction kinetic along with advection and dispersion of pollutant and first order re-aeration to predict the DO

concentration. The classical Streeter and Phelps (1944) model incorporates first order de-oxygenation and re-aeration only. For the pecllet number greater than 4, the dissolved oxygen deficit and DO sag curves have been plotted for different BOD load at the entry. Flexibility of the HCIS model for adopting reaction kinetics and first order re-aeration along with basic transport processes has been demonstrated. The response of the HCIS-R model closely matches with the numerical solution of Streeter-Phelps dispersion model. An in depth study has been done to analyze comparison of the solution obtained by Rinaldi approach with numerical solution indicates that the solution by Rinaldi approach differs much from numerical solution and over estimates DO deficit.

The HCIS, HCIS-A and HCIS-D are linear transport models governing of a single pollutant. The HCIS-R model is a combination of two linear models incorporating decay and aeration. The unit impulse, unit pulse and unit step response functions are fundamental characteristics of a system. Using these basic response functions, the transport of the pollutant in the stream for varying pollutant input can be predicted.

In order to identify the suitability of the HCIS or HCIS-A model for a particular  $C-t$  profile, it is required to know the corresponding parameters of the HCIS and HCIS-A models. In this study, the parameters of the HCIS and the HCIS-A models are estimated using least squares optimization method for a given sets of observed  $C-t$  profile. The suitability of the model is identified by comparing the tracer velocities estimated using the parameters of the HCIS and the HCIS-A models with the mean flow velocity. The model for which the estimated tracer velocity matches with the mean flow velocity is the appropriate model. This helps in selection of the appropriate model for a given  $C-t$  profile.

River width computed using regime channel theory for high flow matches with actual river width observed from satellite data. The Longitudinal dispersion co-efficient has been ascertained from Seo & Cheong's (1998) empirical formulae having river geometry predicted using regime channel theory.

The hybrid CIS model has been used to predict stream water quality down stream of a pollutant disposal site in an Indian river (River Brahmani) successfully. During high and low flow periods the BOD concentration at Talcher attains a value of 14 mg / L and 21

mg / L respectively. Since the river flow has limiting assimilation capacity for the pollutant load, prior treatment of waste load at Tikira the effluent disposal site is essential. By assessing the assimilating capacity of the River Brahmani particularly in the stretch between Rengali and Talcher, regulation for pretreatment of waste has been suggested before dumping to the river.

### **8.3 SCOPE OF FUTURE STUDY**

In nature adsorption/desorption processes may follow non-linear, non-equilibrium isotherm. The study could be extended for adsorption/desorption processes following non-linear, non-equilibrium isotherm.

Depending upon nature of river/stream (influent or effluent), the pollutant transport is influenced by the aquifer's interaction. The HCIS model usage can be extended to study the pollutant transport in influent and effluent streams.

Modeling of thermal discharge to the streams holds importance in modeling of non-conservative pollutant transport. The study can be extended to incorporate temperature effects while modeling non-conservative pollutant transport.

In a stream the sediment transport governs the pollutant transport; therefore the effect of sediment transport on pollutant transport needs to be investigated.

The pollutants are discharged near the bank of a river; near the disposal site the entire width of the river does not take part in transport. In such situation, the river having large width can not be treated as a linear channel, therefore the transport of pollutant to be studied as a two dimensional process.

## REFERENCES

---

1. Abramowitz, M., and Stegun, I. A. (Eds). (1970). Handbook of mathematical functions. Dover Publications Inc., New York.
2. Adrian, D. D., Alshawabkeh, A. N. (1997). Analytical dissolved oxygen model for sinusoidally varying BOD. J. of Hydro. Engg. ASCE., Vol. 2, No. 4, 180-185.
3. Adrian, D. D., Yu, F. X., and Barbe, D. (1994). Water quality modeling for a sinusoidally varying waste discharge concentration. Water Resour. Res., 28 (5), 1167-1174.
4. Anand Prakash. (1977). Convective dispersion in perennial streams. J. of Envir. Engg. Div., ASCE. 103 (2), 321-339.
5. Aris, R. (1956). On the dispersion of a solute in a fluid flowing through a tube. Proc. Royal Soc. London Ser. A 235, 67-77.
6. Asai, K., Fujisaki, K., and Awaya, Y. (1991). Effect of aspect ratio on longitudinal dispersion coefficient. In Environmental Hydraulics, Lee and Cheung (Ed.), Vol. 2, Balkema, Rotterdam, The Netherlands. 493-498.
7. Bajracharya, K., and Barry, D. A. (1992). Mixing cell models for nonlinear non-equilibrium single species adsorption and transport. Water. Res., 29 (5), 1405-1413.
8. Bajracharya, K., and Barry, D. A. (1995). Analysis of one dimensional multispecies transport experiments in laboratory soil columns. Envir. International, Vol. 21, No. 5, 687-691.
9. Bajracharya, K., and Barry, D.A. (1993). Mixing cell models for nonlinear equilibrium single species adsorption and transport. Journal of Contaminant Hydrology 12, 227-243.
10. Bajracharya, K., and Barry, D.A. (1994). Note on common mixing cell models. Journal of Hydrology 153, 189-214.
11. Banks, R. B. (1974). A Mixing Cell Model for Longitudinal Dispersion in Open Channel. Water Resour. Res., 10(2), pp. 357-358.

12. Bansal, M. K. (1971). Dispersion in Natural Streams. J. of Hydraul. Div Proc., Am. Soc. Civ. Eng., HY 11, pp. 1867-1886.
13. Barnet, A.G., (1983). Exact and approximate solutions of the advection dispersion equation. In XXth IAHR Congress Moscow, Hydro. Tech. Inst, Sept 1983, Baz1, 3, 180- 190.
14. Barnwell, T. O (1985). Rates, Constants and Kinetics Formulations in Surface Water Quality Modeling 2e. Environmental Research Laboratory, U.S. E. P. A
15. Barry, D. A., Bajracharya, K. (1995). Optimised Muskingum-Cunge solution method for solute transport with equilibrium Freundlich reactions. J. of Contan. Hydro. 18, 221-238.
16. Bear, Jacob, (1972) Dynamics of fluids in porous media. American Elsevier Publishing Company, Inc., New York, 764p.
17. Bear, Jacob and Bachmat, Y. (1990). Theory and applications of transport in porous media. Kluwer Academic Publishers, Dordrecht, The Netherlands.
18. Beer, T., and Young, P. C. (1983). Longitudinal Dispersion in Natural Streams. J. Environ. Eng. Div., Am. Soc. Civ. Eng., 109(5), pp. 1049-1067.
19. Beltaos, S. (1978). An interpretation of longitudinal dispersion data in rivers. Report no. SER 78-3, Transportation and surface water div., Alberta Research Council, Edmonton, Canada.
20. Beltaos, S. (1980). Longitudinal dispersion in rivers. Jour. Hydro. Div., Proc. Am. Soc. Civil Engrs., 106(1), 151-171.
21. Beltaos, S. (1982). Dispersion in tumbling flow. Jour. Hydraul. Div., Proc. Am. Soc. Civil Engrs., 108(1), 591-612.
22. Bencala, K. E., and R. A. Walters. (1983) Simulation of solute transport in a mountain pool-and riffle stream: a transient storage model. Water Resour. Res., 19(3), 718-724.
23. Bencala, K. E., McKnight, D. M., Zellweger, G. W. (1990). Characterization of transport in an acidic and metal-rich mountain stream based on a lithium traces injection and simulations of transient storage. Water Resour. Res. 26 (5), 989-1000.



24. Berndtson, R. (1990). Transport and sedimentation of pollutants in a river reach: a chemical mass balance approach. *Water Resour. Res.*, 26 (7), 1549-1558.
25. Bevan, K.J., and P.C. Young. (1988). An aggregated mixing zone model of solute transport through porous media. *Jour. Contaminant Hydro.* 3, 129-143.
26. Bhargava, D. S. (1981). Most rapid BOD assimilation in Ganga and Yamuna rivers, *Jour. Env. Engg., ASCE*, 109(1), 174-188.
27. Bidwell, V.J. (1999). State-space mixing cell model of unsteady solute transport in unsaturated soil. *Environmental Modeling & Software* 14, 161–169.
28. Bobba, G., V. P. Singh, and L. Bengtsson. (1996). Application of first order and Monte Carlo analysis in watershed water quality models, *Wat. Resour. Management.* 10, 219-240.
29. Brown, L. C., and Thomas O. Barnwell, Jr. (1987). The enhanced stream water quality models QUAL2E and QUAL2E-UNCAS: Documentation and user manual, US-EPA, ERL, Athens, Georgia.
30. Cameron, D. R., and Klute. A. (1977). Convective dispersive solute transport with combined equilibrium and kinetic adsorption model. *Water Resources Research*, Vol 13 (1), 183 – 188.
31. Castro, N. M., and Hornberger, G. M. (1991). Surface-subsurface water interactions in an alleviated mountain stream channel. *Water resour. Res.*, 27 (7), 1613-1621.
32. Cernik, M., Barmettler, K., Grolimund, D., Rohr, W., Borkovec, M., Sticher, H. (1994). Cation transport in natural porous media on laboratory scale: multi component effects. *Journal of Contaminant Hydrology* 16, 319–337.
33. Chapra, S. C., and Runkel, R. L. (1999). Modeling impact of storage zones on stream dissolved oxygen. *Journal of Environmental Engineering*, Vol. 125, No. 5, 415-419.
34. Chatwin, P. C. (1970). The Approach to Normality of the Concentration Distribution of a Solute in a Solvent Flowing along a Straight Pipe. *J. of Fluid Mech.*, 43, pp. 321-352.
35. Chatwin, P.C. (1971). On the interpretation of some longitudinal dispersion experiments. *Jour. Fluid Mech.*, 48, 689-702.

36. Chatwin, P.C. (1980) Presentation of longitudinal dispersion data. *Jour. Hydr. Div., Am. Soc. Civil Engrs.*, 106(1), 71-83.
37. Chatwin, P.C., and C.M. Allen. (1985) Mathematical models of dispersion in rivers and estuaries. *Annual Review of Fluid Mech.*, 17, 119-149.
38. Cheong, T. S., and I. W. Seo. (2003) Parameter estimation of the transient storage model by a routing method for river mixing processes, *Water Resour. Res.*, 39(4), 1074-1082.
39. Choudhary, N., P. Tyagi, N. Niyogi, and V. P. Thergonhar. (1990). BOD test for tropical countries, *ASCE, Jour. of Env. Engineering*, 118, 298-303.
40. Czernuszenko, W., and Rowinski, P. M. (1997). Properties of the dead zone model of longitudinal dispersion in rivers. *J. of Hydraul. Res.*, 35 (4), 491-504.
41. Czernuszenko, W., and Rowinski, P. M., Sukhodolov, A. (1998). Experimental and numerical validation of the dead zone model for longitudinal dispersion in rivers. *J. of Hydraul. Res.*, 36 (2), 269-280.
42. Dandigi, M. N. and Jeyakumar, K.V. (2003). Municipal wastewater management through eco-friendly treatment systems. *Hydrology and Watershed Management*; edited by B. Venkateswara Rao, K. Ramamohan Reddy, C. Sarala and K. Raju. *Proceedings of International Conference: With a Focal Theme on Water Quality and Conservation for Sustainable Development (18-20 December) Hyderabad*, BS Publications, 1487 p.
43. Day, T.J. (1975). Longitudinal dispersion in natural channels, *Water Resour. Res.*, 11, 909-918.
44. Day, T.J., and I. R. Wood. (1976) Similarity of the mean motion of fluid particles dispersing in natural channels. *Wat. Resour. Res.*, 12(4), 655-666.
45. De Smedt, F. (2006). Analytical solutions for transport of decaying solutes in rivers with transient storage. *J. Hydrol.* 330, 672 – 680.
46. De Smedt, F., Brevis, W., Debels, P. (2005) Analytical solution for solute transport resulting from instantaneous injection in streams with transient storage. *J. Hydrol.* 315 (1-4), 25-39.

47. Deacon, J. R., and N. E. Driver. (1999). Distribution of trace elements in streambed sediment associated with mining activities in the upper Colorado River Basin, Colorado, USA, *Archives of Environmental Contamination and Toxicology*, Vol. 37, No.1, pp. 7-118, DOI: 10.1007/S00244900494.
48. Deng, Z. Q., Bengtsson. L., Singh. V. P. and Adrian, D. D. (2002). Longitudinal dispersion coefficient in single channel streams. *J. of Hydraul. Engg.*, Vol. 128, No. 10, 901-915.
49. Deng, Z. Q., Joao, L. M. P. de. Lima and Singh. V. P. (2005). Transport rate based model for overland flow and solute transport: Parameter estimation and process simulation. *J. of Hydro.* 315, 220-235.
50. Deng, Z. Q., Singh. V. P. and Bengtsson. L. (2001). Longitudinal dispersion coefficient in straight rivers. *J. of Hydraul. Engg.*, Vol. 127, No. 11, 919-927.
51. Dobbins, W.E. (1964). BOD and oxygen relationships in streams, *Jour. of Sanitary Engg. Div., Proc. ASCE*, 90(SA3), 53-78.
52. Donald H. Burn and E. A. McBean. (1987). Application of nonlinear optimization to water quality. *Applied Mathematical Modeling*, Volume 11, Issue 6, December. 438-446.
53. Dooge, J. C. I. (1959). "A general theory of the unit hydrograph." *J. Geophys. Res.*, 64(2), 241-256.
54. Edwards, Richard T. (1998). *The Hyporheic Zone - In River Ecology and Management: Lessons from the Pacific Coastal Ecoregion*, eds. Robert J. Naiman and Robert E. Bilby. New York: Springer-Verlag.
55. Elder, J. W. (1959). The Dispersion of Marked Fluid in Turbulent Shear Flow. *J. of Fluid Mech.*, 5(4), pp. 544-560.
56. Elhadi, N. D., A. Harrington, I. Hill, Y. L. Lau, and B.G. Krishnappan (1984) River mixing-A state-of-the-art report. *Canadian Jour. of Civil Engr.* 11(11), 585-609.
57. Elhadi, N.D., and K.S.Davar. (1976). Longitudinal dispersion for flow over rough beds. *Jour. Hydr. Div. Am. Soc. Civil Engrs.*, 102(4), 483-498.
58. Fick. A. (1855). On liquid diffusion. *Philos. Mag.* 4(10), 30-39.

59. Fischer, H. B. (1966). Longitudinal Dispersion in Laboratory and Natural Streams. Report No. KH-R-12, W. M. Keck Laboratory of Hydraul. and Water Resour., California Institute of Technology, California.
60. Fischer, H. B. (1967). The Mechanics of Dispersion in Natural Streams. *J. of Hydraul. Div., Am. Soc. Civ. Eng.*, 93, pp. 187-216
61. Fischer, H. B. (1968). Dispersion Predictions in Natural Streams. *J. of Sanit. Eng. Div., Am. Soc. Civ. Eng.*, 94, pp. 927-943.
62. Fischer, H. B. (1975). Discussion of Simple Method for Predicting Dispersions in Streams by R. S. McQuiver and T. N. Keefer. *J. of Envir. Eng. Div., Am. Soc. Civ. Eng.*, 101, pp. 453-455.
63. Fischer, H.B., Imberger, J., List, E.J., Koh, R.C.Y., and Brooks, N.H., (1979). *Mixing in Inland and Coastal Waters*. 483 p., Academic press, New York.
64. Fukuoka, S., and Sayre, W.W. (1973) Longitudinal dispersion in sinuous channels, *Jour. Hydraul. Div., Proc. Am. Soc. Civ. Eng.*, 99, 195-218.
65. Ghosh, N. C. (2001). Study of Solute Transport in a River. Ph.D thesis, Dept of Civ. Eng., IIT. Roorkee, INDIA.
66. Ghosh, N. C., and McBean, E. A. (1998). Water quality modeling of Kali River, India. *Water, Air and Soil Pollution*. Vol. 102, 91-103.
67. Ghosh, N.C., G.C. Mishra, and C.S.P. Ojha. (2004) A Hybrid-cells-in-series model for solute transport in a river. *Jour. Env. Engg. Div., Am. Soc. Civil Engr.* 130 (10), 1198-1209.
68. Ghosh, Subimal and Mujumdar, PP (2005) Risk Minimization Model for River Water Quality Management. In *Proceedings Hydrological Perspective for Sustainable Development*, pages pp. 932-939, IIT Roorkee, India.
69. Gradshteyn, I. S., Ryzhik, I. M. (1965). *Table of integrals, series and products*. 4<sup>th</sup> ed. New York: Academic Press.
70. Gray, W. G., and Pinder, G. F. (1976). An Analysis of the Numerical Solution of the Transport Equation. *Water Resour. Res.*, 12, pp. 547-555.

71. Hart, D.R. (1995) Parameter estimation and stochastic interpretation of the transient storage model for solute transport in streams. *Water Resour. Res.* 31 (2), 323–328.
72. Harvey, J. W., Wagner, B. J., and Bencala, K. E. (1996). Evaluating the reliability of the stream tracer approach to characterize stream-subsurface water exchange. *Water Resour. Res.*, 32 (8), 2441-2451.
73. Hauer, F. Richard, and Gary A. Lamberti, eds. (1996). *Methods in Stream Ecology*. San Diego, CA: Academic Press.
74. Hays, J. R., Krenkel, P. A., and Schnelle, K. B. (1966). Mass transport mechanisms in open channel flow, Tech. Report No. 8, Vanderbilt University, Nashville, Tennessee, 138pp.
75. Henderson, F. M. (1966). *Open Channel Flow*. Macmillan, New York.
76. Holley, E. R., and Tsai, Y.H. (1970). Comment on longitudinal dispersion in natural channels by T. J. Day. *Water Resour. Res.*, 13, 505-10.
77. Jain, C. K., and M. K. Sharma. (2002). Adsorption of cadmium on bed sediments of River Hindon : Adsorption models and Kinetics, *Water, Air and Soil Pollution*, Vol. 137, No. 1-4, pp. 1-19.
78. Jain, S. C., (1976). Longitudinal dispersion coefficient for streams. *J. of Envir. Engg., ASCE*, 102 (2), 465-474.
79. Jolanki, D. G. (1997). Basic river water quality models- computer aided learning (CAL) programme on water quality modeling, IHP-V, Technical documents in hydrology, No.13, UNESCO, Paris.
80. Jones, Jeremy B., and Patrick J. Mulholland, eds (2000). *Streams and Ground Waters*. SanDiego, CA: Academic Press.
81. Kafarov, V. (1976). *Cybernetic methods in chemistry and chemical Engineering*. English translation, Mir Publishers, Moscow, 483pp.
82. Keshari, A. K. (2005). Modeling solute transport within groundwater system, in mathematical models in Hydro geochemistry: Assessment of ground water quality & management. Training Manual. School of Envir. Studies, JNU, New Delhi. Pp358.

83. Keshari, A.K. and Bithin Datta. (1995). Integrated Optimal Management of Groundwater Pollution and Withdrawal, Groundwater, September.
84. Kezhong, H., and Yu, H. (2000). A New Empirical Equation of Longitudinal Dispersion Co-efficient. Stochastic Hydraulics 2000, Wang and Hu (Eds), Balkema, Rotterdam.
85. Koussis, A. D., and Rodriguez-Mirasol, J. (1998). Hydraulic estimation of dispersion coefficient for streams. J. of Hydraul. Engg., ASCE, 124 (3), 317-320.
86. Lacey, G. (1930). Stable Channels in Alluvium. Min. Proc. Inst. Civ. Eng. London, Paper No 4736, Vol. 229.
87. Lees, M. J., L. A. Camacho, and S. Chapra. (2000). On the relationship of transient storage and aggregated dead zone models of longitudinal solute transport in streams. Water Resour. Res., 35(1), 213-224.
88. Leij, F. J., and Toride, N. (1998). Analytical solutions for non-equilibrium transport models, in Physical Non-equilibrium in soils modelling and application (Ed. by Selim, H. M., and Ma, L.). Ann Arbor Press, Chelsea, Michigan.
89. Lindley, E. S. (1919). Regime Channels. Proc., Punjab. Eng. Congress, Vol. 7.
90. Liu, H. (1977) Predicting dispersion co-efficient of streams. Jour. Environ. Eng. Div., Am. Soc. Civil Engrs., 103(1), 59-67.
91. Liu, H. (1978). Closure of Discussion on Predicting Dispersion Co-efficient of Streams. J. of Envir. Engrg. Div., ASCE, 104 (4), pp. 825-828.
92. Liu, H., and Cheng, A. H. D. (1980). Modified Fickian model for prediction dispersion. J. of Hydraul. Eng. Div., Am. Soc. Civ. Eng., 106(6), 1021-1040.
93. Loucks, D. P., Stedinger, J. R. and Haith, D. A. (1981). Water resource systems planning and analysis. Prentice – Hall Inc. N.J. USA.
94. Magazine, M. K. (1983). Effect of bed and side roughness on dispersion and diffusion in open channels. Ph.D thesis, University of Roorkee, Roorkee, India.
95. Mahar, P.S. And Bithin, Datta. (1996). Optimal Estimation of Parameters for Coupled Groundwater Flow and Solute Transport Modeling, Proceedings, National Conference: Hydro-96, I.I.T. Kanpur.



96. Marivoet, J. L., and Craenenbroeck, W. V. (1986). Longitudinal dispersion in ship canals. *J. of Hydraul. Res.*, 24 (2), 123-133.
97. Marquardt, D. W. (1963). An algorithm for least squares estimation of non-linear parameters. *J. of Soc. Indust. and Appl. Math.*, 11 (2), 431-441, A1-A9.
98. Martin, J. L and McCutcheon, S. C. (1999). *Hydrodynamics and Transport for Water Quality Modeling*. 794 p, Lewis publishers, Washington, D.C.
99. McCutcheon, S. C., and French, R. H. (1989). *Water quality modeling. Vol. 1: Transport and surface exchange in rivers*. CRC Press Inc., Florida, USA. 334 pp.
100. McCutcheon, S.C., Martin, L., and Barnwell, T. O. (1993). *Water quality handbook of hydrology*. (Ed. David R. Maidment). McGraw Hill, Inc. USA. 11.1-11.73.
101. McQuivey, R. S., and Keefer, T. N. (1974). Simple Method for Predicting Dispersion in Streams. *J. of Envir. Eng. Div., Am. Soc. Civ. Eng.*, 100(4), pp. 997-1011.
102. Mishra, G. C., and Jain, S. K. (1999). Estimation of hydraulic diffusivity in stream aquifer system. *J. of Irri. and Drain. Div.*, 125 (2), 74-81.
103. Mohan, S., and Jegathambal, P. (2002). Subsurface contaminant transport modeling using MT3D-A case study of Palar Basin”, Proceedings, of the National Seminar on Water Resources Systems Planning and Management, Annamalai University, Tamil Nadu. March. pp. B43-B49.
104. Moog Jirka (1998) Analysis of reaeration equations using mean multiplicative error. *J. Environ. Engg, ASCE*, 112, 2, 104 – 110.
105. Morel Seytoux, H. J., and Daly, C. J. (1975). A discrete kernel generator for stream aquifer studies. *Water Resour. Res.*, 11 (2), 253-260.
106. Mujumdar, PP and Saxena, Pavan (2004) A stochastic dynamic programming model for stream water quality management. *Sadhana* 29(Part 5):pp. 477-497.
107. Munavalli, G. R, M.S. Mohan Kumar (2004). Dynamic simulation of multi component reaction transport in water distribution systems. *Water Research*, 38, 1971–1988.
108. Munavalli, G. R, M.S. Mohan Kumar (2005). Water quality parameter estimation in a distribution system under dynamic state. *Water Research*, 39, 4287–4298.

109. Murty Bhallamudi, S., Sorab Panday and Peter S. Huyakorn. (2003). Sub-timing in fluid flow and transport simulations. *Advances in Water Resources*, Volume 26, Issue 5, May. pp 477-489.
110. National Water Commission, National Water Development Agency, Report Feb, 2000, Revised preliminary water balance study Brahmani Basin (Technical study no. 60)
111. Nash, J. E. (1959). "Systematic determination of unit hydrograph parameters." *J. Geophys. Res.*, 64, 111–115.
112. Nordin, C. F., and Troutman, B. M. (1980). Longitudinal dispersion in rivers: The persistence of skewness in observed data. *Water Resour. Res.*, 16 (1), 123-128.
113. Nordin, C. F., Jr., and Sabol, G. V. (1974). "Empirical data on longitudinal dispersion in rivers. USGS." *Water-Resources Investigations*, 20– 74.
114. O'Connor, D. J., and W. E. Dobbins. (1958). Mechanism of reaeration in natural streams, *Trans. ASCE*, 123, 641-684.
115. Oberhettinger, F., and Badii, L. (1973). *Tables of Laplace Transforms*, New York: Springer.
116. Ogata, A. and R. B. Banks (1961) A solution of the differential equation of longitudinal dispersion in porous media .U S Geo. Surv., Prof. Paper no.411-A.
117. Owens, M., R. W. Edwards, and J. W. Gibbs. (1964). Some reaeration studies in streams, *Intl. Jour. Air Water Pollution*, 8, 469-486.
118. Palo, K. C. (2002). A study of assessment of minimum flow in downstream of a dam from ecological considerations, M.Tech, dissertation, IIT Roorkee, INDIA
119. Perk Marcel V., Phillip N. Owens, Lynda K. Deeks, and Berry G. Rawlins. (2006). Streambed sediment geochemical controls in stream phosphorus concentration during base flow, *Water, Air and Soil Pollution*, Vol. 6, No. 5-6, pp.443-451.
120. Pierre, Y. J. (2002). *River Mechanics*. Cambridge University Press, 434 p.
121. Ranga Raju, K. G., Kothiyari, U. C., and Ahmad, Z. (1997). Dispersion of conservative pollutant. Dept. of Civil Engg. Univ. of Roorkee, Roorkee, India.



122. Rinaldi, Soncini-Sessa, Stehfest and Tamura. (1979) Modeling and control of river quality, McGraw hill series in Water Res. And Environ. Engg. Pp. 380
123. Roland Leduc, T. E. Unny and E. A. McBean. (1986). Stochastic model of first-order BOD kinetics. *Water Research*, Volume 20, Issue 5, May. 625-632.
124. Runkel, R. L. (1996). Solution of the advection dispersion: continuous load of finite duration. *J. of Envir. Engg., ASCE*, 122 (9), 830-832.
125. Runkel, R. L. (1998). One Dimensional Transport with Inflow and Storage (OTIS): A Solute Transport Model for Streams and Rivers. USGS Water Resour. Invest. Report No 98-4018., Denver, Colorado.
126. Runkel, R.L., Broshears, R.E. (1991). One dimensional transport with inflow and storage (OTIS): a solute transport model for small streams, Tech. Rep. 91-01, Center for Advanced Decision Support for Water and Environmental System, University of Colorado, Boulder.
127. Runkel, R.L., Chapra, S.C. (1993). An efficient numerical solution of the transient storage equations for solute transport in small streams. *Water Resour. Res.* 29 (1), 211–215.
128. Runkel. R. L., McKnight, D. M., and Andrews, E. D. (1998). Analysis of transient storage subject to unsteady flow: flow variation in an Antarctic stream. *J. N. Am. Benthol. Soc.*, 17 (2), 143-154.
129. Rutherford, J. C. (1994). *River Mixing*, John-Wiley & Sons, Chichester.
130. Sardin, M., Krebs, R., Schweich, D. (1986). Transient mass-transport in the presence of non-linear physicochemical interaction laws: progressive modeling and appropriate experimental procedures. *Geoderma* 38, 115–130.
131. Sardin, M., Schweich, D., Leij, F. J., and Van Genuchten, M. Th. (1991). Modeling the non-equilibrium transport of linearly interacting solutes in porous media: A review. *Water Resour. Res.*, 27, 2287-2307.
132. Sasikumar, K and Mujumdar, PP (1998) Fuzzy Optimization Model for Water Quality Management of a River System. *Water Resources Planning and Management* 124(2):pp. 79-88.

133. Schmid, B.H. (1995). On the transient storage equations for longitudinal solute transport in open channels: temporal moments accounting for the effects of first-order decay. *J. Hydraulic Res.* 33 (5), 595–610.
134. Schmid, B.H. (1997). Analytical solution of the transient storage equations accounting for solute decay. Proceedings of Theme B, Water for a changing Global Community. The 27<sup>th</sup> Congress of the Int. Assoc. for Hydraulic Research. Water Resources Engineering Division/ASCE, August 10–15, 1997, San Francisco, CA, USA, 15–20.
135. Schmid, B.H. (2003). Temporal moments routing in rivers and streams with transient storage. *Adv. Water Res.* 26 (9), 1021–1027
136. Schulz, H.D., Reardon, E.J. (1983). A combined mixing cell/analytical model to describe two-dimensional reactive solute transport for unidirectional groundwater flow. *Water Resources Research* 19, 493–502.
137. Schweich, D., Sardin, M. (1981). Adsorption, partition, ion exchange and chemical reaction in batch reactors or in columns. *Journal of Hydrology* 50, 1–33.
138. Schweich, D., Sardin, M., Gaudet, J-P. (1983). Measurement of a cation exchange isotherm from elution curves obtained in a soil column: preliminary results. *Soil Science Society of America Journal* 47, 32–37.
139. Seepana, Bala Prasad. (2002). Simulation of Solute Transport in Unsteady Stream Flows. Ph.D Thesis, WRDTC, IIT Roorkee, INDIA.
140. Seo, I. W., and Cheong, T. S. (1998). Predicting Longitudinal Dispersion Co-efficient in Natural Streams. *J. of Hydraul. Eng., Am. Soc. Civ. Eng.*, 124(1), pp. 25-32.
141. Seo, I. W., and Cheong, T. S. (2001) A moment based calculations of parameters for the storage zone model for river dispersion, *Jour. Hydr. Eng., Am. Soc. Civ. Eng.*, 127(6), 453-465.
142. Sharma, P. K. and R. Srivastava (2005). Breakthrough curves for reactive transport through porous media, National Conference on Hydraulics and Water Resources - Hydro 2005, Tumkur.

143. Sohrab, M. (1998). Longitudinal dispersion of pollutants in open channels, Ph.D thesis, Department of Civil Eng. University of Roorkee, Roorkee, India.
144. Sooky, A. A (1969). Longitudinal Dispersion in Open Channels. J. of Hydraul. Div., ASCE, 95 (4), pp. 1327-1345.
145. Spiegel, M. R. (1965). Laplace Transforms. Schaum's Outline Series. McGraw-Hill, New York.
146. Srivastava, R., and M.L. Brusseau (1996). Nonideal transport of reactive solutes in heterogeneous porous media: 1. Numerical model development and moments analysis. Journal of Contaminant Hydrology, 24(2), 117-143.
147. Srivastava, R., and T.-C. J. Yeh (1992). A three-dimensional numerical model for water flow and transport of chemically reactive solute through porous media under variably saturated conditions. Advances in Water Resources, 15(5), 275-287.
148. Srivastava, R., P.K. Sharma, and M.L. Brusseau (2004). Reactive solute transport in macroscopically homogeneous porous media: analytical solutions for the temporal moments. Journal of Contaminant Hydrology, 69(1/2), 27-43.
149. Stefan Heinz G., and Demetracopoulos. (1981) Cells in series simulation of riverine transport. Jour. Hydr. Div., Am. Soc. Civil Engrs., 107 (6), 675-697.
150. Streeter, H. W., and Phelps, E. B. (1925). A study of the pollution and natural purification of the Ohio River, Public Health Bulletin No. 146. Public Health Service, Washington, D. C.
151. Sumer, M. (1969). On the Longitudinal Dispersion Co-efficient for a Broad Open Channel. J. of Hydraul. Res., 7 (1), pp. 129-135.
152. Sun, N. Z. (1996). Mathematical modeling of groundwater pollution, Springer-Verlag, New York.
153. Swamee, P. K., Pathak, S. K., and Sohrab, M. (2000). Empirical relations for longitudinal dispersion in streams. J. of Envir. Engg., Vol. 126, No. 11, 1056-1062.
154. Taylor, G. I. (1921). Diffusion by continues movements. Proc. London Math. Soc. Ser. A 20. 196-211.

155. Taylor, G. I. (1953), Dispersion of Soluble Matter in Solvent Flowing Slowly Through a Tube. Proc. R. Soc. London ser., A 219, pp. 186-203.
156. Taylor, G. I. (1954). The Dispersion of Matter in Turbulent Flow through a Pipe. Proc. R. Soc. London ser., A 219, pp. 446-468.
157. Thackston, E. L., and Krenkel, P. A. (1967). Longitudinal Mixing in Natural Streams. J. of Sanit. Engrg. Div., ASCE, 93 (5), pp. 67-90.
158. Thomann, R. V. (1972). Systems analysis and water quality management, McGraw-Hill Book Company, New York.
159. Thomann, R. V., and Mueller, J. A. (1987). Principles of surface water quality modelling and control. Harper & Row Publishers, New York.
160. Valentine, E. M., and I. R. Wood (1979) Dispersion in rough rectangular channels. Jour. Hydr. Div. Am. Soc. Civil Engrs., 105(9), 1537-1553.
161. Van Genuchten, M.T., and Jury, W. A. (1987). Progress in Unsaturated Flow and Transport Modelling. IUGG Rev., 25, pp. 135-140.
162. Van Ommen, H.C., 1985. The mixing cell concept applied to transport of non-reactive and reactive components in soils and groundwater. Journal of Hydrology 78, 201-213.
163. Vander Molen. (1979) Salt balance and leaching requirement. Drainage Principles and Applications, vol. II, Publication no. 16, Intl. Inst. for Land Reclamation and Improvement Wageningen, The Netherlands.
164. Vemula, Subbarao VR and Mujumdar, PP and Ghosh, Subimal (2004) Risk Evaluation in Water Quality Management of a River System. Journal of Water Resources Planning and Management 130(5):pp. 411-423.
165. Verma, A.K., S. Murty Bhallamudi and Eswaran, V. (2000). Overlapping control volume method for solute transport, Journal of Hydrologic Engineering, ASCE, Vol. 5, No. 3, pp. 308-316.
166. Wang G.T. and S. Chen (1996). A new model describing convective-dispersive phenomena derived using the mixing-cell concept. Appl. Math. Modelling, 20.

167. Winter, Thomas C., et al (1998). Groundwater and Surface Water a Single Resource. U.S. Geological Survey Circular 1139. Denver, CO: U. S. Geological Survey.
168. Worman, A. (1998). Analytical solution and time scale for transport of reacting solutes in rivers and streams. *Water Resour. Res.*, 34 (10), 2703-2716.
169. Worman, A., Packman, A.I., Johansson, H., Jonsson, K. (2002). Effect of flow-induced exchange in hyporheic zones on longitudinal transport of solutes in streams and rivers. *Water Resour. Res.* 38 (1), 1001.
170. Yotsukura, N., Fischer, H. B., and Sayre, W. W. (1970). Measurement of mixing characteristics of the Missouri river between Sioux City, Iowa and Plattsmouth, Nebraska. Water Supply paper 1899-G, U.S. Geological Survey, Washington.
171. Young, P. C. (1984). Recursive estimation and time series analysis: An introduction, Springer, Berlin.
172. Young, P. C. and Beck, B. (1974). The modeling and control of water quality in river system. *Automatica*, 10, 455-468.
173. Young, P. C., and Wallis, S. G. (1993). Solute Transport and Dispersion in Channels. Channel Network Hydrology, John Willey & Sons.
174. Yurtsever, Y. (1983). Models for tracer data analysis. In guidebook on nuclear techniques in Hydrology. 381-402. Int. Atomic Energy Agency, Vienna.



### A1. The HCIS Model

The physical processes of solute transport in the HCIS model as shown in Fig.A1 are described as follows: in the plug flow zone, the influent solute undergoes a pure translation without any change in its concentration, and then enters to the first reservoir where it gets thoroughly mixed before entering into the second thoroughly mixed reservoir.

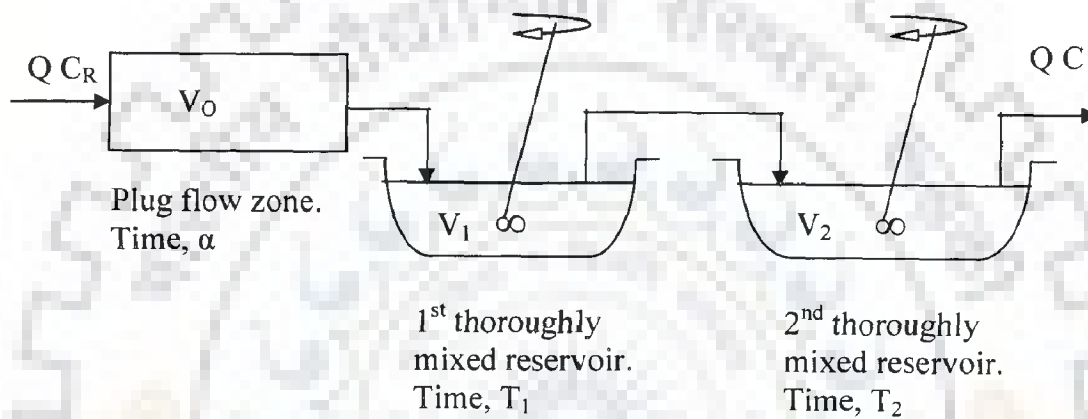


**Fig. A1: The first process unit of the HCIS model**

For a step input boundary concentration,  $C_R$ , in a one-dimensional steady and uniform flow system, with an initial concentration,  $C_i$ , the governing differential equation for the effluent concentration from the first hybrid process unit,  $C_1$  for  $t > \alpha$  (Ghosh *et al*, 2004) is:

$$\frac{dC_1}{dt} + \frac{C_1}{T_2} = \frac{C_R}{T_2} U(t-\alpha) + \frac{C_i - C_R}{T_2} U(t-\alpha) \exp\left[-\frac{(t-\alpha)}{T_1}\right] \quad (A1)$$

in which  $\alpha$  is the time to fill the plug flow zone or the residence time of solute in the plug flow zone (T);  $U(t-\alpha)$  is the unit step function;  $T_1$  and  $T_2$  are the residence times of solute in the 1<sup>st</sup> and the 2<sup>nd</sup> thoroughly mixed reservoirs (T). Solving Eq. A1 for initial condition  $C_1 = C_i = 0$  at  $t = \alpha$ , and boundary concentration,  $C_R = 1$ , the response function of the first hybrid unit to the unit step input concentration is obtained as:

$$K(t) = U(t-\alpha) - U(t-\alpha) \left[ \left( \frac{T_1}{T_1 - T_2} \right) \exp \left\{ -\frac{(t-\alpha)}{T_1} \right\} - \left( \frac{T_2}{T_1 - T_2} \right) \exp \left\{ -\frac{(t-\alpha)}{T_2} \right\} \right]; \quad t \geq \alpha \quad (\text{A2})$$

where,  $K(t)$  = the unit step response function,  $\alpha = V_0/Q$ ;  $T_1 = V_1/Q$ ;  $T_2 = V_2/Q$ ;  $Q$  = flow rate ( $L^3T^{-1}$ );  $V_0$ ,  $V_1$ , and  $V_2$  = volume of the plug flow zone, 1<sup>st</sup> and 2<sup>nd</sup> thoroughly mixed reservoirs respectively ( $L^3$ ). The unit step function,  $U(t-\alpha)$  for  $t \geq \alpha = U(+ve) = 1$ ; and for  $t < \alpha = U(-ve) = 0$ ; and  $t$  = time reckoned since injection of solute. Eq.2 is valid for  $t \geq \alpha$ .

Differentiating  $K(t)$  with respect to  $t$ , the unit impulse response function,  $k(t)$ , which describes the fundamental behaviour of a system, is obtained as:

$$k(t) = \left( \frac{U(t-\alpha)}{T_1 - T_2} \right) \left[ \exp \left\{ -\frac{(t-\alpha)}{T_1} \right\} - \exp \left\{ -\frac{(t-\alpha)}{T_2} \right\} \right]; \quad t \geq \alpha \quad (\text{A3})$$

The characteristics of the unit impulse response function given by Eq.A3 are time to peak, and peak concentration. The time to peak is given by:

$$t_p = \left( \frac{T_1 T_2}{T_1 - T_2} \right) \ln \left( \frac{T_1}{T_2} \right) + \alpha \quad (\text{A4})$$

and, the peak concentration, which occurs at  $t = t_p$ , is:

$$k(t_p) = \left( \frac{\delta(t-\alpha)}{T_1 - T_2} \right) \left[ \exp \left\{ -\frac{T_2 \ln \left( \frac{T_1}{T_2} \right)}{T_1 - T_2} \right\} - \exp \left\{ -\frac{T_1 \ln \left( \frac{T_1}{T_2} \right)}{T_1 - T_2} \right\} \right] \quad (\text{A5})$$

These two characteristics equations (Eqs.A4 and A5) can exclusively be used for estimating the model parameters. In Eqs.A2-A3,  $T_1 \neq T_2$  but they are interchangeable and the interchange does not affect the  $C-t$  profile, time to peak, and peak concentration.

The parameters  $\alpha$ ,  $T_1$  and  $T_2$  can be estimated by several methods, such as: (i) method of partial moments, (ii) a method that uses the zero<sup>th</sup> partial moment, the time to peak and the peak concentration, and (iii) the least squares optimization. The least squares optimization using well-known Marquardt algorithm (Marquardt, 1963) has been found more flexible in estimation of parameters than the other two methods (Ghosh *et al.*, 2004).



Assuming that the river reach downstream of a point source of pollution is composed of a series of equal size hybrid units each having linear dimension,  $\Delta x$  and consisting of a plug flow zone, and two unequal thoroughly mixed reservoirs as shown in Fig.A2.

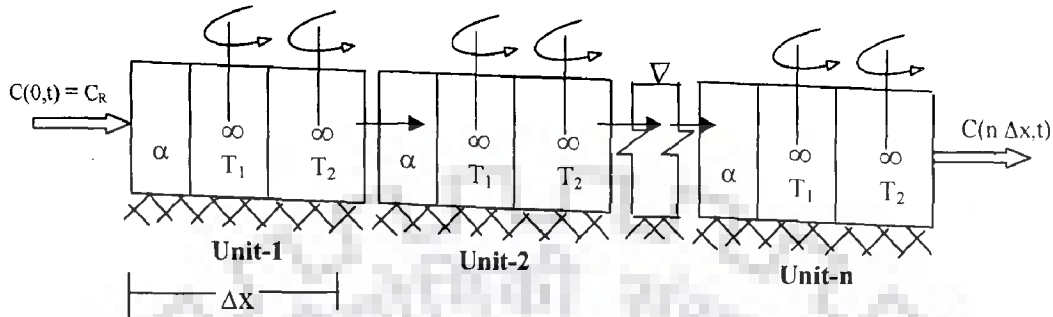


**Fig. A2: A Hybrid-cells-in-series Model ( $\alpha$  = time to replace fluid in the plug flow zone,  $T_1$  and  $T_2$  = residence times of solute in the 1<sup>st</sup> and 2<sup>nd</sup> thoroughly mixed reservoirs respectively,  $\Delta x$  = size of one unit of the hybrid model)**

Using the convolution technique, the response of the  $n^{\text{th}}$  hybrid unit,  $n \geq 2$ , is expressed as:

$$C(n\Delta x, t) = \int_0^t C\{(n-1)\Delta x, \tau\} k(\alpha, T_1, T_2, t-\tau) d\tau \quad (\text{A6})$$

where  $C(\Delta x, \tau) = k(\alpha, T_1, T_2, \tau)$  = output of the 1<sup>st</sup> hybrid unit.

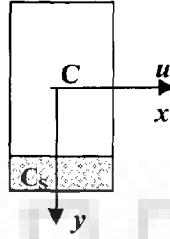
The first and the second moments of Eq.A3 about origin, which describe the mean and the variance of the C-t distribution, obtained by integration between time limit 0 and  $\infty$ , are:

$$M_1 = \alpha + T_1 + T_2 \quad (\text{A7})$$

$$M_2 = \alpha^2 + 2\alpha(T_1 + T_2) + 2(T_1 - T_2)^2 + 6T_1T_2 \quad (\text{A8})$$

where  $M_1$  is the first moment (L);  $M_2$  is the second moment ( $L^2$ ) of the C-t distribution about origin.



**B1. Formulation of Equation for Pollutant Transport in Plug Flow Zone****Fig. B1: A control volume within the plug flow zone, considered for mass balance**

Using chain rule, derivatives of  $C$  and  $C_s$ , with respect to time, can be expressed for a control volume within the plug flow zone (Fig. B1) as follows:

$$\frac{dC}{dt} = \frac{\partial C}{\partial t} + \frac{\partial C}{\partial x} \frac{dx}{dt} \quad (\text{B1})$$

$$= \frac{\partial C}{\partial t} + u \frac{\partial C}{\partial x} \quad (\text{B2})$$

$$\text{and } \frac{dC_s}{dt} = \frac{\partial C_s}{\partial t} + \frac{\partial C_s}{\partial y} \frac{dy}{dt} \quad (\text{B3})$$

$$\text{Since } \frac{dy}{dt} = 0$$

$$\frac{dC_s}{dt} = \frac{\partial C_s}{\partial t} \quad (\text{B4})$$

In the plug flow zone, the rate of change of total mass in a control volume ( $A \Delta x$ ) is equal to negative of rate of change of mass adsorbed in a control volume ( $W_p D_B \Delta x$ ).

Hence,

$$(A \Delta x) \left( \frac{\partial C}{\partial t} + u \frac{\partial C}{\partial x} \right) = - (\phi W_p D_B \Delta x) \frac{\partial C_s}{\partial t} \quad (\text{B5})$$

Rewriting Eq. B5:

$$\frac{\partial C}{\partial t} = -u \frac{\partial C}{\partial x} - \left( \frac{\phi W_p D_B}{A} \right) \frac{\partial C_s}{\partial t} \quad (\text{B6})$$



**C1. The HCIS Model**

The left hand side elements of the Jacobian matrix (Eq. 6.8) are;

$$A(1,1) = \sum_{i=1}^n \left\{ \frac{\partial k_c(i\Delta t)}{\partial \alpha} \frac{\partial k_c(i\Delta t)}{\partial \alpha} \right\} \Bigg|_{\alpha^*, T_1^*, T_2^*}$$

$$A(1,2) = \sum_{i=1}^n \left\{ \frac{\partial k_c(i\Delta t)}{\partial \alpha} \frac{\partial k_c(i\Delta t)}{\partial T_1} \right\} \Bigg|_{\alpha^*, T_1^*, T_2^*}$$

$$A(1,3) = \sum_{i=1}^n \left\{ \frac{\partial k_c(i\Delta t)}{\partial \alpha} \frac{\partial k_c(i\Delta t)}{\partial T_2} \right\} \Bigg|_{\alpha^*, T_1^*, T_2^*}$$

$$A(2,1) = \sum_{i=1}^n \left\{ \frac{\partial k_c(i\Delta t)}{\partial T_1} \frac{\partial k_c(i\Delta t)}{\partial \alpha} \right\} \Bigg|_{\alpha^*, T_1^*, T_2^*}$$

$$A(2,2) = \sum_{i=1}^n \left\{ \frac{\partial k_c(i\Delta t)}{\partial T_1} \frac{\partial k_c(i\Delta t)}{\partial T_1} \right\} \Bigg|_{\alpha^*, T_1^*, T_2^*}$$

$$A(2,3) = \sum_{i=1}^n \left\{ \frac{\partial k_c(i\Delta t)}{\partial T_1} \frac{\partial k_c(i\Delta t)}{\partial T_2} \right\} \Bigg|_{\alpha^*, T_1^*, T_2^*}$$

$$A(3,1) = \sum_{i=1}^n \left\{ \frac{\partial k_c(i\Delta t)}{\partial T_2} \frac{\partial k_c(i\Delta t)}{\partial \alpha} \right\} \Bigg|_{\alpha^*, T_1^*, T_2^*}$$

$$A(3,2) = \sum_{i=1}^n \left\{ \frac{\partial k_c(i\Delta t)}{\partial T_2} \frac{\partial k_c(i\Delta t)}{\partial T_1} \right\} \Bigg|_{\alpha^*, T_1^*, T_2^*}$$

$$A(3,3) = \sum_{i=1}^n \left\{ \frac{\partial k_c(i\Delta t)}{\partial T_2} \frac{\partial k_c(i\Delta t)}{\partial T_2} \right\} \Bigg|_{\alpha^*, T_1^*, T_2^*}$$

The right hand side elements of the Jacobian matrix (Eq. 6.8) are;

$$B(1,1) = \sum_{i=1}^n \left\{ k_o(i\Delta t) \frac{\partial k_c(i\Delta t)}{\partial \alpha} - k_c(i\Delta t) \frac{\partial k_c(i\Delta t)}{\partial \alpha} \right\} \Bigg|_{\alpha^*, T_1^*, T_2^*}$$

$$B(2,1) = \sum_{i=1}^n \left\{ k_o(i\Delta t) \frac{\partial k_c(i\Delta t)}{\partial T_1} - k_c(i\Delta t) \frac{\partial k_c(i\Delta t)}{\partial T_1} \right\} \Bigg|_{\alpha^*, T_1^*, T_2^*}$$

$$B(3,1) = \sum_{i=1}^n \left\{ k_o(i\Delta t) \frac{\partial k_c(i\Delta t)}{\partial T_2} - k_c(i\Delta t) \frac{\partial k_c(i\Delta t)}{\partial T_2} \right\} \Bigg|_{\alpha^*, T_1^*, T_2^*}$$

where, the derivatives coming in these matrices elements can be got by differentiating the unit impulse response  $k_c(i\Delta t)$  with respect to the parameters.

## C2. The HCIS Model with Adsorption

The left hand side elements of the Jacobian matrix (Eq. 6.13) are;

$$A(1,1) = \sum_{i=1}^n \left\{ \frac{\partial k_c(i\Delta t)}{\partial \alpha} \frac{\partial k_c(i\Delta t)}{\partial \alpha} \right\} \Bigg|_{\alpha^*, T_1^*, T_2^*, R_D^*}$$

$$A(1,2) = \sum_{i=1}^n \left\{ \frac{\partial k_c(i\Delta t)}{\partial \alpha} \frac{\partial k_c(i\Delta t)}{\partial T_1} \right\} \Bigg|_{\alpha^*, T_1^*, T_2^*, R_D^*}$$

$$A(1,3) = \sum_{i=1}^n \left\{ \frac{\partial k_c(i\Delta t)}{\partial \alpha} \frac{\partial k_c(i\Delta t)}{\partial T_2} \right\} \Bigg|_{\alpha^*, T_1^*, T_2^*, R_D^*}$$

$$A(1,4) = \sum_{i=1}^n \left\{ \frac{\partial k_c(i\Delta t)}{\partial \alpha} \frac{\partial k_c(i\Delta t)}{\partial R_D} \right\} \Bigg|_{\alpha^*, T_1^*, T_2^*, R_D^*}$$

$$A(2,1) = \sum_{i=1}^n \left\{ \frac{\partial k_c(i\Delta t)}{\partial T_1} \frac{\partial k_c(i\Delta t)}{\partial \alpha} \right\} \Bigg|_{\alpha^*, T_1^*, T_2^*, R_D^*}$$

$$A(2,2) = \sum_{i=1}^n \left\{ \frac{\partial k_c(i\Delta t)}{\partial T_1} \frac{\partial k_c(i\Delta t)}{\partial T_1} \right\} \Bigg|_{\alpha^*, T_1^*, T_2^*, R_D^*}$$

$$A(2,3) = \sum_{i=1}^n \left\{ \frac{\partial k_c(i\Delta t)}{\partial T_1} \frac{\partial k_c(i\Delta t)}{\partial T_2} \right\} \Bigg|_{\alpha^*, T_1^*, T_2^*, R_D^*}$$

$$A(2,4) = \sum_{i=1}^n \left\{ \frac{\partial k_c(i\Delta t)}{\partial T_1} \frac{\partial k_c(i\Delta t)}{\partial R_D} \right\} \Bigg|_{\alpha^*, T_1^*, T_2^*, R_D^*}$$

$$A(3,1) = \sum_{i=1}^n \left\{ \frac{\partial k_c(i\Delta t)}{\partial T_2} \frac{\partial k_c(i\Delta t)}{\partial \alpha} \right\} \Bigg|_{\alpha^*, T_1^*, T_2^*, R_D^*}$$

$$A(3,2) = \sum_{i=1}^n \left\{ \frac{\partial k_c(i\Delta t)}{\partial T_2} \frac{\partial k_c(i\Delta t)}{\partial T_1} \right\} \Big|_{\alpha^*, T_1^*, T_2^*, R_D^*}$$

$$A(3,3) = \sum_{i=1}^n \left\{ \frac{\partial k_c(i\Delta t)}{\partial T_2} \frac{\partial k_c(i\Delta t)}{\partial T_2} \right\} \Big|_{\alpha^*, T_1^*, T_2^*, R_D^*}$$

$$A(3,4) = \sum_{i=1}^n \left\{ \frac{\partial k_c(i\Delta t)}{\partial T_2} \frac{\partial k_c(i\Delta t)}{\partial R_D} \right\} \Big|_{\alpha^*, T_1^*, T_2^*, R_D^*}$$

$$A(4,1) = \sum_{i=1}^n \left\{ \frac{\partial k_c(i\Delta t)}{\partial R_D} \frac{\partial k_c(i\Delta t)}{\partial \alpha} \right\} \Big|_{\alpha^*, T_1^*, T_2^*, R_D^*}$$

$$A(4,2) = \sum_{i=1}^n \left\{ \frac{\partial k_c(i\Delta t)}{\partial R_D} \frac{\partial k_c(i\Delta t)}{\partial T_1} \right\} \Big|_{\alpha^*, T_1^*, T_2^*, R_D^*}$$

$$A(4,3) = \sum_{i=1}^n \left\{ \frac{\partial k_c(i\Delta t)}{\partial R_D} \frac{\partial k_c(i\Delta t)}{\partial T_2} \right\} \Big|_{\alpha^*, T_1^*, T_2^*, R_D^*}$$

$$A(4,4) = \sum_{i=1}^n \left\{ \frac{\partial k_c(i\Delta t)}{\partial R_D} \frac{\partial k_c(i\Delta t)}{\partial R_D} \right\} \Big|_{\alpha^*, T_1^*, T_2^*, R_D^*}$$

The right hand side elements of the Jacobian matrix (Eq. 6.13) are;

$$B(1,1) = \sum_{i=1}^n \left\{ k_o(i\Delta t) \frac{\partial k_c(i\Delta t)}{\partial \alpha} - k_c(i\Delta t) \frac{\partial k_c(i\Delta t)}{\partial \alpha} \right\} \Big|_{\alpha^*, T_1^*, T_2^*, R_D^*}$$

$$B(2,1) = \sum_{i=1}^n \left\{ k_o(i\Delta t) \frac{\partial k_c(i\Delta t)}{\partial T_1} - k_c(i\Delta t) \frac{\partial k_c(i\Delta t)}{\partial T_1} \right\} \Big|_{\alpha^*, T_1^*, T_2^*, R_D^*}$$

$$B(3,1) = \sum_{i=1}^n \left\{ k_o(i\Delta t) \frac{\partial k_c(i\Delta t)}{\partial T_2} - k_c(i\Delta t) \frac{\partial k_c(i\Delta t)}{\partial T_2} \right\} \Big|_{\alpha^*, T_1^*, T_2^*, R_D^*}$$

$$B(4,1) = \sum_{i=1}^n \left\{ k_o(i\Delta t) \frac{\partial k_c(i\Delta t)}{\partial R_D} - k_c(i\Delta t) \frac{\partial k_c(i\Delta t)}{\partial R_D} \right\} \Big|_{\alpha^*, T_1^*, T_2^*, R_D^*}$$

where, the derivatives coming in these matrices elements can be got by differentiating the unit impulse response  $k_c(i\Delta t)$  with respect to the parameters.

## ESTIMATION OF STREAM WATER QUALITY PARAMETER USING REGIME CHANNEL THEORY

### D1. GENERAL

Computation of the pollutant concentration along the river reach and fixation of size of hybrid unit in HCIS model require  $u$  and  $D_L$  *a priori*. Flow velocity,  $u$  can be obtained using flow resistance equation or can be measured in the field. However the estimation of  $D_L$  is not straightforward. A number of approaches to estimate  $D_L$  have been suggested by many investigators (Taylor, 1954; Fischer, 1966; 1967; 1979; Gray & Pinder, 1976). These can be grouped as: (i) Theoretical/analytical approaches, (ii) experimental approaches, and (iii) empirical formulae. Each approach has its own merits and demerits. Interestingly, the value of  $D_L$  of a river if obtained using any of the method does not match with the value of the other methods with hydraulic properties remaining same. Out of these three groups, the third group, i.e., empirical formulae, which mainly suggest estimation of  $D_L$  from river's bulk flow properties and geometry, are less complicated to use. The other two approaches require intensive database. In many riparian streams or rivers, measurements of hydraulic data, such as; stream geometry, flow velocity, etc. are difficult owing to topographical constraints. The regime channel theory that relates flow rate and sediment grain size distribution appears to be sound technique to determine hydraulic data of a stream, knowing flow rate and silt factor *a priori*. The present study is thus focused to investigate a method for determining stream bulk flow properties, which would ease out estimation of  $D_L$  with reasonable accuracy.

### D2. EMPIRICAL METHODS

There are numerous empirical formulae available mostly representing relationship of  $D_L = a_0 d U_*$ . where,  $d$  = depth of flow, &  $U_* =$  shear flow velocity =  $\sqrt{g R S}$ ,  $R$  is hydraulic radius,  $S$  is the bed slope,  $g$  is acceleration due to gravity and  $a_0$  is a constant, which is found to have a value ranging from 8.6 to 7500 (Bansal, 1971). The available empirical formulae suggested by various investigators are tabulated in Table 2.1. From



these empirical formulae, it can be noticed that a number of formulae are of the type  $D_L/U.H = \text{constant}$ . However several researchers have shown that the ratio  $D_L/U.H =$  is not constant. This makes difficulty in estimation of  $D_L$ . Empirical formulae suggest that  $D_L$  is a function of stream flow characteristic and stream geometry. By the non-dimensional analysis (Seo & Cheong, 1998) or by reasonable approximation of the integral relating the dispersion co-efficient in natural streams (Fischer, 1967), the functional relationship pertinent to the dispersion co-efficient has been obtained and given in Eq. (D1).

$$D_L = 5.915 H \left( \frac{W}{H} \right)^{0.62} \frac{U^{1.428}}{U_*^{0.428}} \quad (\text{D1})$$

The dimensionless plot of  $D_L/U.H$  against  $W/H$  of the different empirical formulae suggested by various investigators is shown on log – log scale in Fig D1. The average of distribution of  $D_L/U.H$  versus  $W/H$  computed using different formulae is estimated and found approximately matching with the value estimated using the expression suggested by Seo & Cheong (1998). The plots are shown in Fig. D1. Thus, Seo & Cheong (1998) equation is chosen for estimation of  $D_L$ .

### D3. REGIME CHANNEL CONCEPT

Lindley's (1919) defined that when an artificial channel is considered to carry silty water, both the bed and banks scour or fill and depth, gradient and width changes until a state of balance is attained at which the channel is said to be in regime. Many investigators (Lindley, 1919, Lacey, 1930) recognized that sediment size plays an important role in determining the channel geometry. The approximate relationship suggested by Lindley (1919) to find silt factor is:  $f_L = 8 D_m^{1/2}$ , where  $f_L$  is the silt factor and  $D_m$  is the grain size. Lacey (1930) has suggested couple of empirical relationships to estimate the channel geometry having known the stream flow rate and the silt factor. For a regime channel having average stream flow rate, ( $Q$ ) and silt factor ( $f_L$ ), the channel geometry can be approximated as follows;

$$u = 0.438 Q^{1/5} f_L^{1/3} \quad (\text{D2})$$

$$R_h = 0.47 Q^{\frac{1}{3}} f_L^{-\frac{1}{3}} \quad (D3)$$

$$A = 2.28 Q^{\frac{5}{6}} f_L^{-\frac{1}{3}} \quad (D4)$$

$$P = 4.818 Q^{\frac{1}{2}} \quad (D5)$$

$$S = 0.0003 Q^{-\frac{1}{6}} f_L^{\frac{5}{3}} \quad (D6)$$

where  $u$  is the mean flow velocity (m/s),  $R_h$  is the hydraulic mean radius (m),  $A$  is the cross-sectional area of flow (m<sup>2</sup>),  $P$  is the wetted perimeter (m) and  $S$  is the dimensionless slope (m/m).

The mean grain size is given by:

$$D_m = D_g \exp\left[0.5 \ln(\ln \sigma_g)\right] \quad (D7)$$

where,  $D_m$  is the mean grain size in mm,  $\sigma_g$  is geometric standard deviation of grain size distribution,  $\sigma_g = \frac{1}{2} \left( \frac{D_{84.1}}{D_{50}} + \frac{D_{50}}{D_{15.9}} \right)$ ,  $D_g$  is geometric mean diameter =  $(D_{84.1} D_{15.9})^{\frac{1}{2}}$ . where

$D_{84.1}$ ,  $D_{50}$  and  $D_{15.9}$  are the grain diameters finer than 84.1, 50 and 15.9 % respectively.

Henderson (1966) has also suggested the concept of regime channel according to channel type. Although both the concepts are applicable for wide channel, however, the Lacey's regime channel concept holds some advantages over the Henderson's (1966) theory. These are: (i) field measurement of stream's cross-section can be ignored; (ii) sampling and analyses of streambed material are easier than measurement of stream cross-section.

It is clearly evident that if mean grain size of the streambed sediments is known then silt factor,  $f_L$ , can be determined. Knowing  $f_L$  and  $Q$  and using Eqs. (D2) through (D6), the channel's characteristics and geometry can be ascertained. Having known stream geometry and hydraulic properties, and making use of a suitable empirical formula, one can reasonably estimate  $D_L$ .

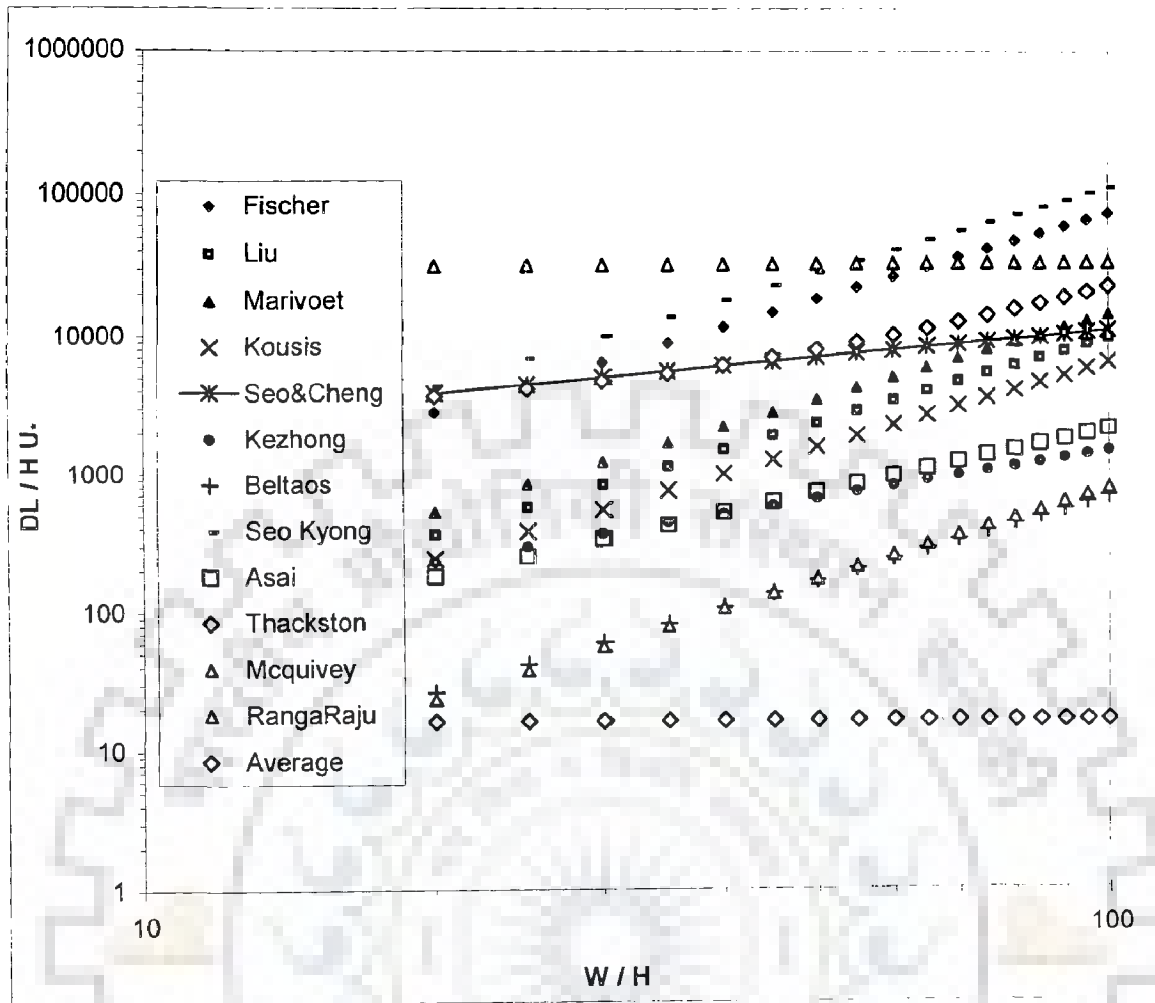


**Fig D1: Variation of  $D_L/H U_*$  versus  $W/H$ ; Using empirical formulae suggested by various investigators for estimation of  $D_L$  in natural streams.**

**E1. MUSKINGUM-CUNGE METHOD (Ponce, V. M, 1989)**

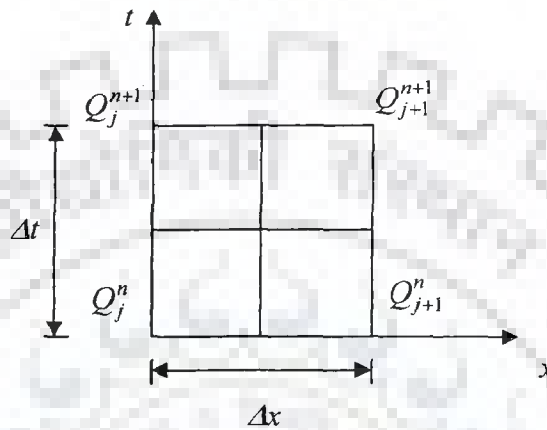


**Fig E1: Space-Time discretization of kinematics wave equation paralleling Muskingum method**

The Muskingum-cunge method can calculate runoff diffusion superficially by varying the weighting factor parameter  $X$ . A numerical solution of the linear kinematic wave equation using a third order accurate scheme ( $C = 1$ ) leads to pure flood hydrograph translation. In this, it is discretized by centering the spatial derivative and off-centering the temporal derivative by means of a weighting factor  $X$ .

$$\frac{X(Q_j^{n+1} - Q_j^n) + (1 - X)(Q_{j+1}^{n+1} - Q_{j+1}^n)}{\Delta t} + c \frac{(Q_{j+1}^n - Q_j^n) + (Q_{j+1}^{n+1} - Q_j^{n+1})}{2\Delta x} = 0 \dots\dots\dots(E1)$$

where  $c$  is wave celerity, and solving Eq. (E1) for the unknown discharge leads to the following routing equation.

$$Q_{j+1}^{n+1} = C_1 Q_j^{n+1} + C_2 Q_j^n + C_3 Q_{j+1}^n \dots\dots\dots(E2)$$

The routing coefficients are

$$C_1 = \frac{c(\Delta t / \Delta x) - 2X}{2(1-X) + c(\Delta t / \Delta x)} \dots\dots\dots(E3)$$

$$C_2 = \frac{c(\Delta t / \Delta x) + 2X}{2(1-X) + c(\Delta t / \Delta x)} \dots\dots\dots(E4)$$

$$C_3 = \frac{2(1-X) - c(\Delta t / \Delta x)}{2(1-X) + c(\Delta t / \Delta x)} \dots\dots\dots(E5)$$

where,  $C$  is courant number. To avoid the numerical diffusion and dispersion the parameter  $X$  and  $C$  have to be chosen as 0.5 and 1.0 respectively.  $D$  is the cell Reynolds number, which can be expressed as follows,

$$D = \frac{q_0}{S_0 c \Delta x} \dots\dots\dots(E6)$$

where  $q_0$  is the reference discharge per unit width,  $S_0$  is channel bottom slope. The choice of reference flow will have a bearing on the calculated results, although the overall effect is likely to be small. For practical applications, either an average or peak flow value can be used as reference flow. The peak flow value has the advantage that it can be readily ascertained, although a better approximation may be obtained by using an average value. The linear mode of computation is referred to as the constant parameter Muskingum-cunge method to distinguish it from the variable parameter Muskingum-cunge method, in which the routing parameters are allowed to vary with flow.